SEPTEMBER 1979

18 and 30 GHz Fixed Service Communication Satellite System Study

CONTRACT NO. NAS 3-21367

FINAL REPORT

HUGHES
HUGHES AIRCRAFT COMPANY
SPACE AND COMMUNICATIONS GROUP

Hughes Ref No. E1992 • SCG 90272R

CONTENTS

		Page
1.	OBJECTIVES AND STATEMENT OF WORK	1-1
2.	INTRODUCTION AND SUMMARY	2-1
	2.1 Satellite Communications at 18 and 30 GHz	2-1
	2.2 Rain Attenuation	2-3
	2.3 System Concepts	2-3
	2.3.1 Trunk Concept	2-3
	2.3.2 Direct to User Concept	2-6
	2.4 Critical Technologies	2-6
3.	TECHNOLOGY ASSESSMENT	3-1
	3.1 Earth Station Baseband and Modems	3-1
	3.1.1 Digital and Analog Terrestrial Interfaces	3-1
	3.1.2 Modulation - Demodulation	3-4
	3.2 Space Diversity System Design and Cost	3-10
	3.3 Earth Station RF Technology	3-22
	3.3.1 Receivers	3-22
	3.3.2 Transmitters	3-26
	3.3.3 Frequency Sources	3-29
	3.3.4 Earth Station Antenna System Considerations	3-33
	3.4 Satellite Repeater	3-38
	3.4.1 Receivers	3-38
	3.4.2 Signal Routing and Switching	3-39
	3.4.3 Satellite Transmitters	3-47
	3.4.4 Frequency Sources	3-53
	3.5 Satellite Antennas	3-53
	3.6 Rain Attenuation	3-55
	3.7 Bibliography	3-57
	3.8 References	3-59
4.	TRUNK CONCEPTS	4-1
	4.1 Trunk Function	4-1
	4.2 Trunk Rain Strategy	4-1
	4.3 System Resources Optimization	4-5
	4.4 Ten Station FDMA Trunk	4-7
	4.4.1 Trunk FDMA Performance Requirements	4-8
	4.4.2 FDMA Link Budget	4-9
	4.4.3 Satellite EIRP and G/T - FDMA Trunk	4-9
	4.4.4 Earth Station Ten Beam FDMA Trunk	4-11
	4.4.5 Satellite Repeater - FDMA Trunk	4-11
	4.4.6 Repeater Weight, Power, and Cost Budget	4-13
	4.4.7 Spacecraft Antenna - Ten Beam FDMA Trunk	4-15
	4.5 Ten Beam FDMA Trunk Satellite	4-15
	4.5.1 FDMA Trunk Satellite Weight, Power, and Cost Budget	4-17
	4.6 Earth Station Cost Breakdown - Ten Beam FDMA Trunk	4-18
	4.7 Ten Beam FDMA Trunk Cost	4-18

4.8 Ten Beam Satellite Switched TDMA Trunk 4-21
4.8.1 TDMA Trunk Link Budget 4-21
4.8.2 Satellite EIRP and G/T - Ten Station TDMA 4-23
4.8.3 Ten Station TDMA Trunk Satellite Repeater 4-23
4.8.4 Trunk TDMA Repeater Weight, Power, and Cost Budget 4-25
4.8.5 Earth Station Ten Beam TDMA Trunk 4-27
4.9 TDMA Trunk Satellite 4-27
4.10 Earth Station Ten Beam TDMA Trunk Cost Breakdown 4-28
4.11 Ten Beam TDMA Trunk Costs 4-28
4.12 Service Investment for Trunk Concepts 4-29
4.12.1 Sensitivity of System Cost to Bit Error Rate 4-29
4.12.2 Sensitivity of System Cost to Data Rate 4-31
4.12.3 Sensitivity of System Cost to Number of Beams 4-31
4.12.4 Sensitivity of Cost to Propagation Reliability 4-33

5. DIRECT TO USER CONCEPTS 5-1
5.1 Antenna Gain Comparison 5-1
5.2 RF Comparison 5-1
5.3 Multibeam Interconnectivity 5-3
5.3.1 Direct Interconnectivity 5-3
5.3.2 Indirect Interconnectivity 5-5
5.4 Multibeam Interconnectivity Without Frequency Reuse 5-5
5.5 Direct to User Traffic Model 5-6
5.6 Spectrum Capacity 5-7
5.7 FDMA Multibeam Concept 5-7
5.7.1 FDMA Multibeam Link Budget 5-9
5.7.2 FDMA Multibeam Satellite EIRP and G/T 5-11
5.7.3 25 Beam Direct to User FDMA Repeater Weight, Power, and Cost Budget 5-12
5.7.4 Direct to User FDMA Earth Station 5-13
5.7.5 Direct to User Earth Station Cost 5-13
5.7.6 25 Beam Direct to User Satellite 5-15
5.7.7 System Investment - 25 Beam Direct to User FDMA 5-17
5.8 Annual Cost of Space Segment and System Control and Maintenance 5-18
5.9 Direct to User Satellite Switched TDMA Concept 5-19
5.9.1 Direct to User TDMA Link Budget 5-19
5.9.2 Direct to User TDMA Satellite 5-21
5.9.3 Direct to User TDMA Earth Station 5-21
5.9.4 Direct to User Earth Station Cost 5-22
5.9.5 Direct to User Annual Service Costs 5-22
5.9.6 Sensitivity of Cost to Number of Beams 5-23
5.9.7 Sensitivity of Cost to Number of Stations 5-24

6. COMPETITIVE ALTERNATIVES 6-1

7. CRITICAL TECHNOLOGY 7-1
7.1 Introduction 7-1
7.2 Multispot Beam Trunk Antennas 7-1
7.2.1 Feed Interference 7-1

7.2.2 Beam to Beam Isolation 7-3
7.2.3 Off-Axis Scan Loss 7-4
7.2.4 Dual Frequency Feeds 7-4
7.3 Direct to User Multispot Beam Antenna 7-5
7.4 Satellite Transmitters 7-5
7.5 FDMA Multiplexers 7-7
7.6 Microwave Switch Matrix 7-7
7.7 Low Noise Amplifiers 7-8

APPENDICES

A. 18/30 GHz Multiple Spot Beam Antenna Study A-1
B. Rain Attenuation and Depolarization at 20/30 GHz B-1
C. Statement of Work C-1

1. OBJECTIVES AND STATEMENT OF WORK

The detailed statement of work (SOW) for this study, including a discussion of the reasons for the study, appears in Appendix C. The study tasks are summarized below. The primary objective of the study was to determine what technology development was most critical for use of the 18 and 30 GHz bands for satellite communications. To this end a number of point to point communication concepts were defined in the SOW. These concepts were to be evaluated, selected baselines optimized, and the system and service costs computed.

Task 1 was to assess the expected 1990's performance and cost of the hardware components of an 18 and 30 GHz satellite system.

Task 2 was the study of a number of potential trunk concepts defined in the SOW. The task was to study the concepts, optimize selected baselines, compute the system cost and the service cost associated with the selected baselines, and compare the variation in service cost influenced by such variables as propagation reliability, data quality, and system size.

Task 3 was a study of direct to user concepts similar to that of the trunk concepts in Task 2.

Task 4 was the comparison of the cost effectiveness of satellite systems at 18 and 30 GHz with existing systems at C and Ku band. The SOW also included a comparison with terrestrial links, but it was agreed among the NASA and the contractors that no effort would be devoted to this comparison in the system studies.

Task 5 was the identification of critical technology developments required to properly use the 18 and 30 GHz bands.

In conjunction with this study, Western Union and IT&T U.S. Telephone and Telegraph Corporation performed studies to assess the potential market for 18/30 GHz satellite communications in the last two decades of this century. Task 6 was to interface with the contractors performing the market demand studies.

2. INTRODUCTION AND SUMMARY

2.1 SATELLITE COMMUNICATIONS AT 18 AND 30 GHz

The World Administrative Radio Council (WARC) has allocated the portion of the spectrum between 17.7 and 20.2 GHz to the downlink, and the portion between 27.5 and 30.0 GHz to the uplink of satellite communications systems which serve fixed earth stations. These bands differ in some respects from C band and Ku band, as indicated below.

1) The 18 and 30 GHz spectrum is 2.5 GHz wide, compared to 500 MHz at C and Ku band.

2) Very narrow spot beams can be generated by satellite antennas which can fit conveniently on a Shuttle launched spacecraft. This allows extensive reuse of the 2.5 GHz wide band.

3) Orbit slot spacing can be reduced below the 3° minimum spacing currently used at Ku band because of the narrow beams achievable with modest earth station antennas; however, the orbital arc is restricted by the requirement to maintain a higher satellite elevation angle at the earth stations than is required at C or Ku band to prevent excessive propagation losses. Nine or ten slots are available to serve the contiguous United States with elevation angles greater than 30°.

4) Rain attenuation of both up and downlink signals is considerably greater at 18/30 GHz than at C and Ku bands. Also, earth station antenna temperatures increase drastically when rain is in the beam.

5) The downlink flux density allowed by WARC at 20 GHz is 33 dB greater than at Ku band and 37 dB greater than at C band. This allows implementation of a very large rain margin relative to the power required for good digital data transmission in clear weather if it is technically and economically advantageous to provide such a margin.

6) A given performance level is more difficult and expensive to achieve at 18/30 GHz than at the lower frequency bands. Performance tends to degrade as the inverse square of the frequency for some important parameters. Also, the maturity of the state of the art in most devices is several years behind that of devices used for C and Ku band.

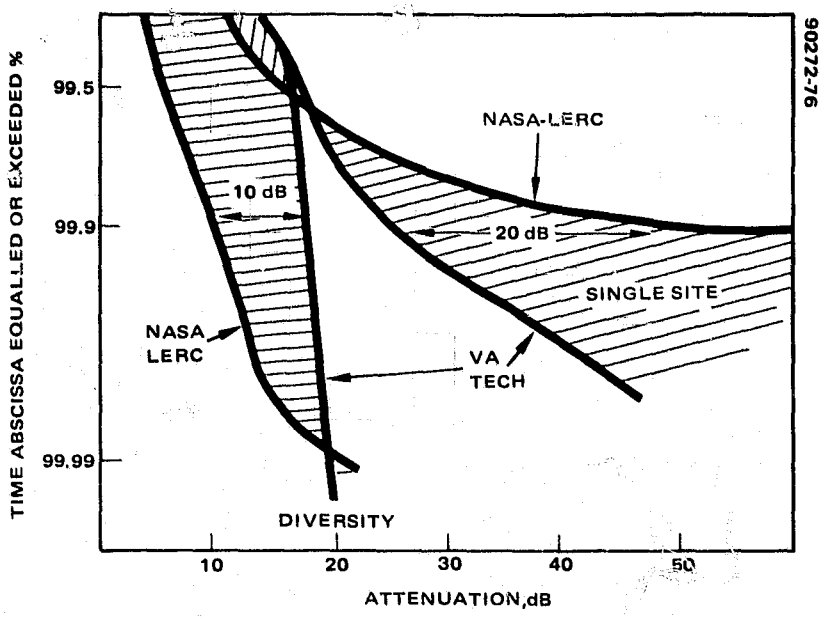

FIGURE 2-1. ATTENUATION STATISTICS COMPARISON – ATLANTA, f = 30 GHz

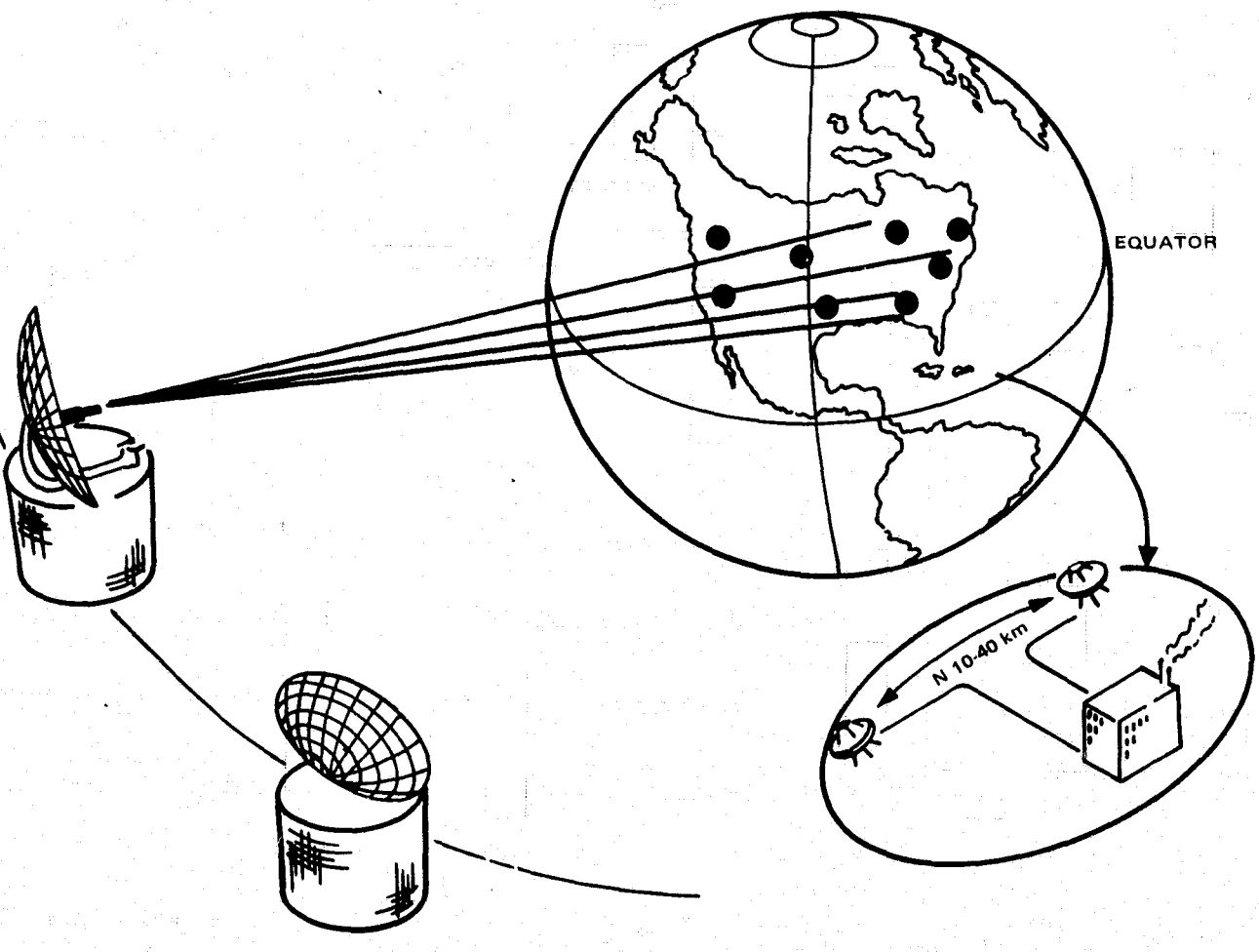

FIGURE 2-2. SATELLITE TRUNK COMMUNICATION SYSTEM

A major objective of this study was to determine how the favorable characteristics of the 18/30 GHz frequency band can be exploited and how the unfavorable characteristics can be overcome.

2.2 RAIN ATTENUATION

The most critical characteristic of the 18/30 GHz frequency band is the rain degradation. At this time there is considerable uncertainty in the statistics of rain attenuation, particularly for terminals using site diversity. Analysis of the data taken from the COMSTAR satellite may provide better definition of the rain statistics for single site terminals in the future; however, little data has been acquired for an analysis of the effect of site diversity.

Rain attenuation statistics at 30 GHz from two predictive models are shown in Figure 2-1. The curves labeled NASA-LeRC are plots of data provided by NASA-Lewis Research Center. The single site NASA-LeRC data is calculated from the model being considered by the International Radio Consultative Committee (CCIR). The diversity curve was obtained by NASA-LeRC by applying a diversity gain factor to the single site data. The other curves are based on a model developed at Virginia Polytechnic Institute. A different approach to diversity gain was taken to generate the diversity curve for this model. Although there is a 20 dB difference between the two single site predictions at a propagation reliability of 99.9 percent, this may not be significant, since even for the more optimistic prediction the rain margin required for 99.9 percent propagation reliability is impractical. The models and their relation to available data are discussed in Appendix B.

The curves of Figure 2-1 are for the 30 GHz uplink band. The curves for the 20 GHz downlink are very similar except that the attenuations expressed in decibels are approximately one-half of those at 30 GHz.

2.3 SYSTEM CONCEPTS

The statement of work (SOW) defines two basic types of satellite communication concepts to be studied: trunk and direct to user.

2.3.1 Trunk Concept

The trunk concept is illustrated in Figure 2-2. In this concept the satellite serves a relatively small number (10 to 40) of heavy traffic centers with individual beams. In each beam there is one terminal which is capable of transmitting and receiving at two sites which are separated by about 15 km, so that the rain degradation of at least one site will be within the rain margin for a very high percentage of the time. Each traffic center has continuous connectivity with each of the other centers. The interconnectivity in the satellite is obtained either through frequency division multiple

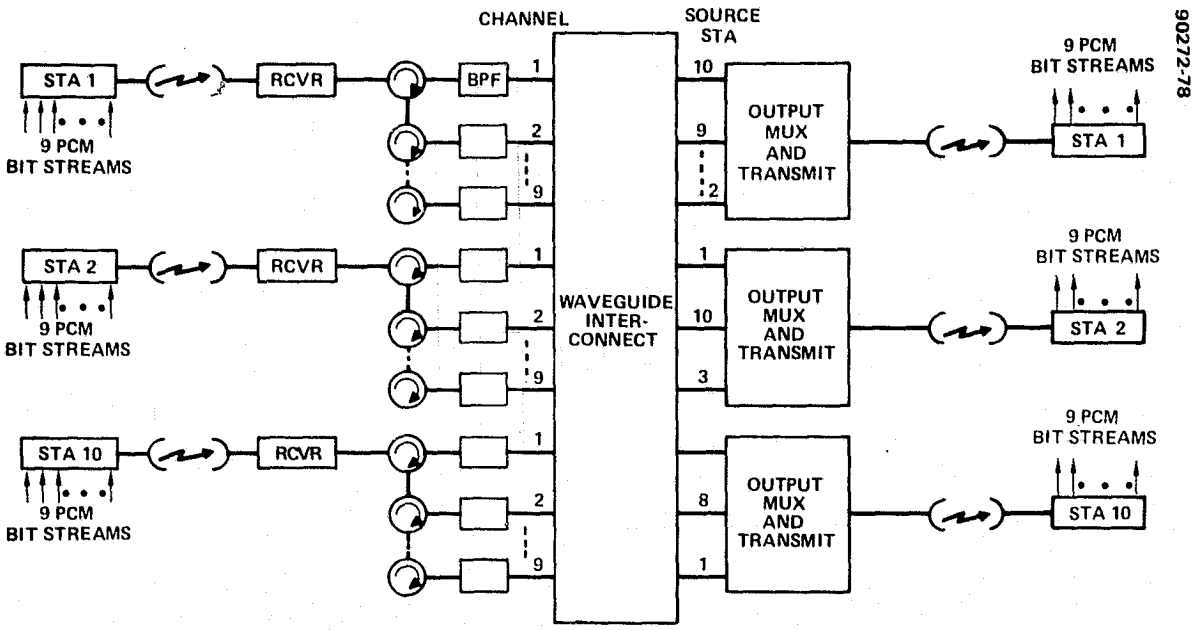

FIGURE 2-3. TEN STATION FDMA TRUNK

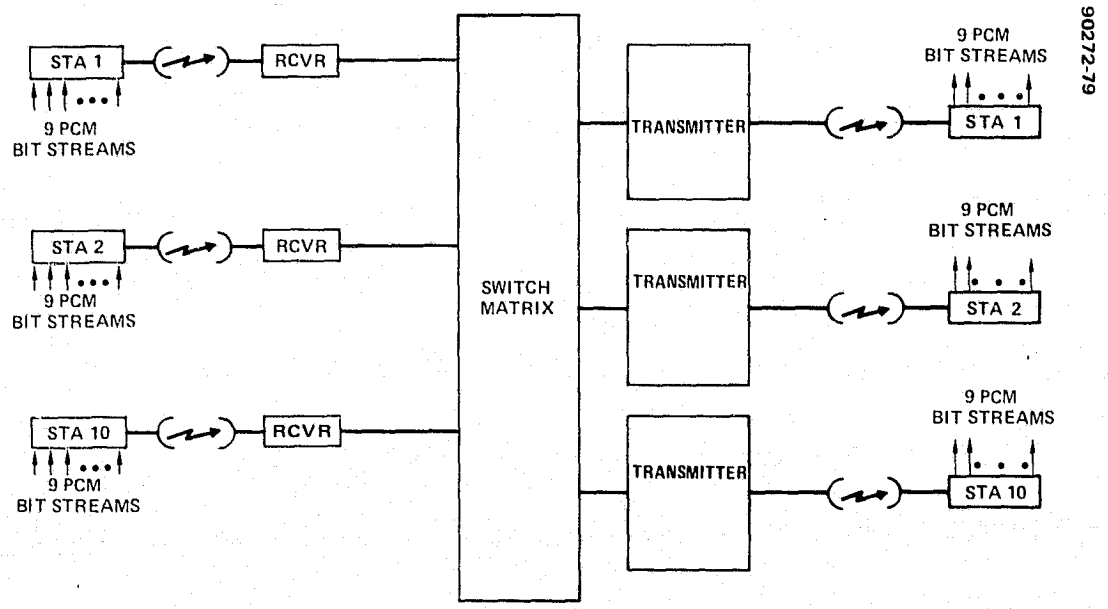

FIGURE 2-4. TEN STATION TDMA TRUNK

access (FDMA) or time division multiple access (TDMA). In an FDMA system the transmitting earth station modulates the data intended for each of the other centers at different carrier frequencies (Figure 2-3). In the TDMA concept the earth station transmits the data for each of the other stations during different time intervals. In both cases the SOW prescribes uniform data rate on all links. Concepts with and without satellite switching were considered. The baseline FDMA concept does not include switching. The addition of switching would allow redistribution of the satellite resources as the traffic demand shifted from link to link during the course of the day. This would eliminate the need to size all links for peak demand, and possibly reduce the cost of the satellite. Because of a lack of data on the variation of demand during the day, it was not possible to determine the value of switching by FDMA systems. The baseline TDMA concept includes satellite switching. A TDMA concept without satellite switching becomes a point to multipoint system. That is, all downlink beams carry the same signal. Then, only one uplink beam can be used at a time, and the frequency spectrum cannot be reused in each beam. Since the traffic is point to point, a TDMA concept without satellite switching does not conserve the spectrum. In addition, it is wasteful of the satellite because all downlink beams radiate continuously, even though only one beam is useful at any time. This would reduce the cost effectiveness of the system. For these reasons, TDMA without satellite switching was not considered. In a TDMA system with satellite switching (SS-TDMA) (Figure 2-4), each station communicates with one and only one other station during a subframe. At the end of the subframe the satellite switch reconfigures so that each station communicates with a different station than it did in the previous subframe. Thus, over a complete frame, each station communicates with each other station. Because the frame duration is a small fraction of a second, it appears to the users that there are continuous links between all stations.

The baseline trunk systems are ten-beam systems. Optimization studies were performed to find the combination of transmitter power, antenna diameter, and receiver type for both the satellite and earth station which minimized the system cost. The satellite carried nearly 25 Gbps of data. The details of the satellite and earth stations for the FDMA and TDMA concepts are described in Section 4.

The cost of the concepts in terms of total investment and investment apportioned to an equivalent 40 MHz transponder and a 64 kbps voice circuit are shown in Table 2-1. These costs include three satellites, three launches, ten dual site terminals (land cost not included) and the diversity links and switches for the terminals, but do not include the terrestrial tails or the central switching offices. Also, it is difficult to translate the investment per transponder or per voice circuit into a tariff because of the uncertainty in the system utilization factor. The very large system capacity is achieved by assuming that each earth terminal used the entire 2.5 GHz spectrum. This is a very unlikely assumption, given the wide disparity in current communications demand between the ten baseline cities.

TABLE 2-1. FDMA-TDMA TRUNK INVESTMENT COST

Item	FDMA		TDMA	
Propagation reliability	99.9%	99.9%	99.99%	99.99%
Total investment, $M	251	273	231	245
Capacity, Gbps	19.4	19.4	22.2**	22.2**
Investment				
$K/40 Mbps channel	518*	562*	374*	397*
$/64 kbps VX circuit	1636*	1801*	1197*	1270*

*Multiply by utilization factor.

**At 90 percent synchronization efficiency.

2.3.2 Direct to User Concept

In the direct to user concept, the satellite serves a large number of stations distributed over the contiguous United States (CONUS), as shown in Figure 2-5. Both multibeam and CONUS beam satellites were defined by the SOW. The advantage of the multibeam satellite antenna is the increased gain associated with the small spot beams. This high gain is critical for the direct to user configuration because the severe rain attenuation associated with single site operation places a great burden on the satellite and earth station resources. In fact, even the 25 beam case studied as a baseline required a very high powered satellite (~10 kW of solar power) to achieve a propagation reliability of 99.5 percent, which was considered minimal by the market study contractors. The use of a low gain CONUS beam antenna made the direct to user concept impractical.

The use of multibeam antennas raises the problem of beam interconnectivity. As in the trunk concepts, interconnectivity can be provided either by FDMA or TDMA; however, the SOW specified that no interconnectivity between beams be provided in the FDMA satellite, but is to be provided through master earth stations in each beam. This results in multihop links, as described in Section 5. In the TDMA concept, interconnectivity of the beams in the satellite is required by the SOW. The baseline TDMA system includes satellite switching as described for the TDMA trunk concept.

The cost of 25 beam direct to user concepts is shown in Table 2-2. The cost shown is for the complete system, since there are no terrestrial tails.

2.4 CRITICAL TECHNOLOGIES

The critical technologies which must be developed to take advantage of the 18 and 30 GHz bands are discussed in Section 7. A major item is the multispot beam antenna, since this element provides the capability for extensive frequency reuse. Also in need of development are the low noise

TABLE 2-2. DIRECT TO USER ANNUAL SERVICE COSTS, $K

Item	Station					
	FDMA			TDMA		
	Small	Medium	Large	Small	Medium	Large
Earth station investment (per station)	277	611	2167	460	580	882
Net earth station revenue (per station)	94	208	736	156	197	300
Revenue required per						
• 64 kbps circuit ($3K)*	16	7.8	6.5	25	7.4	4.4
• 1.5 Mbps circuit ($74K)*	–	134	156	–	180	107
• 6.3 Mbps circuit ($326K)*	–	–	669	–	–	466
	• Not tarrif or lease • Does not account for utilization					

*Share of $398M investment in space segment, TT&C, and master control.

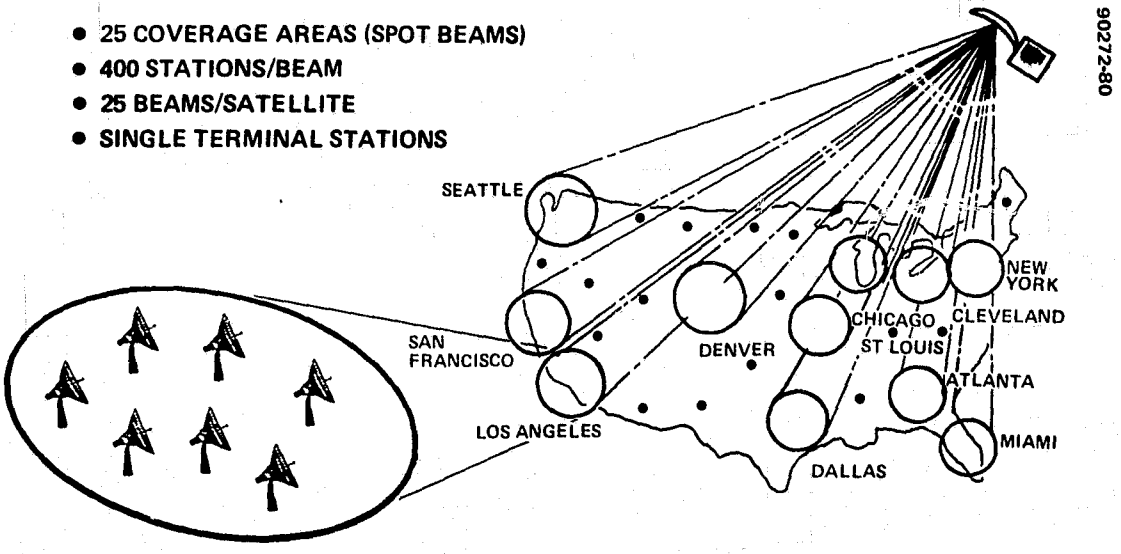

FIGURE 2-5 DIRECT TO USER SYSTEM CONCEPT

and high power amplifiers. The development of these devices in the 18/30 GHz band is several years behind that of the devices for the lower frequencies. Also, for equivalent levels of development, the performance of these devices at 18 and 30 GHz will be inferior to that of the devices used at the lower frequencies.

Although the satellite switch matrices required for SS-TDMA operation do not operate at the carrier frequency, they are more critical to the success of 18 and 30 GHz concepts because of the large number of independent beams which can be generated at these frequencies by a reasonably sized antenna. Although a switch matrix adequate for a 25 beam satellite using the matrix approach can be built with near term technology, the weight and cost of such a matrix becomes impractical as the number of beams increases beyond 25.

3. TECHNOLOGY ASSESSMENT

3.1 EARTH STATION BASEBAND AND MODEMS

3.1.1 Digital and Analog Terrestrial Interfaces

Bell System interfaces are included here (Tables 3-1 and 3-2 and Figures 3-1, 3-2, and 3-3) since they are standard for much of the industry. Representative M13 and M34 costs are shown in Table 3-3. For most of the other interface equipment, costs are readily available and not included here.

TABLE 3-1. STANDARD ANALOG TERRESTRIAL INTERFACES

Channel Type	Bandwidth, kHz	Equivalent VF Channels
Voice frequency	0.200 to 3.400	1
Group	60 to 108	12
Supergroup	312 to 552	60
Mastergroup		
L600, L1 line	60 to 2788	600
U600	564 to 3084	600
U660	312 to 3084	660
Multimaster group		
L3 line	312 to 8284	1860
TD or TH radio BB	60, 312, or 564 to 8284	900 to 1860
Jumbogroup		
L4 line	564 to 17548	3600
Multijumbogroup		
L5 line	3124 to 60556	10800
NTSC-TV	6000	N/A

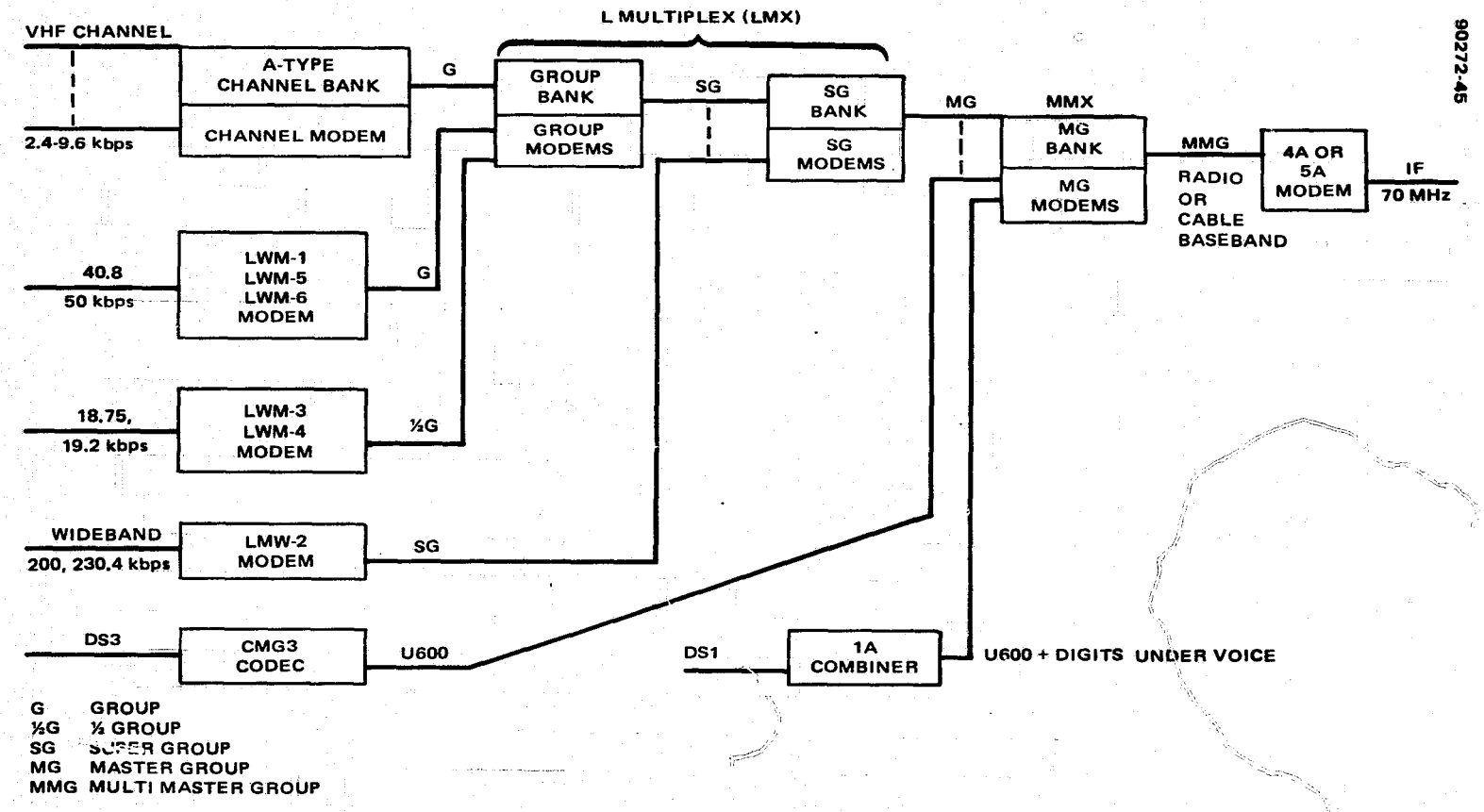

FIGURE 3-1. BELL SYSTEM ANALOG TERRESTRIAL INTERFACES

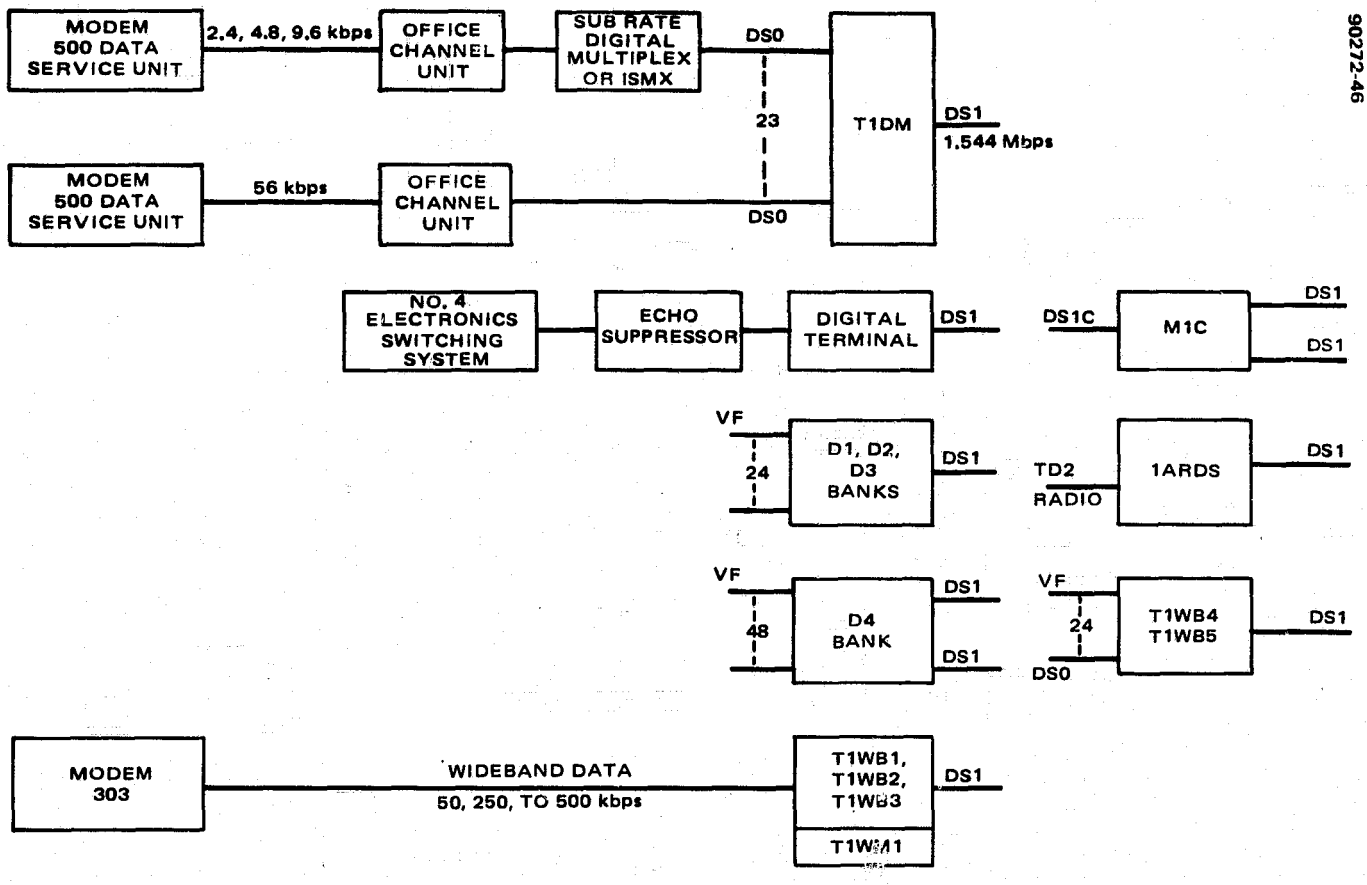

FIGURE 3-2. BELL SYSTEM DS1 DIGITAL TERRESTRIAL INTERFACES

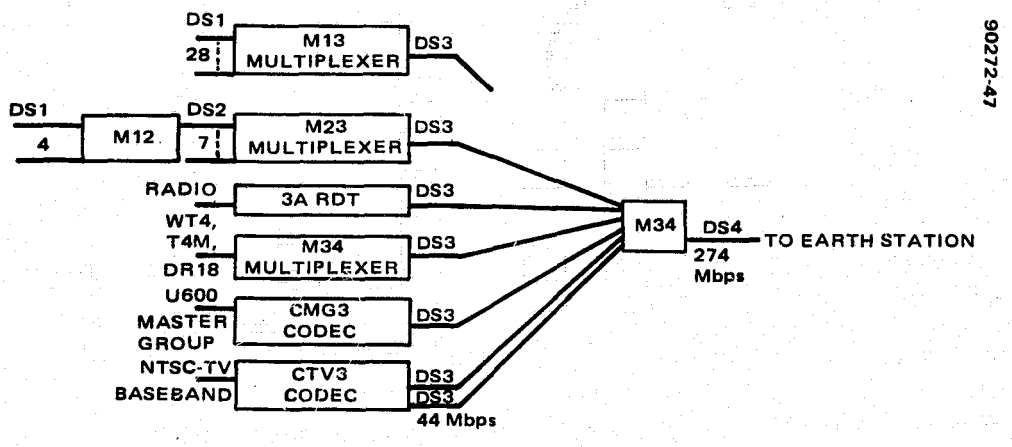

FIGURE 3-3. BELL SYSTEM DS3 AND DS4 DIGITAL TERRESTRIAL INTERFACES

TABLE 3-2. STANDARD DIGITAL TERRESTRIAL INTERFACES

Signal Level	Bit Rate, Mbps	Line Signal	PCM Voice Channels, TDM
DS0	0.064	Three level bipolar	1
DS1 (digroup)	1.544	Three level bipolar, ±6V	24
DS1C	3.152	Three level duobinary	48
DS2	6.312	Three level, B6ZS	96
DS3	44.736	Three level, B3ZS, ±1.5 to ±3V	672
DS4	274.176	Polar binary, NRZ, ±1.25V	4032

TABLE 3-3. M13 AND M34 DIGITAL MULTIPLEX COST ESTIMATES

Manufacturer	Unit Cost, $*
M13:	
Farinon M1-3	36, 522
Raytheon RDM428	25,750 (28 T1 lines)
	48,450 (56 T1 lines)
Rockwell International DMX-13C	62,000 (56 T1 lines)
M34:	
WECO M34	160,000 (6 DS3 channels)

*All units protected

3.1.2 Modulation - Demodulation

A partial list of baseband digital modems for satellite application is given in Table 3-4. Several manufacturers contacted (DCC, Fujitsu, Harris, Motorola, NEC, and TRW) are designing 250 Mbps, TDMA burst modems for SBS and advanced WESTAR, using QPSK modulation and 750 μsec frame lengths. NEC, Hughes, DCC, and others have built experimental modems in the 1 to 4 Gbps range. No existing modems meet the requirements of the 18/30 GHz satellite trunking terminals, which must handle up to nine of the DS-4 level PCM channels (274 Mbps polar signals). Also, no baseband multiplexer capable of combining DS-4 signals is available.

Since high speed multiplexers or wideband, high speed modems are not available at the bit rates of interest, projected costs must be estimated by performing a preliminary design or by extrapolating available units (the approach used here). For the latter case, prices are indicated in Table 3-5.

TABLE 3-4. DIGITAL MODEMS FOR SATELLITE COMMUNICATIONS

Manufacturer	Baseband Data Rate	IF Frequency	Modulation Technique	TDMA Frame, μsec	Burst Mode	CW Mode	Price, $
American Modem Corp.							
Model 1440	To 230 kbps	52 to 88 MHz	BPSK			X	
Model 1460	56 kbps	52 to 88 MHz	QPSK			X	
Digital Communications Corp.(Reference 1)							
Model 1003	(28) T1	70 MHz	QPSK	750	X		300,000*
Model 4007	32 kbps to 10 Mbps	52 to 88 MHz	QPSK		X		
Model 4011	64 kbps	52 to 88 MHz	QPSK		X		
Marconi Electronics							
P3700	240 Mbps	140 MHz	QPSK		X	X	
Multirate	9.6 kbps to 2 Mbps	70 MHz	BPSK/QPSK			X	
NTT (Reference 2)							
TDMA-100M	106.88 Mbps	1.7 GHz	QPSK		X		
TRW (Reference 3)	250 Mbps		QPSK	750	X		30,000

*Price includes modem, multiplexing, and TDMA equipment.

TABLE 3-5. QPSK BURST MODEMS

Modem	Data Rate, Mbps	Cost, $	Reference
Marconi Electronics P3700	240	120,000	4
Motorola (NASA-TDRSS, demodulator only)	Variable to 600	100,000	
TRW (advanced WESTAR)	250	30,000	5

3.1.2.1 Multiplex/Demultiplex

To minimize costly high speed logic, the WECO M34 was designed to utilize 2-ns emitter coupled logic (ECL) for 96 percent of the logic and expensive sub-ns ECL logic for the remaining 4 percent (Reference 1). Two stages of multiplexing were employed. An analogous design for an M4X multiplexer/demultiplexer (muldem) to interface nine DS-4 channels to one DS-X channel at 2.5 Gbps is shown in Figure 3-4.

The M4X cost can be roughly estimated from the M34 cost by appropriate scaling. There are nine low speed inputs rather than the six for the M34. The price ratio of sub-ns to 2-ns ECL varies from 5:1 to 17:1, as shown in Table 3-6. However, when the price of a complete subsystem is considered

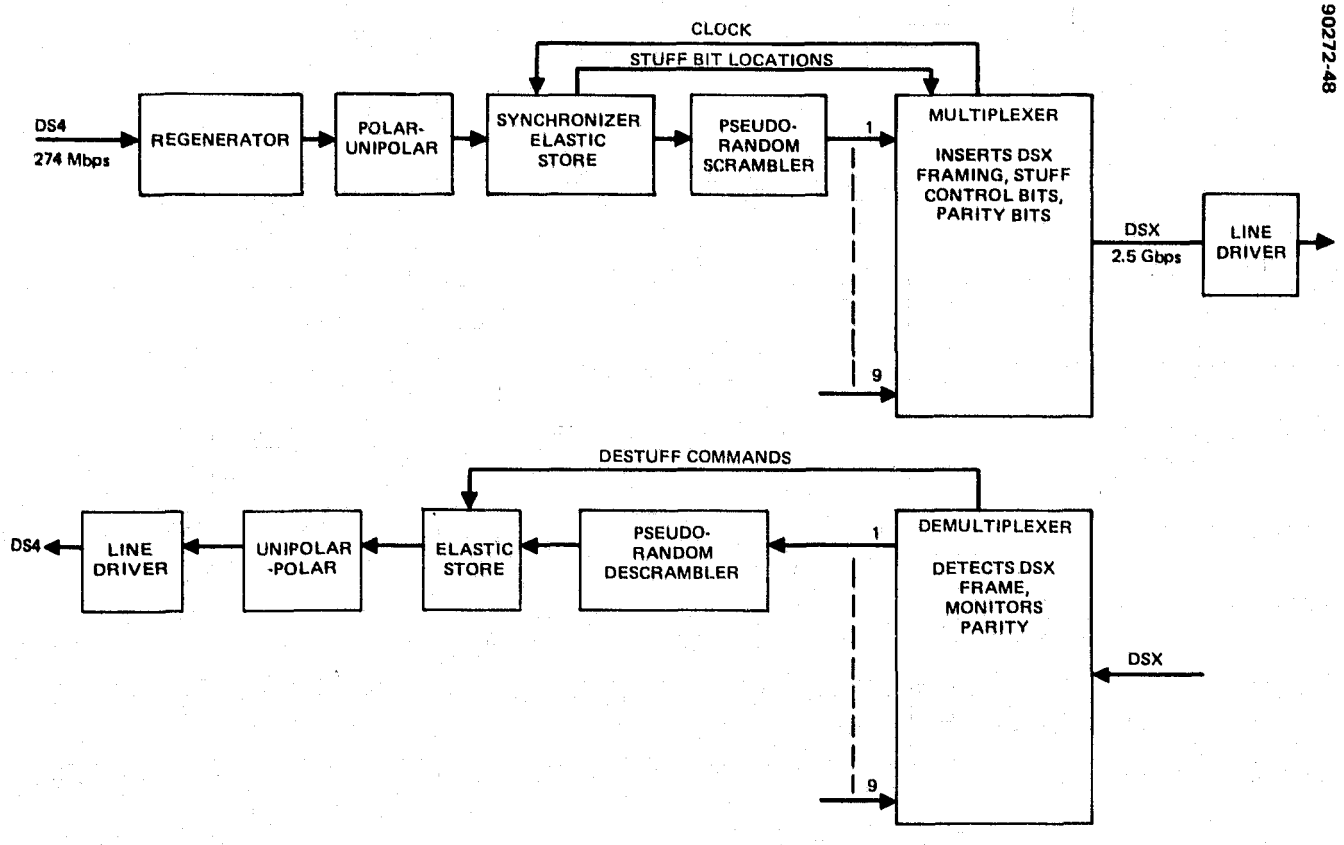

FIGURE 3-4. M4X MULDEM DESIGN FOR SATELLITE TRUNKING TERMINAL

TABLE 3-6. HIGH-SPEED LOGIC PRICE COMPARISON*

Integrated Circuit	Gate Propagation Delay	
	2-ns Series, $	Sub-ns Series, $
Four-bit counter	3.95	43.20
Quad NOR gate	0.45	7.50
Flip-flop	2.95	14.90
Four-bit shift register	7.41	43.20
Dual four-input gate	0.45	7.50
Quad line receiver	0.45	7.50
Subsystem		
Variable delay unit (same number delay bits for comparison)	311.00	859.00

*Based on 1978 100-unit prices for Motorola 10,000 series and 1600 series ECL

(PC board, IC chips, connectors, associated low speed logic, etc.), the ratio is less. For the variable delay unit, as an example, the price ratio between sub-ns and 2-ns logic implementation is 2.76:1, if the number of bits of delay is held fixed. For the present analysis, this ratio will be considered typical. Assume that 96 percent of the M4X logic can be made from sub-ns ECL and only 4 percent requires the custom GaAs devices (the same ratio between high speed and low speed ECL as in the M34). Also assume the price ratio of the custom GaAs devices to the sub-ns ECL is the same as for the sub-ns ECL to 2-ns ECL. Then

$$\frac{\text{M4X price}}{\text{M34 price}} = (2.76)\,(9/6) = 4$$

so the estimated M4X price is

$$4 \times 160,000 = \$640,000.$$

3.1.2.2 Modem Cost Estimate

The 2.5 Gbps (DS-X level) PCM bit stream from the M4X muldem can be used to directly modulate (QPSK) the 30 GHz carrier or an IF signal. Similarly, the 18 GHz input can be downconverted and demodulated or directly demodulated (using recent MIC technology). In either case, the basic elements of the modem illustrated in Figure 3-5 are required. For a continuous (non-burst) system, the dashed boxes (compression/expansion buffers which provide guard intervals, preamble generator/detector, burst synchronizer, and TDMA controls) are not required.

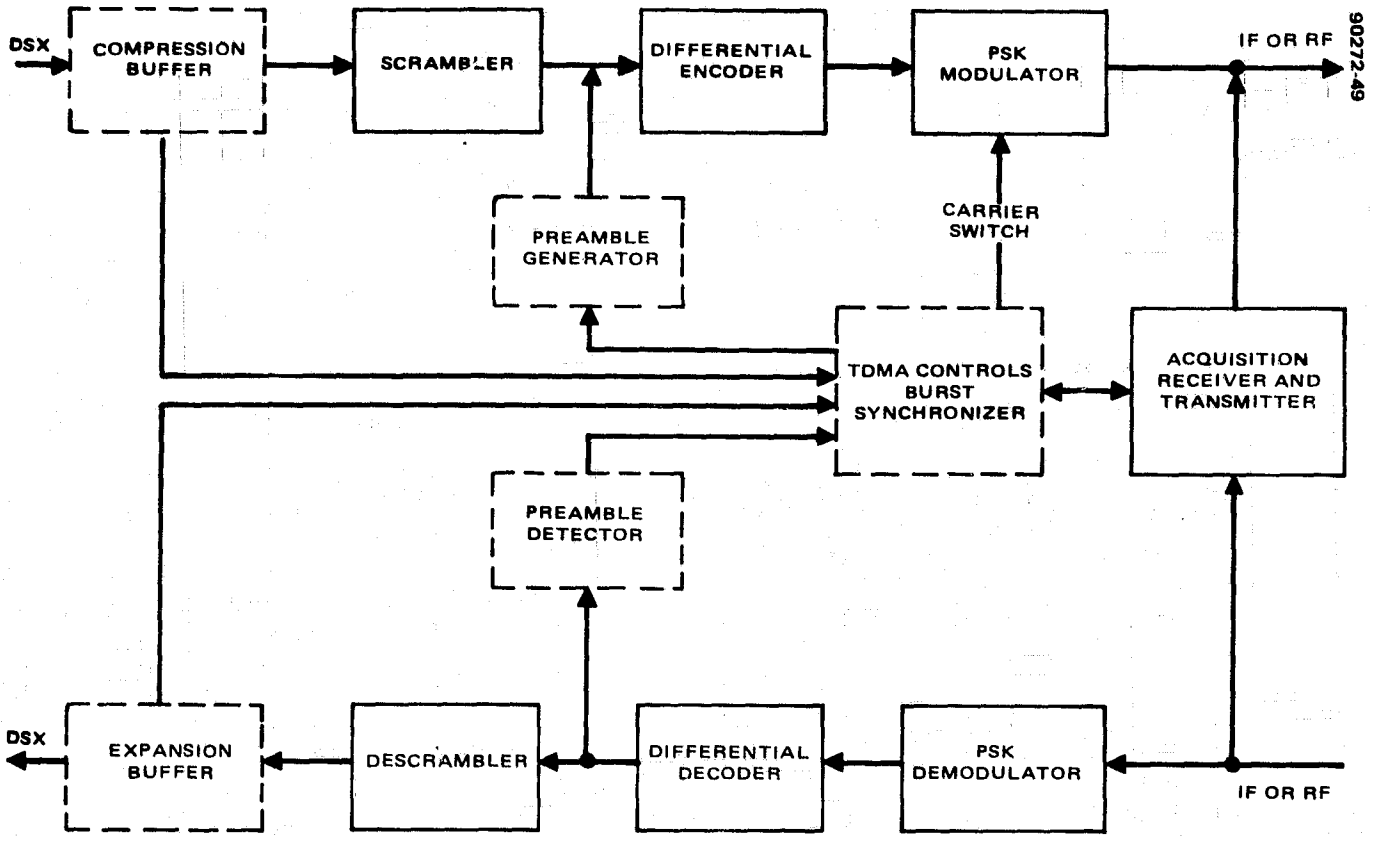

FIGURE 3-5. HIGH SPEED BURST MODEM FOR SATELLITE TRUNKING TERMINAL

Experimental modems capable of 2.5 Gbps have been described in the literature. (References 6 and 7.) One method for minimizing the amount of high speed circuitry is the use of QASK modulation instead of QPSK, (Reference 7). A large amplitude and a small amplitude QPSK signal are combined to obtain a 16-level APSK signal. This provides twice the data rate without a bandwidth increase when compared with QPSK, but at 4 dB less power.

From Table 3-5 it can be seen that burst modems capable of handling 1 or 2 DS4 channels are in the $120,000 price range. Continuous-carrier QPSK modems are less expensive, but no firm prices could be obtained. A lower limit is an unofficial price of $30,000 for the 250 Mbps QPSK modulator/demodulator modules alone. These involve high speed ECL technology. If it is assumed that (see Figure 3-6) the buffers and scramblers are implemented in parallel on the DS4 channels and that only a few high speed GaAs FET devices are required, then crude estimates for the modem costs are obtained by scaling.

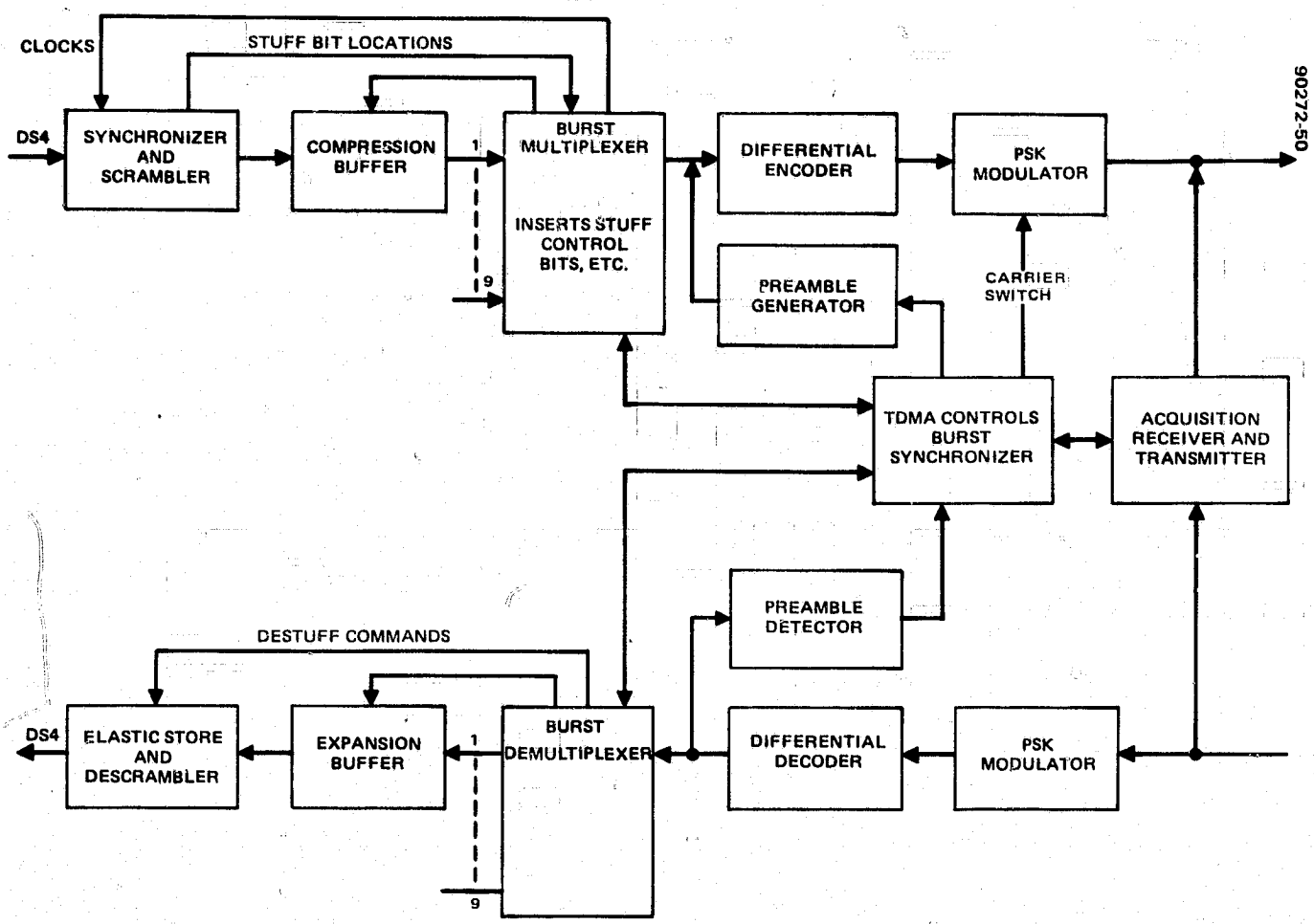

FIGURE 3-6. COMBINATION BURST MODEM/MULDEM FOR SATELLITE TRUNKING TERMINAL

$$\text{DSX burst modem cost} \approx 9(\$120,000) + C$$

$$\text{DSX CW modem cost} \approx 9(\$30,000) + C$$

where C is the cost of the GaAs FETs and custom design high speed circuitry. A value of $150,000 for C seems reasonable, based on development costs for 10 terminals.

3.1.2.3 Technology Assessment

Standard MSI and LSI logic families are available (Fairchild F100K ECL and Motorola MECL III lines with subnanosecond gate-propagation-delays) for multiplexing and modulation of PCM bit streams to 500 or 600 Mbps. Muldems and modems for processing higher bit rates must rely on devices such as the GaAs MESFET, MOSFET, and TED. Some of these will be available by 1980 on a custom basis in SSI or MSI (References 8, 9, and 10).

In the future, there is also the possibility of using integrated-optic and acousto-optic devices for gigabit speeds. Digital muldems using mode-locked injection lasers with traveling wave electro-optic switches and optical waveguide modulators are feasible as integrated circuits (Reference 11).

3.2 SPACE DIVERSITY SYSTEM DESIGN AND COST

The cost of the space diversity system required to minimize rain fades has been estimated by pricing available products and by making preliminary designs of the subsystems which are not off the shelf.

Figure 3-7 indicates the overall diversity arrangement. The alternate earth stations are separated by 10 to 20 miles from the regular stations. An auxiliary channel is required for proper operation. The transmit switches prevent both stations, such as A and B, from transmitting simultaneously, which

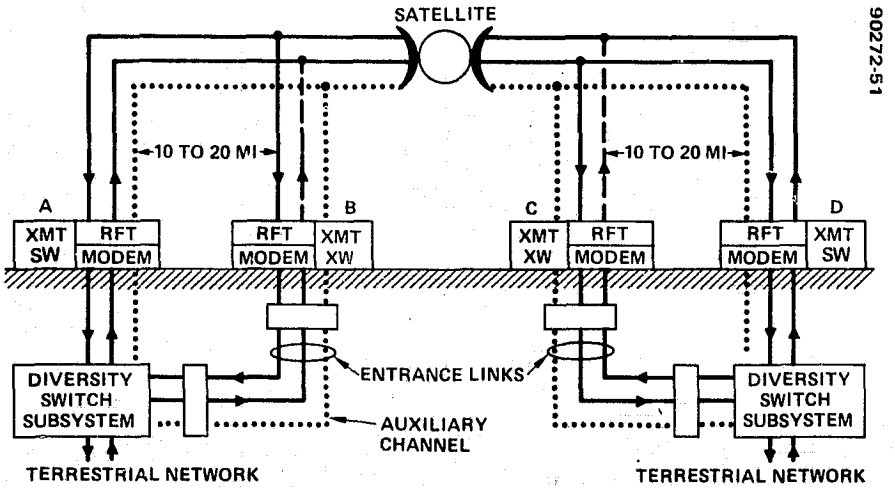

FIGURE 3-7. ALTERNATE EARTH TERMINALS MINIMIZE RAIN FADES

would garble the communications. As an example, suppose that the transmission from A has faded but reception at A is still acceptable; D will detect the fade at both D and C, so it will notify A to switch to B.

Table 3-7 indicates alternatives for the diversity link between the regular and alternate earth stations. For light density traffic, including spur feeders, Farinon introduced its version of the DR18, designated the DM18, in 1979.* For the 1980-85 period, several manufacturers (including Farinon) are planning on digital radio systems with 120 to 137 Mbps in a 40 MHz channel. Only the terrestrial 6 and 11 GHz microwave and fiberguide alternatives are analyzed in this section. The fiberoptic data are from Harris, although by 1980 several others including Rockwell will be offering complete systems. The combinations of most interest are baseband diversity switching at the DS3 (Figure 3-8) or at the DS4 (Figure 3-9) levels. The relative costs are shown in Figure 3-10.

TABLE 3-7. DIVERSITY LINK BETWEEN REDUNDANT GROUND STATIONS

System	Nominal Repeater Spacing, mi.	RF Band, GHz	Capacity of One-Way System-Channel* (Bandwidth, Bit Rate Equivalent VF Channel)	Number of Two-Way System-Channels (Working ÷ Protection)	Number of Two-Way Equivalent VF Channels per System
Microwave radio, WECo DR18 (QPSK, dual polarization)	2 to 5	17.7 to 19.7	220 MHz 274.176 Mbps 4032 channels	7/1	28,224
Microwave radio, WECo 3A-RDS (QPSK, dual polarization)	13 to 20	10.7 to 11.7	40 MHz 44.736 Mbps 672 channels	20/2 (400H protection switch)	13,440
Microwave radio, Rockwell MDR-6 (8 PSK, dual polarization)	15 to 25	5.925 to 6.425	30 MHz 2 x 44.736 Mbps 1344 channels	10/1 (MDS-10 protection switch)	13,440
Digital coaxial cable, WECo T4M	1.15	–	274.176 Mbps 4032 channels	9/1	36,288
MM waveguide, WECo WT4 (two level)	25	40 to 110	525 MHz 274.176 Mbps 4032 channels	59/3	237,888
Optical fiber	3 to 4	–	274.176 to 548.352 Mbps 4032 to 8064 channels	9/1	36,288 to 72,576
Microwave radio, Rockwell MDR-11 (8 PSK)	15 to 25	10.7 to 11.7	40 MHz 90.258 Mbps (2XDS3) 1344 channels	10/1	13,440

*RF channel, coaxial tube, fiber

*Telephone Engineer and Management, April 15, 1979, pp 100-104.

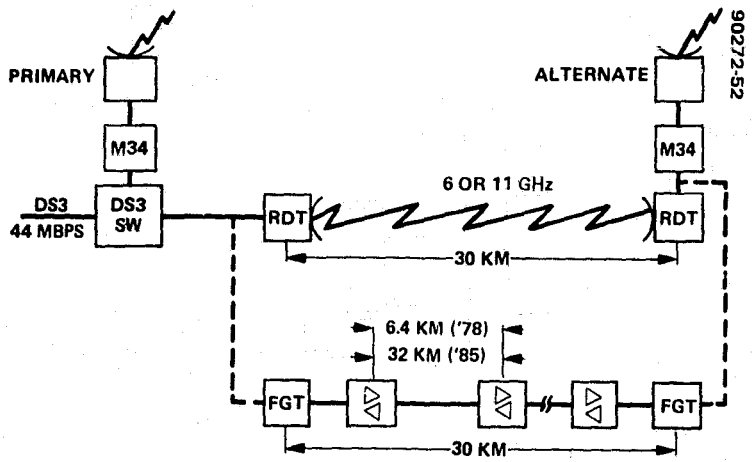

FIGURE 3-8. DS3 DIVERSITY SWITCHING OPTIONS

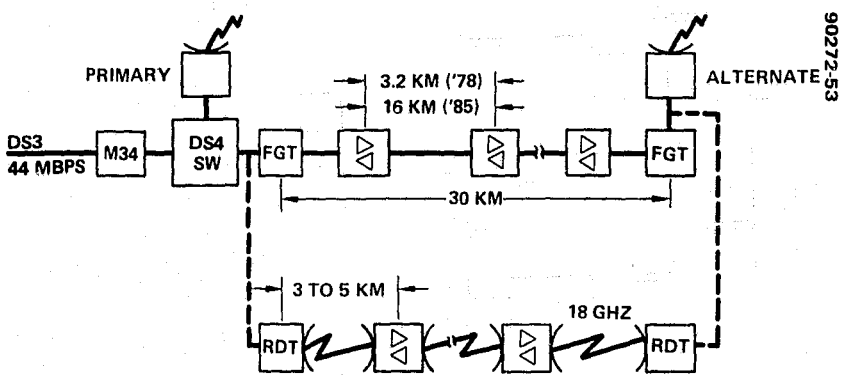

FIGURE 3-9. DS4 DIVERSITY SWITCHING OPTIONS

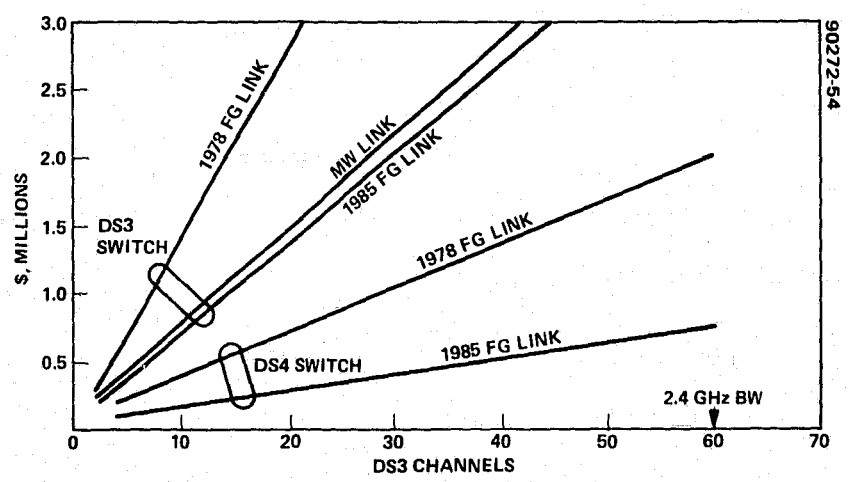

FIGURE 3-10. SPACE DIVERSITY INTERCONNECT COST

Evidently, it is preferable to switch at DS4 and use fiberoptic interlinks. The fiberoptic costs are based on the assumption that the conduit and manholes provided by Telco are shared with other services. The use of 90 Mbps (two DS3) radio channels suffers the disadvantage of requiring M34 multiplexers at both the regular and alternate earth stations.

The material costs used in this section can be converted to installed costs by using a 1.5 factor which is typical for such systems. Annual charges can be estimated by using 25 percent (outside plant) or 33 percent (central office) of the installed costs.

The variable time delay and frame detection units are not available off the shelf. The cost was estimated using ECL III logic for the high speeds.

The M13 and M34 cost data are summarized in Table 3-3. The cost formulas used to derive Figure 3-10 are given in Table 3-8 for the most significant options. Figures 3-11 through 3-14 and Tables 3-9 through 3-19 give the detailed steps used to derive the cost formulas from circuit diagrams and component costs.

TABLE 3-8. SPACE DIVERSITY SYSTEM COST

Option: DS3 switch with microwave link (see Tables 3-9 and 3-18)

Cost = $\$60{,}000 + \$43{,}000\ N_3 + \$160{,}000\ M_{34}$

Where N_3 = number of DS3 channels

M_{34} = number of M34 multiplexes

Option: DS4 switch with fiberguide link (see Tables 3-10 and 3-16)

Cost = $\$22{,}000 + \begin{cases} \$190{,}000\ N_4 \text{ (1978)} \\ \$\ 70{,}000\ N_4 \text{ (1985)} \end{cases}$

Where N_4 = number of DS4 channels

TABLE 3-9. 44 Mbps DIVERSITY SWITCH SUBSYSTEM COST ESTIMATE

Module	Unit Price, $	Required Quantity	Cost for N DS3 Channels
Variable delay unit	1,870	2N	$ 3,740N
Transmit switch	100	2M	200M
Rockwell MDS-10			
Common equipment	12,250	1	12,250
Per channel equipment	1,875	N	1,875N
Rockwell MCS-11			
Master unit	6,000	1	6,000
Remote unit	3,400	1	3,400
Total			$21,650 + $5,615N + $200M

Note: M = N/6 rounded up to nearest integer

TABLE 3-10. 300 Mbps DIVERSITY SWITCH SUBSYSTEM COST ESTIMATE

Module	Unit Price, $[1]	Required Quantity	Cost for N DS4 Channels
VDU	9,450	2N	$18,900N ($25,740N)[2]
FDU	2,535	4N	10,140N
SLU	805	N	805N
Transmit switch	100	2N	200N
Rockwell MDS-10[3]			
Common equipment	12,250	1	12,250
Per channel equipment	1,875	N	1,875N
Rockwell MCS-11 (Aux channel telemetry)			
Master unit	6,000	1	6,000
Remote unit	3,400	1	3,400
Total			$31,920N + $21,650

1. For estimated prices, the component costs were multiplied by 6
2. Figures in parentheses correspond to 600 Mbps data rate
3. Used to estimate cost of components not affected by high speed data (MDS-10 operates on two DS-3 signals)

TABLE 3-11. VARIABLE DELAY UNIT(DDU)

DS3 VDU (44 Mbps)
- 4K bits delay
- ECL/bipolar logic
- $1900 cost

DS4 VDU (274 Mbps)
- 32K bits delay
- ECL III/ECL logic
- $9500 cost

TABLE 3-12. 44 Mbps VARIABLE DELAY UNIT PARTS COST ESTIMATE

Module	Motorola Code	Unit Cost, $			Quantity	Total Costs, $	
		1 to 24	24 to 99	100 to 999		1 to 24	100 to 999
Four-bit counter	MC10178	4.94	4.54	3.95	8	39.52	31.60
Quad NOR gate	MC10101L	0.56	0.52	0.45	4	2.24	1.80
JK flip-flop	MC10135L	3.69	3.39	2.95	4	14.76	11.80
Four-bit shift register	MC10141L	9.26	8.52	7.41	4	37.04	29.64
Quad 2-input and gate	MC10104L	0.56	0.52	0.45	1	0.56	0.45
Quad line receiver	MC10115L	0.56	0.52	0.45	1	0.56	0.45
Quad latch	MC10153	3.66	3.37	2.93	3	10.98	8.79
1K RAM	MCM10146	19.50	17.95	15.60	8	156.00	124.80
Subtotal					33	261.66	209.33
Two-sided PCB		@ $0.40/in^2			60 in^2		24
Dip sockets		@ $1.00			33		33
Connectors							20
Control logic (misc. chips)							25
Total							311.33

Note: 1. Fairchild or Motorola ECL logic
2. Up to 4K bits delay

TABLE 3-13. 300 Mbps VARIABLE DELAY UNIT PARTS COST ESTIMATE

Module	Motorola Code	Unit Cost, $			Quantity	Total Costs, $	
		1 to 24	24 to 99	100 to 999		1 to 24	100 to 999
Four-bit counter	MC1654L	64.80	54	43.20	2	129.6	86.4
Quad NOR gate	MC1662L	11.25	9.40	7.50	4	45	30
RS flip-flop	MC1666L	22.35	18.60	14.90	4	89.4	59.6
Four-bit shift register	MC1694L	64.80	54	43.20	16	1,036.8	691.2
Dual gate	MC1660L	11.15	9.40	7.50	1	11.25	7.5
Quad receiver	MC1692L	11.15	9.40	7.50	1	11.25	7.5
Four-bit counter	MC10178L	4.94	4.54	3.95	6	29.64	23.7
Quad latch	MC10153L	3.66	3.37	2.93	3	10.98	8.79
1K RAM	MCM10146L	19.50	17.95	15.60	32	624	499.20
Subtotal					69	1,987.92	1,413.89
Two-sided PCB (drilled, etched)		@ $0.40/in^2			120 in^2		48
Dip sockets		@ $1.00			69		69
Connectors							20
Control logic (misc. chips)							25
Total							1,575

Note: 1. Fairchild or Motorola ECL III logic
2. Up to 32K bits delay
3. Add $570 to total for up to 64K bit delay

TABLE 3-14. SYNCHRONIZATION UNIT PARTS COST ESTIMATE

Module	Motorola Code	Unit Cost, $			Quantity	Total Costs, $	
		1 to 24	24 to 99	100 to 999		1 to 24	100 to 999
Triple 2-input OR gate	MC1672	11.25	9.40	7.50	1	11.25	7.50
Quad line receiver	MC1692	11.25	9.40	7.50	1	11.25	7.50
Four-bit counter (÷16)	MC1654	64.80	54	43.20	2	129.60	86.40
Subtotal					4	152.10	101.40
Control logic (misc. chips)							25
Two-sided PCB			@ $0.40/in^2		10		4
Dip sockets			@ $1		4		4
Total							134.40

Note: Fairchild or Motorola ECL III logic

TABLE 3-15. FRAME DETECTOR UNIT PARTS COST ESTIMATE

Module	Motorola Code	Unit Cost, $			Quantity	Total Costs, $	
		1 to 24	24 to 99	100 to 999		1 to 24	100 to 999
Four-bit shift register	MC1694	64.80	54	43.20	4	259.2	172.8
Dual 4-input AND gate	MC1660	11.25	9.40	7.50	3	33.75	22.5
Triple 2-input OR gate	MC1672	11.25	9.40	7.50	6	67.50	45
Four-bit latch	MC10153	3.66	3.37	2.93	4	14.64	11.72
RS flip-flop	MC1666	22.35	18.60	14.90	1	22.35	14.90
Quad receiver	MC1692	11.25	9.40	7.50	1	11.25	7.50
Four-bit counter	MC1654	64.80	54	43.20	1	64.80	43.20
Subtotal						473.49	317.62
Decision logic (misc. chips)							25
Dip sockets					20		20
Connectors							20
Two-sided PCB (drilled, etched)			@ $0.40/in^2		100 in^2		40
Total							422.62

TABLE 3-16. FIBERGUIDE DIVERSITY LINK COST ESTIMATE

Module	Unit Cost, $		Required Quantity	Cost for N DS4 Channels, $	
	1978	1985		1978	1985
Terminal	8,500	2,500	2 N	17,000 N	5,000 N
Repeater	8,500	2,500	9 N (N)	76,500 N	2,500 N
Fiber-PR	2/meter	1/meter	30 N KM	60,000 N	30,000 N
Repeater apparatus case (per repeater)	25		9 N (N)	225 N	25 N
Conduit and manhole (per fiber-PR)	10/KM		30 N KM	300 N	
Connectors	25	10	40 N (8N)	1,000 N	80 N
Total				155,000 N	(38,000 N)

TABLE 3-17. FIBERGUIDE COST ESTIMATE

	Price Estimates, $		
	1978	1980	1985
Harris Corp.			
Terminal (T/R)	8,500	5,000	2,500
Line repeater (two regenerators)	8,500	5,000	2,500
Siecor Optical Cables			
10-F (premium, 6 dB/Km, 400 MHz-Km, 10 fibers)	20.80/m		10 m
Connectors (per fiber-end)	10 to 50		10

1. Repeater spacing for DS3 rate: 6.4 km (1978), 32 km (1985)
2. Polar binary PCM modulation
3. Rates to 300 Mbps (1978)
4. Repeater spacing for DS4 rate: 3.2 km (1978), 16 km (1985)

TABLE 3-18. MICROWAVE DIVERSITY LINK COST ESTIMATE

Item	Unit Cost, $	Required Quantity	Total Cost of N DS3 Channels, $
Radio terminal (two DS3)	37,300	N	37,300 N
Tri-Ex Tower Corp.			
TKD 40-3 (40 ft)	1,980	1	1,980
TKD 100-6 (100 ft)	7,615	1	7,615
Andrew Cal, Corp.			
200 ft elliptical waveguide and connector			
11 GHz	1,840	1	1,840
6 GHz	2,396	1	2,396
Auto. dehydrator			
1930 B	750	2	1,500
Dual-polarization antenna			
6 ft diam	4,800		
8 ft diam	5,800	4	23,200
10 ft diam	7,100		
Total			$38,531 + $37,300 N

1. A maximum of 20 DS3 duplex channels can be accommodated in each of the 6 GHz and 11 GHz bands
2. Two antennas are needed at each station to avoid multipath fades

TABLE 3-19. DIGITAL MICROWAVE RADIO TERMINAL COST ESTIMATE

Manufacturers Code	Price for Two DS3 Channels, $
Raytheon Model 8410 (11 GHz, 8 PSK, 40 MHz/channel)	37,300 (SDP)
Raytheon Model 6200 (6 GHz, 8 PSK, 30 MHz/channel)	38,000 (SDP)
Rockwell MDR-11-5 (11 GHz, 8 PSK)	46-53,000 (HS)
Rockwell MDR-6 (6 GHz, 8 PSK)	45-52,000 (HS)
Farinon DM11-2A (11 GHz, QPSK, 40 MHz)	55,790 (SDP)
Farinon DM6-2A (6 GHz, QPSK, 30 MHz)	55,790 (SDP)

1. Allocated bands are 10.7 to 11.7 GHz or 5.9 to 6.5 GHz
2. Assume link is one hop (no repeater stations)
3. Radio terminals include space diversity protection (SDP) or hot-standby (HS) and TWT output stage
4. RDT includes radio and modulation equipment

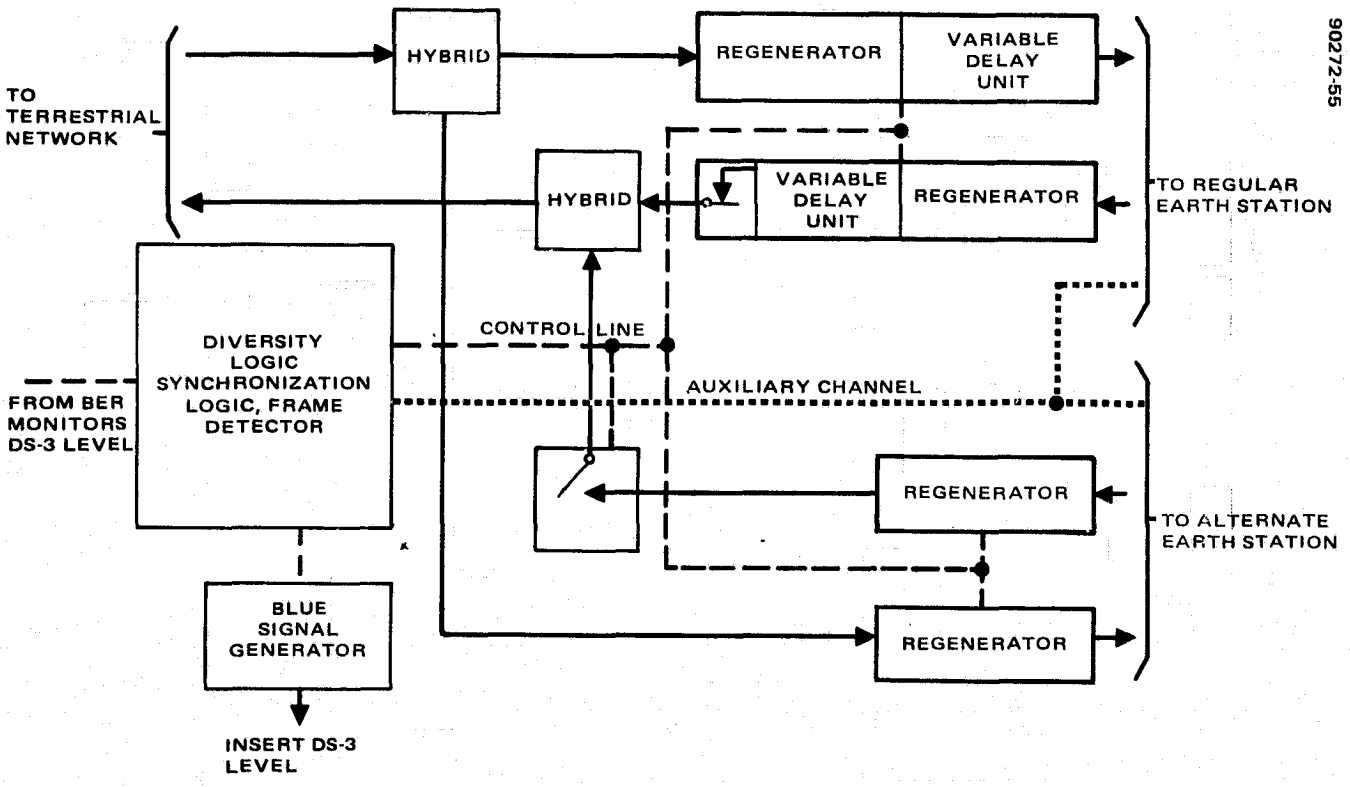

FIGURE 3-11. AUTOMATIC DIVERSITY SWITCH SUBSYSTEM

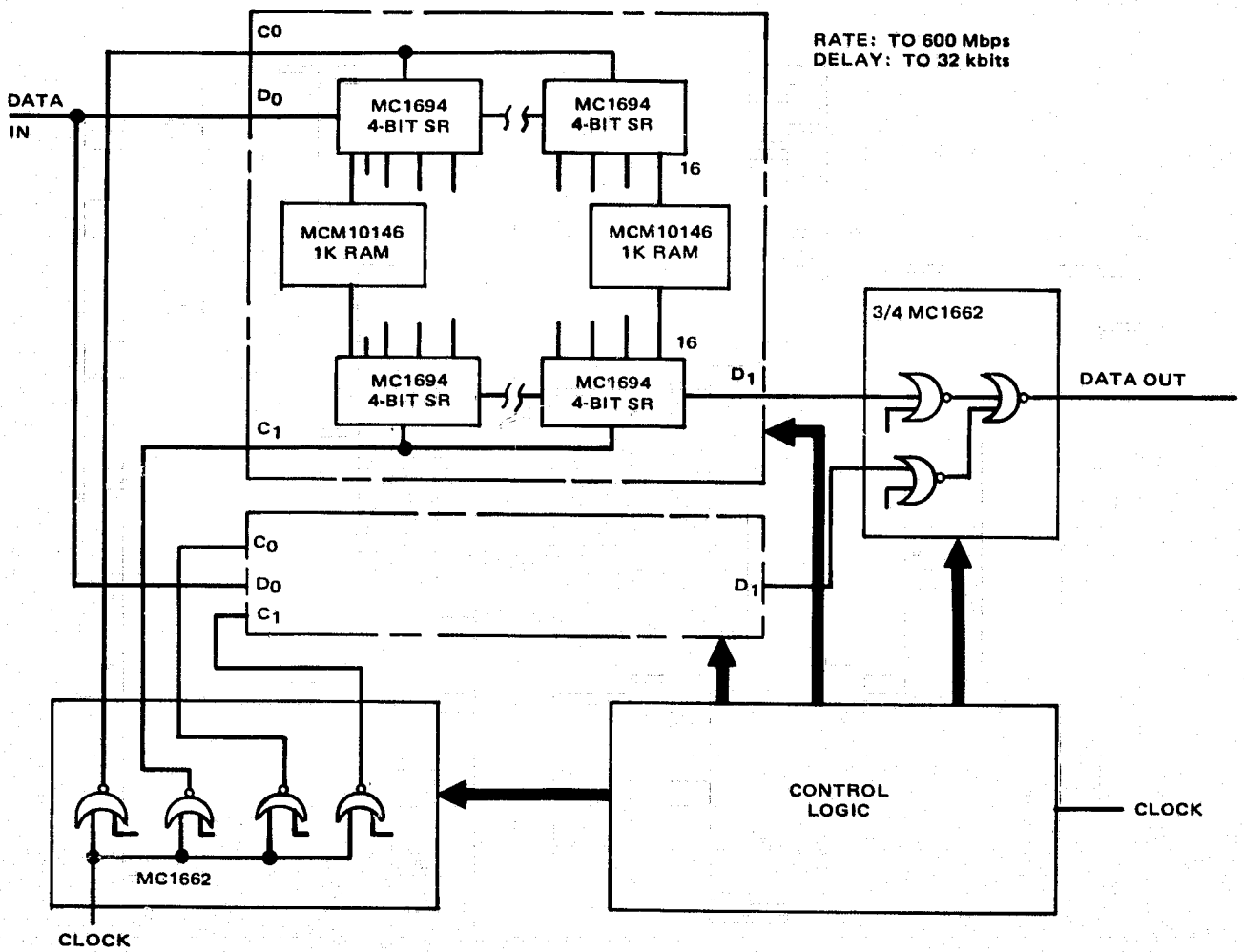

FIGURE 3-12. VARIABLE DELAY UNIT

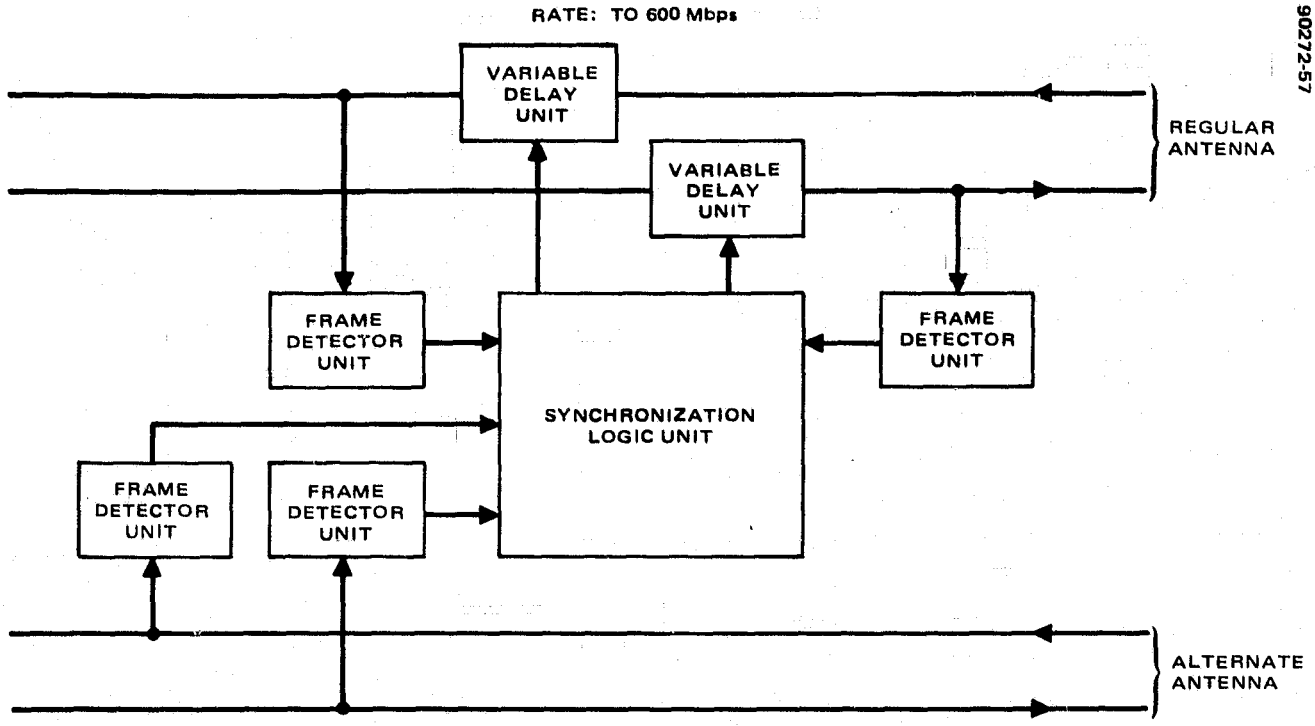

FIGURE 3-13. SYNCHRONIZATION LOGIC UNIT INTERFACES

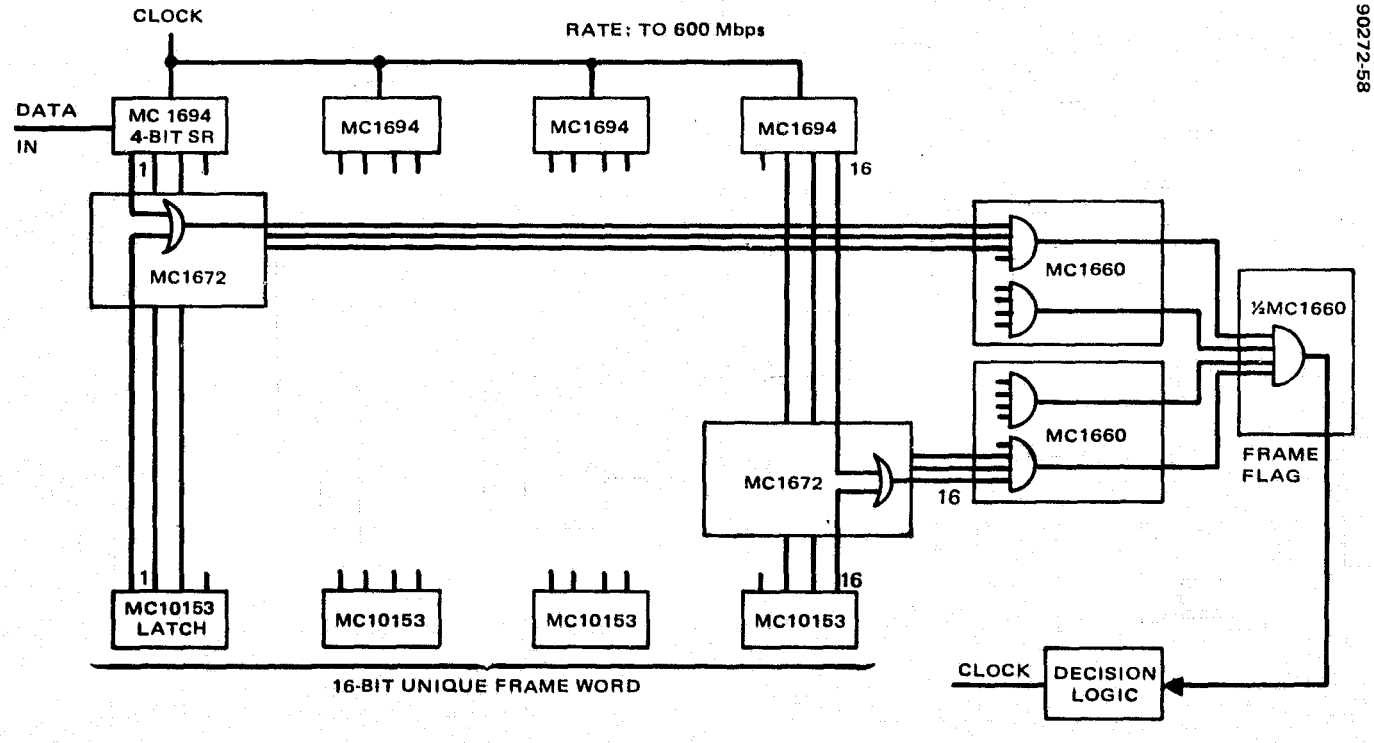

FIGURE 3-14. FRAME DETECTOR UNIT

3.3 EARTH STATION RF TECHNOLOGY

3.3.1 Receivers

3.3.1.1 Low Noise Front Ends

The highest performance at present and projected into the 1980's will be achieved by use of parametric amplifiers. Improvements in GaAs varactor diode technology and solid state millimeter-wave pump sources have made practical parametric amplifier systems operating at 20 GHz and higher possible.

Parametric amplifiers are capable of relatively flat amplitude response over bandwidths of 10 to 15 percent without serious degradation of noise temperature performance. The lower noise temperatures will generally be observed at the low frequency end of the working bandwidth.

Nearly all parametric amplifiers employ a form of temperature stabilization in order to achieve gain stability. Generally, cryogenic (helium cycle) cooling and thermoelectric cooling offer the most promising performance over systems operating at near ambient temperatures as shown in Table 3-20. Unfortunately, the highest performance systems are very

TABLE 3-20. LOW NOISE AMPLIFIER TEMPERATURE PERFORMANCE AT 20 GHz

Amplifier	Performance, °K		1978 Cost, $K	
	1978	1985	1-10	100
Parametric, ambient	160	100	30	20
Parametric, cooled	100	70	70	55
Mixer, ambient	530	300	3	2
Mixer, cooled	230	140	16	12
GaAs FET, ambient*	630	300	8	5
GaAs FET, cooled*	360	120	18	14

NOTE: Assume IF NF - 0.7 dB
*1/2 micron gate 1978
1/4 micron gate 1985

expensive and may cost in excess of $60,000 1978 dollars, including $15,000 for the helium cycle refrigerator. Critical packaging, low RF loss thermo isolators, and dewar design make the overall system very expensive. Furthermore, the growth potential for parametric amplifiers into the mid-1980 period is limited, since the technology is mature.

On the other hand, GaAs FET devices constitute a new and rapidly expanding technology. Worldwide FET research and development is vigorous and dynamic and can be expected to continue the improving FET performance trend in the immediate years ahead. Figure 3-15 is a plot of GaAs FET device noise figure versus time for 12 GHz devices.

Noise figures in the order of 4.5 dB in the 15 to 21 GHz region have been observed. These values could approach 2 to 3 dB at room temperature according to theory by use of smaller gates and optimized doping profiles.

Hughes Research Laboratories are currently developing GaAs FETs for low noise amplification which employ gate geometries with true 0.5 and 0.25 micron lengths formed by electron beam lithography. Preliminary measurements on these devices have demonstrated gains of 9 dB at 21 GHz with 4.5 dB noise figures at room temperature.

GaAs FET devices are in their infancy and might achieve performance comparable to that of uncooled parametric amplifiers between 1985 and 1990. Furthermore, they represent a cost-effective, highly reliable LNA design.

Bandwidths of 10 percent or more are practical with FET amplifiers with only a small decrease in potential low noise performance.

Direct mixer front ends are also attractive since they offer a simple, cost-effective approach. The use of cooled mixers using properly terminated GaAs diodes may prove to be competitive with GaAs FET devices in terms of both performance and cost (see Table 3-20).

Traditionally, satellite earth station design has utilized a common LNA driving a power divider feeding individual receivers or downconverters. The use of mixer front ends without preamplification would limit the receiving system to one channel operation since paralleling would significantly increase noise temperature of the system.

3.3.1.2 Downconverters

Off the shelf 20 GHz downconverter hardware is not yet available. Thus costs were derived from estimates of the costs of the individual components within a typical downconverter. Detailed block diagrams of two types of downconverters are shown in Figure 3-16.

The major advantage of the dual conversion mode lies in the simplicity of changing channels if the 2.5 GHz bandwidth is eventually channelized: only

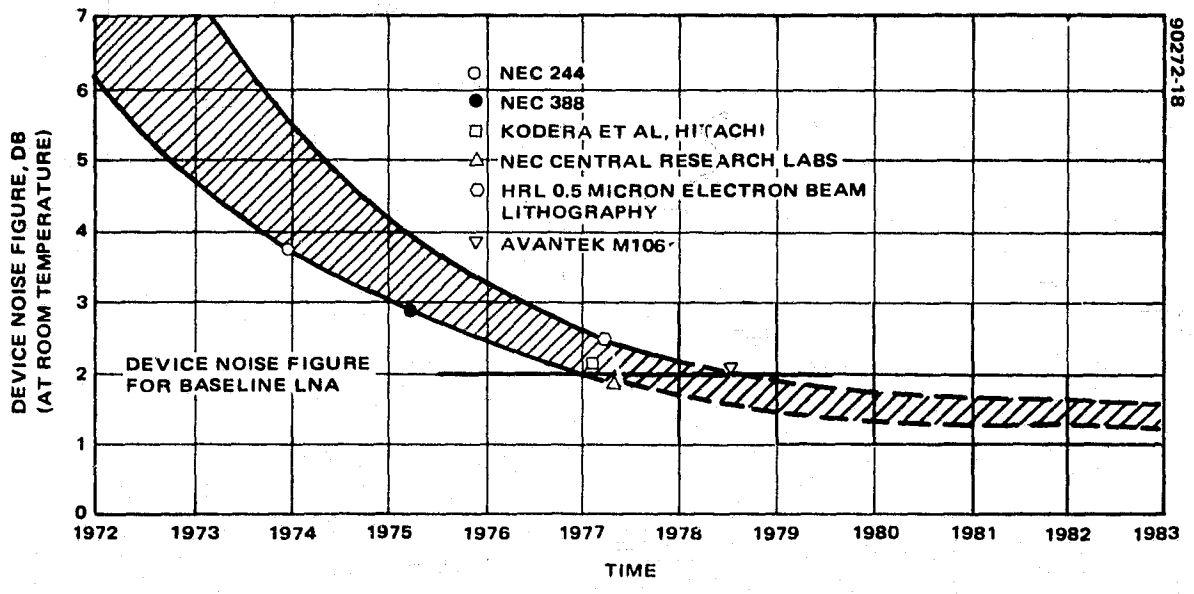

FIGURE 3-15. GaAs FET NOISE FIGURE AT 12.0 GHZ VERSUS TIME

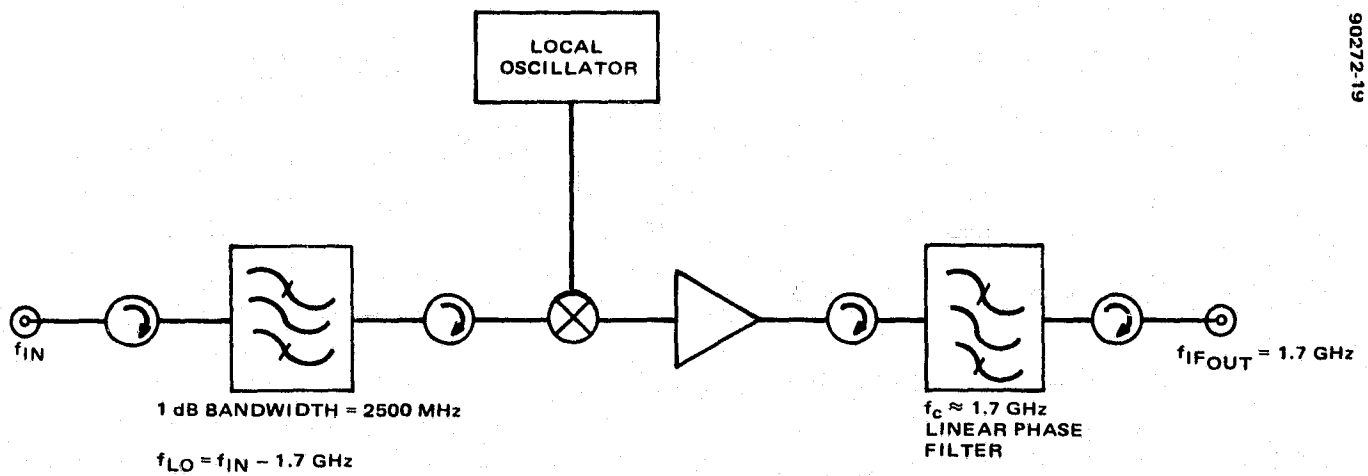

a) SINGLE CONVERSION

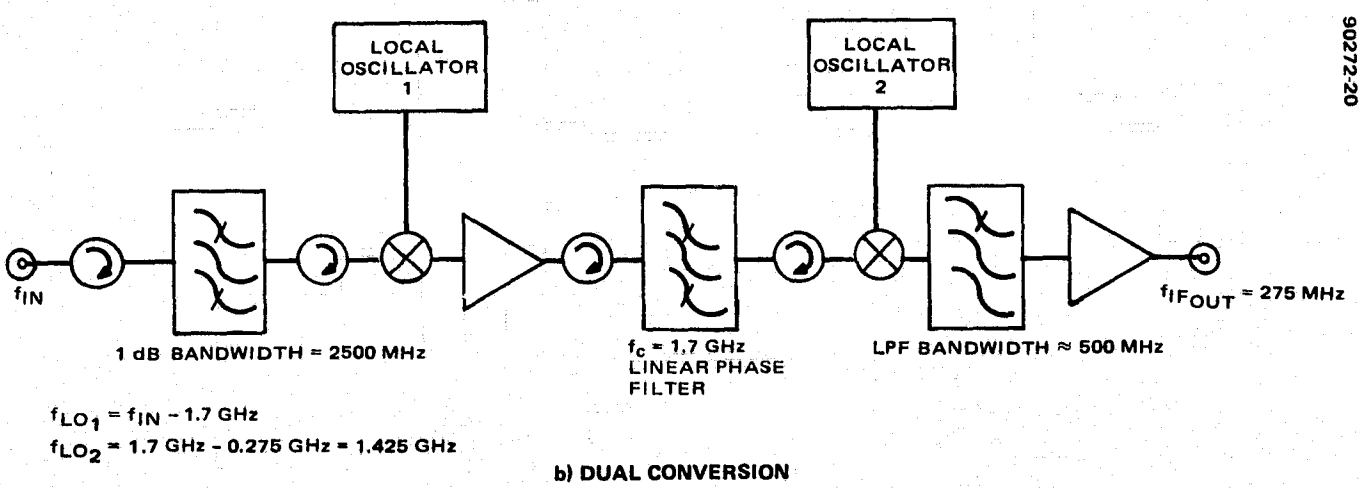

b) DUAL CONVERSION

FIGURE 3-16. DOWNCONVERTERS

the second LO frequency will need to be changed, while the single conversion scheme will require a filter and LO frequency change.

The major cost contribution items derive from the critical requirements of the filters. If the peak-to-peak group delay variation over the band is three ns or less, there will be not more than one dB degradation in bit error rate (BER). Furthermore, a self-equalized (linear phase) microwave filter can be realized with a -25 dB bandwidth equal to 1.6 times the linear phase bandwidth. While there are tradeoffs to be made, the BER and bandwidth criteria are good guidelines.

Channel bandwidths must also be considered if the 2.5 GHz bandwidth is sliced into individual channels. For a 274 megabit system, several modulation schemes can be considered. Two multiphase PSK schemes are summarized in Table 3-21.

The recommended bandwidths take into consideration 20 to 25 MHz for stationkeeping, beacons, and other uses if eleven 4 phase PSK or sixteen 8 phase PSK channels are mechanized. There seems to be an advantage of nearly 1.5 in capacity by using 8 phase PSK. Another advantage lies in the fact that the filter skirt requirements are not as stringent for the 8 phase PSK system since a larger guard band is available.

The estimated costs of a complete downconverter are shown in Table 3-22.

TABLE 3-21. MULTIPHASE PSK SCHEMES

PSK Modulation	Linear Phase BW, mHz	-25 dB BW, mHz	Recommended Channel BW, mHz
4 phase	137	219.2	225
8 phase	91.33	146.1	155

TABLE 3-22. DOWNCONVERTER COSTS

Class	Quantity	
	20	100
Single conversion	$18,500	$12,500
Double conversion	$20,000	$13,500

3.3.2 Transmitters

3.3.2.1 Solid State

Only limited data have been published on Ka band solid state hardware. Several years ago RCA developed a 160 mW output, 22 GHz amplifier with 4.8 dB of gain using a 1 micron gate FET. Texas Instruments more recently developed a device capable of 800 mW at 18 GHz using a one-half micron gate FET.

Other workers are striving to develop devices capable of operation at higher frequencies with significant power capability. It is known that reducing gate length increases device gain but does not increase the power output capability. Smaller gate sizes of much less than one-half micron do not offer significant advantages since the reduction of cross-sectional area increases losses. Some receiver low noise FET devices utilizing one-quarter micron gates have been developed. Techniques are being considered to compensate for the increased losses but the practical limit for power FET devices in the 30 GHz band may be in the order of one-quarter to one-tenth micron by the 1980's.

One-half micron devices should be practical at 30 GHz based upon presently known GaAs FET characteristics. It should be possible to achieve one-half watt per millimeter gate structure width at these frequencies. Practical structures should range from one-half to 1 millimeter in size, thus yielding devices with 200 to 500 mW potential by the mid-1980's.

Power combining is quite difficult at these (30 GHz) frequencies using conventional planes, branch line, and tandem hybrids. Other schemes, such as radial structures, are being considered whereby up to ten devices may be paralleled with bandwidths of 10 percent. Thus, completely solid state sources with 2 to 5 watt capability may be available by 1985.

This technology is so new that it is nearly impossible to estimate product costs. Historically, costs on similar lower frequency 6 GHz hardware have decreased to be competitive with low power TWT devices used as intermediate power amplifiers.

It may be expected that similar economic trends will result in economical applications for 30 GHz hardware, particularly where high reliability and maintenance cost are considered.

Other devices such as locked oscillators derived from Gunn diodes and IMPATT diodes are capable of generating RF power at 30 GHz. Gunn devices operate at lower power (50 to 500 mW) and noise figure when compared with IMPATT devices. IMPATT devices have more power potential, however, and can be mechanized either as amplifiers or locked oscillators.

IMPATT amplifiers are not new, but improved devices of both silicon and GaAs are available. GaAs IMPATT devices offer potential for higher

efficiency but have lower reliability than silicon devices. Power levels up to several watts per device may be possible in the 1980's. The use of radial structures may permit solid state power levels of 5 to 10 watts and perhaps more by 1990.

GaAs FET devices, however, are a new and rapidly expanding field. They have potential for higher efficiency and longer life, and they operate at lower voltages and junction temperatures. They offer advantages of being less susceptible to the formation of intermodulation products in contrast to IMPATT devices, and they may be the solid state devices of the future.

3.3.2.2 TWT Power Amplifiers

Most wideband services require an amount of RF power significantly greater than what may be expected from parallel solid state devices. At present, vacuum tube technology (TWT or Klystrons) appears to be the only possible means of developing substantial power levels. Tube technology is mature, highly competitive, and producing tubes in substantial quantities. Significant improvements affecting cost or performance are not anticipated in the near future.

In any event, the technology exists to cover the power spectrum from 10 watts to several kilowatts or more. The major advantages of TWT tubes is their excellent bandwidth response in contrast to the limited 50 to 100 MHz bandwidth of Klystrons. Klystrons are less costly and may offer economic advantages if the 30 GHz band is channelized in the 1980 time frame.

Other tube devices such as the Gryrotron are under development. Unfortunately, these devices require relativistic electron velocities and therefore operate at very high voltage (50 to 100 kV) and generate very high power in the order of 200 kW at 28 GHz. Present developments are narrow-banded (0.2 percent) and susceptible to spurious oscillations.

The burden of the medium to high power amplifiers to be used at 30 GHz will undoubtedly employ TWTs. Cost is plotted as a function of power in Figure 3-17.

The high voltage power supply and control subsystem accounts for a significant portion of the cost of a high power amplifier. Large, heavy power supplies providing precise regulation are required for stable TWT operation. Tube protection logic circuits such as waveguide arc sensor-suppressors, sequencing, overload tripouts, and high voltage crowbar devices contribute to costs.

Generally simple support circuitry is required at power levels up to 50 watts, and more complex designs are required for higher power levels. The higher power TWTs (400 to 600 watts) do not have permanent magnet beam focusing structures and require a solenoid with associated power supply and control circuits. Furthermore, helix TWTs have limited power capability at 30 GHz, thus necessitating the use of more costly coupled cavity

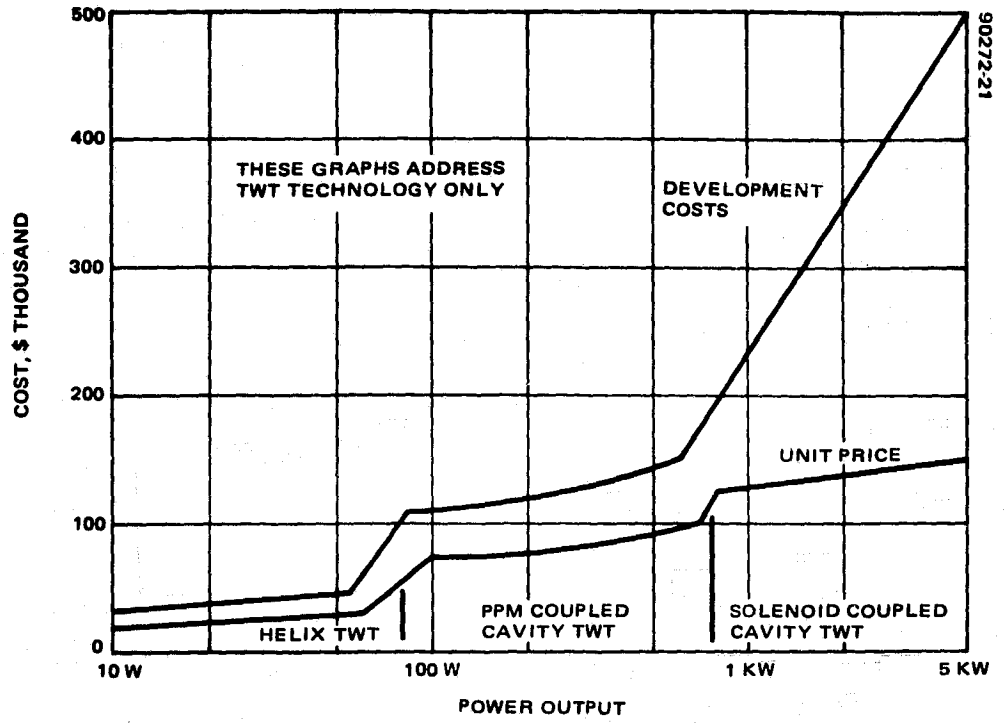

FIGURE 3-17. EARTH STATION TRANSMITTER COST

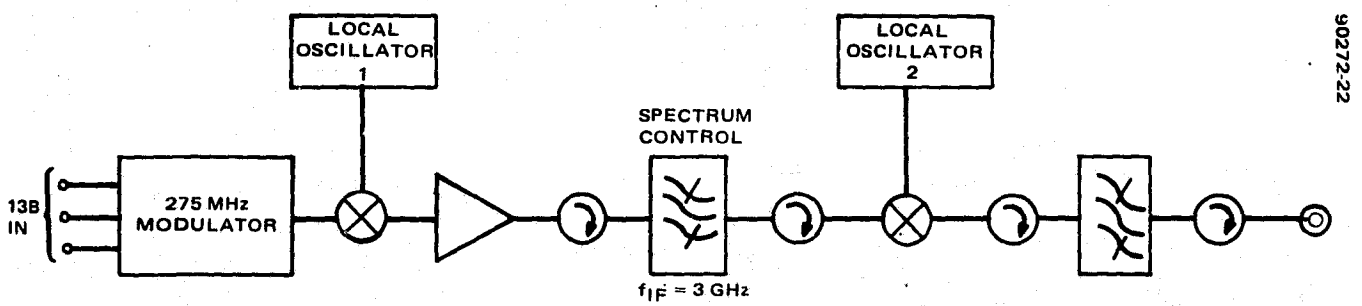

$f_{LO_1} = 3.0 - 0.275 = 2.725$ GHz

$f_{LO_2} = f_{OUT} - 3.0$ GHz

a) DUAL CONVERSION

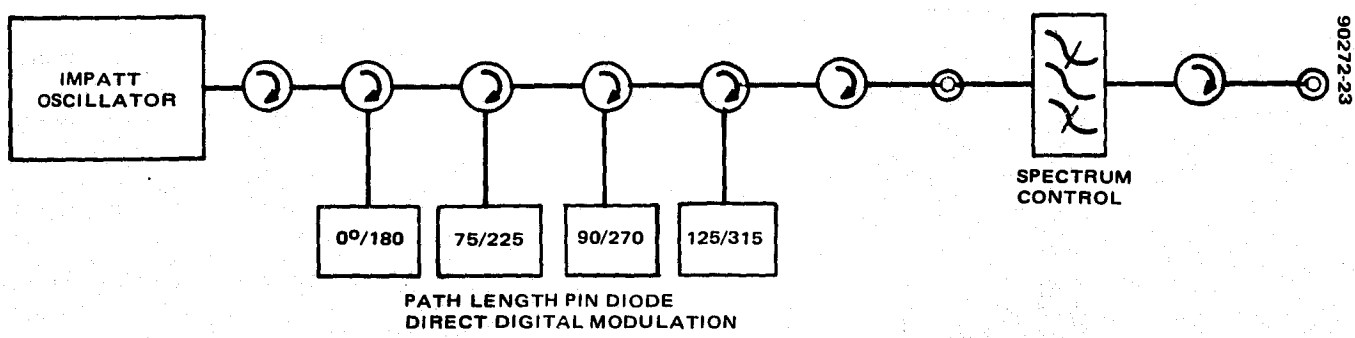

b) IMPATT EXCITER MODULATOR

FIGURE 3-18. UPCONVERTERS

designs at approximately the 50 watt level. The discontinuities shown in Figure 3-17 are indicative of these factors.

3.3.2.3 Upconverters

The problems associated with converting intermediate frequencies to 30 GHz are nearly identical to those of downconverting from 20 GHz as discussed in 3.3.1.2.

Dual conversion is recommended not only for simplicity of changing channels by changing the second LO frequency, but also for permitting the spectrum control bandpass filter characteristics to remain unchanged with carrier frequency changes. Figure 3-18 shows a typical configuration for dual conversion. Costs are shown in Table 3-23 but do not include the modulator.

A highly cost-effective IMPATT oscillator with a path length pin diode direct digital modulation scheme is also shown in Figure 3-18. This approach permits power outputs of at least +20 dBm to be developed and includes an 8 phase PSK modulator. The unit has poor frequency stability and must employ differentially encoded digital data for the modulators. Furthermore, the spectrum control filter must operate at 30 GHz and would require changing in order to change channels.

3.3.3 Frequency Sources

In general, up/downconverters employ low phase noise, high stability oscillators to ensure adequate system performance. Frequency sources covering the stability range of 1×10^{-4} to 1×10^{-11} were considered since no standards have been agreed on for 18 and 30 GHz fixed service satellite communications.

Some 20 GHz terrestrisl microwave systems utilize an IMPATT diode local oscillator operating on the output frequency with no frequency conversion mixers. Simple QPSK modulators using path length type PIN diodes permit direct digital modulation of the transmitted signal. Such systems are reliable, simple, and low in cost. It is doubtful that they will have applications for ground station use since their stability is dependent upon temperature control of the IMPATT diode diamond heat sink and associated cavity. Frequency stabilities of the order of 1×10^{-4} have been achieved, however.

TABLE 3-23. UPCONVERTERS

Class	Costs	
	20	100
IMPATT	$10,500	$6,700
Dual conversion	13,000	3,700

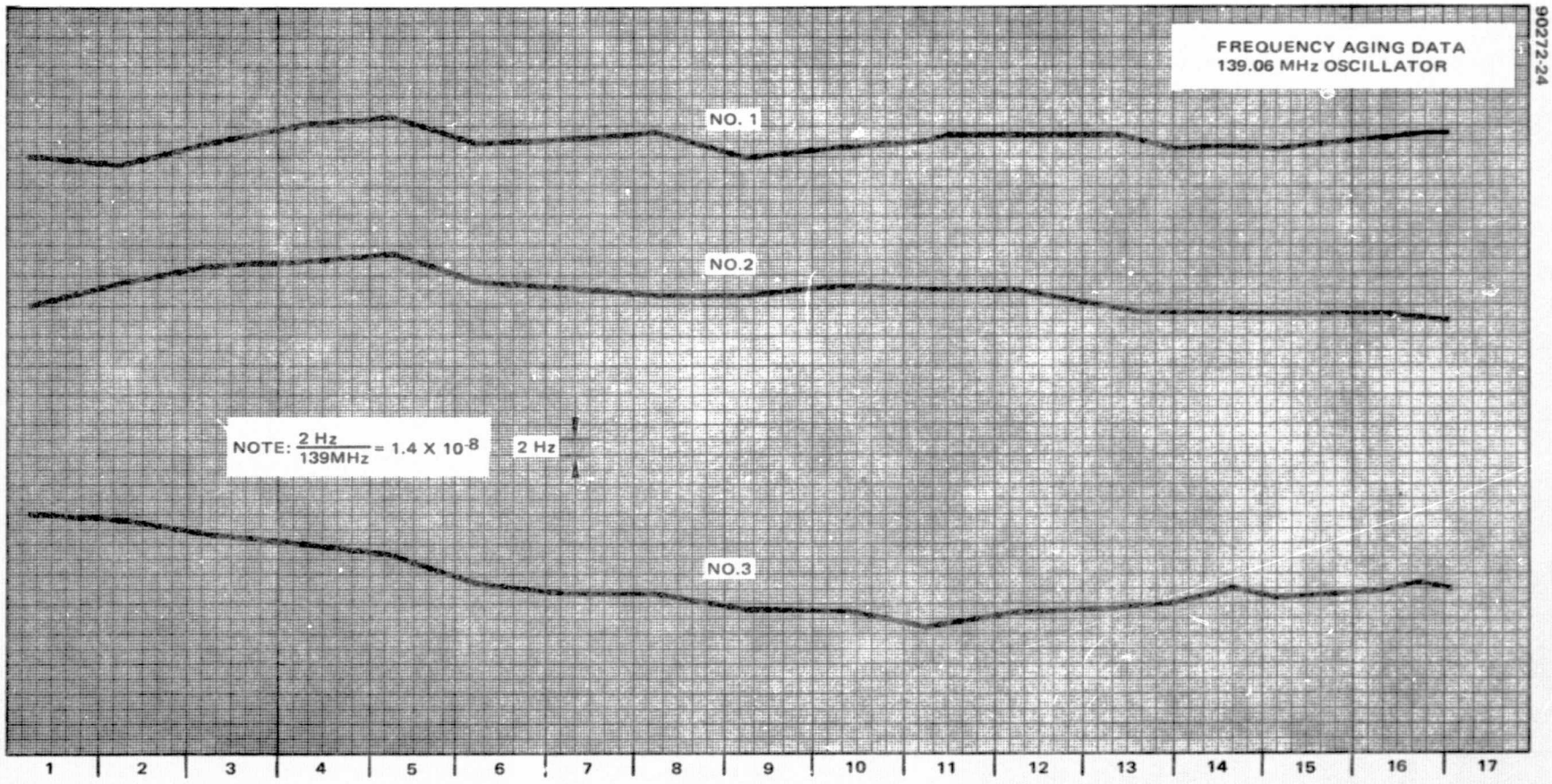

FIGURE 3-19. OSCILLATOR STABILITY – VHF QUARTZ

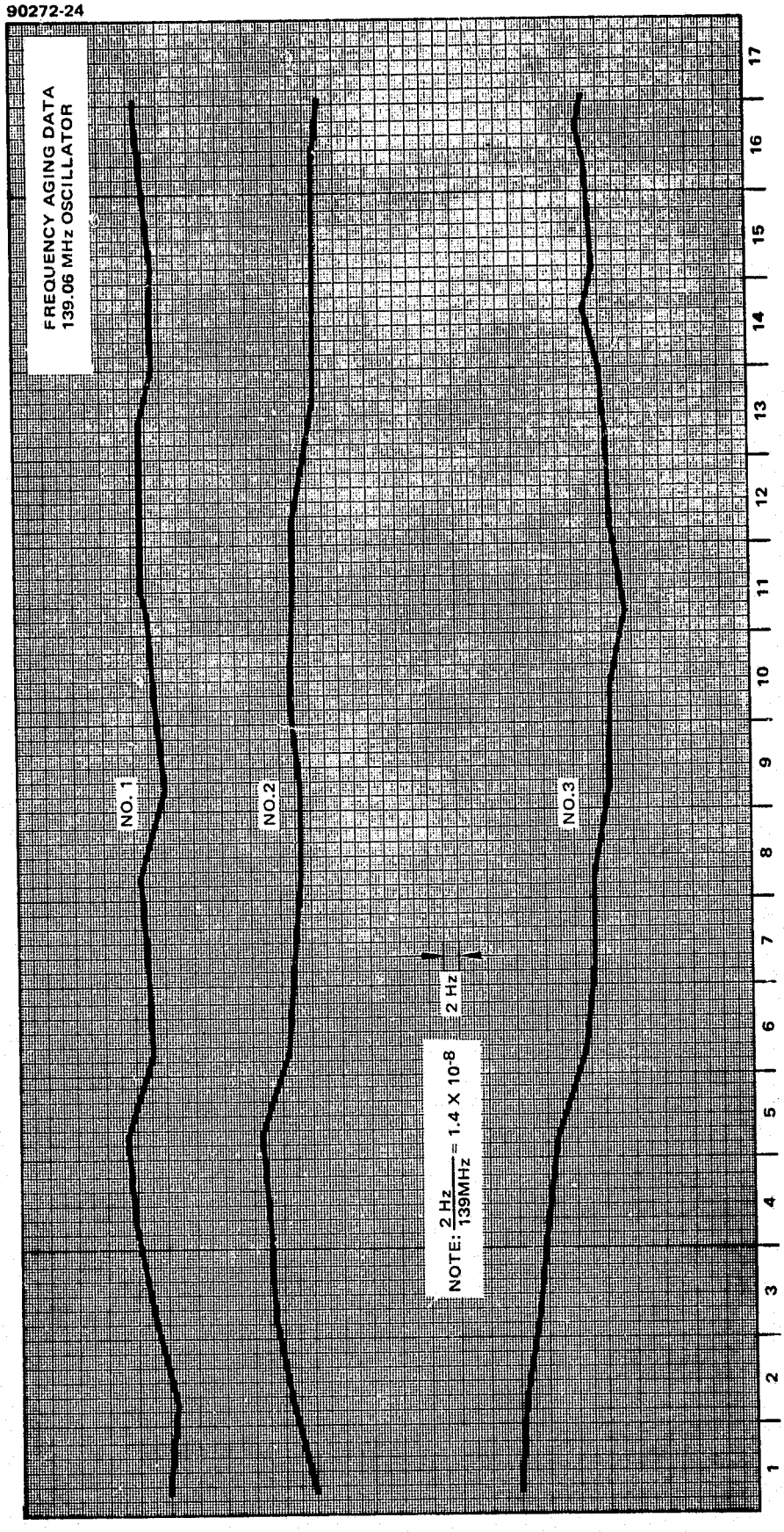

FIGURE 3-19. OSCILLATOR STABILITY – VHF QUARTZ

More conventional frequency sources consist of quality crystal oscillators. The low phase noise oscillators consist of a VHF crystal oscillator and buffer amplifier and employ a control oven. Frequency control is provided by seventh overtone cut quartz crystal in the frequency range of 110 to 133 MHz. A VHF oscillator will provide improved FM noise characteristics in the frequency range of interest over that attainable from low frequency oscillators since smaller multiplication factors are involved. Long term stability has measured better than 5×10^{-8} over a 3 month period.

Three oscillator models operating at VHF have been on life test during the past two years at Hughes. The stability in a laboratory environment is indicated in Figure 3-19. Performance over a temperature range of 20° to 105°F resulted in a frequency stability of 3.6×10^{-8}. The expected performance characteristics of the oscillator are shown in Table 3-24.

Some forms of communications schemes such as single channel per carrier required stabilities significantly better than 1 kHz at the output frequency. Higher frequency stability may be required than a conventional crystal oscillator is capable of providing, since 30 GHz is nearly five times higher than present 6 GHz uplinks to the spacecraft. Long term stability several orders of magnitude better than that of crystal oscillators can be achieved by making use of the atomic resonance of rubidium (Rb 87) to control the frequency of the quartz oscillator to accuracy levels better than 1×10^{-9}.

Present rubidium oscillators can be extremely compact, long-lived, and have high spectral purity. The low noise spectral purity is important since higher multiplication factors are involved due to the normal 5 to 10 MHz output frequency of rubidium oscillators. Typical characteristics are shown in Figure 3-20.

The costs are shown in Table 3-25. The rubidium oscillator high cost can be more effectively amortized by using only one device as a station master oscillator which serves as a reference for less stable locked oscillators used in the other station subsystems.

TABLE 3-24. EXPECTED PERFORMANCE CHARACTERISTICS OF OSCILLATOR

Crystal	28 to 32 MHz, selectable
Output power	0 to +3 dBm
Frequency stability	
Long term	$\leq 5 \times 10^{-8}$ for 6 months after warmup
Temperature	$\leq 5 \times 10^{-8}$, 0° to 40°C
FM noise	< 0.5 Hz rms in 50 to 15,000 Hz band
DC power	
Heater	< 0.8 W at 70°F
Oscillator	~ 0.4 W
Size	3 x 3 x 2 in

OUTPUT	10 MHz SINEWAVE 0.5 V RMS INTO 50 OHMS, HEATING GROUND OPTION: 5 MHz, 1 MHz	
SIGNAL TO NOISE (SSB 1 Hz BW)	$>$120 dB AT 100 Hz AND $>$145 dB AT 1000 Hz FROM CARRIER	
INPUT POWER	13 W AT 24 VDC, 25°C AMBIENT; 22 TO 32 VDC; PEAK CURRENT DURING WARM-UP, 1.8A	
WARM-UP CHARACTERISTICS	$<$10 MINUTES TO REACH 2×10^{-10} AT 25°C AMBIENT	
LONG TERM STABILITY (DRIFT)	$<4 \times 10^{-11}$/MONTH	$<1 \times 10^{-11}$/MONTH
SHORT TERM STABILITY	3×10^{-11} τ = 1 SEC 1×10^{-11} τ = 10 SEC 3×10^{-12} τ = 100 SEC	1×10^{-11} τ = 1 SEC 4×10^{-12} τ = 10 SEC 1×10^{-12} τ = 100 SEC
TRIM RANGE	2×10^{-9}	1×10^{-9}
ENVIRONMENTAL EFFECTS		
VOLTAGE VARIATION	$<1 \times 10^{-11}$/10%	
OPERATING TEMPERATURE	$<6 \times 10^{-10}$ FROM -40°C TO +65°C OPTION: $<10 \times 10^{-9}$ FROM -54°C TO +65°C	$<1 \times 10^{-10}$ FROM -25°C TO +65°C OPTION: $<4 \times 10^{-10}$ FROM -54°C +65°C
STORAGE TEMPERATURE	-54°C + 75°C	
MAGNETIC FIELD	$<4 \times 10^{-11}/AM^{-1}$ (3×10^{-11}/0.1 MILLITESLA). OPTIONAL SHIELD AVAILABLE.	
ALTITUDE	$<1 \times 10^{-11}$/MBAR (SEA LEVEL TO 21,000 M)	
HUMIDITY	95% MIL-T-5422F	
SHOCK	MIL-STD-810C, METHOD 516.2, PROCEDURE I	
VIBRATION	MIL-STD-810C, METHOD 514.2, PROCEDURE I	
GENERAL INFORMATION		
SIZE	100 MM x 99 MM x 112 MM (3.9 IN. x 3.9 IN. x 4.4 IN.)	
WEIGHT	1.3 KG (2.9 LBS), WITH OPTIONAL HEAT SINK EEK-10, 1.55 KG (3.5 LBS)	
ELECTRICAL PROTECTION	AN INTERNAL DIODE AND FUSE PROTECTS AGAINST REVERSED POLARITY CONNECTION	
CONNECTORS	COAXIAL CONNECTOR OSM 211; MATES WITH OSM-501-3 OR EQUIVALENT. EIGHT PUSH-ON CONNECTORS PINS. OPTION: WINCHESTER CONNECTOR PN: SRE-20PJ; MATES WITH SRE-20SJ.	
WARRANTY	1 YEAR; LAMP AND RESONANCE CELL – 5 YEARS	

90272-25

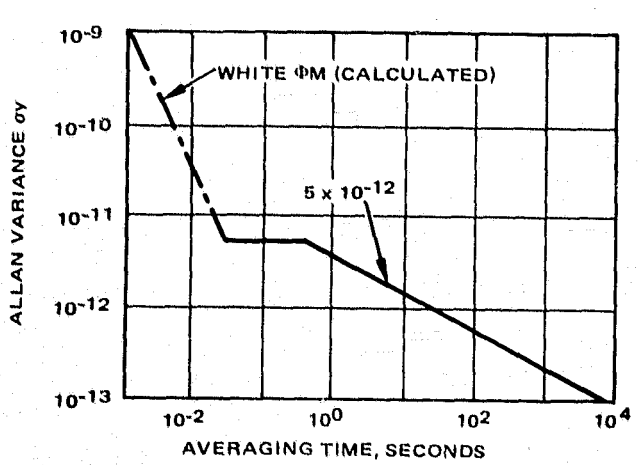

TIME DOMAIN STABILITY

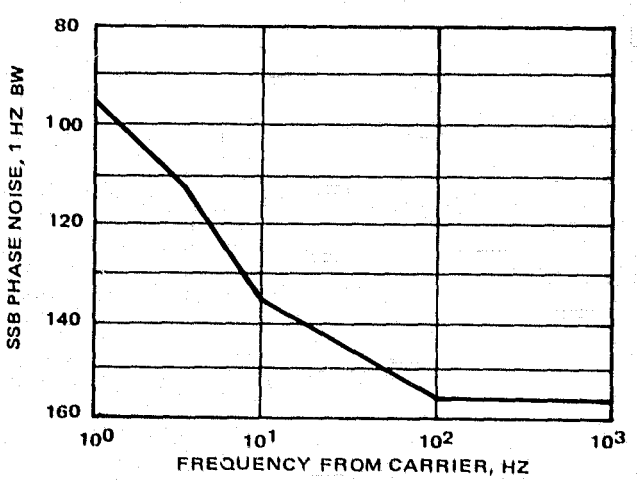

FREQUENCY DOMAIN STABILITY

FIGURE 3-20. RUBIDIUM OSCILLATOR CHARACTERISTICS

TABLE 3-25. FREQUENCY SOURCE COSTS

Class	Costs	
	1-10	100
Rubidium	$5030	$4000
10 mHz quartz	775	600
VHF quartz	500	400

3.3.4 Earth Station Antenna System Considerations

Many earth stations may be required in the communication system, so earth station costs, especially the antenna subsystem cost, must be as low as possible.

Table 3-26 provides a brief overview of the antenna equipment to be considered and the related tradeoffs. The evaluations of cost, while not absolute, generally can indicate the present trends. It may be concluded from this table that, at the present time and in the near future, the prime focus and cassegrain fed parabolic antennas are the most cost-effective approaches to most earth station requirements.

The effect of random phase errors due to surface tolerance has been analyzed by Ruze and others. The loss due to random phase errors is given by

$$L = e^{-\left(4\frac{\pi\sigma}{\eta}\right)^2}$$

where σ is the RMS surface error. This equation applies at high F/D ratios. Figure 3-21 shows the loss at 30 GHz for several values of F/D. Antennas used at Ku band have surface errors of approximately 0.035 inch in an operational environment, including manufacturing and thermal losses. At 14 GHz a loss of about 0.7 dB results for F/D = 0.3. At 30 GHz the loss increases to 3.5 dB for the same F/D. At 20 GHz the loss is 1.6 dB. To obtain performance at 30 GHz equivalent to the performance of a Ku band antenna at 14 GHz, surface precision of about 0.015 inch is required. The cost of antennas with this precision is quite high because of the many measurements and adjustments required and the high cost of tooling. Figure 3-22 shows a plot of cost versus diameter for Ku band (0.035 inch) and Ka band (0.015 inch) antennas. Costs include limited motion autotrack. The Ku band data are an extrapolation of recent antenna purchases and catalog prices at smaller diameters (<8 meters). The Ka band data are from a manufacturer with experience with even more precise radio astronomy antennas (ESSCO). This manufacturer recommends radomes for the size and precision shown.

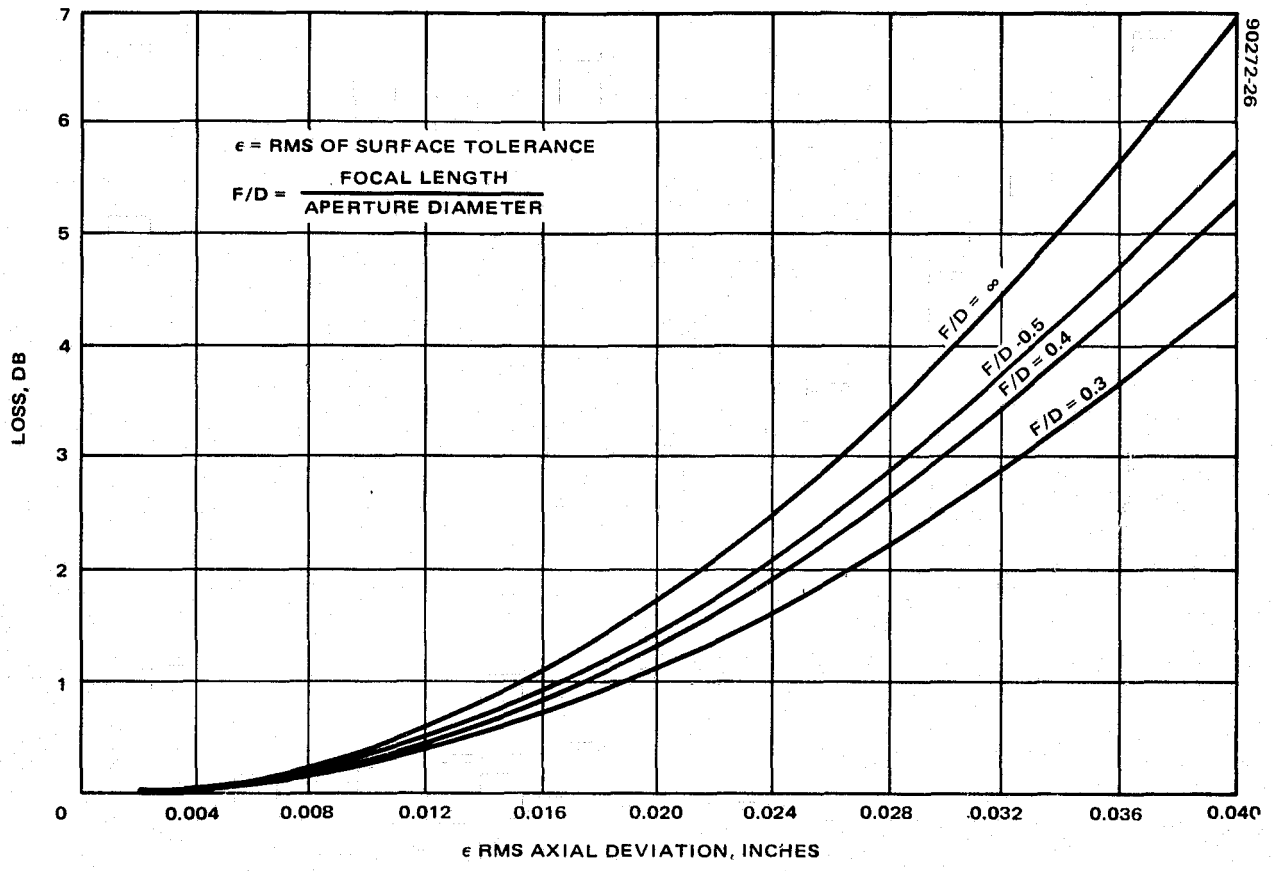

FIGURE 3-21. EFFECTS OF SURFACE TOLERANCE ON GAIN LOSS AT 30 GHZ

TABLE 3-26. ANTENNA EQUIPMENT CHARACTERISTICS AND TRADEOFFS

Antenna Equipment	Comments	Relative Cost
Paraboloid reflector, prime focus feed	Simplest configuration, sidelobes higher due to spillover, temperature higher due to earth contribution direct to sides of feed.	Lowest
Paraboloid reflector, cassegrain feed	Low sidelobes, subreflector is hyperbolic shape in front of reflector focus, easy to connect to LNA and diplexer.	Medium/low
Paraboloid reflector Gregorian feed	Low sidelobes, subreflector is elliptical shape beyond reflector focus, easy to connect to LNA and diplexer, probably more difficult to align, not commonly used but occasionally available because of probable low sidelobe performance.	Medium
Shaped reflector with offset feed	Very low sidelobe performance, low gain, feed easy to support, low blockage, not generally used for earth terminals because of cost and low gain.	High
Array	Generally narrowband, low sidelobes, electronically steerable, easy to mount on buildings, efficiency dependent upon design.	Very high
Horn	Very low sidelobes, high gain, physically difficult to mount and steer, difficult to use on top of building in medium and large sizes.	High
Reflectors		
Metal	Common fabrication technology, used for all sizes of reflectors.	Low
Fiberglass	Common fabrication technology, used for small and medium sized reflectors.	Low for small reflectors, higher for larger sizes due to labor and tooling costs.

The Ka band costs apply either with or without radomes; however, the achievement of this performance without radomes is questionable, especially at winds greater than 20 mph. Radomes have generally been considered poor candidates for use at these frequencies because of potentially large radome losses in the presence of rain; however, this manufacturer provides data showing these losses to be under 1 dB for all applicable levels of rain if the radome surface is properly coated to prevent filming. When the difference in surface loss is taken into account, the cost can be compared as a function of gain (see Figure 3-23).

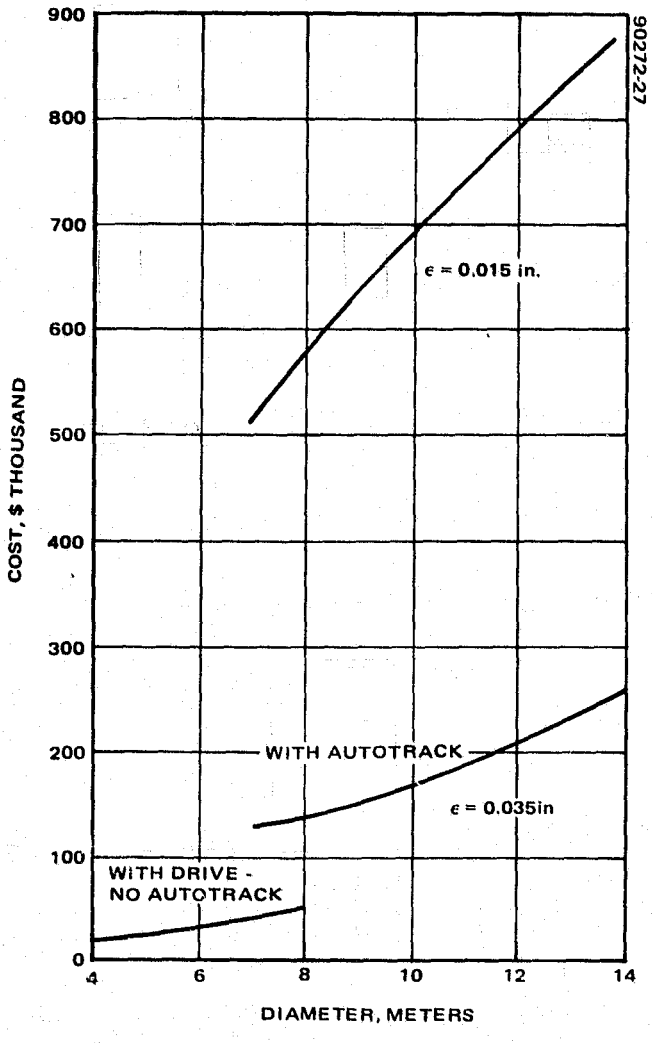

FIGURE 3-22. COST AS A FUNCTION OF DIAMETER

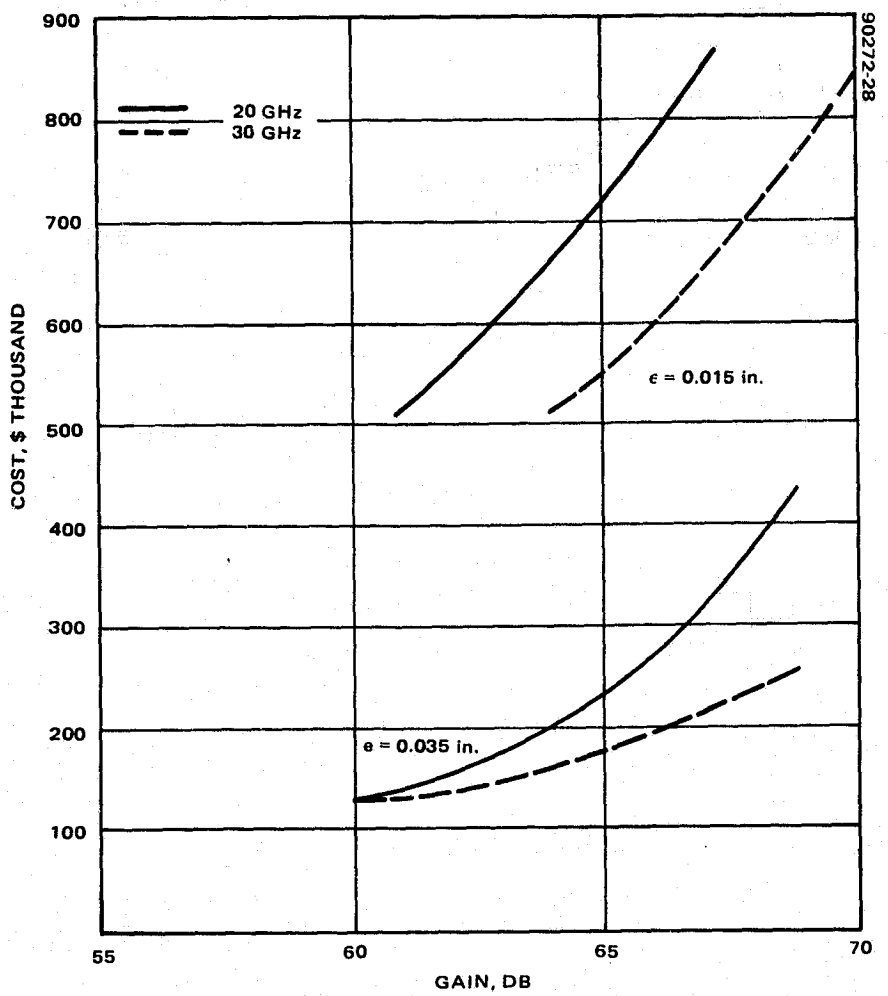

FIGURE 3-23. COST AS A FUNCTION OF GAIN

3.4 SATELLITE REPEATER

3.4.1 Receivers

The characteristics of low noise amplifiers are summarized in Table 3-27.

3.4.1.1 FET Low Noise Amps

Production of the first low noise FETs with gate lengths less than 0.25 μm is expected in the next year. Theoretical calculations predict that this will lead to noise figures of approximately 3 dB at 30 GHz, but circuit designers with experience in flight hardware production lean toward a more conservative forecast of 4 to 5 dB. Accompanying gains of around 7.5 dB are expected.

At 18 GHz, 7 dB gain has already been obtained with a noise figure of 2.3 dB from a 0.5 μm gate FET. With a shorter gate and proper tuning, somewhat higher gains should be possible with noise figures comparable to these predicted above.

The amplifier weight is determined primarily by the isolators, waveguide, and packaging used. Those listed in Table 3-27 are based on waveguide input, output, and circulators. The weight could be reduced through the use of MIC circulators and MIC output; however, the greater loss in MIC would degrade both noise figure and gain. The cost is determined by the amount of labor required for production, most of which consists of tuning.

3.4.1.2 30 GHz Paramps

Paramps can offer even lower noise figures than FETs; however, low noise figure is achieved at the expense of bandwidth and reliability.

TABLE 3-27. LOW NOISE AMPS

Type	NF, dB	Gain, dB	BW, %	DC Power	Weight, oz	Recurring Cost, $K
FET						
30 GHz LNA	4-5	7.5	≥10	0.05	7	35 (2 stage)
18 GHz LNA	<4	12	≥10	0.05	7	30 (2 stage)
18 GHz Hi	4	15	>10	0.05	7	35 (4 stage)
Paramp	~2.5	18	~5	12.0	16	70

NOTES:

1) All values per stage except FET weight and cost
2) Weight of FET amps are relatively constant with regard to the number of stages.
3) Paramp development costs $250K. Performance varies with risk. Also, noise figure varies with bandwidth.

Low noise figure and wide bandwidth both require high pump frequencies which are inconsistent with the high reliability required in a satellite application. A realistic pump frequency for a satellite application might be 90 GHz, although some designers might estimate higher potential frequencies. With this pump frequency a combination of 2.5 dB noise figure and 5 percent bandwidth appears reasonable.

3.4.1.3 Mixers

Two types of mixers will be available for use in the transponder. Those using Schottky barrier diodes have found the widest use to date. These mixers are capable of around 4 dB conversion loss and noise figures very nearly equal to the loss. The other possibility is the use of a dual gate FET which provides conversion gain, but has higher noise figures. FET mixers are considered poor candidates for this application because developmental efforts in this frequency range have been relatively low level. Their applicability should lie more in the area of integrated receivers where several components are mounted on a single chip.

The cost of the mixers themselves should be relatively low. Most of the cost listed in Table 3-28 is due to the local oscillator.

3.4.2 Signal Routing and Switching

3.4.2.1 Microwave Switching Devices

Switch element technology for the 1990 time frame is not expected to differ significantly from the microwave component technology of today. For very high isolation redundancy switch applications, existing mechanical designs will still be in use. These mechanical units now provide million cycle lifetimes, and for applications that require only periodic switching they will remain effective design alternatives. Of more important interest to high technology satellites, however, are the options available for beam switching or high speed phase control, and here the challenge will concentrate on ferrite versus solid state switching.

TABLE 3-28. MIXERS

Conversion Type	Gain, dB	NF, dB	BW, %	DC, watts	Weight, oz	Cost, $K
30/18 GHz Schottky Diode 30/F IF/18	-4	4	>10	8	32	36
30/18 FET	+3	8	10	8	32 Includes L.O.	40*

*FET Mixer Development Cost $175K

Ferrite switches generally have the advantage of higher power handling capability because of lower power densities. Also, they achieve lower insertion losses because of less dissipation of the waveguide modes as compared with the circuit losses of TEM modes. Often, lower VSWR can be achieved by matching a single major discontinuity at the ferrite as compared with matching out many widely spaced diode or FET discontinuities.

Solid state switch elements have the advantage over ferrite switches of significantly faster speeds. Also these devices generally offer size and weight advantages, and are more easily reproducible for volume requirements. As a side benefit there is some lessening of temperature sensitivity. Semiconductor device alternatives are PIN diodes, Schottky diodes, and microwave FETs. PIN diodes are the most common device choice because they offer good speed, good isolation, good power handling capability, and potentially broadband operation. Switching speeds of 1 nanosecond to 50 ns have been achieved with PIN diodes, depending on the type of circuit choice (series, parallel, or combined series/parallel) with corresponding isolations of 20 to 40 dB. Power handling capability can be extended to 250 watts average for parallel reflective circuits. DC bias power can be relatively high compared with ferrite or mechanical alternatives, with 300 mW continuous holding power required for a typical fast driver/diode combination, although 20 mW is possible for slower requirements. Schottky diode devices have some advantage over PINs for higher speeds, but realistic applications are limited to low power loaded line switch elements because of poor isolation. FET switch devices provide some interesting tradeoffs because they can be made with very high speed or very low dc bias power. A C band switch matrix using FETs has recently been developed at Hughes which is capable of 1 ns transition time or 1 mW continuous dc holding power for a driver/device combination. For slower applications, a high power FET switch is possible using the Hughes-developed resistive-gate FET capable of controlling 50 watts average power with negligible bias driver holding power. Some disadvantages of FETs as compared with PINs is lower isolation (approximately 20 dB) and a higher insertion loss for either high RF power or low dc bias power.

Projected comparative performance of IF switch types is shown in Table 3-29.

TABLE 3-29. MICROWAVE SWITCHING DEVICES

Device	Speed ns	DC Power, mW	Loss, dB	Isolation, dB	Weight, oz	Cost, $
PIN diode	1 50	300 20	1.5 1.5	30 30	2	2000
FET	0.05 10	100 0.01	3.0 3.0	20 20	2	3000
Ferrite	1000	0	0.5	20	3	2000
Mechanical	100,000	0	0.25	60	4	3000

3.4.2.2 SS-TDMA Switch Matrices

The switch matrix in an SS-TDMA system connects the N input ports to the N output ports in a simultaneous connection combination. In the Hughes system description, this switch matrix is located after the receivers but before the main power amplification. In principle, this switching can take place at baseband or at a suitable microwave IF; however, because of the high data rates being discussed, a baseband switch matrix would require complex GaAs large scale integration (LSI). Implementation of the switch matrix using microwave switch elements is a straightforward extension of existing technology and has been studied continuously at Hughes since 1973.

There are many possible configurations that a microwave switch matrix (MSM) might take. It is possible to utilize a biplanar construction in which a layer of N input lines punch through to a second layer of N output lines in a microwave analogy to crossbar switching. This approach provides smallest size but it introduces variable group delay per path and difficult feedthrough interconnects. At Hughes, the preferred implementation for further study has been a "cubic" arrangement in which the N input lines fan out to N^2 elements oriented orthogonal to the first. In this way, the NxN matrix is composed of 2N identical single pole N throw (SPNT) switch modules. By proper switch control selection the N input ports are simultaneously connected to some permutation of the N output ports. The cubic arrangement is shown in Figure 3-24.

The Switch Module

The switch module circuit can be implemented in a variety of ways. The two that have been investigated at Hughes are the center junction circuit and the power divider circuit. The center junction design is a straightforward SPNT switch with a switch element at each output port, one of which is turned on. The advantages of this center junction design approach are maximum potential bandwidth, lowest overall insertion loss, and slightly smaller size. The disadvantage of this approach is that switch elements are closely spaced together and the crowding of parts around the junction makes rework repair difficult, and also requires special care in placement of resonant inductors.

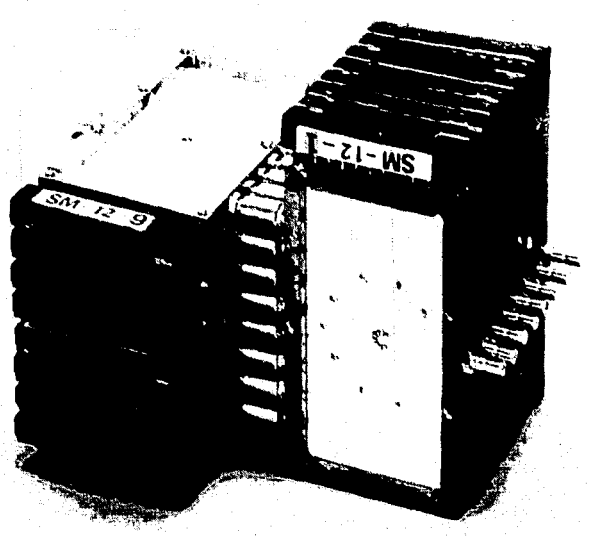

90272-29

FIGURE 3-24. CUBIC MICROWAVE SWITCH MATRIX

An alternative circuit layout to achieve the SPNT module is a power divider approach wherein the input signal is split into N equal outputs, each of which is then switched on or off. The disadvantage to this approach is much higher insertion loss (module output power is only one portion from sequential 3 dB dividers); however, several important advantages are acquired. The foremost advantage is a physical separation of devices that allows the possibility of using packaged switch devices or the possibility of special substrate mounts that can be easily tested before assembly and easily removed later.

The Switch Device

Choice of switch device is essentially independent of the overall circuit choices that have been discussed. The two dominant candidates for this SS-TDMA application are the PIN diode and the GaAs FET. The PIN is a common switch element with a known reliability history. PIN switches can be made which have high speed, high RF power, high isolation, and broad bandwidth, although these parameters do not necessarily occur in the same design. The FET used as a microwave switch is a new application offering its own potential benefits, but also introducing new limitations and unresolved questions. The PIN has been shown in previous studies to be capable of 10 ns switch delay time measured from logic command input to RF amplitude change. This speed is quite fast and perfectly compatible with TDMA applications as we now see them. However, these speeds are achievable only at the expense of sizable dc power dissipation in the driver circuit. The microwave FET is an alternative to the PIN diode as the active element of a microwave switch. Good quality microwave FETs are now available for use at Ku band frequencies. These microwave transistors have been used predominantly as amplifiers, and the parameters required for good amplifier operation are also important for good switching operation; the high f_{max} for the amplifier correlates to fast speed for the switch; the high I_{DSS} for the amplifier correlates to low ON insertion loss for the switch, and the low C_{DG} for minimizing feedback in the amplifier also improves the isolation for the switch. Research revealed four main reasons for preferring FETs to PINs for the microwave switch:

1) The FET biasing input is inherently isolated from the RF line and requires minimal block/choke separation.

2) There is a possibility with the FET of achieving insertion gain rather than loss.

3) There is the possibility of achieving essentially zero dc power dissipation in driving the switch to its on and off states.

4) The FET provides a distinct speed advantage over the PIN.

The second and third conditions are, however, mutually exclusive. Since dc power has been a major concern for Hughes system designs, the minimal dc power configurations have received the most extensive investigation.

Center Frequency

The choice of center frequency for the microwave switch matrix has been the subject of several studies. Factors involved in the consideration are: 1) a link operating frequency of 14 to 12 or 30 to 20 GHz, 2) interconnectability to a 6 to 4 GHz communications link, 3) percentage bandwidth constraints on the switch, 4) availability of transistor amplifier design, and 5) placement of local oscillator harmonics from the upconverter relative to the receive band.

In a 30/20 GHz system with 2500 MHz of bandwidth, the microwave IF could conceivably be chosen as low as 1250 MHz. However, since this would require transistor amplifiers to operate from dc to 2500 MHz, this is an unlikely choice. Another conceivable choice is 20 GHz, since no output upconverter stage would be necessary, but then the transistor amplifiers would be unnecessarily expensive. Obviously the probable choice lies between these two extremes. Percentage bandwidth is one of the more critical constraints, not only for the amplifier but also, more importantly, for tuning to maximize channel-to-channel isolation. The preponderance of work at Hughes has been for 500 MHz bandwidths for which a center frequency of 4 GHz has proven both convenient and effective. For 2500 MHz bandwidth, this center frequency would have to rise, but it is too early to predict an optimum choice. Cursory inspection suggests that 8 GHz as a center frequency IF may be reasonable.

Matrix Order

The order of the matrix, whether 8 x 8, 16 x 16, or 50 x 50 has a nonlinear impact on size, weight, power, and cost. The length of a single module increases almost linearly with order (slightly more to allow partition channels to reduce higher order modes); hence, volume increases as the cube of the order. The existing Hughes design in its breadboard form is very compact and, hence, weight can also be expected to increase as the cube of the matrix order. Bias power is dependent on the number of switch elements which is related to the NxN matrix order by a factor $2N^2$. If FETs are used in minimum power design configurations, the total dc power will fortunately remain low. The cost is dependent mainly on the number of switch elements, which increases as the square of the matrix order; however, at higher matrix orders it is not clear how control signals will be brought in and interfaced to the RF switch elements; hence, some additional consideration must be given for added technical risk.

Performance and Cost Characteristics

Performance comparisons will be made with the research performed on switch matrices at Hughes.[1] There are several assumptions that have been made. First, the switching transition time requirement is nominal

[1] R. Gaspari and H. Yee, "Microwave GaAs FET Switching", IEEE MTT-S International Microwave Symposium Digest, June 1978, (IEEE cat. 78CH1355-7 MTT).

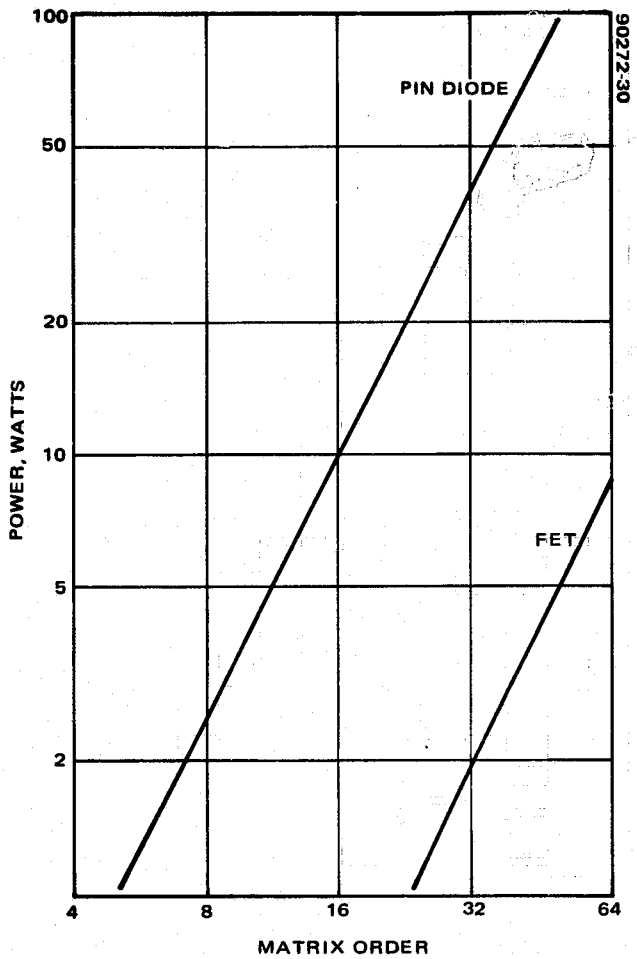

FIGURE 3-25. MATRIX POWER REQUIREMENTS

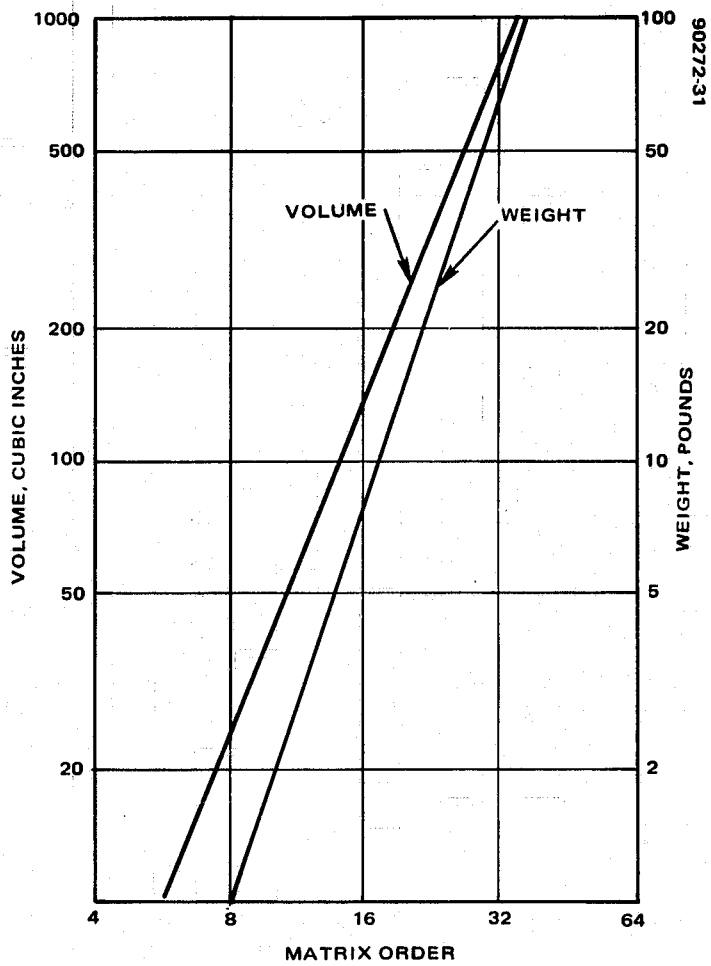

FIGURE 3-26. SWITCH MATRIX SIZE AND WEIGHT

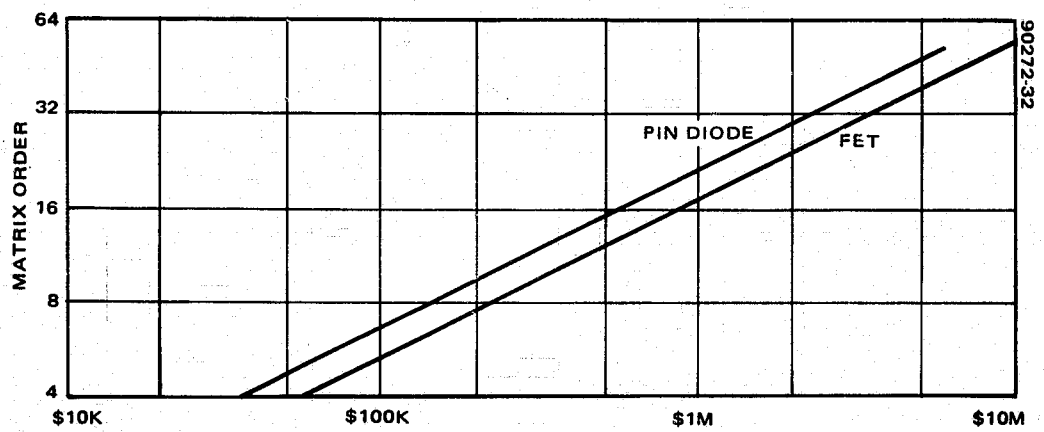

FIGURE 3-27. RECURRING COST PER SWITCH MATRIX

(30 to 50 ns), so that PINs are usable. Second, the isolation requirement is nominal (30 to 50 dB), so that FETs are usable. These two assumptions are reasonable, based upon frame time partition and beam-to-beam isolation in the antenna. The dc power requirements are shown as a function of the matrix order in Figure 3-25. The FET bias power is based on a 1 mW per switch element dissipation for driver/device combination; since there are $2N^2$ devices in an NxN matrix, a 64 x 64 matrix would consume a theoretical 8.192 watts. The PIN bias power is based on a 20 mW per switch element dissipation, which is consistent with a 50 ns switch time. Size and weight projections are shown in Figure 3-26. The estimated size of a 32 x 32 switch matrix is about 10 x 10 x 7 inches, but because of the density of substrates, carriers, connectors, and support frames, the weight is 64 pounds. By comparison, a 64 x 64 matrix would weigh 512 pounds. Both size and weight are independent of the choice of FET or PIN switch element.

Cost is the factor most difficult to project without a complete set of performance specifications. Some projections are shown in Figure 3-27. The FET implementation is estimated at 1.5 the cost of the PIN implementation. The cost of devices is a significant percentage of the total cost, partly because flight quality devices are much more expensive than their commercial counterparts, and also because attrition is high due to confined geometry and multiple driver and control line interconnections. Ideally, if the chip contained the driver plus device and the switch element, the unit could be assembled in a half day with no tuning, and the cost would be about $500K per switch matrix, based on 1978 dollars.

3.4.2.3 FDMA Multiplexers

In an FDMA trunk repeater, switching and routing are provided by input and output multiplexers as shown in Figure 3-28. The weight and cost of the filters in these multiplexers are a result of the requirements for out-of-band rejection, in-band phase and amplitude distortion, and power loss. Ideally, these requirements would be the result of a complex tradeoff study which would compare the cost of achieving the required combination of bit rate and bit error rate by minimizing the distortion and interference due to the filters (hence, minimizing the RF resources (EIRP and G/T) required to compensate for these distortions) with the cost of satisfying the communication requirements by increasing the energy per bit and relaxing the filter requirements. Such analysis is beyond the scope of the present study; however, for the purpose of the system concept studies reported in Sections 4 and 5, the weight and cost of filters with the performance characteristics of SBS satellite multiplexers was assessed for an input and output multiplexer at 20 GHz.

The input multiplexer filters are eight section, four finite frequency loss pole, dual mode elliptic function filters. The filters are circulator coupled. Fabrication is of thin walled Super Invar.

The weight of the filters plus the required circulators and isolators is 0.8 pound per channel, and the cost is $14K per channel.

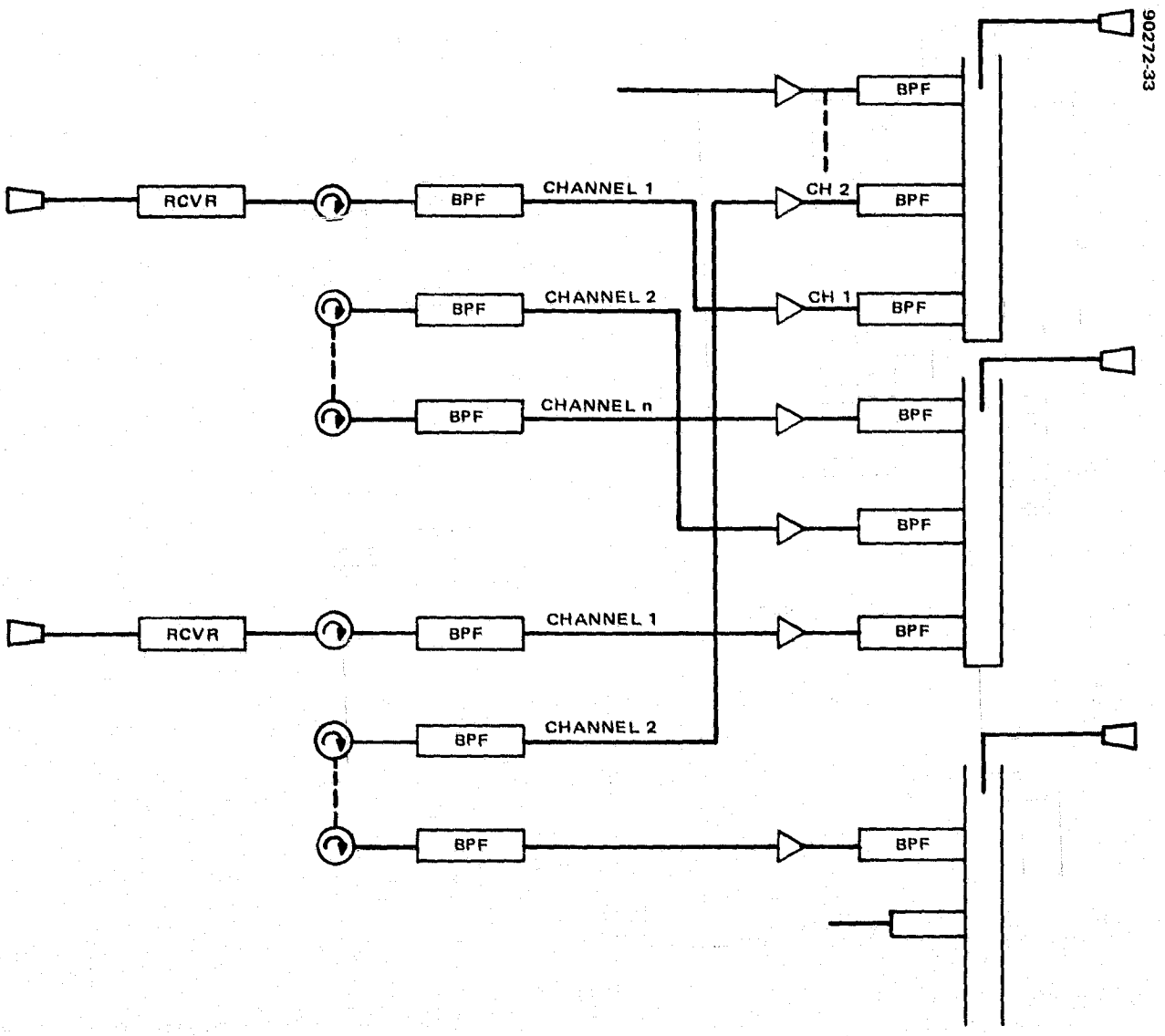

FIGURE 3-28. INPUT AND OUTPUT MULTIPLEXERS

The use of an odd-even output multiplexer configuration in conjunction with a single antenna feed would result in a 3 dB hybrid loss. It is assumed that channels would be configured in a single short circuited manifold. Such a multiplexer becomes increasingly difficult to design and tune as the number of channels increases. The nine channel output multiplexer for the baseline FDMA concept will be extremely difficult to fabricate to operate at 20 GHz.

The filters are in a six section, four pole configuration. The weight per channel is 0.53 pound, and the cost per channel is $10K for a reasonably low number of channels. The rate at which the cost per channel will increase as the number of channels increases beyond nine is not known.

3.4.3 Satellite Transmitters

3.4.3.1 Solid State Amplifiers

Primary solid state candidates for satellite high power amplifier devices at 20 GHz are the IMPATT diode and the GaAs FET transistors. Although development of the IMPATT diode is well ahead of the GaAs FET at this time, it appears that worldwide FET research will lead to GaAs FET devices which will be more appropriate for this application in the 1990's than the IMPATT diode. The FET is expected to be superior for the following reasons:

1) The FET is intrinsically a stable broadband device with no power-bandwidth tradeoff as observed in negative resistance amplifiers. There are no parametric harmonic or subharmonic oscillations, and the noise figure is typically 20 dB less than IMPATT amplifiers. In addition, there is no recovery time associated with loss of injection locking during QPSK switching which can degrade the bit error rate performance of injection locked amplifiers.

2) It appears that power FETs will prove to be more efficient than the IMPATTs. In addition to reducing primary power requirements, this higher efficiency will lead to lower junction temperatures. Because of the small size of the junction at this frequency, heat dissipation will be a vital factor in device reliability.

A single IMPATT diode has a power capability of 3 watts. No GaAs FET devices suitable for use as high power amplifiers are now available. Theoretical considerations indicate a potential of 3 to 5 watts per chip for the GaAs FET, but practical considerations related to efficiency, bandwidth, and reliability could place a limit of 1 to 2 watts, depending on the level of effort applied to these devices. For high power amplifiers of greater capacity, it will be necessary to combine chips. Low loss waveguide power combiners can be designed for this application. An example of power combining to achieve a 4.5 watt amplifier with 0.75 watt chips is shown in Figure 3-29.

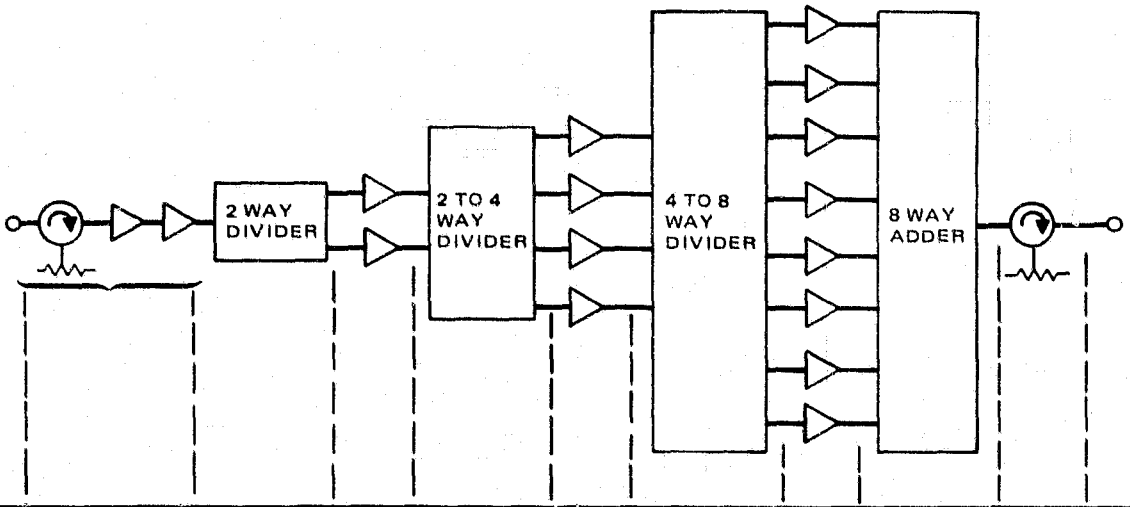

GAIN, dB	+15.25	-0.25	+7.0	-0.25	+5.0	-0.25	+4.0	-0.25	-0.25	+30
POWER, dBW	-7.95	-8.20	-1.20	-1.45	+3.55	+3.3	+7.3	+7.05	+6.8	+6.55
POWER, W	0.16	0.15	0.76	0.72	2.26	2.14	5.37	5.07	4.8	4.52
POWER ADDED EFFICIENCY, %	11	–	14	–	18	–	20	–	–	10.4
POWER DISSIPATED, W	1.3	–	4.7	0.04	10.5	0.12	21.6	0.28	0.27	38.8
COMPONENT VALUES										NET

FIGURE 3-29. 20 GHZ, 4.5 WATT FET AMPLIFIER (ASSUMES 0.75 WATT MAXIMUM PER CHIP)

As the number of chips which must be combined to achieve the required output power increases, the cost of the amplifier increases rapidly due to the labor intensive nature of power combiner fabrication. The relation of cost to power output, assuming that 2 watt chips are developed, is shown in Figure 3-30. The dc power required by the amplifier is shown as a function of output power in Figure 3-31.

The weight of the GaAs FET amplifier itself does not grow very much with power output, remaining in the 1 pound region over the practical output range; however, it is not known at this time what the weight penalty will be to maintain the device junction at a temperature consistent with long life. The weight to power relationship shown in Figure 3-32 allows a significant amount of weight for spreading the heat dissipated in the device. It may be that this weight can be reduced by the use of heat pipes, or it may be that the problem of transferring the heat from the junction to the case limits the output level of these devices. This is an area requiring investigation before the implications of solid state technology to 20 GHz high power amplifiers can be accurately assessed.

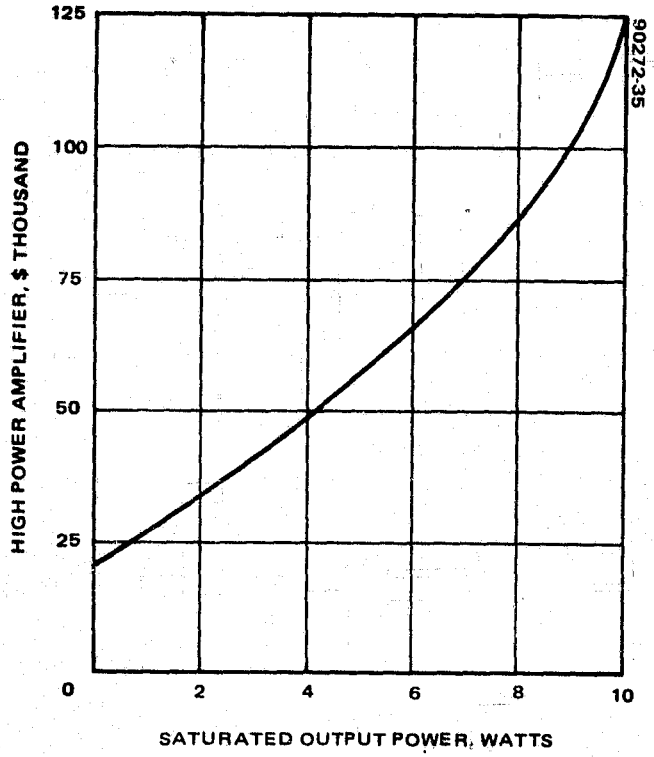

FIGURE 3-30. COST OF GaAs FET HIGH POWER AMPLIFIERS

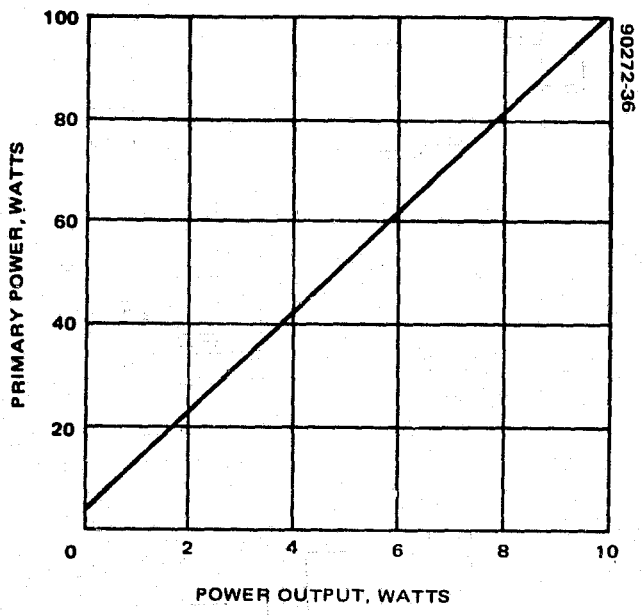

FIGURE 3-31. GaAs HIGH POWER AMPLIFIER POWER REQUIREMENTS

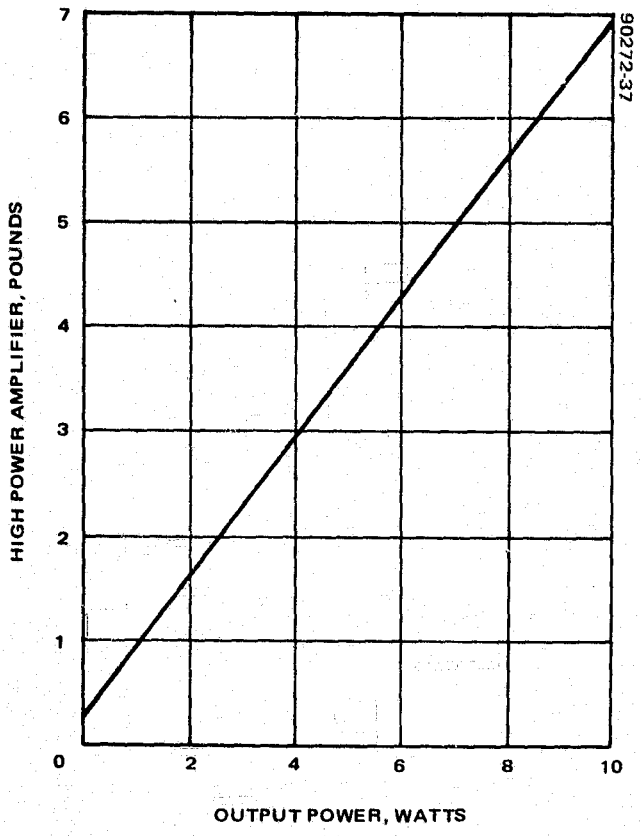

FIGURE 3-32. GaAs HIGH POWER AMPLIFIER WEIGHT

3.4.3.2 20 GHz Traveling Wave Tubes

Helix TWTs

Figure 3-33 illustrates the range of output power which may be covered by helix TWTs. There is considerable confidence that a 100 watt TWT will be developed by 1990. A 200 watt tube is a possibility, but requires technological developments which may not be achievable in a 10 year period.

Figures 3-34 and 3-35 show the variation of recurring and nonrecurring cost with output power. The increased cost for the multimode TWT is due primarily to increased testing. For power outputs greater than about 70 watts, the cost exceeds that of a coupled cavity; however, the weight is considerably lower. Figure 3-36 illustrates the weight versus output power. The lower curve is possible, depending on the success of future technological developments in the area of lightweight collectors.

The efficiency of Helix TWTs operating at saturations is illustrated in Figure 3-37. The multistage collector also provides greater efficiency for backed-off operation.

20 GHz Coupled Cavity TWTs

Coupled cavity TWTs would be considered for satellite high power amplifiers requiring more than 100 watts output at saturation. In the range between 100 and 300 watts, coupled cavity TWTs will cost approximately $100K per TWT with a nonrecurring cost which would vary from $500K to $1,000K.

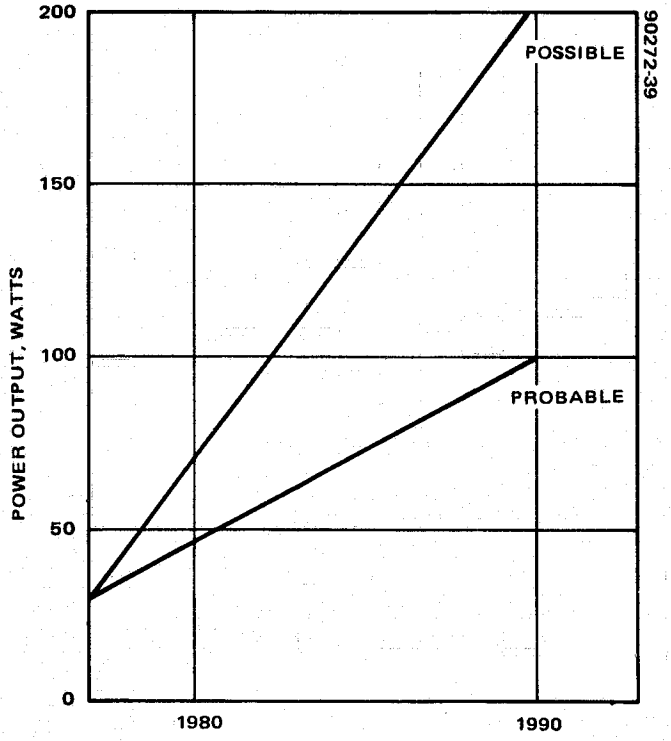

FIGURE 3-33. OUTPUT POWER RANGE FOR 20 GHZ HELIX TWT

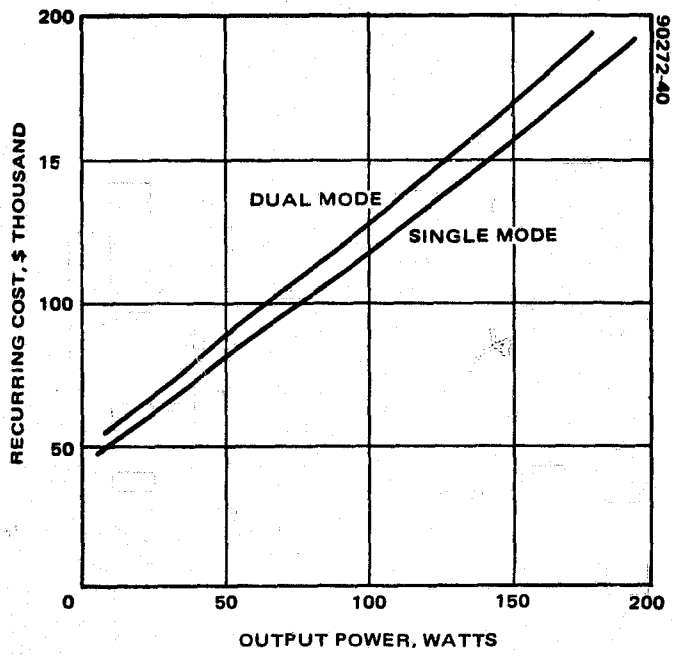

FIGURE 3-34. RECURRING COST VERSUS OUTPUT POWER-HELIX TWT

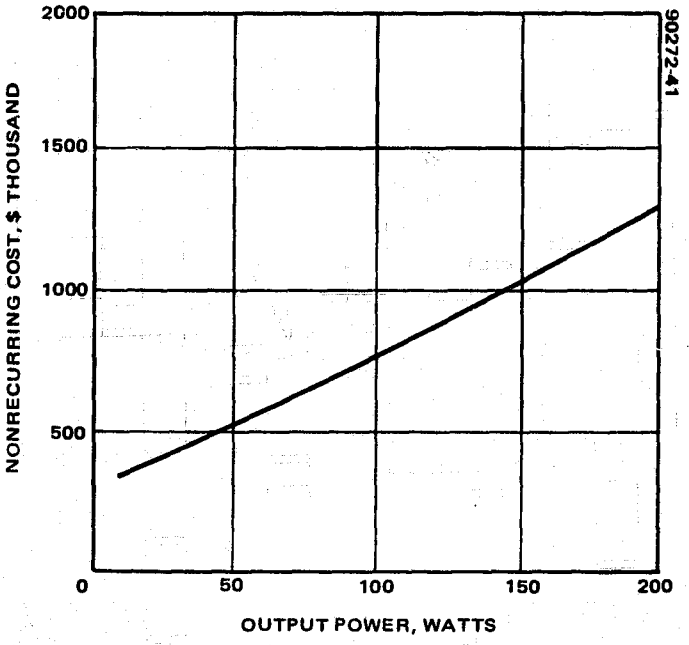

FIGURE 3-35. NONRECURRING COST VERSUS OUTPUT POWER-HELIX TWT

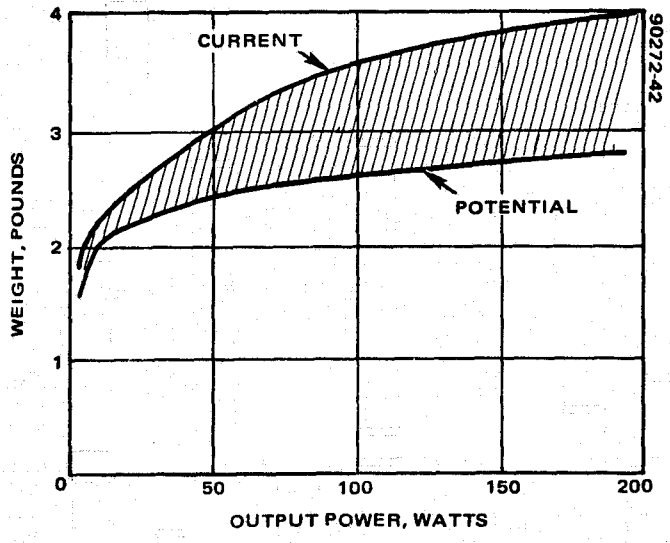

FIGURE 3-36. WEIGHT VERSUS OUTPUT POWER-HELIX TWT

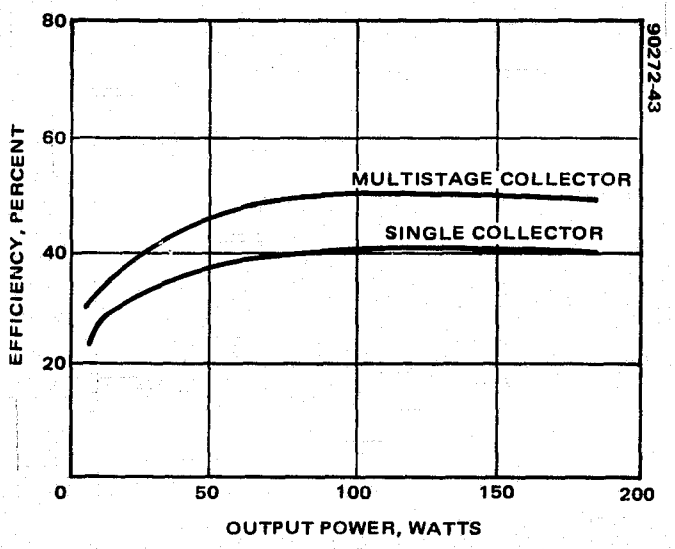

FIGURE 3-37. EFFICIENCY VERSUS OUTPUT POWER-HELIX TWT

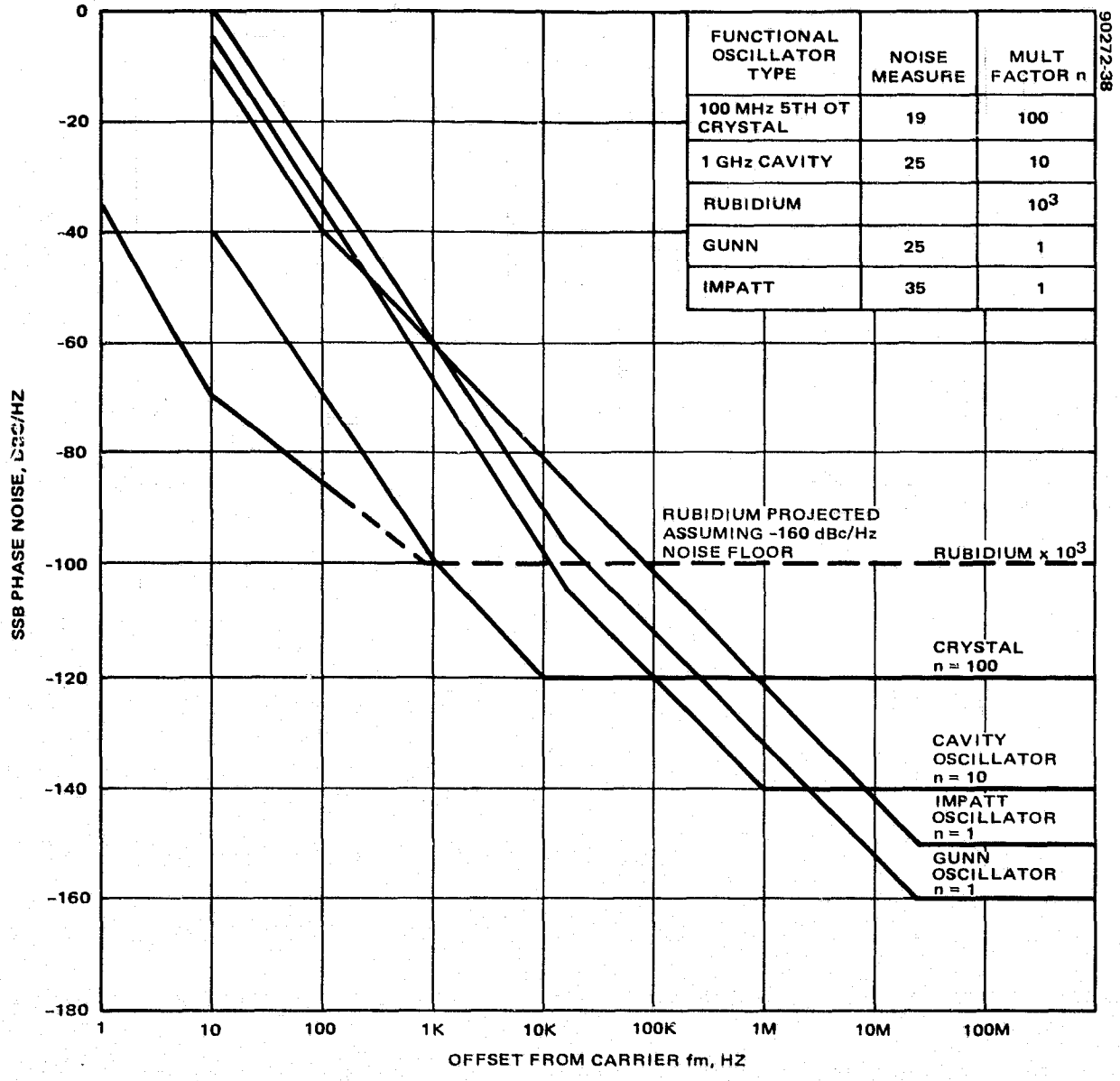

FIGURE 3-38. OSCILLATOR NOISE FROM SOURCES MULTIPLIED BY 10 GHZ

The weight of the TWT would be between 18 and 20 pounds. Efficiency would be between 40 and 45 percent for a TWT designed for a bandwidth equal to 5 percent of the carrier frequency. A requirement for a 10 percent bandwidth would decrease the efficiency; however, for the systems specified for this study, there is no requirement for bandwidths greater than about 5 percent.

3.4.4 Frequency Sources

Figure 3-38 shows typical relative noise performance of various types of oscillators after frequency multiplication to 10 GHz. A basic noise floor of -160 dBc/Hz is assumed for each fundamental oscillator. A practical local oscillator would obtain a compromise between high and low offset noise by phase locking a Gunn diode oscillator to a crystal or possibly rubidium reference oscillator. Adjustment of the loop bandwidth to the crossover point for the device chosen produces an overall noise spectrum controlled by the reference oscillator within the loop bandwidth where the noise performance of this oscillator is superior, and by the Gunn oscillator outside the loop bandwidth where the reverse is true.

The stability of the phase locked system is controlled by the reference oscillators. Typical stabilities are 5×10^{-11} per day for crystal oscillators and 10^{-11} to 4×10^{-11} per month for rubidium standards.

3.5 SATELLITE ANTENNAS

The satellite multispot beam antenna is perhaps the most critical technology item in an 18 and 30 GHz satellite system. It is this element which provides the great increase in spectrum capacity by beam-to-beam frequency reuse, and provides the high gain which compensates for the increased rain degradation at these frequencies. Also, the multispot beam antenna design is specifically and intimately related to the concepts being considered. For these reasons, an extensive analysis of the relation of the antenna performance characteristics such as gain, off axis scan loss, sidelobe performance, and beam isolation to the antenna design parameters has been performed. This analysis is reported in Appendix A.

The weight and cost of reflectors is given as a function of diameter in Figure 3-39 for offset parabolas made of aluminum honeycomb covered with graphite phase sheets.

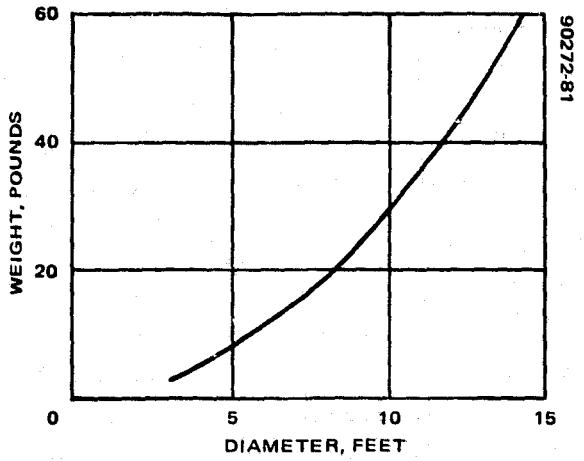

a) WEIGHT OF REFLECTOR

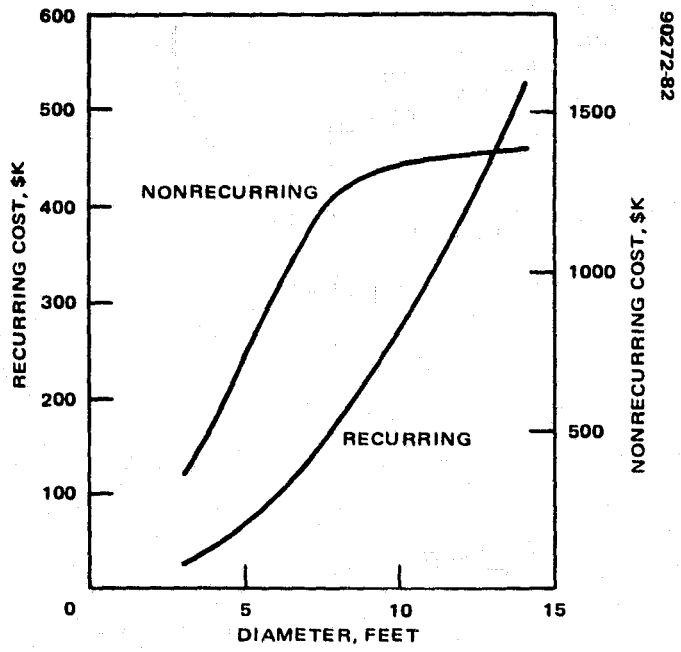

b) COST OF REFLECTOR

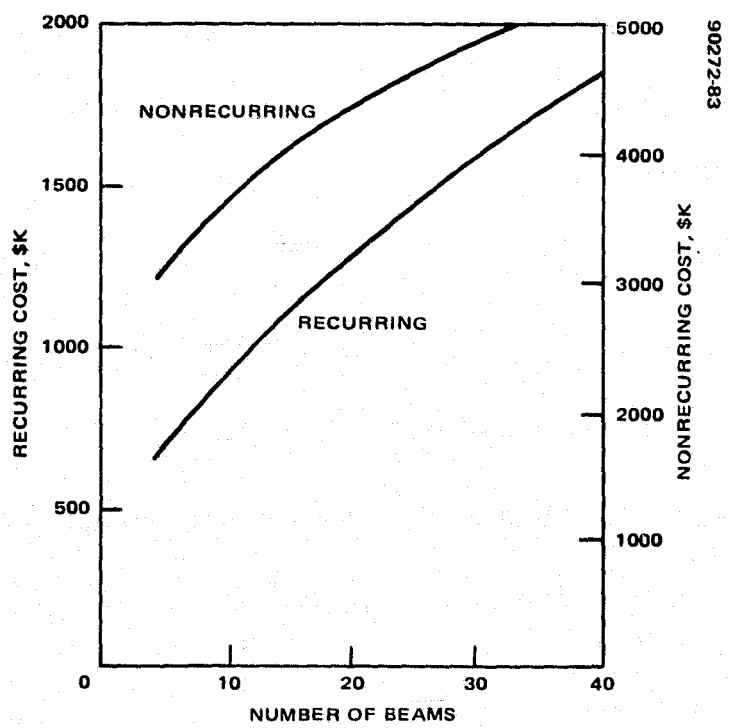

c) ANTENNA MICROWAVE COSTS

FIGURE 3-39. WEIGHT AND COST OF REFLECTORS AS A FUNCTION OF DIAMETER

3.6 RAIN ATTENUATION

Rain attenuation is a major problem which affects the 18 and 30 GHz bands more severely than at the lower communication frequencies used heretofore for satellite communications. Figure 3-40 shows the models used in this study to estimate the rain attenuation as a function of propagation reliability for the system concepts discussed in Sections 4 and 5. Table 3-30 presents the baseline rain attenuation statistics provided by NASA/LERC for single site stations. Table 3-31 presents these statistics for diversity sites. A discussion of the status of rain attenuation statistics and models is included as Appendix B.

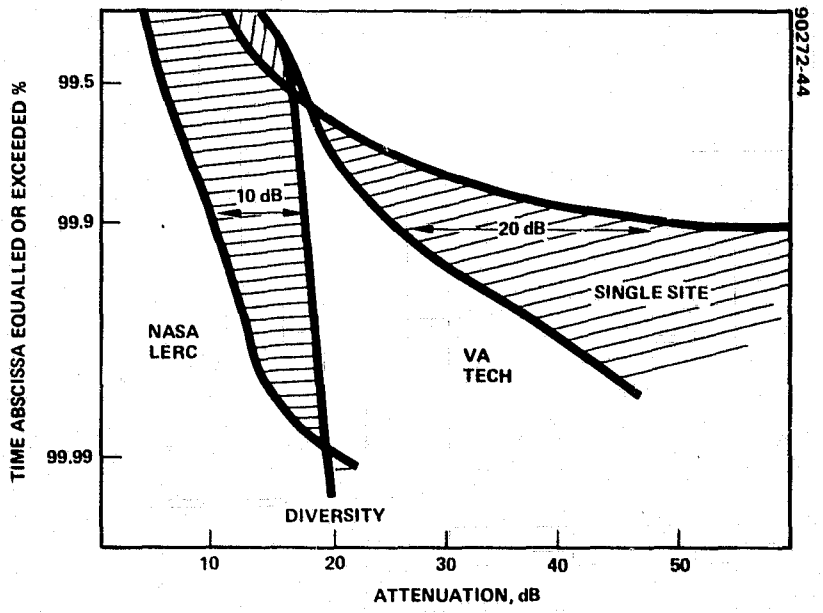

FIGURE 3-40. ATTENUATION STATISTICS COMPARISON– ATLANTA, f = 30 GHZ

TABLE 3-30. ESTIMATES FOR SINGLE STATION RAIN MARGINS–NASA/LeRC

Location \ Rain Reliability*	99.5		99.9	
	20	30	20	30
Atlanta	6.49	14.07	26.46	51.48
Chicago	4.85	10.67	11.79	27.55
Cleveland	5.25	11.51	13.50	24.36
Dallas - Ft. Worth	4.45	9.91	23.54	46.17
Denver	1.98	4.61	7.88	16.64
Kansas City	5.09	11.21	22.78	44.66
Los Angeles	2.91	6.76	7.66	16.49
Miami	8.66	18.55	38.15	72.66
New York	6.53	14.19	13.86	28.53
San Francisco	4.12	9.26	8.40	17.94
Seattle - Tacoma	8.04	17.52	13.41	27.99

*Assumes equal probabilities on uplink and downlink; i.e.,

Combined reliability with respect to rain = (Rel. uplink) (Rel. downlink)

TABLE 3-31. ESTIMATES FOR REQUIRED RAIN MARGINS FOR TWO-STATION DIVERSITY–NASA/LeRC

Location \ Rain Reliability*	99.5		99.9		99.95		99.99	
	20	30	20	30	20	30	20	30
Atlanta	2.68	5.03	5.07	10.10	6.29	12.75	10.18	20.37
Chicago	2.37	4.31	3.93	7.71	6.79	9.51	8.11	16.21
Cleveland	2.50	4.62	4.46	8.85	5.41	10.86	7.91	15.81
Dallas - Ft. Worth	2.07	3.64	4.20	8.27	5.54	11.10	11.42	22.11
Denver	1.60	3.64	4.16	8.22	3.76	7.31	6.57	12.82
Kansas City	2.28	4.11	4.43	8.75	5.60	11.19	10.25	20.45
Los Angeles	1.92	3.35	3.38	6.64	4.38	8.68	6.74	13.59
Miami	2.90	5.52	5.98	11.99	7.64	15.46	16.60	32.65
New York	2.99	5.72	5.21	10.50	6.24	12.64	8.87	17.87
San Francisco	2.24	4.05	3.97	7.83	4.90	9.78	7.03	14.20
Seattle - Tacoma	3.74	7.53	6.36	13.03	7.52	15.43	10.15	20.78

*Assumes equal probabilities on uplink and downlink; i.e.,

Combined reliability with respect to rain = (Rel. uplink) (Rel. downlink)

3.7 BIBLIOGRAPHY

TWTs

1) Sherba, "Designing High Efficiency TWT's," Microwaves, July 1973.

2) Kaisel, "Microwave Tube Technology Review," Microwave Journal, July 1977.

IMPATTs

1) Midford, et al, "New Solid State Components for Millimeter Wave Systems," Microwave Journal, November 1971.

2) Baprawski, et al, "Phase Locked Solid-State MM-wave Sources," Microwave Journal, October 1976.

3) Day, "Gunn Oscillators – A Decade Later," Microwave Systems News, April 1978.

4) Kramer, "Solid-State Technology for Millimeter Waves," Microwave Journal, August 1978.

FETs

1) Strid and Duder, "Intermodulation Behavior of GaAs Power FETS," IEEE International Microwave Symposium, San Diego, California, 1978.

2) Krumm, et al, "A 30-GHz GaAs FET Amplifier," IEEE International Microwave Symposium, San Diego, California, 1978.

3) Cuccia and Ho, "The Impact of the FET on the Satellite Transponder – A Technology Perspective," AIAA 7th Communications Satellite Systems Conference, Sand Diego, California, 1978.

4) Akinaga, et al, "FET Low Noise Amplifier for Satellite Communications," AIAA 7th Communications Satellite Systems Conference, San Diego, California, 1978.

5) Cooke, "Microwave Field Effect Transistors, 1978," Microwave Journal, April 1978.

6) Turner, "The Versatile FET Expands Its Horizons," Microwave Systems News, February 1978.

7) Technical Staff, "GaAs FETS Market and Technology Review," Microwave Journal, February 1978.

8) DiLorenzo, "GaAs FET Development – Low Noise and High Power," Microwave Journal, February 1978.

Parametric Amplifiers

1) Nussbaum and Sard, "Broadbanding a Ku-Band Parametric Amplifier," Microwave Journal, November 1977.

2) Wheelan, "Present and Future Millimeter Wave Pumped Paramps", 6th European Microwave Conference, 1976.

3) Lopriare, et al, "ESA Activities for Millimeter Wave Space Communications", AIAA 7th Communications Satellite Systems Conference.

Mixers

1) Cardnasmengs, "New Diodes Cut the Cost of Millimeter-wave Mixers", Microwaves, September 1978.

2) Kelly, "Low Noise Millimeter Wave MIC Mixer", IEEE Transactions on Microwave Theory and Techniques, November 1976.

Frequency Sources

1) Hamilton "FM and AM Noise in Microwave Oscillators," Microwave Journal, June 1978.

Microwave Switches

1) Gaspari, et al, "Microwave GaAs FET Switching", Hughes Aircraft Company Space and Communications Group, El Segundo, California, MTT-s International Microwave Symposium Digest, June 1978.

Passive Components

1) Raue, "High Performance Millimeter Wave Receiver and Transmitter Component Development", AIAA Tech Communications Satellite Conference, San Diego, California, 1978.

Related Systems

1) Solman, et al, "The Ka-Band Systems of the Lincoln Experimental Satellites LES-8 and LES-9", AIAA 7th Communications Satellite Conference, San Diego, California, 1978.

2) O'hara, et al, "The Satellite Transponder Performance for the Experimental Communications Satellite (ECS)", AIAA 7th Communications Satellite Conference, San Diego, California, 1978.

Baseband

1) A.S. Acampora and R.E. Langseth, "Baseband Processing in a High-speed Burst Modem for a Satellite-switched TDMA System," Fourth International Conference on Digital Satellite Communications, 1978, p. 131.

2) H. I. Mansell, et al, "The M13 and M34 Digital Multiplexers," ICC, 1975, pp 48-5 to 48-9.

Diversity

1) J. R. Jones et al, "An Optical T4 Trunking System," ELECTRO '78.

2) J.R. Jones and D.F. Hemmings, "Optical Fiber T-Carrier Transmission Systems," NTC '78.

3) C.R. Patisaul, "Performance Predictions for a High-speed Digital Optical Cable Video Trunking System," ICC '78.

4) L.P. Yeh, "Fibre-Optic Communication Systems," Telecommunications, September 1978, pp. 33-38.

5) T. Watanabe et al, "Space Diversity System for TDMA Satellite Links," Fourth International Conference on Digital Satellite Communications, 1978, p. 319.

6) J. Wyatt, "Fiber Optic System for Satellite Intrafacility Links," Harris Corporation, February 10, 1978.

7) P. Brostrup-Jensen et al., "WT4 System," ICC '78.

8) K.C. Kao and M.E. Collier, "Fibre-Optic Systems in Future Telecommunication Networks," Telecommunications, April, 1977.

3.8 REFERENCES

1) "High Speed TDMA Terminal Model 1003," Digital Communications Corporation.

2) K. Miyauchi, et al, "Digital Techniques for Domestic Satellite Communication System of NTT," AIAA 78-601, 1978.

3) J.D. Barnla and F.R. Zitzmann, "Digital Communications Satellite System of SBS," EASCON '77.

4) P. N. Sargeaunt, "A 120 Mbit/s QPSK Modem for TDMA Applications," ICC 1977.

5) J. Ramasastry, et al, "Advanced Westar SS/TDMA System," 4th Int. Conf. on Dig. Sat. Commun., 1978.

6) M. Washio and T. Katoh, "Experimental Study on a New 1.6 GBPS 16-Level APSK Modem," NTC 1977, pp. 05:6-1 to 05:6-6.

7) D. F. Horwood, et al, "Experimental 2 GBPS MM Wave System and 4 GBPS QASK Modulator," ITC 1978, pp. 521-530.

8) L. J. Micheel and G. G. Rabanus, "Integrated Gigabit Logic – State of the Art Assessment and Performance Projections," Proc. IEEE MTT-S, 1978, pp. 50-53.

9) R. C. Eden, "GaAs Integrated Circuits: MSI Status and VLSI Prospects," Proc. IEEE IEDM, 1978, pp. 6-11.

10) C. R. Ryan, "A Multi-gigabit Signal Processing System," Proc. IEEE MTT-S, 1978, pp. 54-57.

11) M. Izutsu, et al, "Broadband $LiNb0_3$ Optical Waveguide Modulator," Technical Digest of 1977 Int. Con. on Integrated Optics and Optical Fiber Communication, pp. 137-140.

4. TRUNK CONCEPTS

This section addresses the design, cost, and technology associated with trunk concepts as they are defined under Task 2 of the SOW.

4.1 TRUNK FUNCTION

The relationship between the user and the trunk satellite communication (Satcom) system analyzed below is illustrated in Figure 4-1. The user collects the data from the subscribers at a central switching office in each city in the network. The subscribers input is in the form of voice, data and video. The user conditions the subscriber data and organizes it into a group of pulse code modulated (PCM) bit streams with each bit stream containing the data for a single city in the network. This data is transferred to the satellite earth station where it is provided as an input to the Satcom system. The Satcom system then transmits the data in each bit stream to the destination city. At the destination earth station the user is provided a set of PCM bit streams, each bit stream containing the data from a single city in the network. The user then distributes this data to the subscribers. For a ten beam trunk, the bit rate of each PCM bit stream is at the DS-4 level, 274 Mbps, although the ability to fit nine 274 Mbps signals in the 2.5 GHz spectrum when frequency division multiple access (FDMA) is used is questionable. The statement of work specifies that all links carry the same bit rate. If more than ten beams are provided, the bit rate of each link drops proportionately to fit the total data at each city within the 2.5 GHz spectrum.

4.2 TRUNK RAIN STRATEGY

There are several options for dealing with the variable rain attenuation associated with the 20/30 GHz bands. Figure 4-2 illustrates the downlink options. In Figure 4-2a the transmitter power is constant at a level consistent with the worst rain fade that the system is designed to cope with. The solar panels must then be sized for this worst case rain fade. For example, if the propagation reliability requirement imposes a 9 dB worst case margin, the panel must be eight times as large as that required for clear weather. The batteries would also be eight times as large because the rain margin is required during eclipse. An alternate approach is illustrated in Figure 4-2b. The transmitted power in clear weather contains a rain margin which is just sufficient to cover very frequent rain fades. The margin to cover infrequent severe rain fades is provided by a high power mode into

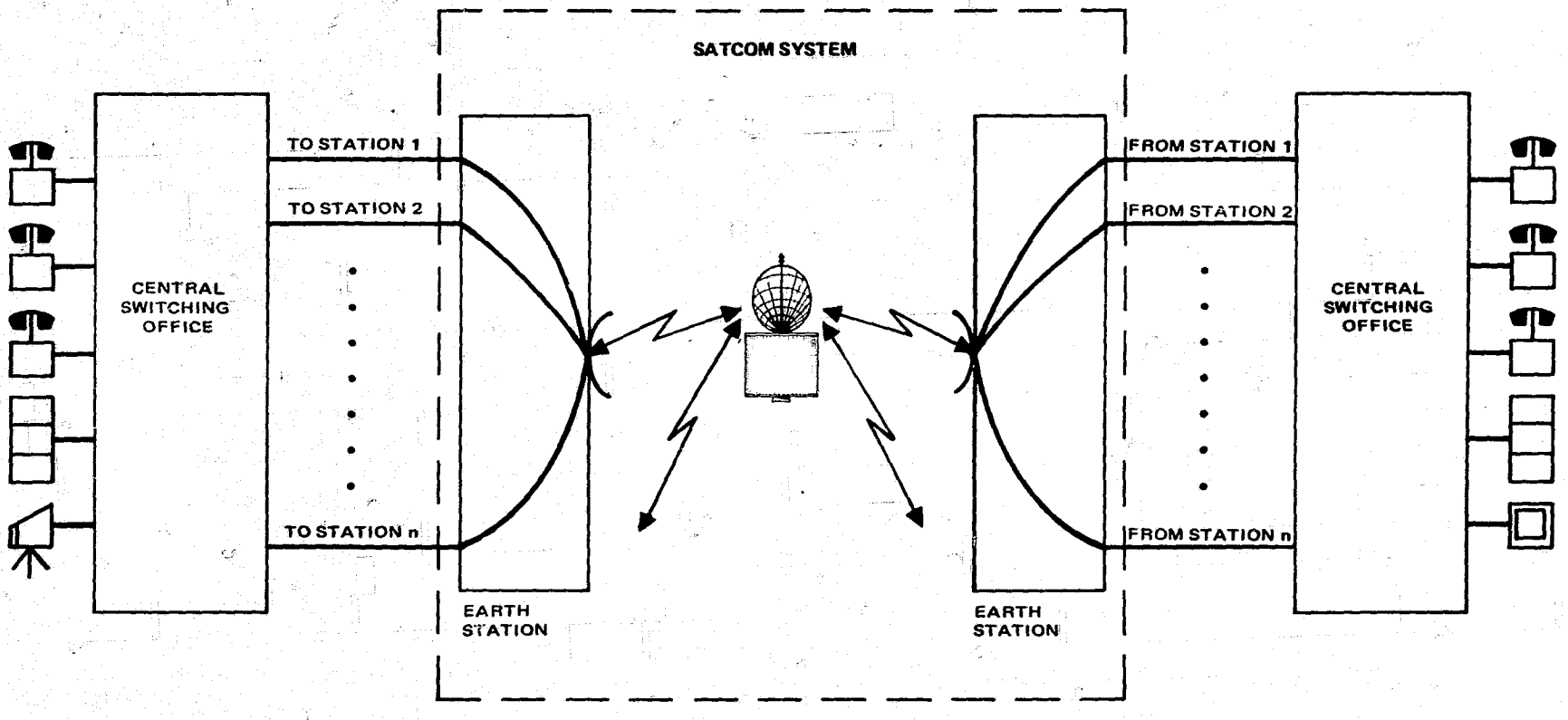

FIGURE 4-1. SATCOM TRUNK FUNCTION CONCEPT

which the transmitter can be switched when necessary. The primary power for these periods of high power operation is supplied by the batteries. By this technique the solar panel size is minimized. As long as the total duration of the high power modes during a day is less than the duration of the longest eclipse, the batteries also do not require as much capacity as they would if a constant rain margin were provided. Two methods of providing the variable rain margin are illustrated in Figures 4-2c and 4-2d. In Figure 4-2c the power output is varied by varying the drive to the high power amplifier. The saving in primary power is limited because an amplifier operating in a backed off condition is inefficient. If the amplifier is solid state essentially no primary running power is saved when the amplifier drive is backed off. If the amplifier is a TWT a considerable power saving occurs if the tube has multiple collectors; however, the efficiency is still less than if a multimode amplifier is operated in saturation as shown in Figure 4-2d. If a TWT is used, the power supply voltages are changed to vary the output saturation level. The use of a solid state amplifier as a multimode amplifier requires investigation. A possible approach is to bypass and switch off the output stages. On/off switching raises reliability questions. It may be possible to reduce output and primary power by changing power supply voltages.

The tradeoff between constant and variable rain margins depends on rain fade statistics which are not available, at least for earth station spatial diversity. In a constant output system the battery is sized to provide the energy required during eclipse. Also, the solar panel capacity is increased to provide sufficient additional power to recharge the battery before the next eclipse (24 hours later). In a variable power system, the energy drained by the high power mode during a 24 hour period must be added to the battery capacity and solar panel recharge capacity. Although, in no case need the battery or solar panel capacity be larger for a multimode satellite than for the constant rain margin case, the saving could become insufficient to justify the added complexity and the degradation of the carrier-to-interference ratio associated with unequal transmitted powers. In the absence of adequate data, the variable rain margin approach was adopted for the trunk baselines. A 2 dB constant margin was assumed to avoid too frequent switching. The appropriate threshold value would depend on the rain fade statistics.

The control of downlink transmitter power would be exercised by the telemetry, tracking, and command (TT&C) station based on power received levels monitored at each receiving station. If received power dropped below threshold at a station it would be assumed that the cause was downlink rain fade because the uplink power received at the satellite is held constant by providing power control at the earth station transmitter. This uplink power control must be provided to maintain the carrier-to-interference ratio as well as to maintain constant drive to the satellite transmitter. If the uplink transmitter power was constant, the signal received by the satellite from a rain impacted terminal would be less than that received from an adjacent terminal experiencing clear weather, and would be reduced relative to the sidelobe in the adjacent beam. Uplink power control is also exercised by the TT&C station based on readings of power monitors at the output of each satellite receiver.

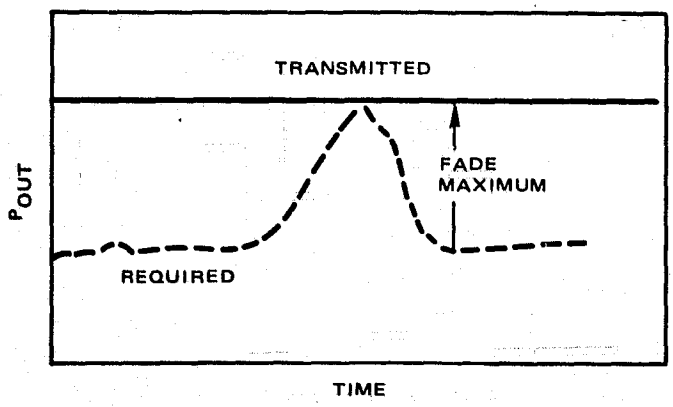

EXCESSIVE BURDEN
ON POWER SYSTEM

9 dB MAX FADE

8x (SOLAR PANEL AND
BATTERY)

90272-2

a) CONSTANT TRANSMITTED POWER

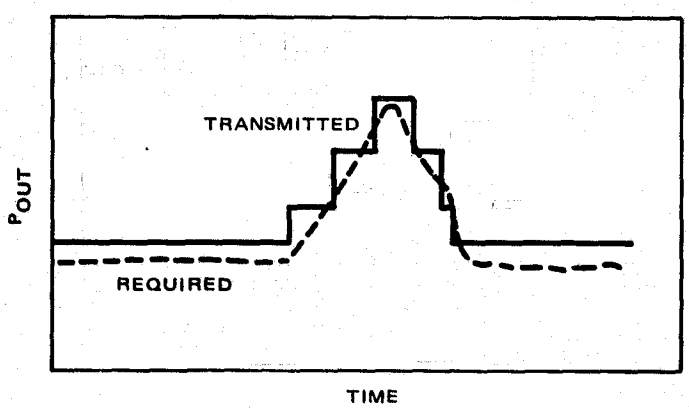

b) VARIABLE TRANSMITTED POWER

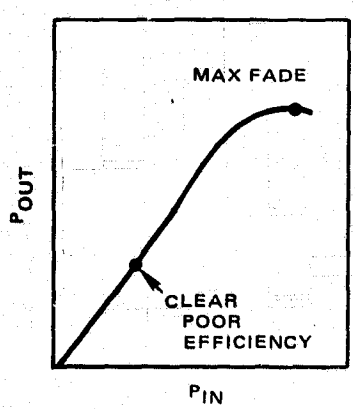

c) VARIABLE TRANSMITTED POWER–DRIVE VARIATION

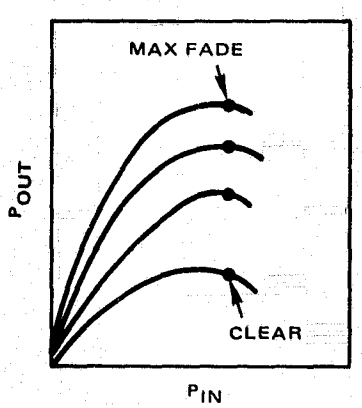

d) MULTIMODE TRANSMITTER

FIGURE 4-2. DOWNLINK RAIN STRATEGY FOR TRUNK CONCEPTS

4.3 SYSTEM RESOURCES OPTIMIZATION

Tradeoff studies were performed to determine a set of RF parameters which would minimize the total system cost of each of the concepts. The parameters which are subject to tradeoff are shown in Figure 4-3. For each of the satellite parameters, the cost associated with a particular value is composed of the several parts shown below (see Table 4-1).

1) Cost of hardware – development plus cost of three satellites.

   The development cost does not include basic device development costs. For example, it is assumed that solid state chips for use in high power amplifiers or low noise amplifiers will have been developed to the expected performance independently of the satellite program; however, the cost of developing an integrated receiver or transmitter using these chips is part of the satellite cost.

2) Weight associated with an RF parameter. The weight of the device adds to the system cost in the following two ways:

   a) The increase in the weight of a device associated with improved performance (for example, higher transmitter power or increased antenna gain) is found from emperical data to be correlated with an increase in the cost of the satellite bus.

   b) The increased communication weight imposes an increase in structural weight, and to some extent attitude control weight. The total satellite bus weight increase leads to increased requirements for stationkeeping and apogee injection fuel. All of these weight increases add to the size of the perigee kick motor. The increase in Shuttle launch weight is thus many times the increase in communication

TABLE 4-1. COST OF ON-ORBIT COMMUNICATION PAYLOAD

Cost = communication payload cost + satellite bus cost + STS launch cost

Satellite bus cost = 0.0290 x communication payload weight
+ 0.0022 x communication payload power (BOL)
+ 19.2
= 2.00 x communication payload weight
+ 0.394 x communication payload power
+ 865

$$\text{STS launch cost} \approx \frac{6 \times \text{satellite weight (EOL)}}{6500 \text{ lb}} \times \$34.5 \text{ M}$$

Applying $K_1, K_2 \ldots K_6$: for three satellites in orbit

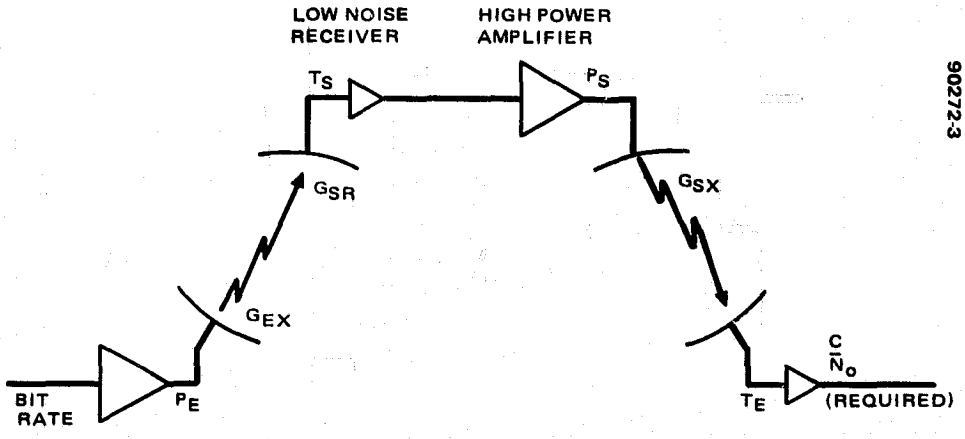

FIGURE 4-3. COST TRADEOFF PARAMETERS

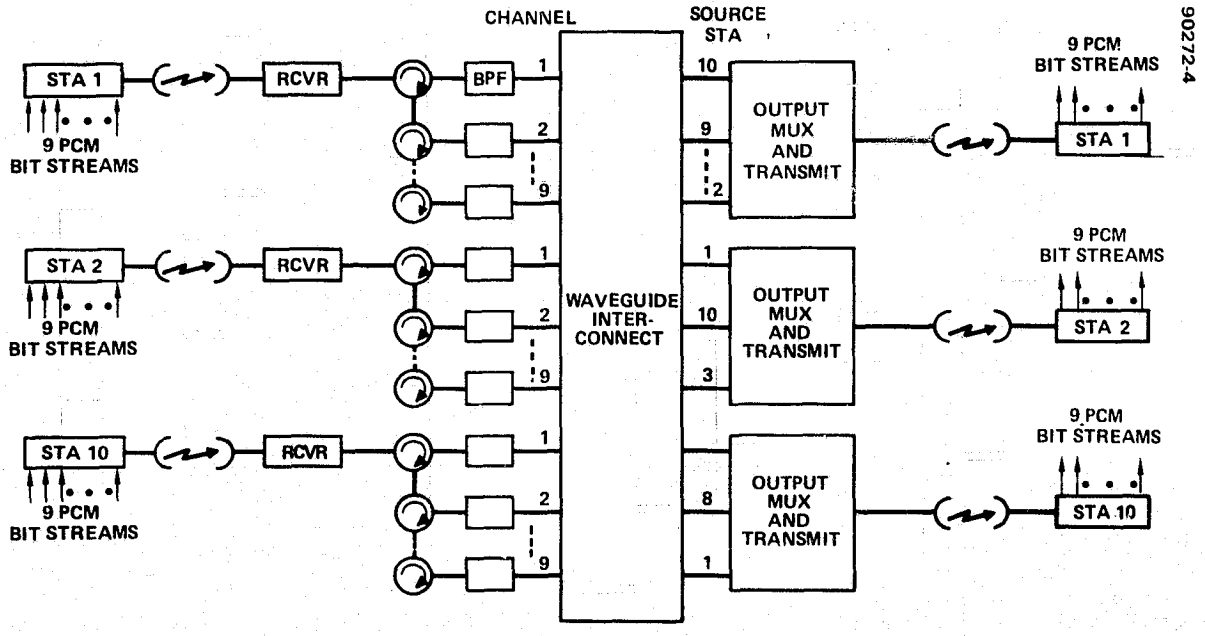

FIGURE 4-4. TEN STATION FDMA TRUNK

payload weight. The cost of a Shuttle launch is assumed to be $530 per pound placed in low earth orbit in 1978 dollars.

When the factors mentioned above are taken into account, the total incremental cost attributable to a 1 pound increase in communication payload weight is approximately $48,000 per pound for three satellites in orbit. Of course, this assumes that the fraction of the Shuttle weight capability used by the vehicle is at least as great as the fraction of the Shuttle payload bay length occupied by the vehicle. It is good design practice to make the weight and length fractions approximately equal to take advantage of the full Shuttle capability associated with the launch cost. In this case, the cost of weight used in the tradeoff is valid.

3) Cost of satellite power – An increase in power supplied to the communication system adds to the system cost in three ways:

   a) Increased power requirements add to the cost of the satellite solar panels, batteries, and associated electronics.

   b) The increased power system weight adds to the cost and weight of the satellite structure.

   c) The increased weight associated with the increased power increases the Shuttle launch cost.

When the above factors are taken into account, the cost of a single spacecraft in orbit is increased by $6000 for a spinning satellite and $4200 for a body stabilized satellite per incremental watt of power supplied to the communication payload. When a multimode transmitter is used, the power cost is based on low power mode operation; however, the cost of the additional battery capacity for the high power periods must be included.

The tradeoff model varies satellite RF parameters and computes sets of earth station parameters which are able to provide the required link performance. For each set of RF parameters, the cost of the earth station hardware associated with the RF parameters is added to the satellite cost discussed above. The earth station cost depends on the number of stations. The set of parameters which leads to the lowest total system cost is then selected. In practice, the selection of parameters is modified to reflect uncertainty in the cost models for the device. For example, the cost trades indicated larger earth station antennas than those selected would be optimum; however, because the decrease in system cost was modest and there is considerable uncertainty in the cost model for large antennas at these frequencies, a less than optimum antenna size was chosen.

4.4 TEN STATION FDMA TRUNK

A block diagram of the ten beam FDMA trunk is shown in Figure 4-4. Each of the nine pulse code modulated bit streams (one for each other city in the network) is quadrature phase shift key (QPSK) modulated on a separate

carrier at the earth station. The nine carriers are transmitted to the satellite where they are processed in a common receiver. The receiver amplifies them to as high a level as permitted by considerations of intermodulation distortion, and downconverts to the downlink frequency band. The nine carriers are then separated in an input multiplexer. Each carrier is then connected by a hard-wired waveguide interconnect to the appropriate downlink transmitter. A channel assignment can be developed so each of the nine carriers arriving at a downlink transmitter is in a separate frequency channel. The nine carriers are transmitted on the downlink beam to the receiving station, which demodulates the carriers and provides the resulting bit streams to the user.

The space segment of the trunk system includes three satellites: an operational satellite, an on-orbit spare, and a ground spare. Each beam contains a single earth station which has two sites approximately 15 km apart to provide spatial diversity to minimize rain fades. The optimum separation distance cannot be determined from the data currently available on rain attenuation.

The ground rules for this study are: 1) complete interconnectivity be provided, and 2) all links have the same capacity. The baseline system is to have ten beams, a bit error rate (BER) of 10^{-6}, and a propagation reliability of 99.9 for a one-way link.

4.4.1 Trunk FDMA Performance Requirements

The baseline performance requirement is for a bit error rate (BER) of 10^{-6} (Table 4-2). A degradation of 2.5 dB is assessed for co-channel interference from adjacent beams.* An impairment margin of 3.0 dB was provided for satellite distortion and demodulator performance. A bit rate of 215 Mbps was assumed for FDMA, even though 288 MHz are allocated to each channel. This was done because of the uncertainty of whether contiguous multiplexers can be fabricated at this frequency with acceptable losses.

TABLE 4-2. TRUNK FDMA PERFORMANCE REQUIREMENTS

BER = 10^{-6}	→	$\frac{E_b}{N_o}$ = 10.6 dB
15-17 dB $\frac{C}{I}$ ratio	→	$\Delta\frac{E_b}{N_o}$ = 2.5 dB
Impairments margin	→	3.0 dB
Bit rate 215 Mbps	→	83.3 dB
Required C/N_o		99.4 dB

*J. J. Spilker, Digital Satellite Communications, Prentice Hall, 1977.
A. S. Rosenbaum, Bell System Technical Journal, February, 1969.
V. K. Prabhu, Bell System Technical Journal, March, 1969.

4.4.2 FDMA Link Budget

The link budget for a 215 Mbps channel in the ten beam FDMA trunk is given in Table 4-3. This budget is for a New York to Atlanta link. The uplink budget is for the maximum rain case because only the saturated power of the earth station transmitter is significant. The downlink budget shows both the clear weather case and the maximum rain case, since the low power mode drives the satellite solar power requirements and the high power mode sizes the satellite transmitters. The clear weather budget provides 2 dB for rain attenuation to prevent too frequent mode switching and to avoid operation in the high power mode for extended periods of time, which would defeat the purpose of the multimode transmitter. The earth station and satellite EIRP and G/T are detailed in the section that follows. As might be expected for a system with three satellites and ten earth stations, it is desirable to have a strong uplink to minimize degradation of the downlink. The link shown is one of the more difficult links in the system because it combines relatively high rain attenuation and relatively low satellite antenna gain because of off axis scan loss. Sizing the system based on this link is somewhat pessimistic.

4.4.3 Satellite EIRP and G/T – FDMA Trunk

In the baseline FDMA design each channel is amplified by an individual GaAs FET amplifier (Figure 4-5). The saturated power in the high power mode is 0.7 watts if the system is designed for 99.9 percent. The power output in the low power mode is 0.34 watt. The output losses were specified by NASA and are based on the performance of the Japanese Communication Satellite.

TABLE 4-3. TRUNK FDMA LINK BUDGET

Parameters	Uplink		Downlink		
	99.9%	99.99%	99.9%	99.99%	Clear Weather
EIRP, dBW	77.9	88.1	48.7	54.2	44.8
Pointing loss – transmit	0.4		0.4		
Atmospheric loss	0.7		1.0		
Rain attenuation	10.2	20.4	5.1	10.2	2.0
Path loss	212.9		210.2		
Polarization loss	0.2		0.2		
Pointing loss receive	0.6		0.2		
G/T	25.1		40.1	39.7	40.9
K	228.6		228.6		
C/N_0	106.6	106.6	100.3	100.3	100.3
Uplink noise degradation				0.9	
C/N_0 (link)				99.4	
C/N_0 (required) = 10.6 (E_B/N_0) +2.5 (interference) + 10 log 215×10^6				96.4	
Impairments margin				3.0	

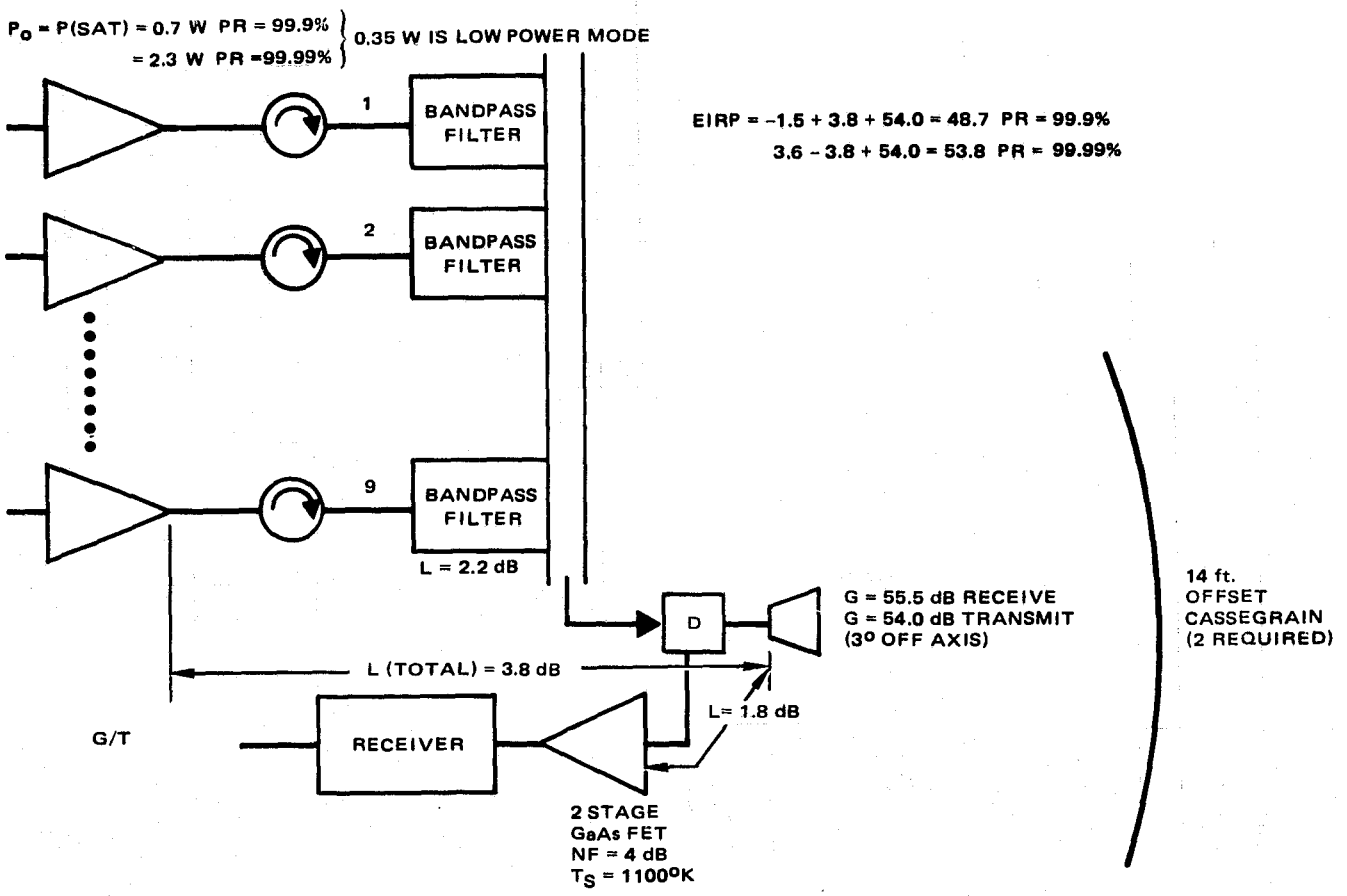

FIGURE 4-5. SATELLITE EIRP AND G/T – FDMA TRUNK

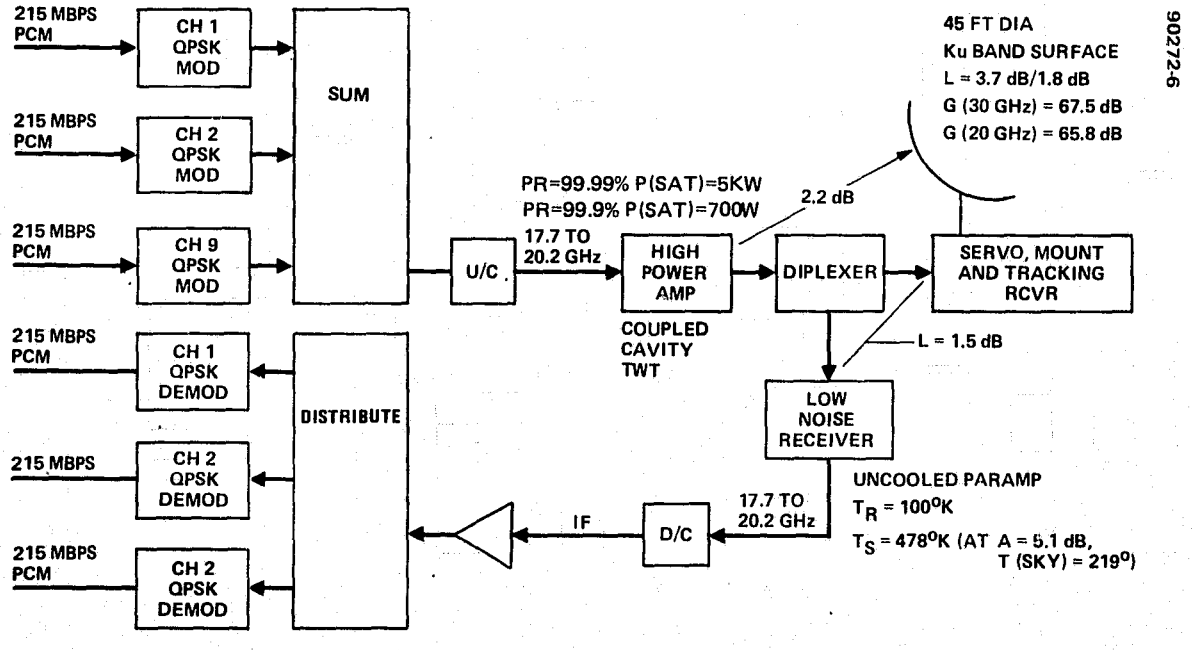

FIGURE 4-6. EARTH STATION TEN BEAM FDMA TRUNK

The 2.2 dB loss for the output multiplexer is probably pessimistic because the channel data rate is only 215 Mbps, despite an allocation of 288 MHz per channel. This data rate allows relatively relaxed out of band rejection requirements which might permit a significantly lower loss in the output filter than that shown. The antenna gains at transmit and receive are 2.5 and 4.5 dB less than theoretical gain for a 14 foot antenna and 55 percent efficiency because of increased surface loss at these frequencies and off axis scan loss. The surface error achievable at reasonable cost is estimated at about 0.020 inch rms, leading to a surface loss of 0.8 dB at 20 GHz and 1.7 dB at 30 GHz. The off axis scan loss is 1.7 dB at 20 GHz and 2.8 dB at 30 GHz. The system receive temperature of 1100°K is based on a 4 dB noise figure for the two-stage GaAs FET receiver and an antenna temperature of 290°K.

4.4.4 Earth Station Ten Beam FDMA Trunk (Figure 4-6)

RF optimization studies indicate that a relatively large earth station antenna (45 foot diameter) is optimum. The gain of this antenna is reduced by 3.7 dB at 30 GHz and 1.8 dB at 20 GHz by surface losses. These losses are for a surface precision of 0.035 inch rms, including all effects, and F/D = 0.35. The earth station high power amplifier (HPA) saturated power is 700 watts if the system is designed for 99.9 percent propagation reliability and 5 kW for 99.99 percent. This power allows for nine 215 Mbps channels and a 6 dB output power backoff to reduce intermodulation distortion to an acceptable level. The antenna has limited motion monopulse autotracking capability with an accuracy of 0.006°, 3σ. An uncooled parametric amplifier was selected as the low noise amplifier. A thermoelectrically cooled parametric amplifier would reduce the receiver temperature by about 30°K, but when the noise due to input loss and the increased sky noise in the presence of a rain which produces a 5.1 dB fade are taken into account, this improvement has a small effect on system noise temperature.

The input pulse code modulated (PCM) bit streams at 215 Mbps are each modulated on individual carriers by a QPSK modulator. The carrier spacing is 278 MHz.

4.4.5 Satellite Repeater – FDMA Trunk

The satellite repeater is shown in Figure 4-7. The FDMA receiver is single conversion. Its output is nine carriers equispaced between 17.7 and 20.2 GHz. The input multiplexer is in an odd-even configuration for ease of assembly. The output of the filters are connected to the appropriate downlink amplifier by a waveguide interconnect. Single conversion was chosen because dual conversion would have required an upconverter in each of the 90 channels. A major question is that of transmitter redundancy. In a 12 or 24 channel CONUS beam satellite, the loss of a transmitter reduces the capacity of the system but does not affect the interconnectivity of users. In this system the loss of a transmission channel loses a link. If complete interconnectivity of the cities is required, no transmission channel can be allowed to fail. Table 4-4 gives the probability of all links being available for various redundancy configuration for 7 and 10 years. A GaAs FET amplifier failure rate of 70 failures per 10^9 hours (70 FIT) was assumed, based on manufacturer data at 12 GHz. A 12/9 redundancy was selected for the high power amplifiers.

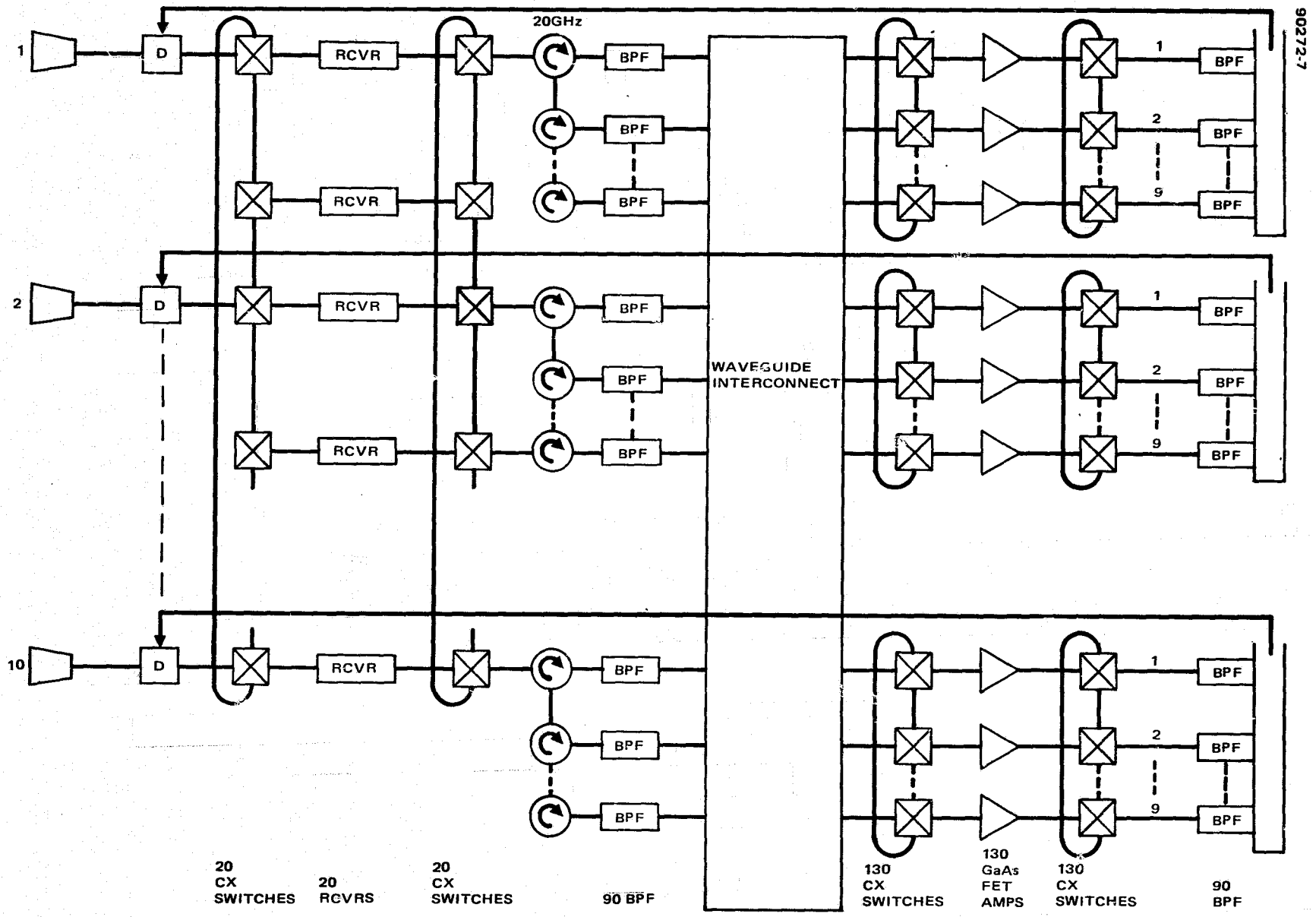

FIGURE 4-7. TEN BEAM FDMA TRUNK REPEATER

TABLE 4-4. HIGH POWER AMPLIFIER REDUNDANCY – GaAs FET RELIABILITY EQUAL TO 70 FAILURES PER 10^9 HOURS (70 FIT). TWO FOR ONE RECEIVER REDUNDANCY

Number Of Beams	Number of Amplifiers Per Beam	Amplifier Redundancy	Probability of No Channels Lost	
			7 Years	10 Years
10	9	None*	0.10	0.05
	9	None	0.169	0.078
	9	12 for 9*	0.612	0.459
	9	12 for 9	0.978	0.956
	9	11 for 9	0.969	0.932
	9	10 for 9	0.842	0.715
	9	5 for 3	0.977	0.953
	9	4 for 3	0.920	0.842
	1	None	0.805	0.725
	1	11 for 10	0.961	0.924
20	19	22 for 19	0.944	0.869
	19	23 for 19	0.957	0.911
	1	22 for 20	0.963	0.898
	1	23 for 20	0.968	0.914
40	39	42 for 39	0.653	0.280
		45 for 39	0.916	0.835
		5 for 3	0.889	0.769

*Nonredundant receivers.

Any of the 12 amplifiers can operate on any of the 9 channels associated with a downlink beam by means of the crossover switches which allow any HPA in the group of 12 to replace any failed HPA in the group. Loss of a receiver leads to loss of a city from the network, so 20 for 10 redundancy is provided; i.e., any of 20 receivers can be switched into any beam. The use of ring around redundancy in this manner may lead to unacceptable losses on either the input or output. A repeater layout is required to estimate the effect of this redundancy implementation on the losses.

4.4.6 Repeater Weight, Power, and Cost Budget

A breakdown of the weight, power, and cost of the components of the satellite FDMA trunk repeater are given in Table 4-5. The power requirement for the GaAs FET HPAs is for the low power mode which is used to size the solar panels. Additional power is available in the spacecraft batteries for high power mode operation up to 120 channel minutes per day.

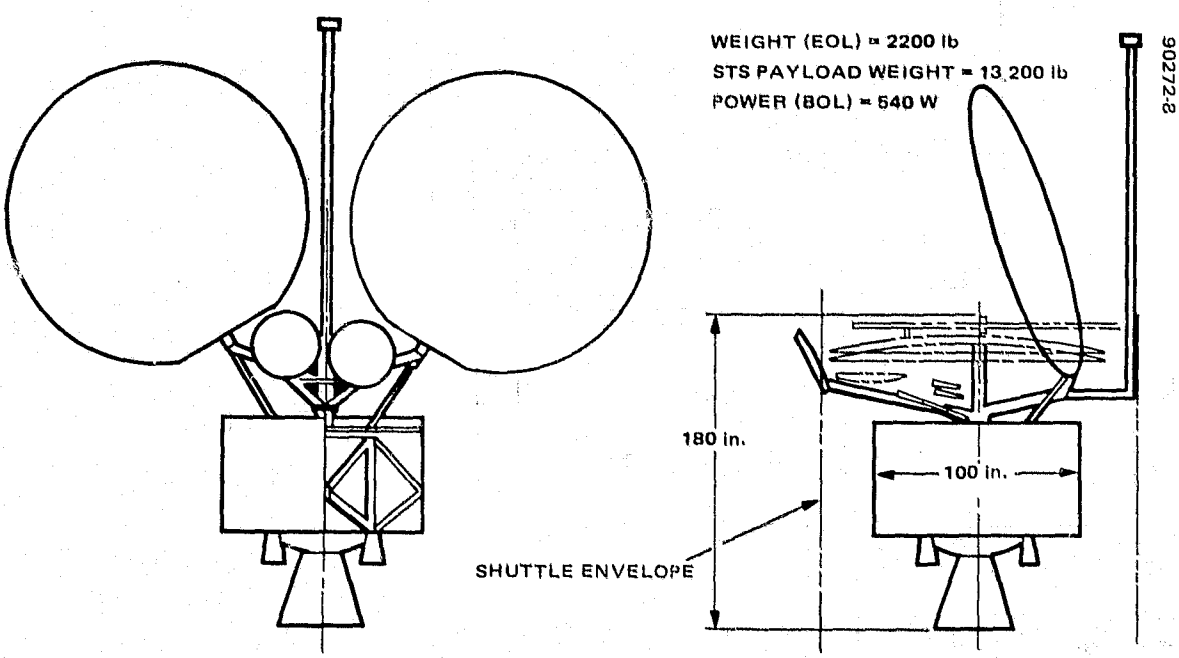

FIGURE 4-8. TRUNK SATELLITE

TABLE 4-5. TRUNK FDMA REPEATER WEIGHT, POWER, AND COST BUDGET

Component	Quantity (Operating + Redundant)	Weight, lb		Power, W		Cost, $K	
		Unit	Total	Unit	Total	Unit	Per Satellite
Redundancy switches (30 GHz)	20	0.30	6.0	–	–	6	120
Receivers	10 +10	2.5	50.0	7	70	150	3,000
Redundancy switches (20 GHz)	20	0.45	9.0	–	–	6	120
Input multiplexer	90	0.82	73.8	–	–	14	1,260
Redundancy switches (20 GHz)	130	0.45	58.5	–	–	6	780
High power amplifiers (0.7 W)	90 + 40	0.74	96.5	3.1*	279	24	3,120
Redundancy switches (20 GHz)	130	0.45	58.5	–	–	6	780
Output multiplexer	90	0.53	47.7	–	–	10	900
Miscellaneous repeater			40.0				1,500
Total hardware			440.0		349		11,580
Labor (Project management controls, test, and integration							1,850
Total recurring – three satellites							40,280
Nonrecurring							7,000
Total							47,280

*Output power = 0.35 watt in clear weather.

4.4.7 Spacecraft Antenna – Ten Beam FDMA Trunk

The components of the ten beam trunk antenna are listed in Table 4-6 with their associated weight and cost. The reflectors are fabricated of graphite over aluminum honeycomb. In addition to the main reflectors, subreflectors, and their supports, the antenna system requires a mechanism to deploy the reflectors and to rotate the main reflectors to provide elevation tracking. Azimuth tracking is accomplished by positioning the despun platform of the dual spin satellite. In addition to the ten feeds for ten communication beams, a set of monopulse tracking feeds provides tracking signals for elevation and azimuth tracking.

4.5 TEN BEAM FDMA TRUNK SATELLITE

The baseline satellite is shown in Figure 4-8. A dual spin configuration was selected as a model; however, a body stabilized spacecraft could also be used. No tradeoff between the two configurations was performed.

TABLE 4-6. SPACECRAFT ANTENNA – TEN BEAM FDMA TRUNK

Component	Weight, lb	Cost ($K)			
		Engineering		Manufacturing	
		Nonrecurring	Recurring	Nonrecurring	Recurring
Two main reflectors; 14 ft diameter	116	1365	250	83	548
Two 3 ft subreflectors	6	340	21	22	8
Structure (including deployment activator)	75	230	60	22	164
Stress, thermal qualification test, and GSE		1260	5	160	30
Total mechanical	197	3195	336	287	750
		Nonrecurring		Recurring	
Microwave					
Independent of N		1520		280	
Dependent on N (N = 10)	15	2250		690	
Total microwave	15	3770		970	
Total antenna	212	7250		2056 (per satellite)	

A number of options are available within the class of dual spin satellites. The spacecraft diameter could be expanded to fill the Shuttle payload envelope diameter to obtain a roll to pitch ratio greater than 1 and, hence, an inherently stable spinner. This is the LEASAT approach. However, even with the 14 foot diameter, the size and location of the antennas would make it difficult to achieve an adequate roll to pitch ratio. Since a 100 inch diameter solar array can easily provide the required power, it is not advantageous to provide the additional structure required by the larger diameter. The resulting configuration is a Gyrostat and requires a more complex attitude control system than the stable spinner configuration.

The solid antenna is folded during launch as shown in Figure 4-8. The subreflectors must also be stored and deployed. The antenna tracks an earth based beacon about two axes. The azimuth tracking motion is provided by the despin of the payload portion of the spacecraft. The elevation tracking motion is provided by the mechanisms which deploy the antennas.

The perigee kick motor (PKM) is integrated into the spacecraft to minimize the length of Shuttle payload bay occupied by the spacecraft. A liquid apogee motor (LAM) is also used for this purpose. Since the time of interest is still many years away, no specific PKM (e.g., SSUS-A) was assumed.

The TT&C subsystem operates at C band during the launch phase and at 20/30 GHz during the operational phase of the mission. Commands

are received on omni antennas. Telemetry is transmitted at 20 GHz over the communication antennas during normal orbital operations. If antenna pointing is lost, telemetry transmission can be commanded to the 20/30 GHz band omni antenna.

The attitude control system primary sensor is the monopulse tracking system associated with the communication antenna. To point the tracking feed boresight at the 30 GHz beacon, the control system varies the angular position of the despun platform which contains the communication payload and varies the angular position of the communications antennas about the deployment axis to null out the monopulse tracking error signals. It is possible that because of thermal distortion, the two antennas will require independent positioning. This would require a second monopulse system as well as an additional axis in the deployment mechanism to provide independent azimuth tracking, since platform despin is common to both antennas.

Although GaAs solar cells are expected to be available in the 1990's, the power system is assumed to use existing solar cell technology, since the characteristics of this technology are well defined and the power requirements of this communication payload are relatively low because of the very high antenna gain. Nickel hydrogen batteries are assumed, allowing an 80 percent depth of discharge and minimizing the battery penalty associated with the multimode transmitter.

The PKM is assumed to be a motor sized for this mission which is integrated into the spacecraft to minimize length and, hence, Shuttle launch cost. An SSUS-A has the capacity required for this mission. An LAM is used for the same reason.

4.5.1 FDMA Trunk Satellite Weight, Power, and Cost Budget

The weight, power, and cost of the satellite subsystems is shown in Table 4-7. The cost, weight, and power estimates of the communication payload were based on the analysis summarized in the previous sections. The cost and weight data for the other subsystems was developed using a model based on communication satellites built or being built by Hughes. This model relates cost and weight to communication payload weight and satellite power requirements. Where appropriate, the data provided by the model was modified to reflect projected technology developments and peculiarities of this mission. The power subsystem weight was changed to reflect the use of NiH2 rather than NiCad batteries, and the use of a dual power mode in the communications high power amplifier which requires additional battery capacity. The weight and cost of the structure were estimated independently of the model to reflect the lighter weight technology used in LEASAT, while using an 8.5 foot satellite diameter rather than the LEASAT 14 foot diameter.

The nonrecurring cost assumes that an existing spacecraft bus is suitable for modification to this mission. In view of the fact that launch would be in the 1990's, this assumption appears reasonable.

TABLE 4-7. TEN BEAM FDMA TRUNK SATELLITE WEIGHT, POWER, AND COST BUDGET

Subsystem	End of Life Weight, lb	Power, W	Cost, $K	
			Nonrecurring	Recurring, Three Satellites
Repeater	440	349	7,000	40,280
Antenna	212	–	7,250	6,168
Communication payload	652	349	14,250	46,448
Telemetry, tracking, and command	72	60	1,580	3 140
Attitude and antenna pointing contract	65	25	1,534	2,023
Power (including losses and margins)	265	98	914	3,390
Structure	1,147	–	1,543	5,210
Propulsion	253	–	2,182	5,489
Total hardware	2,454	587	22,003	65,700
Program management and support			15,551	20,658
Total cost of three satellites at manufacturing			123,278	
G&A and fee			32,217	
Total satellite investment			155,495	

4.6 EARTH STATION COST BREAKDOWN – TEN BEAM FDMA TRUNK

The costs associated with a typical dual site earth terminal in the ten beam FDMA trunk system are shown in Table 4-8.

The cost of the antenna does not include installation or the antenna foundation. These are included in earth station installation and civil works.

Receivers and transmitters are redundant at each of the dual sites. This redundancy could be eliminated by considering the alternate site as providing the redundancy. Then operation would be interrupted only when a failure was in effect at one site and rain degradation was excessive at the other site. When the very large amount of data being handled by these terminals is considered, it appears that the modest cost saving does not justify the added risk. One spare QPSK modem is provided at each site.

The diversity cost is for a system which handles each of the nine input baseband PCM signals before modulation combining. This system is described in Section 3.

4.7 TEN BEAM FDMA TRUNK COST

The total cost of the ten beam FDMA trunk Satcom system is shown in Table 4-9. The space segment sum includes the purchase cost of three satellites and the cost of launching all three. The earth station cost does not

TABLE 4-8. EARTH STATION COST BREAKDOWN, TEN BEAM FDMA TRUNK

Item	Quantity	Cost, $K		
		Unit	Single Terminal	Total Dual Terminal
Antenna (45 ft diameter) (reflector, mount, deicer, and monopulse tracker – limited motion)	1	253	253	506
Receiver (uncooled parametric amplifier, downconverter, IF strip)	2	80	160	320
Transmitter (upconverter, high power amplifier)	2	115	230	460
QPSK modems	10	40	400	800
Controls and monitoring	1		50	100
Miscellaneous hardware			110	220
Diversity switch and links				630
Earth station hardware			1202	3034
Management, System Engineering, Integration and Test, Product Assurance (33%)				1011
Civil work (building, antenna foundation)			150	300
Installation			135	270
Total manufacturing cost				4465
G&A and fee				1161
Total (excluding site costs)				5626

TABLE 4-9. TEN BEAM FDMA TRUNK SYSTEM COST, $M

Item	Cost
Satellite cost (three satellites)	156
Launch cost (three launches)	24
Earth station cost	56
TT&C	15
Total system cost*	251

*Includes G&A and profit.

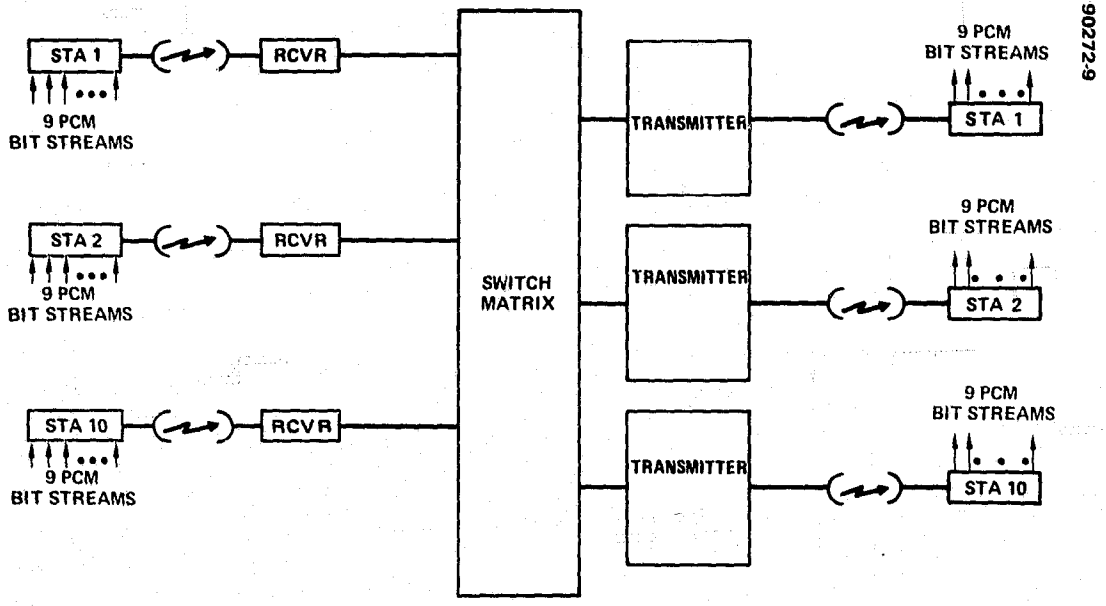

FIGURE 4-9. TEN STATION TDMA TRUNK

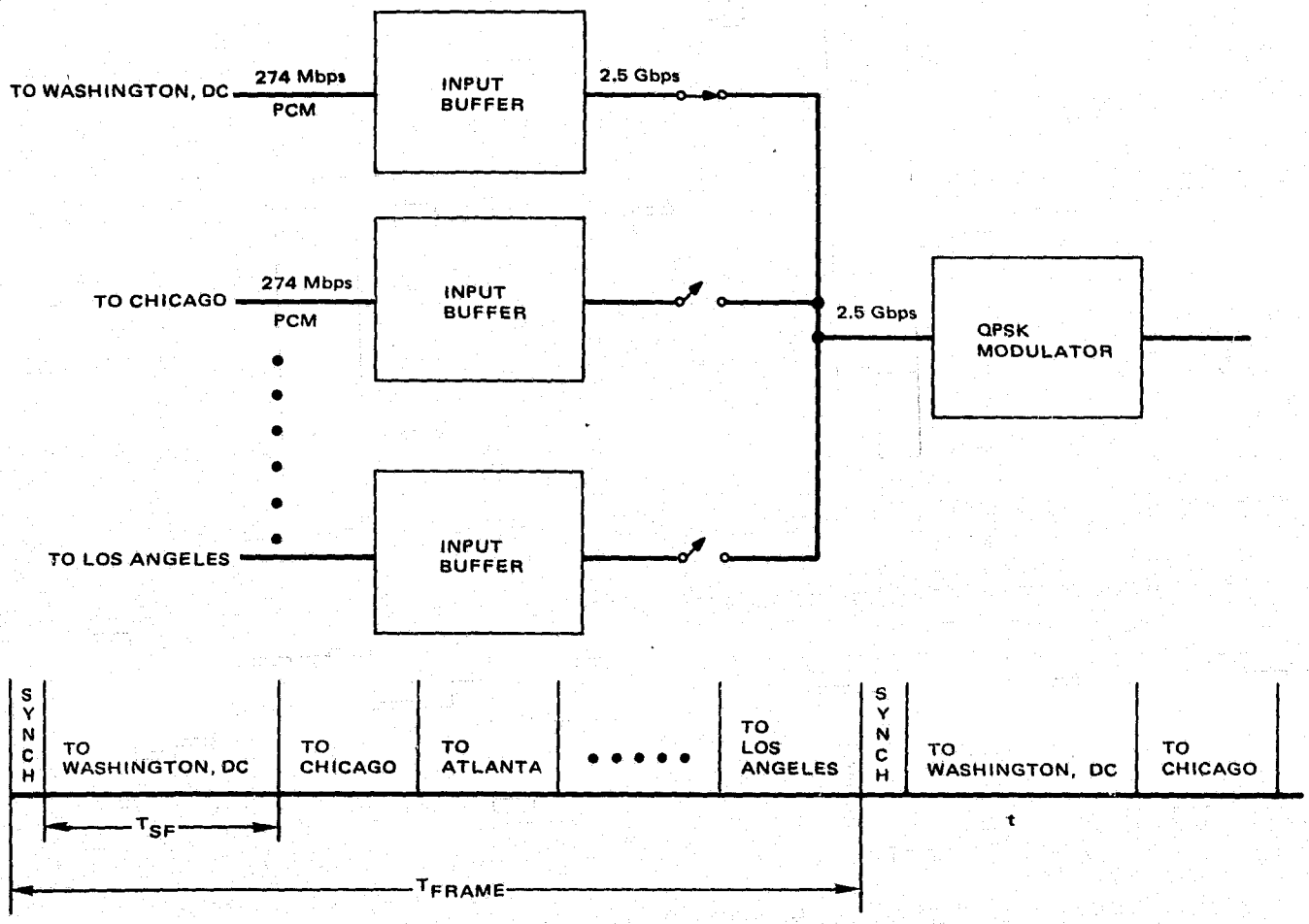

FIGURE 4-10. SATELLITE SWITCHED TDMA MULTIPLEXING

include the terrestrial tail to the user central switching office. The TT&C cost includes the cost of monitoring the effects of rain on both uplink and downlink signals and controlling the earth station and satellite response. All costs include manufacturer's G&A and profit.

4.8 TEN BEAM SATELLITE SWITCHED TDMA TRUNK

A block diagram of the ten beam TDMA trunk is shown in Figure 4-9. In contrast to the FDMA earth terminal which individually modulates each of the nine baseband PCM signals, the TDMA terminal multiplexes the buffered baseband signals to form a single PCM baseband signal at a data rate which is roughly nine times the rate of the input signals (Figure 4-10). The output rate is made slightly higher than the total input rate to allow for guard times, preambles, and synchronization codes. A 10 percent allowance for these requirements is conventional; however, because of the small number of data bursts per frame in this system, somewhat better efficiency can be realized.

The input buffers are filled at the input data rate of 274 Mbps continuously. The input buffers are read out one at a time at the burst rate of approximately 2.5 Gbps. Since each buffer contains data meant for a specific downlink beam, the terminal communicates data to each of the other terminals in the system during each frame.

The 2.5 Gbps signal occupying the 27.5 to 30.0 GHz band is received by the spot beam antenna and amplified and downconverted to IF in the receiver associated with that beam. The satellite switch matrix connects each of the receiver outputs to a different downlink beam. Thus, at any time, each terminal is transmitting to a different receiving terminal. At the end of the subframe the switch matrix reconfigures so that in the next subframe each station communicates with a different station than it did on the previous subframes. Over a frame, each station transmits to every other terminal for a subframe.

4.8.1 TDMA Trunk Link Budget

The trunk TDMA link budget is given in Table 4-10.

In the TDMA concept each beam carries a single RF channel. In the baseline concept, the TDMA carrier is at a data rate equal to nine DS-4 channels (9 x 274.6 Mbps = 2471.4 Mbps). Then, for a 10^{-6} BER (E_6/N_o = 10.6 dB), 2.5 dB for interference degradation, and 3 dB for impairments, the required C/N_O = 110.0 dB. This is 10.6 dB higher than each of the nine 215 Mbps channels in the baseline FDMA trunk. The total data rate per beam is higher for the TDMA trunk because of the absence of guard bands. This is balanced somewhat by the need for guard times between the data bursts.

The earth station G/T decreases by 0.4 dB when the rain attentuation increases to 10.2 dB because of an increase in sky temperature.

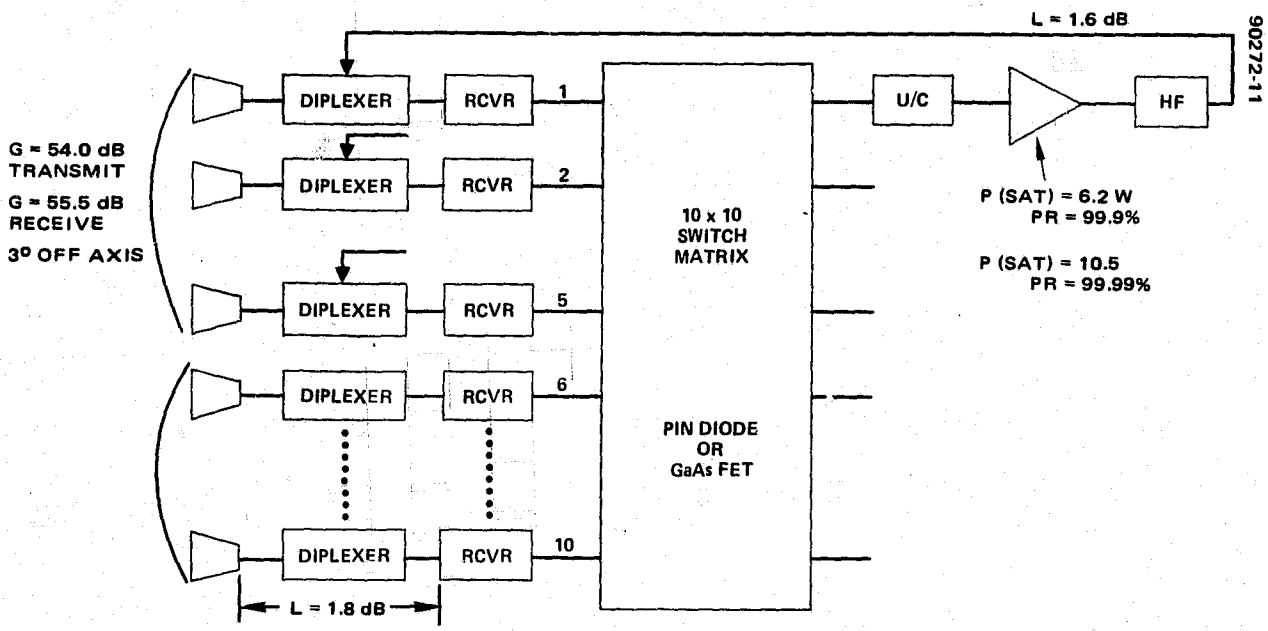

FIGURE 4-11. SATELLITE REPEATER EIRP AND G/T – TEN STATION TDMA

TABLE 4-10. TRUNK TDMA LINK BUDGET

Parameters	Uplink		Downlink		
	99.9%	99.99%	99.9%	99.99%	Clear Weather
EIRP, dBW	86.8	97.0	62.6	68.1	58.7
Pointing loss, transmit	0.4		0.4		
Atmospheric loss	0.7		1.0		
Rain attenuation	10.2	20.4	5.1	10.2	2.0
Path loss	212.9		210.2		
Polarization loss	0.2		0.2		
Pointing loss, receive	0.6		0.2		
G/T	25.1		37.4	37.0	38.2
K	228.6		228.6		
C/N_o	115.5		111.5	111.5	111.5
Uplink degradation				1.5	
C/N_o				110.0	
C/N_o				104.5	
Margin				5.5	
2.5 dB for interference					
3.0 dB for impairments					

4.8.2 Satellite EIRP and G/T – Ten Station TDMA

The satellite EIRP and G/T is shown in Figure 4-11.

The 90 solid state output amplifiers are replaced by 10 TWTAs operating at a higher saturated power. The 6.2 watts required of the TWTAs for 99.9 percent propagation reliability is within the potential range of solid state amplifiers; however, since the performance characteristics of GaAs FET amplifiers at this power output are less well known than those of TWTs, the baseline is designed with TWTs. If the GaAs FET amplifiers demonstrate a very superior reliability relative to TWTs, the output power requirement could be reduced somewhat by increasing the gain of the earth station antenna and by increasing the power of the earth station HPA to further reduce uplink noise degradation. To achieve a propagation reliability of 99.99 percent with the baseline rain model, it is necessary to increase the satellite amplifier outputs 10.2 watts. This is well within the demonstrated capability of helix TWTs.

The output loss of the repeater is reduced by 2.2 dB from the FDMA value because of the elimination of the output multiplexer.

4.8.3 Ten Station TDMA Trunk Satellite Repeater

The input and output multiplexers of the FDMA repeater are replaced by a 10 x 10 switch matrix (Figure 4-12). In the baseline TDMA system in which the 90 links carry uniform traffic levels, the matrix is switched at

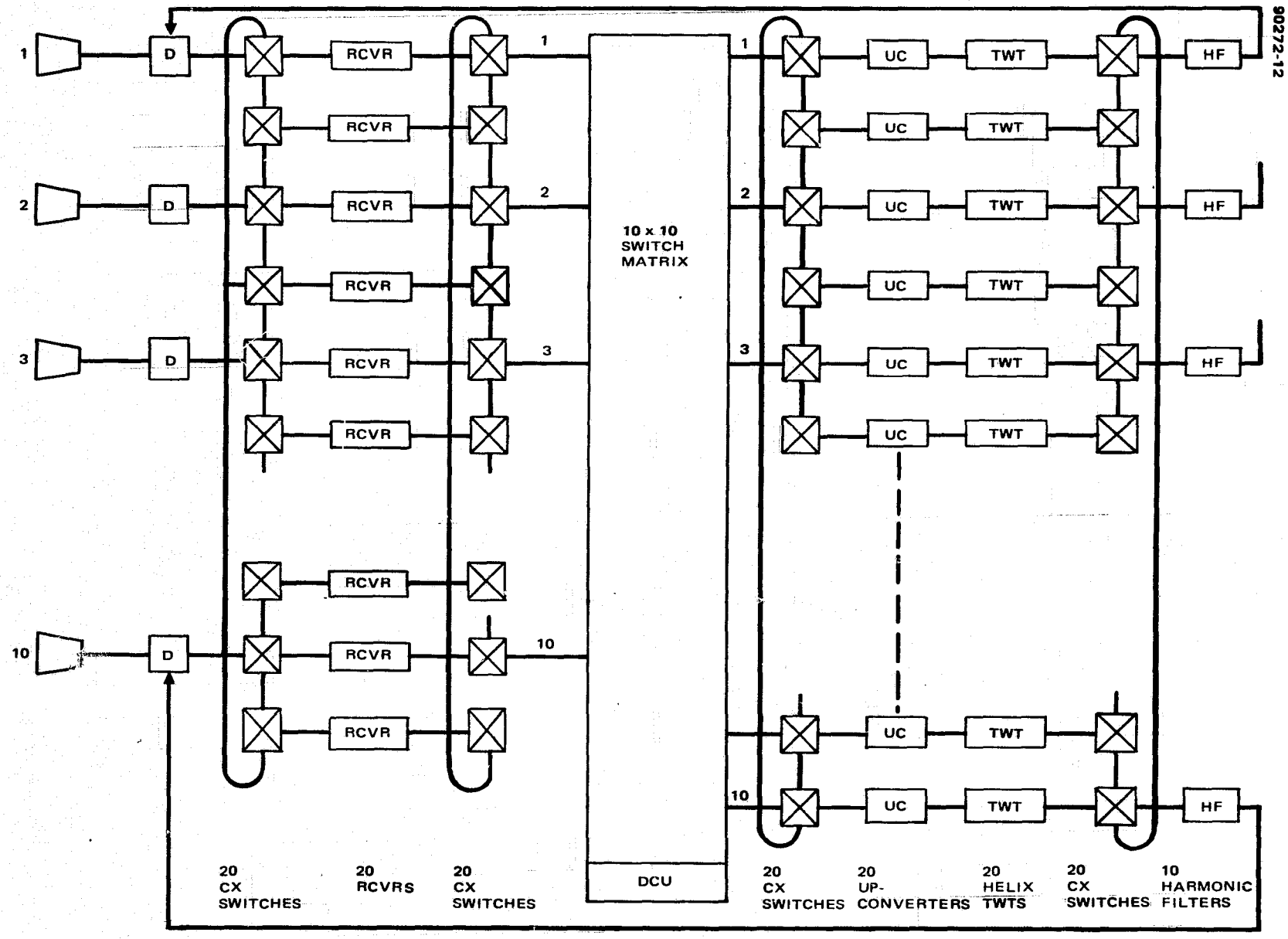

FIGURE 4-12. TEN BEAM TDMA TRUNK REPEATER

fixed intervals by a clock. In a system which accommodated varying traffic, the matrix would be switched by a programmable controller. The TDMA synchronization and switching is discussed in a later section.

The receivers in the TDMA repeater are dual conversion to provide a signal at an IF frequency suitable to the satellite switch matrix. Choice of an optimum IF frequency would require additional study. A frequency of 12 GHz was used for repeater sizing and costing. Criteria for choosing an IF frequency are discussed in the technology section of this report.

The receiver redundancy is implemented in the same manner as in the FDMA repeater, since this part of the system is unchanged between FDMA and TDMA except for the use of dual conversion in the TDMA system.

Reliability studies indicate a 15 for 10 redundancy for the output amplifiers. As in the FDMA configuration, any amplifier may replace any other amplifier.

4.8.4 Trunk TDMA Repeater Weight, Power, and Cost Budget

The major weight, power, and cost elements of the repeater for the ten beam TDMA trunk are shown in Table 4-11. The power requirement for the HPAs (16.1 watts) is based on the low power mode transmitted power of 2.2 watts. The repeater is considerably lighter than the FDMA repeater because of the elimination of the input and output multiplexers and the reduction in the number of channels from 90 to 10 (130 to 15, including redundancy).

TABLE 4-11. TRUNK TDMA REPEATER WEIGHT, POWER, AND COST BUDGET

Component	Quantity (Operating + Redundant)	Weight, lb		Power, W		Cost, $K	
		Unit	Total	Unit	Total	Unit	Per Satellite
Redundancy switches (30 GHz)	20	0.30	6.0	—	—	6	120
Receivers	10 + 10	2.5	50.0	7	70	150	3,000
Redundancy switches (20 GHz)	20	0.45	9.0	—	—	6	120
10 x 10 switch matrix	1 + 0.5	—	3.0		4.0	340	510
Redundancy switches (20 GHz)	20	0.45	9.0	—	—	6	780
High power amplifiers (6.2 W)	10 + 5	5.92	88.7	16.1*	161	74	1,120
Redundancy switches (20 GHz)	20	0.45	9.0	—	—	6	120
Upconverters	10 + 5	0.80	12.0	1.5	1.5	40	600
Miscellaneous repeater and spares			30.0				1,500
Total hardware			216.7		231		7,536
Labor (project management, controls, test, and integration)							1,342
Total recurring — three satellites							26,643
Nonrecurring							6,000
Total							32,643

*Output power = 2.2 watts in clear weather.

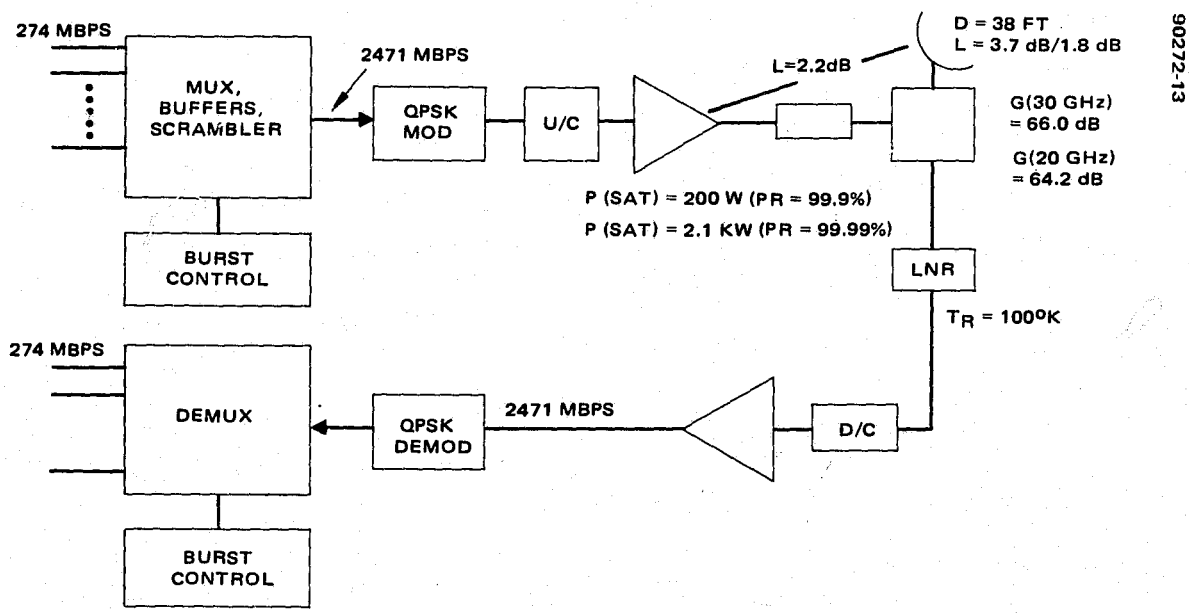

FIGURE 4-13. EARTH STATION TEN BEAM TDMA TRUNK

4.8.5 Earth Station Ten Beam TDMA Trunk

The optimized RF values for the TDMA earth station differ from those of the FDMA station for several reasons. Since the TDMA earth station transmits a single carrier rather than the nine carriers transmitted by the FDMA stations, the transmitter can be operated in saturation. The satellite has a single transmitter per beam rather than nine per beam as in the FDMA case (Figure 4-13).

The nine QPSK modems of the FDMA terminal are replaced by a single modem with a 2471 Mbps data rate to handle the nine 274 Mbps input channels. The required average rate is 2471 Mbps. The burst rate must be higher to account for guard times, preambles, and synchronization codes. An efficiency of well over 90 percent can be achieved with the small number of stations accessing the satellite.

4.9 TDMA TRUNK SATELLITE

The satellite configuration and operating modes are essentially the same as those of the FDMA satellite; however, the difference in weight and power between the FDMA and TDMA repeaters affects the other satellite subsystems to some extent. The satellite weight, power, and cost breakdown is shown in Table 4-12.

TABLE 4-12. TEN BEAM TDMA TRUNK SATELLITE WEIGHT, POWER, AND COST BUDGET

Subsystem	Weight, lb	Power, W	Cost, $K	
			Nonrecurring	Recurring (Three Satellites)
Repeater	217	231	6,000	26,643
Antenna	212	–	7,250	6,168
Communication payload	429	231	13,250	32,811
Telemetry, tracking, and command	58	46	1,211	2,408
Attitude control and antenna pointing	55	20	1,534	1,841
Thermal	(1)	48	(2)	(2)
Power (including losses and margins)	183	69	842	2,969
Structure	979	–	1,427	4,107
Propulsion	210	–	2,084	5,052
Total hardware	1,914	414	20,347	49,188
Program management and support			10,990	16,536
Total cost of three satellites at manufacturing			97,061	
G&A and fee			25,235	
Total satellite investment			112,297	

(1) Included in structure.
(2) Included in structure and in program management and support.

4.10 EARTH STATION TEN BEAM TDMA TRUNK COST BREAKDOWN

The costs associated with a typical dual site earth terminal in the ten beam TDMA trunk are shown in Table 4-13.

The remarks concerning the RF portion of the FDMA terminals apply equally here. A single QPSK modem with a 2.471 Gbps output data rate replaces the nine 215 Mbps QPSK modems of the FDMA terminal. Again, a single spare modem is provided at each site.

The diversity switch and link are the same as for the FDMA terminals, since the input to the stations are nine individual PCM baseband signals in both cases.

4.11 TEN BEAM TDMA TRUNK COSTS

The total cost of the ten beam TDMA trunk system is shown in Table 4-14. The space segment includes the cost of placing all three satellites in synchronous orbit. The earth segment cost includes the cost of synchronizing the TDMA signals.

TABLE 4-13. EARTH STATION COST BREAKDOWN, TEN BEAM TDMA TRUNK

Item	Quantity	Cost, $K		
		Unit	Single Terminal	Total Dual Terminal
Antenna (38 ft diameter) (reflector, mount, feeds, deicer, and limited motion monpulse tracker)	1	193	193	386
Receiver (uncooled parametric amplifier, down-converter, IF strip)	2	80	160	320
Transmitter (upconverter, high power amplifier)	2	93	186	372
QPSK modem (2.5 Gbps)	2	510	1020	2040
Controls and monitoring	1			100
Miscellaneous hardware			156	312
Diversity switch and links				630
Earth station hardware			1715	4060
Management, System Engineering, Integration and Test, Product Assurance				1353
Civil work (building, antenna foundation)			140	280
Installation			125	250
Total manufacturing cost				5943
G&A and fee				1545
Total (excluding site costs)				7488

TABLE 4-14. TEN BEAM TDMA TRUNK SYSTEM COSTS, $M

Item	Cost
Satellite cost (three satellites)	122
Launch cost (three launches)	19
Earth station cost	75
TT&C	15
Total system cost	231

4.12 SERVICE INVESTMENT FOR TRUNK CONCEPTS

The investment required for each 40 Mbps of capacity and for each 64 kbps full duplex circuit is shown in Table 4-15. The 40 Mbps cost is required by the statement of work. This cost provides a comparison to the cost of 40 MHz transponders used on many satellites. The 64 kbps circuit would satisfy voice traffic without requiring any compression of the voice signal. The costs shown are the investment required to make the capacity available. Before these costs can be converted to tariffs, it is necessary to determine the utilization of this capacity.

4.12.1 Sensitivity of System Cost to Bit Error Rate

The variation of system cost to the required bit error rate (BER) is shown in Figure 4-14. The effect on the system of varying the BER requirement is to vary the requirement for energy per bit (E_b/N_o) and, hence, for carrier-to-noise density ratio (C/N_o). The curves in the figure reflect this variation in C/N_o; however, the curves are somewhat misleading because the degradation due to interference between beams was held constant at 2.5 dB, and the degradation due to bandlimiting, group delay distortion, intermodulation distortion, modulator and demodulator imperfections and other distortions was held constant at 3 dB. In reality, the degradation of the signal would vary

TABLE 4-15. FDMA-TDMA TRUNK INVESTMENT COST

Item	FDMA		TDMA	
Propagation reliability	99.9%	99.99%	99.9%	99.99%
Total investment, $M	251	273	231	245
Capacity, Gbps	19.4	19.4	22.2**	22.2**
Investment				
$K/40 Mbps channel	518*	562*	374*	397*
$/64 kbps VX circuit	1636*	1801*	1197*	1270*

*Multiply by utilization factor.
**At 90 percent synchronization efficiency.

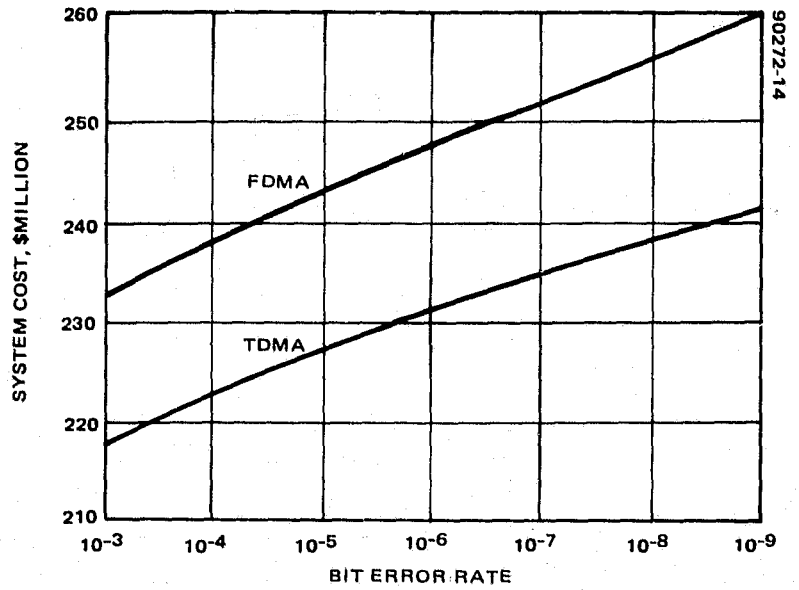

FIGURE 4-14. 18/30 GHZ SYSTEM COST VERSUS BIT ERROR RATE (INCREASED DEGRADATION BY INPAIRIMENTS AT VERY LOW BIT ERROR RATES: $<10^{-7}$)

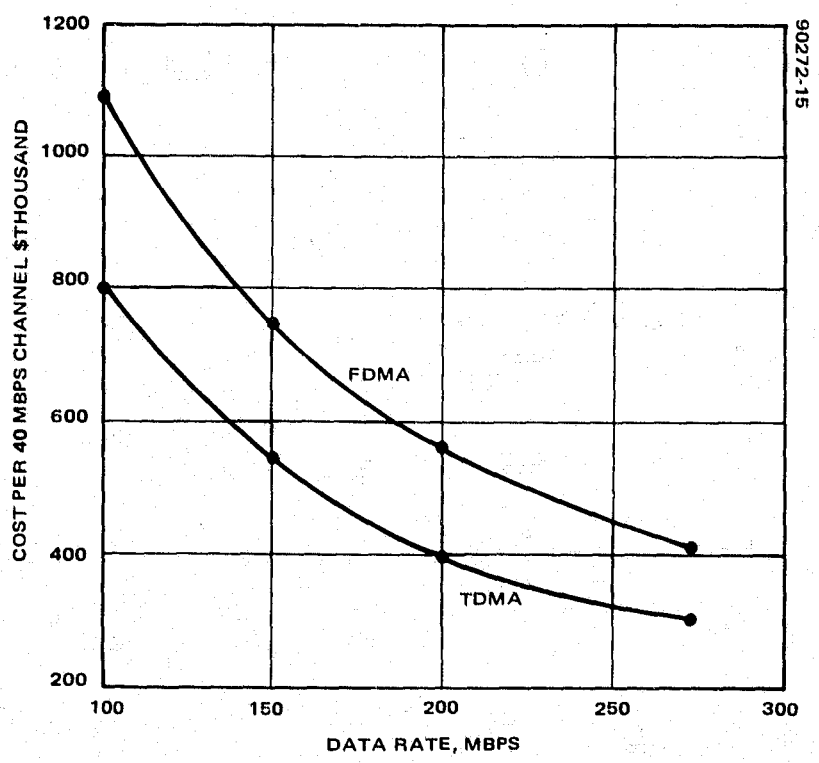

FIGURE 4-15. COST PER 40 MBPS CHANNEL VERSUS DATA RATE

considerably as E_b/N_o varies. As E_b/N_o increases, the BER for uncoded data tends to asymptote to a value set by the impairments. As E_b/N_o decreases, noise tends to mask the impairments so that the degradation decreases. If these factors are taken into account, the costs associated with very low bit rates such as 10^{-9} would increase considerably above that shown. The more practical way of achieving these low BER values is to use coding. The use of coding by increasing the bandwidth occupancy sacrifices data capacity to achieve the required BER with reasonable C/N_o. Likewise a reduction of the BER requirement to 10^{-3} would reduce the cost more than is shown by the curves.

4.12.2 Sensitivity of System Cost to Data Rate

The sensitivity of system cost to the channel data rate is shown in Figure 4-15. The number of channels is held constant so that the system capacity varies with data rate. The channel bandwidth is 2.5 GHz/9 = 277.8 MHz. The baseline data rate is 274.6 Mbps for the TDMA system and 215 Mbps for the FDMA system. The cost is expressed as cost per 40 Mbps, as specified in the statement of work, to account for both the variation in system total cost and the variation in capacity of the system. The curves show that as the data rate increases the unit cost of data decreases because the system capacity is increasing faster than the system cost. The BER is held constant as the data rate varies. Also, the effect of impairments such as interference, distortion, and imperfect modulation and demodulation on the required value of C/N_o were assumed to be constant with data rate. This assumption may be unrealistic for the FDMA case at high data rates because of the uncertainty in the spectral characteristics of realizable output multiplexers.

4.12.3 Sensitivity of System Cost to Number of Beams

The sensitivity of cost to the number of beams (N_B) in the system is shown in Figure 4-16. The data rate per beam and BER are held constant. The total system cost increases with N_B as more earth terminals, satellite amplifiers, antenna feeds, and filters or switches are added; however, the system capacity which grows linearly with N_B increases faster than the system cost for TDMA concepts so that the unit cost of data decreases with N_B. In the FDMA system this economy of scale is defeated by rapid increase in the number of filters in the system and the difficulty of fabricating multiplexers with the number of channels required (39 channels for 40 beams). A 39 channel FDMA system may not be achievable at any reasonable cost.

Because the analysis is based on the same data rate on all channels and for all beams, the curves are probably not realistic. The traffic demand will vary greatly from beam to beam and channel to channel so that the increased capacity provided by the increased number of beams will not be used.

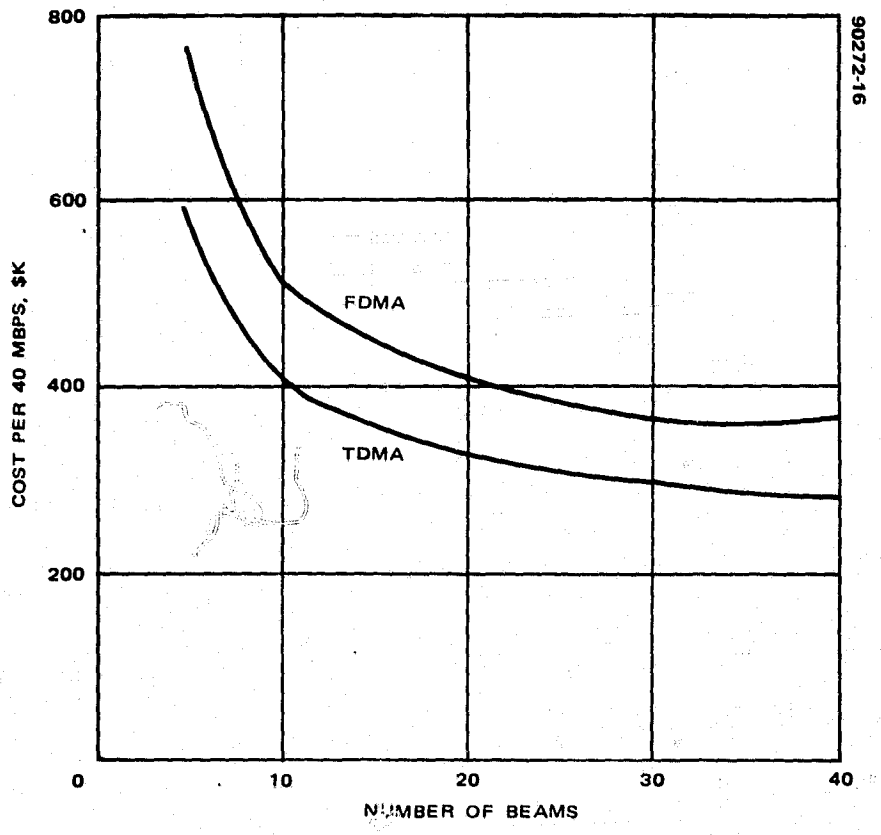

FIGURE 4-16. SERVICE COST PER 40 MBPS CHANNEL VERSUS NUMBER OF BEAMS

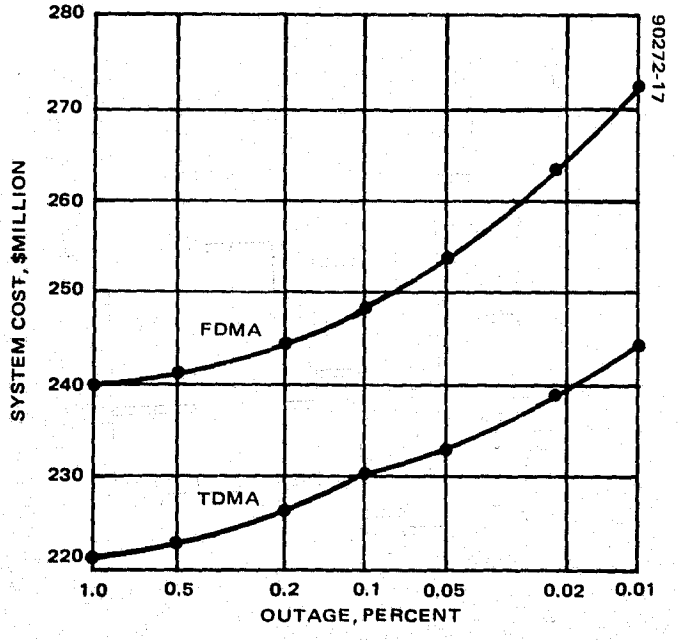

FIGURE 4-17. 18/30 GHz SYSTEM COST VERSUS OUTAGE

4.12.4 Sensitivity of Cost to Propagation Reliability

The sensitivity of system cost to propagation reliability is shown in Figure 4-17. It can be seen that the increase in cost required to reduce the outage from 0.1 to 0.01 percent is less than 10 percent with the model used to estimate rain attenuation with site diversity. Thus, if the model for diversity improvement is reasonably valid, a propagation reliability of 99.99 percent can be assumed for the trunk systems.

5. DIRECT TO USER CONCEPTS

The direct to user concept is illustrated in Figure 5-1. The satellite antenna system generates a number of equispaced spot beams which are large enough that every point in the 48 contiguous states is within one of the beams. Intersection of the beams at the half power beamwidth appears to be optimum. For this study the terminals are taken as uniformly distributed over CONUS. The number of terminals to be considered range from 1000 to 10,000 (originally the upper limit was 100,000, but NASA and the contractors agreed to reduce the upper limit to 10,000). Site diversity is not to be considered for the direct to user concepts; therefore, higher rain attenuation or lower propagation reliability must be considered. The number of beams used to cover CONUS ranges from 4 to 40.

5.1 ANTENNA GAIN COMPARISON

The satellite antenna gain of the trunk system is limited by antenna size. The gain in the direct to user system is limited by the requirement to cover the specified region with a limited number of spot beams (Figure 5-2). Thus, for a 25 beam system, the spots must have half power beamwidths of at least 1.1°, which corresponds to a gain of about 43.3 dB. In general, the gain is proportional to the number of beams, so that the burden on the earth station RF components and the satellite transmitter can be alleviated by increasing the number of beams. Unfortunately, the larger the number of beams the greater the interconnectivity problem. For the baseline 25 beam system, the direct to user satellite downlink (20 GHz) antenna gain is 14.5 dB lower than for the trunk concept, assuming that the downlink beam is no larger than the uplink beam. On the other hand, the direct to user system has a considerable antenna advantage over conventional CONUS coverage satellites.

5.2 RF COMPARISON

The pertinent elements of the 25 beam direct to user and trunk concepts (independent of the number of beams) are compared in Table 5-1. In addition to the 14.5 dB antenna disadvantage, the increased rain degradation resulting from single site operation is significant. To make the direct to user concept technically viable, the propagation reliability is limited to 99.5 percent compared to the baseline 99.9 percent of the trunk concept. Also, the satellite

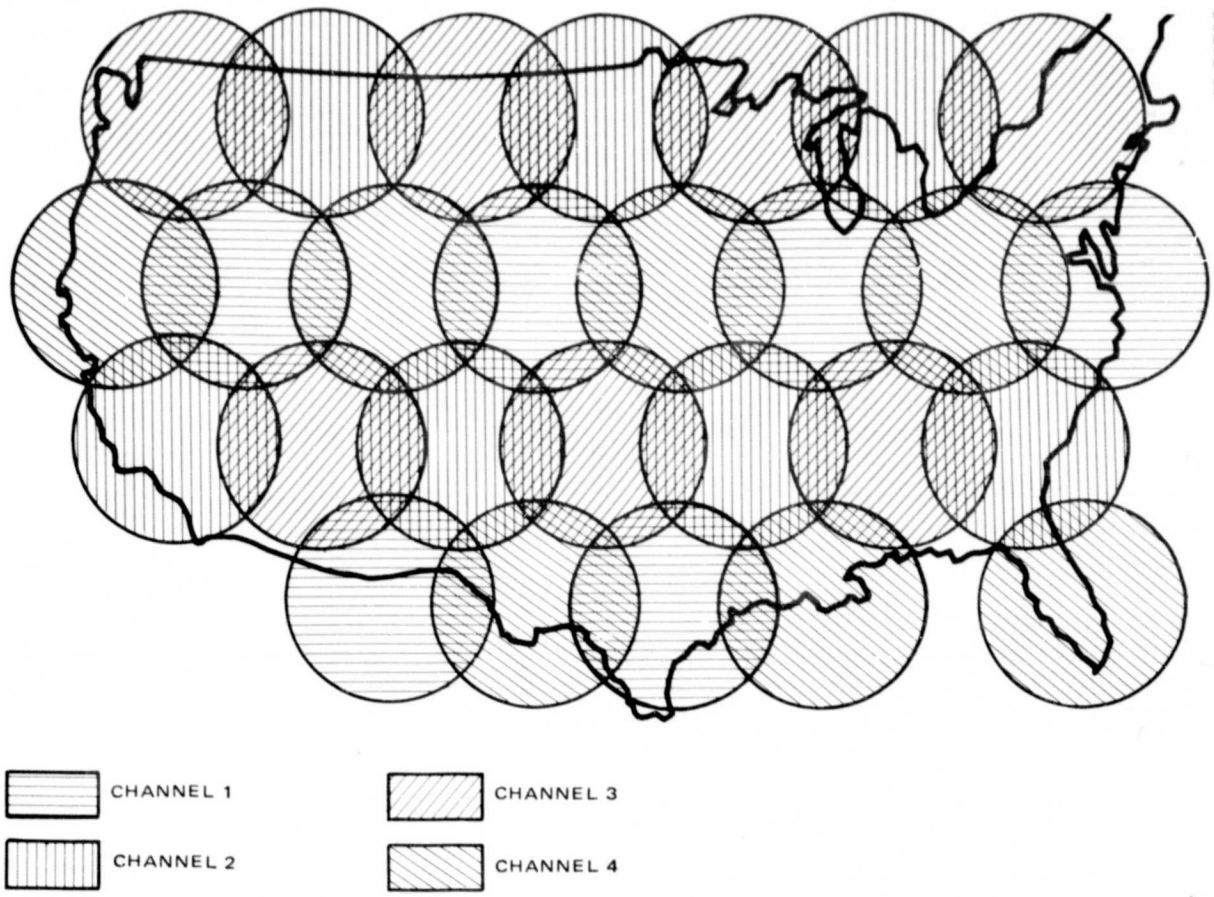

FIGURE 5-1. DIRECT TO USER CONCEPT

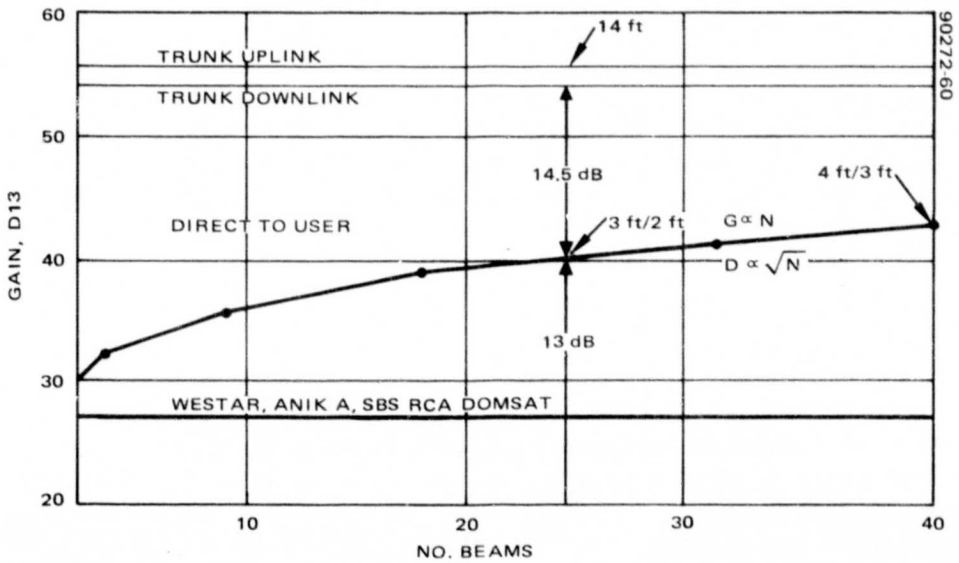

FIGURE 5-2. ANTENNA GAIN COMPARISON

TABLE 5-1. RF COMPARISON COST/MBPS

Element	25 Beam Direct-To-User, dB	Trunk Spot Beam, dB	Δ, dB
Downlink			
Satellite antenna gain	42.5	54.0	-11.5
Edge loss	-3.0	0	-3.0
Rain degradation	-7.5 (99.5%)	-6.4 (99.9%)	-1.1
Earth station antenna gain	59.6	65.8	-6.2
			-21.8
Uplink			
Rain attenuation	-14.1 (99.5%)	-7.8 (99.9%)	-6.3
Antenna gain-receive	42.5	55.5	-13.0
Edge loss	-3.0	0	-3.0
Total			-22.3

transmitter burden is increased by the severe limitations imposed on earth station antenna size by cost and zoning considerations. Thus, both the satellite and earth station transmitters have to make up over 20 dB of disadvantage relative to the trunk system for the same data rate. This disadvantage relative to the trunk does not necessarily mean that the direct to user concept is not viable. The station portion of the trunk system was, after all, extremely cost effective.

5.3 MULTIBEAM INTERCONNECTIVITY

Much of the network traffic in a multispot beam system will be between stations in different beams. Beam to beam interconnection can be a difficult technological problem if beam to beam frequency reuse is employed.

Terminals in different beams can be interconnected in two ways:

1) Directly through the 18/30 GHz satellite transponder

2) Indirectly through master stations in each beam which communicate with each other, either through an auxiliary satellite payload or through terrestrial links

5.3.1 Direct Interconnectivity

Direct interconnectivity in a 18/30 GHz satellite transponder with beam to beam frequency reuse requires input and output multiplexers for an FDMA system or a switch matrix for an SS-TDMA system. If the number of

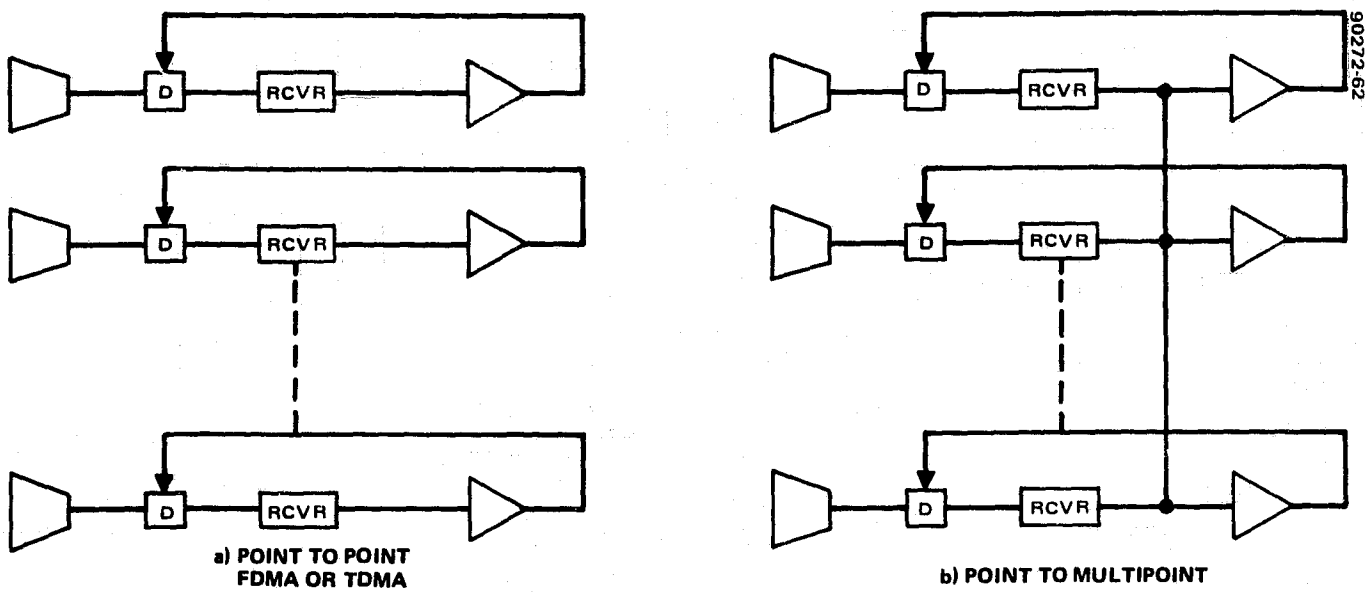

FIGURE 5-3. DIRECT TO USER WITH NO SATELLITE SWITCHING

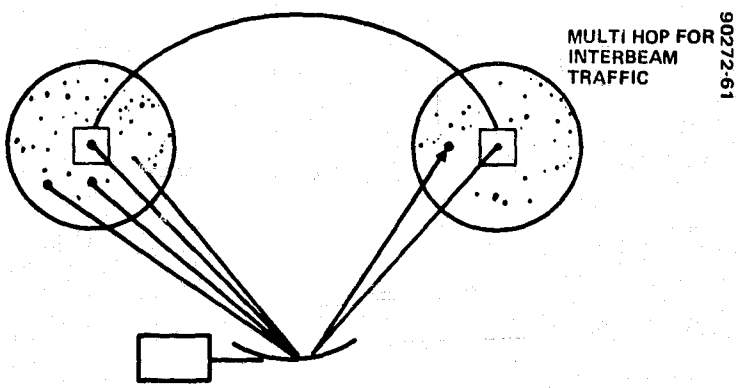

FIGURE 5-4. DIRECT TO USER GROUND CONNECTED MULTIBEAM

beams is reasonably small, direct interconnectivity is manageable. FDMA multiplexing of up to 10 or 12 beams appears manageable, although such a multiplexer has not been built at 20 GHz. An SS-TDMA switch matrix capable of handling 40 beams also appears to be within reason, although, again, an IF switch matrix of this size does not exist. As the number of beams increases beyond these levels, the FDMA multiplexer, especially the output multiplexer, becomes increasingly difficult to realize, and the cost, weight, and complexity of the SS-TDMA switch accelerate. These problems are discussed in 3.4.2, 7.5, and 7.6.

5.3.2 Indirect Interconnectivity

Indirect interconnectivity through master stations simplifies the satellite transponder considerably; however, the quality of the links is compromised, and the spectral efficiency of the system is reduced. In such a system, all uplink signals are retransmitted in the same beam in which they were received (Figure 5-3a). Traffic which is intended for terminals in other beams is collected at the master station and relayed by the master station in the originating beam through terrestrial links or through an auxiliary satellite payload to the master station in the destination beam. This master station then relays the data through the 18/30 GHz satellite transponder to the receiving terminal. Thus, the link suffers multihop transmission; two hops if the master stations communicate through terrestrial links, and three hops if they communicate through a satellite (see Figure 5-4). Even dual hopping is considered by communication carriers to be an extremely serious degradation to a voice signal. Such a system is primarily useful for data transmission and facsimile.

Note also that the spectral capacity consumed by such a system is three times that required for a directly connected system.

The above options are summarized in Table 5-2.

5.4 MULTIBEAM INTERCONNECTIVITY WITHOUT FREQUENCY REUSE

A multispot beam system can be interconnected in the satellite transponder as shown in Figure 5-3b. In this configuration, each uplink signal is transmitted on all downlink beams; consequently, the spectrum cannot be reused from beam to beam. Also, the satellite transmitter power requirement is not lower than would be required if a single area beam were used, because all signals are transmitted to all of CONUS. On the other hand, neither multiplexers nor switch matrices are required, and the links are single hop. This is essentially a point to multipoint system, and is not considered further in this study.

TABLE 5-2. MULTIBEAM INTERCONNECTIVITY

System	FDMA	TDMA
Ground	Multihop	Reduced capacity (point to multipoint)
Satellite	Multiplexer (N^2 filters)	Satellite switch matrix Weight $\propto N^3$ Cost $\propto N^2$

5.5 DIRECT TO USER TRAFFIC MODEL

To provide a basis for configuration of direct to user systems, one of the market study contractors (Western Union) supplied a model for a 10,000 station network. The model which is meant only to be typical and is not an estimate of future demand comprises three types of stations as shown in Table 5-3. The stations are characterized as small, medium, and large according to the number of each of four classes of circuit ends provided at the station. These numbers do not represent the number of end users or the average demand, but the number of simultaneous circuits in which the station can engage; i.e., the peak instantaneous demand which a single station can impose on the satellite. The number of each station type in the network is shown in the left hand column. For networks of fewer than 10,000 stations, the same proportion of station types is maintained.

The number of satellite links required to support this network of stations depends on a number of factors which are not defined, such as the population of users and the variation with time and direction of the traffic flow; however, assuming uniform conditions and conventional statistical relations between blockage probabilities and amount of traffic versus the number of circuits, an estimate was developed. This estimate is shown in the bottom row of Table 5-3.

TABLE 5-3. DIRECT TO USER TRAFFIC MODEL (WU)

	Number of Circuits/Station (Full Duplex)			
	Voice Circuits	56 kbps Circuits	1.5 Mbps Circuits	6.3 Mbps Circuits
Large stations, 125	240	20 data	2 data 1 video	1 video
Medium stations, 1275	60	5 data 2 video	1 video	—
Small stations, 8600	12	1 data 1 video	—	—
Total, 10^4 stations	212 K	28.8 K	1675	125
Links required in satellite (full duplex)	65K		~500	~50

5.6 SPECTRUM CAPACITY

Because adjacent beams overlap at the 3 dB beamwidth, the spectrum cannot be reused in every beam as it is in the spot beam trunk system. Spectrum capacity is summarized in Table 5-4. The problem of beam to beam isolation is discussed in the antenna technology section of this report. In summary, if uplink power control is provided at the earth stations it appears possible to reuse the spectrum every other beam without recourse to multifeed beam generation. Uplink power control is required to achieve any spectrum reuse whatever (beyond that which is available with cross polarization), because if earth stations all continuously transmit sufficient power to overcome the maximum rain attenuation, a station whose signal is attenuated will have C/I ratio degraded to an unacceptable level. With the spectrum reused every other beam and cross polarization used as well, the 2.5 GHz spectrum need only be shared by two beams, each beam having 1.25 GHz available; however, when the link budget requirements for the direct to user systems are taken into account, it is apparent that the capacity of the system will be power limited rather than spectrum limited. Full use of the 1.25 GHz spectrum on each of 25 beams requires a 62 kW prime power capacity; this would exceed the capability of a Shuttle launch as well as require a very expensive spacecraft. To deal with a reasonable spacecraft, the baseline design will be confined to 200 MHz per beam, or 5 GHz overall capacity. The number of satellite voice circuits which can be provided by such a satellite (31×10^3) are probably inadequate for the 10,000 station network detailed in Table 5-3; however, this satellite would be consistent with a 5000 station network.

5.7 FDMA MULTIBEAM CONCEPT

In the FDMA multibeam concept a total data rate of 200 Mbps is available through the satellite. At any time, this capacity is shared by some combination of small, medium, and large stations. Figure 5-5 shows the

TABLE 5-4. SPECTRUM CAPACITY

Spectrum Reuse	Number of Beams	Bandwidth/ Beam	Total Bandwidth	Number of Full Duplex (10^4 Stations)		
				Voice 50%	1.5 MHz, 25%	6.3 MHz, 25%
Four beam cells plus cross polarization	10	1.25 GHz	12 GHz	75×10^3	1000	240
	25		32 GHz 62 kW	200×10^3	2500	600
	40		50 GHz	300×10^3	4000	950
Baseline	25	1.25 GHz allocated 200 MHz used	32 GHz allocated 5 GHz used 10 kW	31×10^3	416	100
Required for 10^4 stations				65×10^3	500	50

Note: uplink boost control required

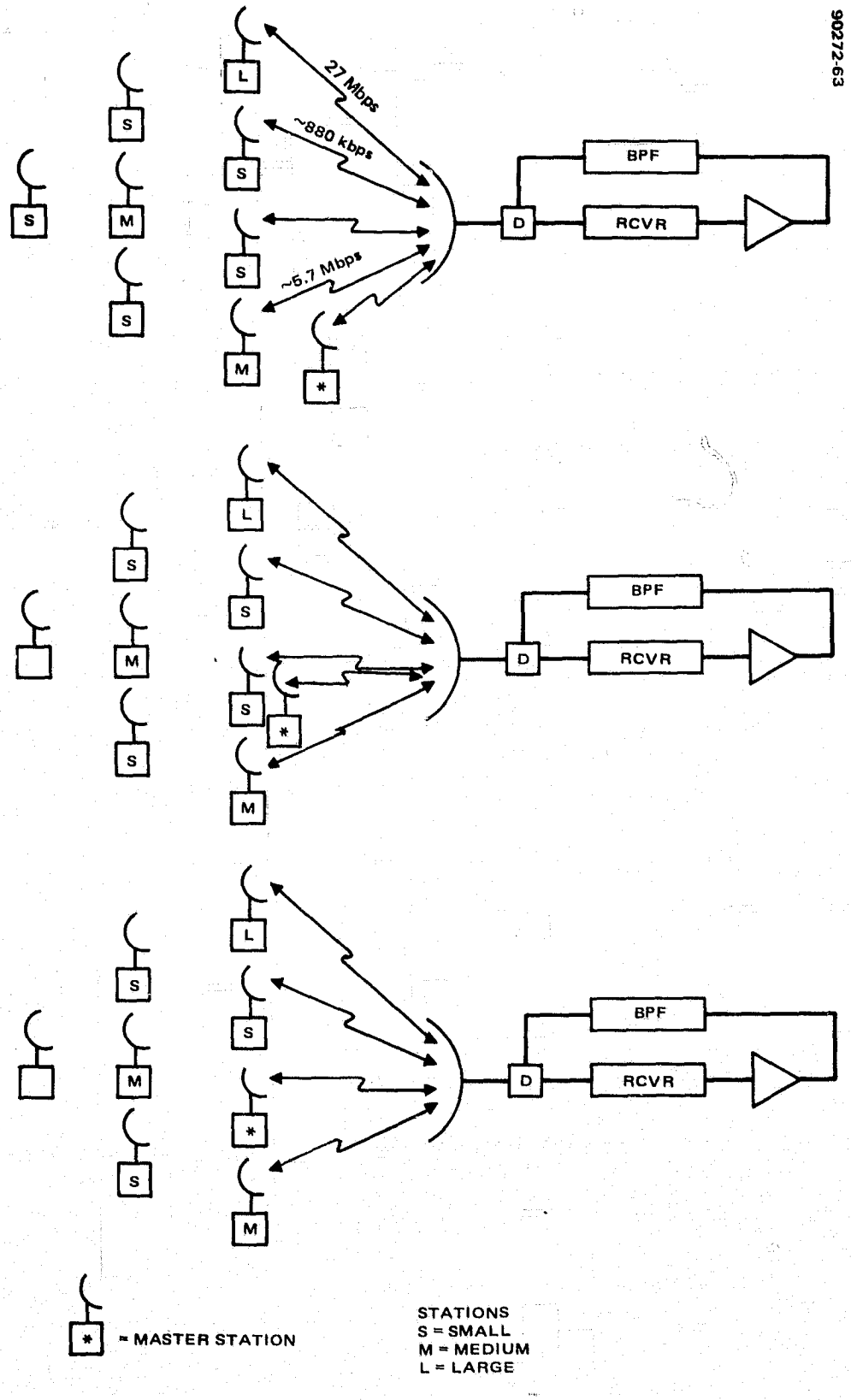

FIGURE 5-5. MULTIBEAM FDMA CONCEPT

total data rate which can be generated by each of these stations. This total data rate is composed of a combination of voice, low rate data, 1.5 Mbps data and video, and 6.3 Mbps video. At any time most stations will be generating less than their maximum data rate. The earth station EIRP and G/T are sized to handle the maximum station data rates shown. The satellite transponder power is sized to handle 200 Mbps. The optimization of the RF resources, which is primarily a trade between satellite transmitter power and earth station transmitter power and antenna gain, is based on the distribution of station sizes between large, small, and medium given in the previous station, assuming 5000 stations total.

There is one master station in each beam. This station receives all traffic destined for other beams and transmits all traffic originating in other beams.

5.7.1 FDMA Multibeam Link Budget

The link budgets for the 25 beam FDMA system are shown in Table 5-5. The link requirements for each service are based on a bit error rate of 10^{-6}, which requires Eb/N_0 = 10.6 dB and a carrier to interference ratio of 16 to 17 dB, which degrades Eb/N_0 by about 2.5 dB. Thus, for the 64 kbps voice channel, C/N_0 (required) = 10.6 + 2.5 + 10 log 64 x 10^3 = 61.1 dB. A 3 dB margin for satellite and earth station modem impairments is provided. The satellite EIRP and earth station EIRP and G/T are the result of tradeoff studies between the various RF parameters involved. The primary variables are the satellite transmitter power, the earth station transmitter power, and earth station antenna diameter. The satellite antenna gain is fixed at both transmit and receive frequencies by the spot size. The parameters which

TABLE 5-5. FDMA MULTIBEAM LINK BUDGET

	Uplink			Downlink		
	Voice	1.5 Mbps	6.3 Mbps	Voice	1.5 Mbps	6.3 Mbps
EIRP, dBW	51.0	64.7	70.9	25.4	39.2	45.4
Pointing loss	-0.4	-0.4	-0.4	-0.4	-0.4	-0.4
Path loss	-212.9	-212.9	-212.9	-210.2	-210.2	-210.2
Atmospheric loss	-0.7	-0.7	-0.7	-1.0	-1.0	-1.0
Rain attenuation (PR = 99.5%)	-14.9	-14.9	-14.9	-6.5	-6.5	-6.5
Polarization loss	-0.2	-0.2	-0.2	-0.2	-0.2	-0.2
Pointing loss	-0.6	-0.6	-0.6	-0.2	-0.2	-0.2
G/T	19.4	19.4	19.4	30.2	30.2	30.2
$C/N_0 = C/T + 228.6$	69.3	83.1	89.3	65.6	79.4	85.6
Uplink noise degradation				-1.5	-1.5	-1.5
C/N_0 (link)				64.1	77.9	84.1
C/N_0 (required)				61.1	74.9	81.1
Margin for impairments				3.0	3.0	3.0

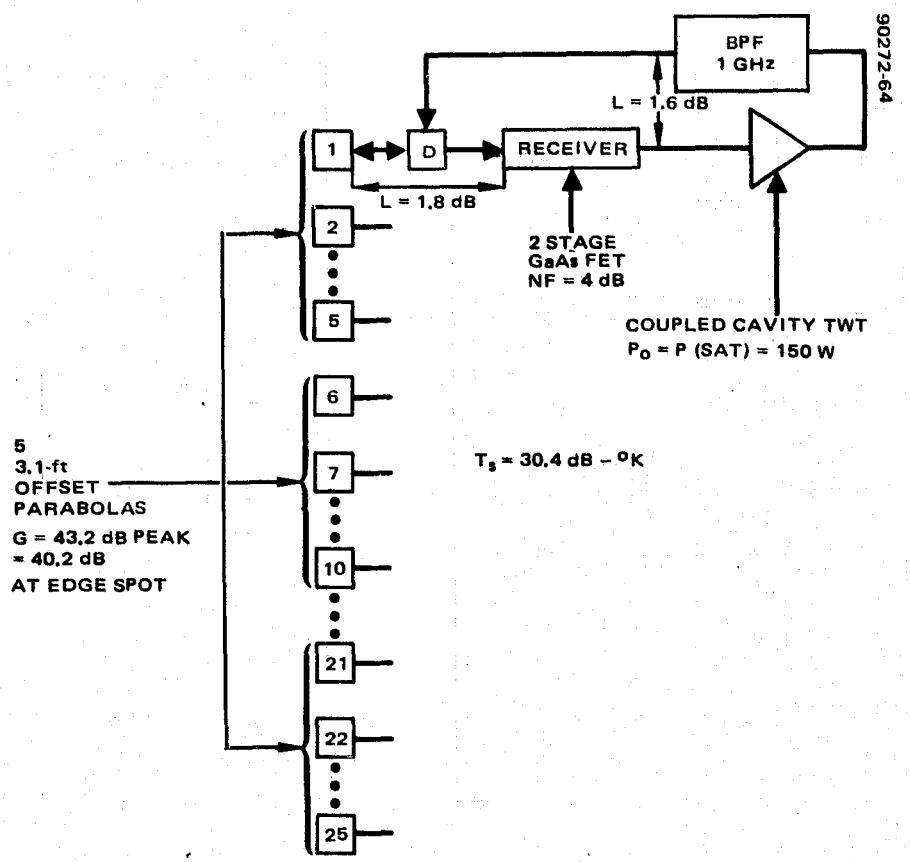

FIGURE 5-6. DIRECT TO USER SATELLITE FDMA EIRP AND G/T

provide the EIRP and G/T values in Table 5-5 are discussed in subsections that follow.

The link budget applies to transmitting and receiving stations at the edge of the beam in the New York area. This link has a relatively severe requirement both as regards rain attenuation and position in the satellite antenna spot beam; however, a link between stations in a spot in the Gulf Coast region would have considerably greater rain attenuation or poorer propagation reliability.

5.7.2 FDMA Multibeam Satellite EIRP and G/T

The satellite EIRP requirements for each type of service shown in the link budget are based on a total EIRP for each downlink beam of 60.4 dBW. This EIRP supports 200 Mbps, so that the EIRP for each service is reduced from 60.4 dBW by the ratio of the service bit rate to 200 Mbps.

The EIRP is achieved as shown in Figure 5-6. The high power amplifier is a 150 watt coupled cavity TWT. An output circuit loss of 1.6 dB was provided by NASA. (Actually, 3.8 dB, including a 2.2 dB output filter loss which is eliminated here because the lack of interconnectivity between beams eliminates the need for an output multiplexer.) This loss represents a heat source of 46 watts per beam, or 1156 watts for a 25 beam spacecraft in addition to imposing a large additional requirement on the satellite power subsystem. It would be a major objective of the design of such a satellite to reduce this loss to 0.5 to 0.6 dB. The antenna gain at the edge of each spot is 3 dB lower than the peak gain of 43.2 dB. It is assumed that a surface precision of 0.0010 inch, including environmental effects, would be achieved at reasonable cost for these small antennas, thus limiting the surface loss to 0.2 dB. The EIRP is then given by

P (150 W)	21.8 dBW
L	-1.6 dB
G	40.2 dB (at edge of spot)
EIRP	60.4 dBW (at edge of spot)

The high power amplifiers are operated in saturation. Since only a small portion of the available spectrum is occupied, it should be possible to maintain an adequate carrier to intermodulation ratio by causing much of the intermodulation distortion to fall between signal channels.

The satellite receive temperature is established by a two-stage GaAs FET followed by a GaAs mixer downconnecting to 20 GHz. The resulting receiver noise figure is 4 dB. If the input circuit loss is 1.8 dB and the temperature of the earth facing antenna is 290°, the system temperature is given by

$$T_s = NF \times L \times 290 = 1120°K = 30.4\ dB\text{-}°K$$

If the input circuit loss was reduced to 0.8 dB, T_s would decrease by 1 dB to 871°K.

The satellite antenna gain at 30 GHz is slightly less than at 20 GHz because of increased surface loss (0.5 dB). The antenna is larger at 20 GHz to give the same spot diameter at both frequencies (see Section 3). Thus, the gain differs only by the difference in surface loss. The G/T is given by

$$\begin{array}{l} G = 39.8 \text{ dB (at edge of spot)} \\ \underline{T = 30.4 \text{ dB}} \end{array}$$

$$\frac{G}{T} = 9.4 \text{ dB (at edge of spot)}$$

5.7.3 25 Beam Direct to User FDMA Repeater Weight, Power, and Cost Budget

The weight, power, and cost budget of the satellite repeater for the 25 beam direct to user satellite is summarized in Table 5-6. The repeater is simple in configuration due to the lack of interconnectivity, but is burdened by the large number of 150 watt coupled cavity TWTs. Reliability studies indicate that 10 spares for the 25 operating TWTs are adequate if any of the TWTs can be applied to any channel and if the TWT failure rate is 2000 failures in 10^9 hours (2000 FITs). The true failure rate for TWTs is uncertain,

TABLE 5-6. 25 BEAM DIRECT TO USER FDMA REPEATER WEIGHT, POWER, AND COST BUDGET

Component	Quantity	Unit Weight, lb	Total Weight, lb	Unit Power, W	Total Power, W	Unit Cost, $K	Cost Per Satellite, $K
Redundancy switches, 30 GHz	35	0.30	10.5	–	–	6.0	210
Receivers	25 + 10	2.50	87.5	7	245	150.0	5,250
Redundancy switches, 20 GHz	35	0.45	15.7	–	–	6.0	210
Redundancy switches, 20 GHz	35	0.45	15.7	–	–	6.0	210
High power amplifiers, 150 W	25 + 10	37.5	1,313.8	375	9,375	181.9	6,366
Redundancy 20 GHz	35	0.45	15.7	–	–	6.0	210
Bandpass filters	25	0.5	12.5	–	–	0.5	12
Miscellaneous repeater	–	–	–	–	–	–	1,250
Total hardware			1,471.3		9,620		13,718
Labor (Project management contracts, test and integration)							2,050
Total recurring, three satellites							47,300
Nonrecurring							4,000
Total							51,300

and higher and lower rates have been calculated by different investigators. Similar redundancy is assumed for the receivers. Although the receiver failure rate is lower, the penalty for excess redundancy is small compared to that for the TWTs. The ring around redundancy assumed for the receivers and TWTs was described in Section 4.

5.7.4 Direct to User FDMA Earth Station (Figure 5-7)

The system cost optimization leads to the choice of a 22 foot diameter earth station antenna. Although an antenna of this diameter minimizes the cost of the system RF resources it may be difficult to site in the desired locations. If antenna diameter is restricted to 15 feet there will be a significant cost impact on other parts of the system. The antennas have surface precision consistent with Ku band operation (E=0.035 inch) as discussed in Section 4. The losses are 3.7 dB at 30 GHz and 1.7 dB at 20 GHz. The antennas track the spacecraft in response to position commands which are received from the central TT&C station. A microprocessor at the earth station converts the TT&C command to a command to the two-axis antenna drive motors. A pointing accuracy of 0.02° (3σ) can be achieved by this method at very small cost compared to providing autotrack at each station.

The power required on the uplink varies between large, medium, and small stations because of the variation in the bandwidth each station uses when all of the stations circuits are in use. This maximum bandwidth depends on the number of modems of each type which the station possesses. For an output circuit loss of 1.7 dB:

$$\begin{aligned} EIRP &= 18.2 - 1.7 + 60.8 = 77.3 \text{ large station} \\ &= 11.4 - 1.7 + 60.8 = 70.5 \text{ medium station} \\ &= 3.3 - 1.7 + 60.8 = 62.4 \text{ small station} \end{aligned}$$

The receivers use GaAs FET front ends operating at ambient temperature. A noise figure of 3 dB is projected. If input circuit loss is 1.5 dB, the system temperature in the presence of a 6.5 dB rain fade (T_{sky} = 239°K) is 761°K (28.8 dB°K) and

$$\frac{G}{T} = 59.0 - 28.8 = 30.2 \text{ dB}$$

The modems produce a modulated carrier for each baseband input. The voice channels are assumed to be analog and are frequency modulated. All other inputs are assumed to be digital and are QPSK modulated.

5.7.5 Direct to User Earth Station Cost

The cost elements of the FDMA earth stations are listed in Table 5-7. The antenna includes a motorized drive capable of positioning the antenna in response to commands and a de-icer. The cost is similar to the cost of recently purchased Ku band antennas. Some reduction in cost would be available if antennas for 5000 stations were ordered.

The cost of the electronics do not include redundancy. Replacement of transmitter TWTs is assumed to be included in the maintenance cost. The

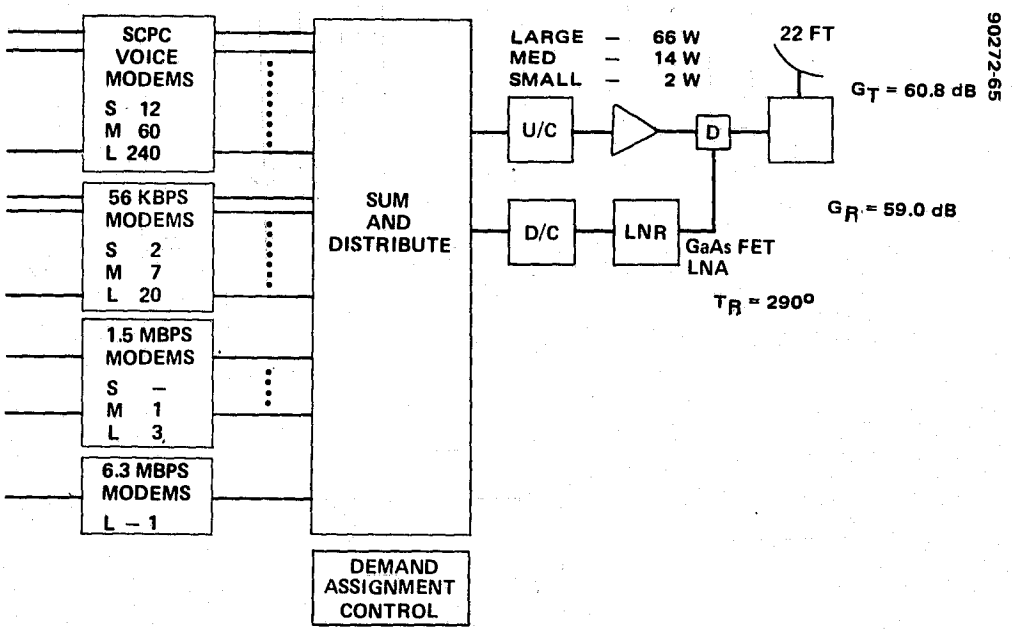

FIGURE 5-7. DIRECT TO USER FDMA EARTH STATION

TABLE 5-7. DIRECT TO USER FDMA EARTH STATION COST, $K

Breakdown	Earth Station		
	Small	Medium	Large
Antenna	34	34	34
Transmitter	20	35	83
Receiver	15	15	15
Modems (and associated equipment)	82	253	977
Shelter, cabling, etc.	5	9	28
Total equipment	156	346	1137
Labor (project engineering, system engineering, quality assurance, test, management)	52	115	379
Total equipment and labor	208	461	1516
Contingency	12	24	104
Total manufacturing cost	220	485	1720
G&A plus profit	57	126	447
Total cost (FOB factory)	227	611	2167

modems are single carrier per channel (SCPC) as specified in the statement of work. The cost of modems for the large station is inflated by the number of modems required (240 modems for voice alone). It might be possible to reduce this cost by using FDM rather than SCPC for the voice traffic, but sacrificing some bandwidth efficiency. On the other hand, the SCPC modem costs are current costs. These costs might come down in response to the large order represented by this system.

5.7.6 25 Beam Direct to User Satellite

The 11.8 kW end of life power requirement dictates a body stabilized spacecraft with deployed sun tracking solar panels as shown in Figure 5-8. Over the 10 year lifetime, the solar panel output can be expected to degrade to 64 percent of the beginning of life output. The beginning of life output of 18.4 kW would require a panel area of 70 m^2 with GaAs cells. These cells are expected to be available for long life application by the period of interest with a power density of about 264 W/m^2. This is nearly twice the power density of current silicon cells. The solar power is provided by two wings as shown in Figure 5-8. Each wing is 3 by 12 meters, although the width to length ratio is subject to optimization based on considerations primarily of attitude stability and availability of existing configurations. The batteries are nickel-hydrogen.

The antenna system is composed of five reflectors, each with five beams. This configuration is required to allow complete coverage of CONUS with overlapping beams using present feed technology. This problem is discussed in Appendix A.

The weight, power, and cost budget for the satellite is shown in Table 5-8. The weight of the power subsystem reflects the use of GaAs solar cells and nickel-hydrogen batteries. The nonrecurring costs are based on

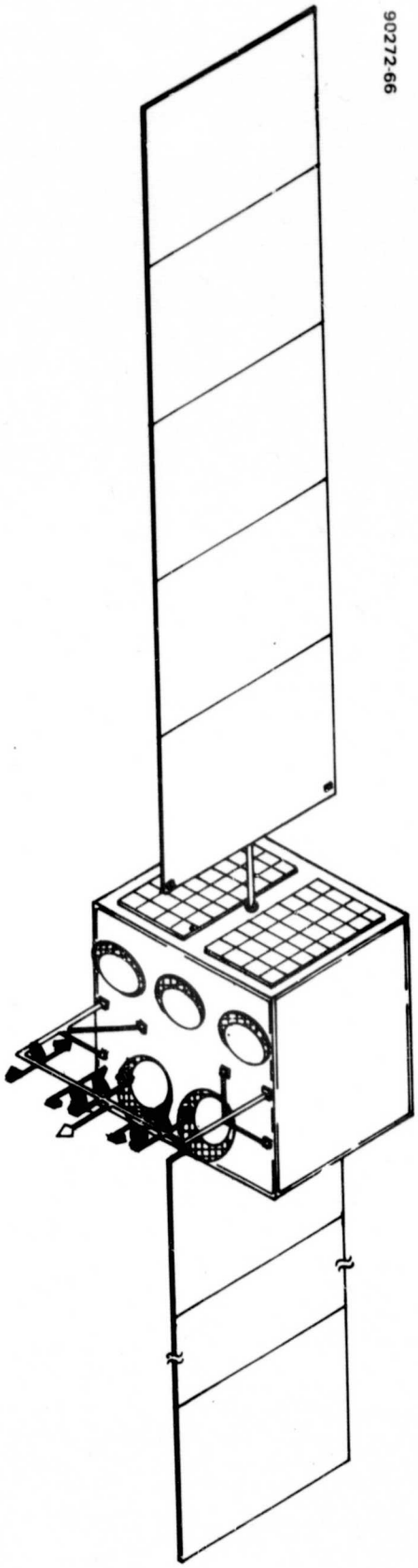

FIGURE 5-8. 25 BEAM DIRECT TO USER SPACECRAFT

TABLE 5-8. 25-BEAM DIRECT TO USER SATELLITE WEIGHT, POWER, AND COST

Subsystem	Weight, kg	Power, W	Non Recurring Cost, $M	Recurring Cost for Three Satellites, $M
Repeater	667	9,620	4.0	47.3
Antenna	23	—	6.3	6.4
Communication payload	690	9,620	10.3	53.7
Telemetry, tracking, and command	29	54	1.2	2.6
Attitude control	82	150	1.5	8.5
Power	911	1,965	2.7	9.0
Structure	964	—	2.8	11.2
Propulsion	191	—	3.1	8.9
Total subsystems	2,867	11,789	21.6	94.0
Program management and support			14.9	36.8
Total manufacturing cost			36.5	130.8
Total satellite manufacturing cost — three satellites plus design and development			167.3	
G&A and fee			43.5	
Satellite investment cost — three flight satellites			210.8	

the assumption that a basic satellite bus exists which is applicable to this mission.

Program management and support includes program management, program control, system engineering, system test, and environmental testing and launch support.

5.7.7 System Investment — 25 Beam Direct to User FDMA

The total investment of $2 billion required for a 25 beam system in which 5000 earth stations communicate on an FDMA SCPC basis is described in Table 5-9. Five thousand stations were chosen as a baseline because it

TABLE 5-9. 25 BEAM DIRECT TO USER SYSTEM INVESTMENT — 5000 EARTH STATIONS

Item	Cost, $M
Satellite (three flight satellites)	210.8
Launch (three launches)	56.8
TT&C	15.0
Total space segment and TT&C	282.6
4,300 small earth stations	1,191.1
535 medium earth stations	348.0
65 large earth stations	140.8
Total earth segment	1,719.9
Total system	2,002.5

appears that this is the maximum number of stations which can be reasonably supported by a spacecraft with acceptable blockage. The cost for other numbers of stations or other mixes of large, small, and medium stations can easily be calculated from the data in the table if the total spacecraft capacity is held constant.

It can be seen in the table that the system investment is dominated by the earth station cost. Since the number and mix of stations will be determined by market demand which is not yet known, the overall investment cost has limited significance. It is more useful to examine the annual revenue required for individual circuits. This data will be provided in a later section.

5.8 ANNUAL COST OF SPACE SEGMENT AND SYSTEM CONTROL AND MAINTENANCE

The annual cost of those system elements which are independent of the number and type of earth stations is shown in Table 5-10. The total investment for the space segment and its control, and for a master station in each beam is approximately $400 million. The cost of its master stations depends on what fraction of the traffic is interbeam. Because of the lack of interconnectivity in the satellite, the master station must communicate all of the interbeam traffic to master stations in other beams. It must also retransmit all traffic received from other master stations to the satellite for retransmission to the user stations. The master stations must perform these functions with minimal degradation of the signal. The degradation will be minimized by regenerating the data of the master station or by employing high EIRP and G/T at the master stations. The latter approach appears less costly and more reliable; however, a tradeoff has not been done

TABLE 5-10. ANNUAL COST OF SPACE SEGMENT AND COMMON SYSTEM CONTROL AND MAINTENANCE

System Element	Cost, $M
Space segment investment	283
TT&C	15
25 master stations	100
Total common investment	398
Annual depreciation of common investment	40
Return of common investment	62
System control and maintenance	5
Total common system annual cost	107
Net common system cost per:	($K)
64 kbps full duplex circuit	2.7
1.5 Mbps full duplex circuit	63.3
5.3 Mbps full duplex circuit	279.0

between regeneration and strong RF performance. The cost of the regeneration approach cannot be assessed without greater knowledge of the interbeam traffic. It appears that the cost of providing interconnectivity through the satellite would be less expensive than providing 25 master stations. In addition, it would eliminate the multiple hop, making the service more applicable and drawing more traffic.

The depreciation is based on a 10 year life for the common system elements. A post-tax return on investment of 11 percent is provided. This is equivalent to a pre-tax profit of about 22 percent.

The annual cost of controlling the spacecraft and providing demand assignment and other monitoring central control of the earth stations constitutes the system control and maintenance cost.

The annual cost of $107 million is apportioned to each of the services in proportion to the fraction of the system capacity of 5 GHz required by the circuit. The total annual revenue requirement for a circuit is determined by adding this cost to the portion of the cost of an earth station which is attributable to a circuit.

5.9 DIRECT TO USER SATELLITE SWITCHED TDMA CONCEPT

The direct to user satellite switched (SS) TDMA concept is illustrated in Figure 5-9. In each beam, at any time, one station is transmitting to the spacecraft. The instantaneous data rate is 200 Mbps, independent of the size of the earth station. Each of the 25 signals being received during a subframe is connected by the switch matrix to the appropriate downlink beam. Each downlink carries one 200 Mbps signal which is intended for a specific station. Over a complete frame, each beam is connected during a subframe to each other beam.

The satellite repeater is the same as the satellite repeater described for the TDMA system, with the addition of the 25 x 25 switch matrix.

5.9.1 Direct to User TDMA Link Budget

The TDMA link budget differs from the FDMA link budget in that:

1) All links are at a 200 Mbps QPSK rate. The C/N_o required for all links with $C/I \sim 18$ dB is then C/N_o (required) = 13.1 + 10 log 200×10^6 = 96.1

2) All earth stations have to handle a higher data rate than any of the FDMA stations, and thus require higher EIRP.

The TDMA link budget is shown in Table 5-11.

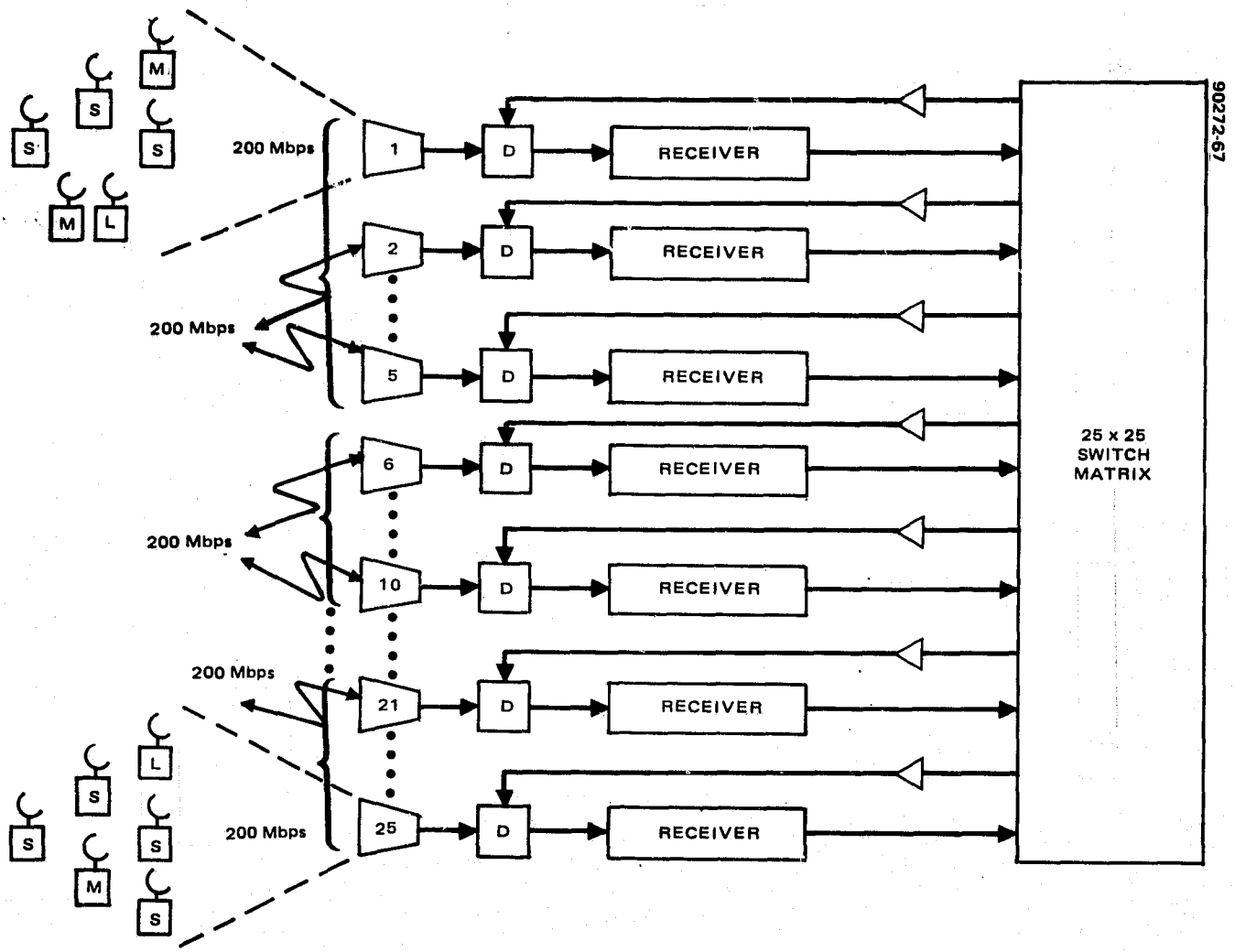

FIGURE 5-9. DIRECT TO USER SATELLITE SWITCHED TDMA CONCEPT

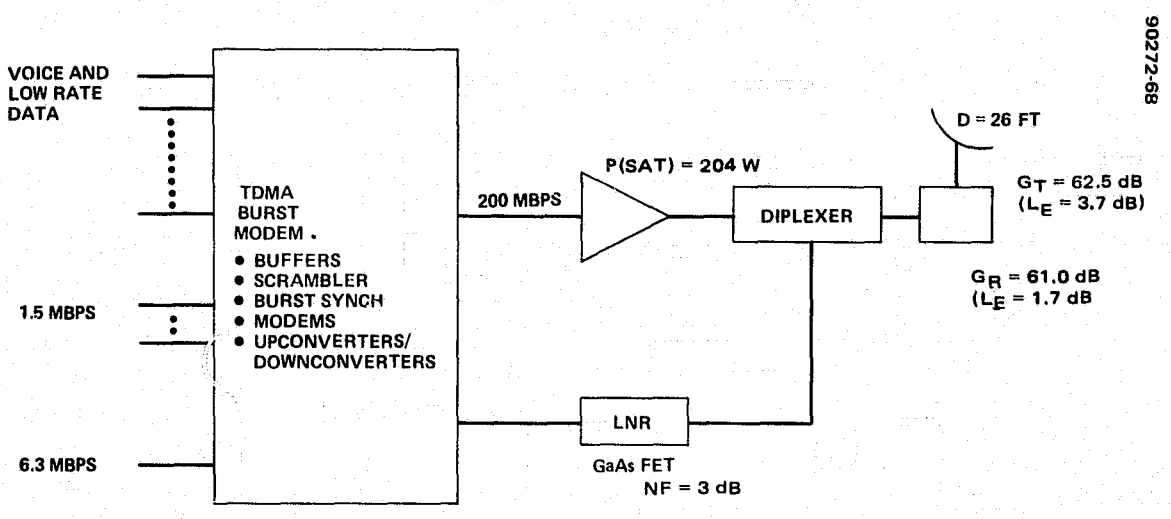

FIGURE 5-10. DIRECT TO USER TDMA EARTH STATION

TABLE 5-11. DIRECT TO USER TDMA LINK BUDGET

Parameter	Uplink	Downlink
EIRP	83.9	60.4
Pointing loss	-0.4	-0.4
Path loss	-212.9	-210.2
Atmospheric loss	-0.7	-1.0
Rain attenuation (propagation reliability = 99.5%)	-14.9	-6.5
Polarization loss	-0.2	-0.2
Pointing loss	-0.6	-0.2
G/T	19.4	31.6
$C/N_0 = C/T + 228.6$ dB	102.2	102.0
Uplink noise degradation	—	2.9
C/N_0 link	—	99.1
C/N_0 (required) (200 Mbps)	—	96.1
Margin for impairments	—	3.0

5.9.2 Direct to User TDMA Satellite

The satellite for the 25 beam TDMA system is essentially the same as that of the 25 beam FDMA system, with the addition of a 25 x 25 microwave switch matrix to provide interconnectivity. The switch adds about 40 pounds and negligible power load to the spacecraft, and has a recurring cost of about $3 million per spacecraft, including the increased cost of test and integration of the repeater. The impact on annual cost per circuit given in subsection 5.8 is negligible.

5.9.3 Direct to User TDMA Earth Station

In the TDMA system (Figure 5-10) each station uses the same 200 Mbps burst rate, whatever its baseband capacity. This increases the earth station RF burden, particularly for the majority of stations which require an average data rate of less than 1 Mbps. The RF cost is minimized for the TDMA system by a larger earth station antenna than the FDMA system station antenna to minimize system cost. The 26 foot diameter poses a siting problem, as described in the FDMA earth station section.

Assuming an output circuit loss of 1.7 dB, the EIRP is given by

$$EIRP = 23.1 - 1.7 + 62.5 = 83.9 \text{ dBW}$$

The receive temperature is 28.8 dB/°K, as for the FDMA earth station

$$G/T = 62.5 - 28.8 = 33.7 \text{ dB}$$

The individual SCPC modems of the FDMA earth station are replaced by a single 200 Mbps burst modem with a complement of input/output circuits appropriate to the size of the station. Each input circuit has a compression buffer which reads in data at the baseband rate and which is read out in 200 Mbps bursts. Each output circuit has an expansion buffer which is loaded by 200 Mbps bursts and is read out at the baseband rate.

5.9.4 Direct to User Earth Station Cost

The cost breakdown for the TDMA earth station is shown in Table 5-12. The RF costs do not include redundancy. The modem costs, which are considerably lower than the FDMA modem costs for the large stations, are somewhat questionable since, unlike SCPC voice modems, there are no existing modems which match the baseband inputs of these stations to 200 Mbps outputs. In general, the TDMA modem costs shown project considerable cost reduction from todays comparable costs. This projection appears consistent with the trend in digital electronics.

5.9.5 Direct to User Annual Service Costs

The annual revenue requirements for three types of circuits are shown in Table 5-13. The revenue requirements are the sum of the space segment annual costs attributable to an individual satellite circuit from the previous section and the portion of the cost of an individual earth station attributable to the circuit. The earth station cost attributable to a circuit is the earth station total cost times the fraction of total earth station capacity represented by the service. For example, a 64 kbps voice circuit is approximately one-fourteenth of the small station capacity (12 voice circuits, two 56 kbps data circuits) and $64 \times 10^3 / 27.3 \times 10^6$ of the large station capacity. It can be seen that service costs are lower for the large stations due to economy of scale.

TABLE 5-12. DIRECT TO USER TDMA EARTH STATION COST, $K

Breakdown	Station		
	Small	Medium	Large
Antenna	45	45	45
Transmitter	95	95	95
Receiver	15	15	15
TDMA burst modem	100	154	250
Shelter, cabling, etc.	5	9	28
Total equipment	260	318	433
Labor	87	106	144
Total equipment and labor	347	242	577
Contingency	18	36	123
Total manufacturing cost	365	460	700
G&A plus profit	95	120	182
Total cost (FOB factory)	460	580	882

TABLE 5-13. DIRECT TO USER ANNUAL SERVICE COSTS, $K*

Item	Station					
	FDMA			TDMA		
	Small	Medium	Large	Small	Medium	Large
Earth station investment	277	611	2167	460	580	882
Net earth station revenue (per station)	94	208	736	156	197	300
Revenue required per						
• 64 kbps circuit ($3K)**	16	7.8	6.5	25	7.4	4.4
• 1.5 Mbps circuit ($74K)**	–	134	156	–	180	107
• 6.3 Mbps circuit ($326K)**	–	–	669	–	–	466

*Not tarrif or lease; does not account for utilization.
**( ) Space segment revenue required per circuit.

The service costs shown do not define the cost to the ultimate user because they do not account for the utilization of the system. Since the subsystem will not be fully utilized throughout its life, the cost will be higher.

5.9.6 Sensitivity of Cost to Number of Beams

If the system capacity is held constant and the number of spot beams is varied, the principal effects are:

1) Antenna gain varies, thus varying the requirements for satellite and earth station transmitter power. The increase in antenna gain with increasing number of beams decreases RF costs.

2) Satellite antenna cost varies somewhat. The number of reflectors is unchanged.

3) The cost of satellite interconnectivity varies. For the FDMA as defined in the SOW, there is no interconnectivity and thus no effect; however, if interconnectivity were provided, the number of filters required would vary as the square of the number of beams. In a TDMA satellite the order of the switch matrix will vary with the number of beams. The weight of the switch matrix tends to vary as nearly the third power of the order, and the cost varies as the square of the order. Cost and weight of microwave switch matrices are given as a function of matrix order in Section 3.

The variation of total system investment as a function of the number of beams is shown in Figure 5-11. While the cost savings obtained by increasing the number of beams from 25 to 40 is modest, the cost increase when the number of beams is reduced to 10 is significant. Note that over the range specified in the SOW (10 to 40 beams), the variation in cost of the switch matrix is insignificant.

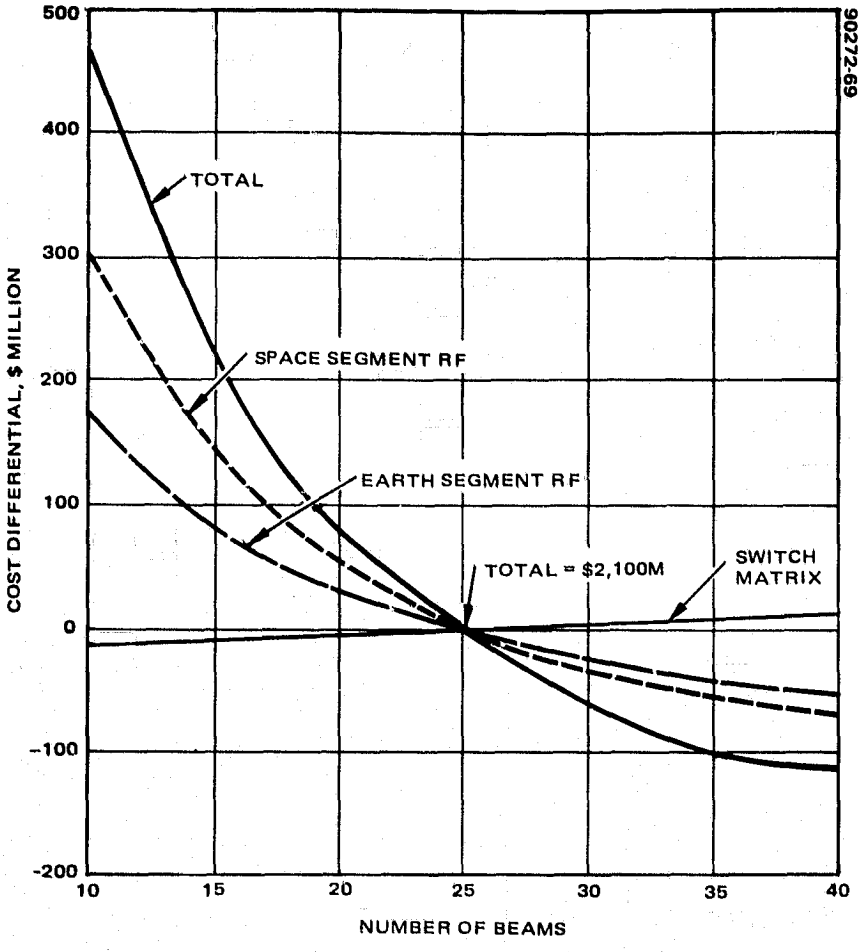

FIGURE 5-11. SENSITIVITY OF COST TO NUMBER OF BEAMS (TOTAL SYSTEM CAPACITY HELD CONSTANT, BURST RATE, AND THUS EIRP, IS INVERSELY PROPORTIONAL TO NUMBER OF BEAMS)

5.9.7 Sensitivity of Cost to Number of Stations

The effect on the system cost and the annual cost of a circuit of varying the number of earth stations depends on the assumptions made about the system capacity and the number of modems at the stations. If it is assumed that the satellite capacity is maintained at 5 GHz and the station sizes remain the same; i.e., the number of each type of circuit in the station remains the same, and their mix remains the same as for the baseline, then the annual cost of a circuit will remain the same, as presented in subsection 5.9.5. The availability of satellite circuits will vary, and will depend on the traffic demand, which is not known.

6. COMPETITIVE ALTERNATIVES

Task 4 requires a comparison of the concepts in Sections 4 and 5 with current Domsat systems. Such a comparison can have only limited objectives because of important differences between the concepts in this report and current Domsat systems which are unrelated or slightly related to the frequency band. However, one apparently valid conclusion to be drawn from such a comparison is that if current Domsats are economically viable, then the concepts considered in Sections 4 and 5 of this report are extremely cost effective if the traffic demand exists. This conclusion is derived from the data in Table 6-1.

In Table 6-1 the cost of both space segments and individual earth stations for the trunk and direct to user TDMA concepts are compared to those costs for current Domsats. The costs are normalized to cost per 40 Mbps to make the comparison consistent. The cost of the current Domsat space segment is based on earlier programs inflated to 1979 dollars. The cost of the current Domsat space segment includes three Atlas/Centaur launches rather than the less expensive shuttle launches assumed for the 20/30 GHz systems. Because the current Domsat parameter of interest in this comparison is what a user would pay for the system, this difference in launch assumptions is justified. Even assuming that the 20/30 GHz costs are optimistic compared

TABLE 6-1. SPACE SEGMENT AND EARTH STATION COST COMPARISONS

Item	20/30 GHz		Current Domsat (Typical)
	10 Beam TDMA Trunk	25 Beam Direct to User TDMA	
Propagation reliability, %	99.9	99.5	99.99
Space segment cost, $M*	140	265	160
Satellite capacity, Mbps	24,710	5,000	1,000
Space segment cost per 40 Mbps, $K	224	2,120	6,400
Earth station (RF only), $K	2,863**	285	NA
Earth station burst rate, Mbps	2,471	200	NA
Earth station cost per 40 Mbps, $K	46	57	NA

*Includes three satellites plus three launches.
**Dual site.

to actual costs that the current Domsat price is based on, it can be seen that the economy of scale that results from the great capacity of the multibeam spacecraft makes them very cost effective. The propagation reliability of the 20/30 GHz systems is lower than that of the current Domsat. If the costs associated with a trunk system at 99.99 percent were used rather than those for 99.9 percent, the result would not be significantly changed. The same cannot be said for the direct to user systems at 20/30 GHz.

The earth stations also benefit from the economy of scale associated with high data rates; however, this economy of scale could as easily be achieved at C or Ku band. At any rate, the 20/30 GHz earth station costs appear economically viable.

7. CRITICAL TECHNOLOGY

7.1 INTRODUCTION

This section discusses the technological developments which are most critical to exploiting the two most important features of the concepts discussed in Sections 4 and 5; namely, the application of a relatively unused frequency band and the use of a fairly large number of spot beams.

7.2 MULTISPOT BEAM TRUNK ANTENNAS

The problems associated with a multispot beam antenna are illustrated in Figure 7-1.

The orientation of the spot beams is dictated by the location of the earth stations in the system. When these stations are close together, two problems arise. In order for the beams to have a small angular separation, the feeds associated with the beams must be closely spaced, perhaps causing physical interference. In the trunk baseline, two reflectors were used to alleviate this problem. Closely spaced beams also introduce an isolation problem. In the trunk system, spatial isolation was augmented by cross polarization.

A problem corollary to the feed crowding problem is that of providing feeds at both the transmit and receive bands. If separate feeds are used at both 20 and 30 GHz for each beam, the feed crowding problem is aggravated. If a single feed is used it is difficult to optimize the feed for both bands.

When the area of coverage is a great many beamwidths, as it is in the baseline trunk concept, the beams which are displaced from the antenna mechanical boresight can suffer significant gain loss.

7.2.1 Feed Interference

Feed interference occurs when the separation of phase centers for two feeds is less than the physical dimension of the feeds. The phase centers for two feeds whose beams are separated by a specified angle move apart as the focal length increases. For a given F/D, the focal length increases with diameter. Thus, increasing diameter relieves feed crowding. Increasing F/D has a smaller effect on feed crowding because it causes feed size to increase. Figure 7-2 shows how the ability to provide separate beams for

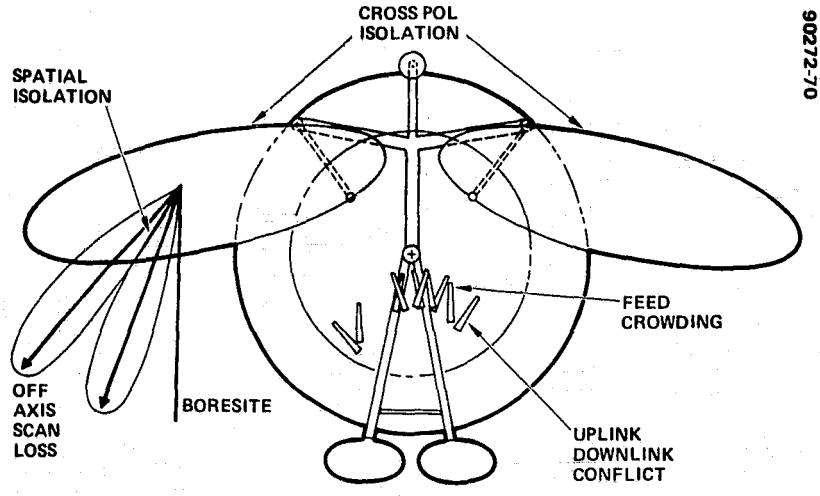

FIGURE 7-1. TRUNK ANTENNA CONFIGURATION

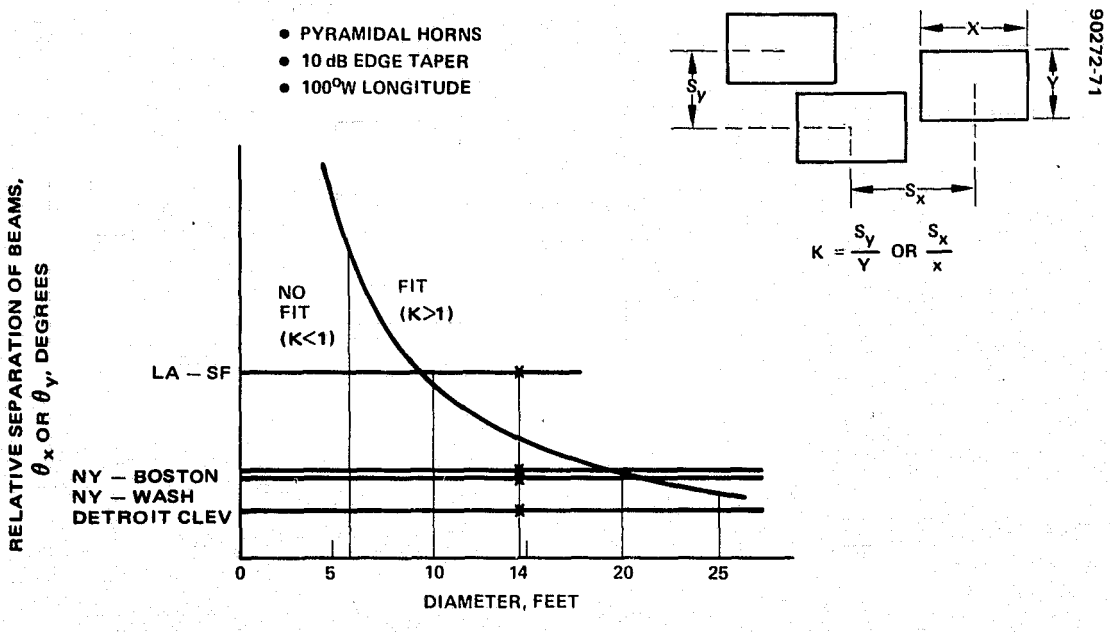

FIGURE 7-2. FEED SEPARATION VERSUS DIAMETER

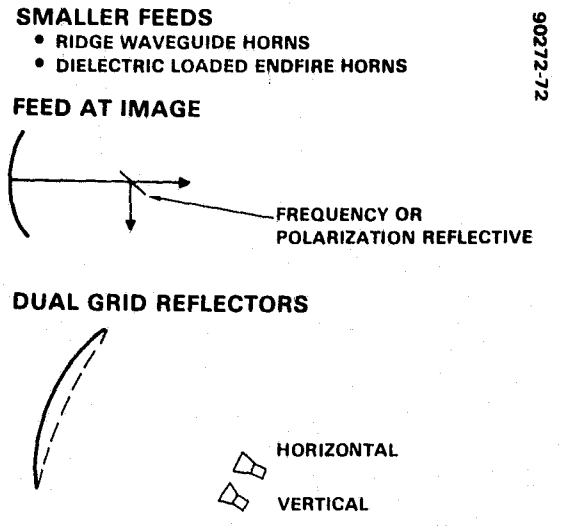

FIGURE 7-3. POTENTIAL IMPROVEMENTS TO FEED CROWDING

several pairs of cities varies with diameter. Of the baseline city pairs, only the New York and Washington feeds would interfere if they shared a reflector. For a 20 beam system, other cases of interference would occur. The baseline solution avoided the technology problem by providing separate reflectors for interfering feeds. There are other potential technological solutions (Figure 7-3). The baseline system used conventional pyramidal horns for feeds. Smaller feeds might be realized using ridge waveguide horns or dielectric loaded endfire horns; however, a number of serious technical problems must be solved before these techniques are practical. Another approach is to provide two possible locations for each feed. This can be done using a frequency or polarization sensitive surface to create an image of the focal point. The same effect can be produced by dual grid reflectors which simulate two reflectors with different focal points. These techniques also require development.

7.2.2 Beam to Beam Isolation

Beam to beam isolation is enhanced by increasing the antenna diameter to narrow the mainlobe of the antenna pattern and by increasing F/D and reducing obstruction to hold down the sidelobe level. The diameters required for two levels of C/I for the baseline are shown in Figure 7-4. The C/I values in the figure are theoretical and may be optimistic by 2 dB. A C/I of about 17 dB produces acceptably low data degradation for a QPSK signal; however, if a multimode transmitter is used as in the trunk baseline of Section 4, an additional margin equal to the difference in power between the low and high modes is required because of the increased level of interference when an adjacent beam is boosted. Multifeed techniques can reduce sidelobes, but must be developed for this type of application.

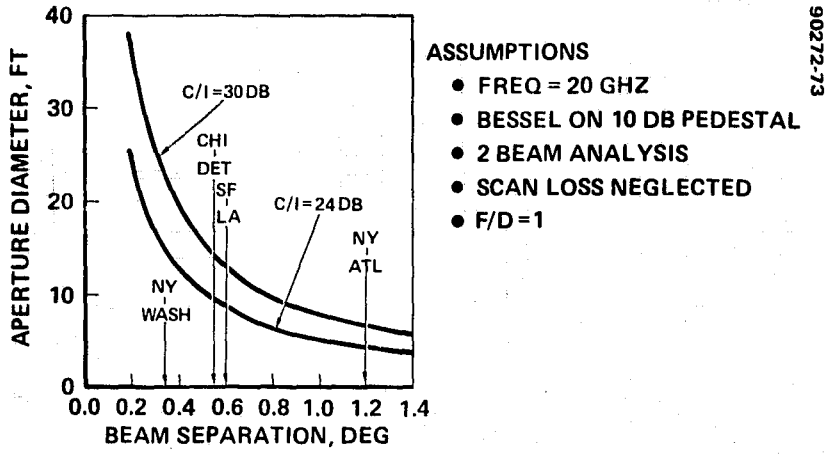

FIGURE 7-4. APERTURE SIZE VERSUS BEAM SEPARATION

7.2.3 Off-Axis Scan Loss

Increasing antenna diameter alleviates the problems discussed above; however, as the beam shrinks, the spacing between the antenna boresight and cities at the edge of coverage becomes a greater number of beamwidths, and the off-axis scan loss increases. Thus, the advantages in gain and beam isolation obtained from increased diameter by cities near boresight are at least partially lost by those cities displaced from the boresight. Figure 7-5 shows gain variation with angular separation from boresight for several configurations. For an offset parabola on a spinning spacecraft, available focal length is limited by the Shuttle diameter if feeds are not deployed or folded optics utilized. A body stabilized spacecraft allows somewhat greater focal lengths but still suffers practical limitations. For offset parabola antennas the effective F/D is less than one-half the F/D calculated using aperture diameter. Thus, a diameter of about 10 feet is maximum before off-axis scan loss becomes excessive. The baseline solution was to use an offset cassegrain configuration to allow adequate focal length. The subreflecter configuration assumed provided an F/D of 1.17 which provides adequate off-axis gain performance and appears to provide adequate C/I performance. The reason for the low gain shown at 30 GHz in Figure 7-5c is that a single feed was used for both frequencies and optimized for 20 GHz. Another option is to use a lens antenna, but lens antennas are very heavy or very complex.

7.2.4 Dual Frequency Feeds

Feed placement problems are simplified if dual frequency feeds are used; however, significant losses can occur, as shown in Figure 7-5, where the offset cassegrain gain at 30 GHz is greatly reduced from the theoretical value because the feed is optimized for 20 GHz.

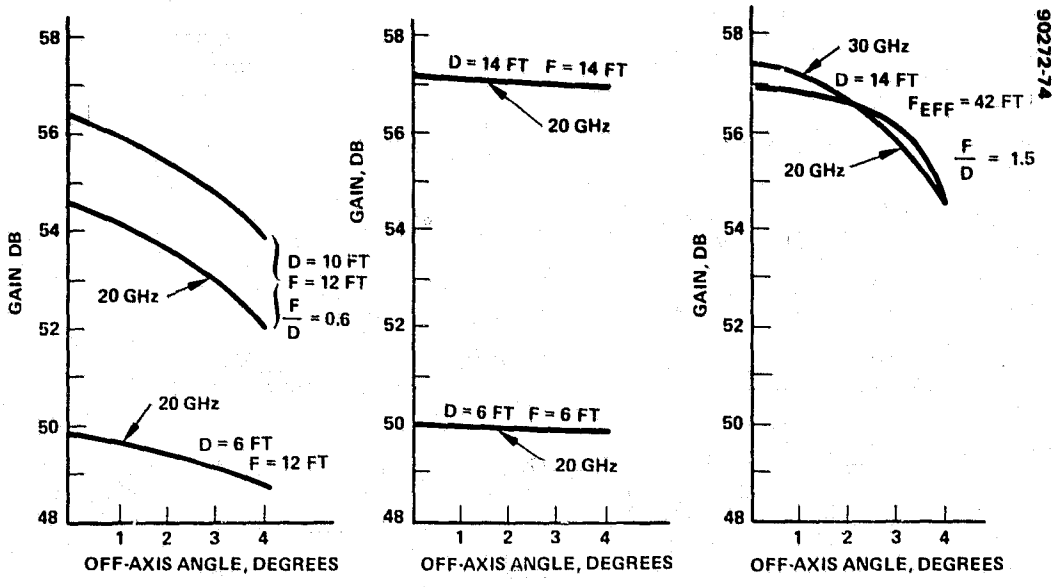

NOTE: GAIN VALUES DO NOT INCLUDE ANY LOSSES

FIGURE 7-5. OFF-AXIS GAIN LOSS COMPARISON

7.3 DIRECT TO USER MULTISPOT BEAM ANTENNA

Problems similar to those affecting the trunk antenna arise with the direct to user antenna. If continuous coverage is required over a large area, the feed interference problem becomes severe. In the baselines of Section 5, five reflectors were used. Technological development of smaller feeds or multifeed beam techniques might reduce the number of antennas required. Beam isolation requirements dictate good sidelobe suppression.

The direct to user antenna is sized by the spot size required for coverage of the specified area by the specified number of beams. Ideally, the spot size is the same at both 20 and 30 GHz. This requires separate antennas of different diameter for receive and transmit, or development of reflectors which have different effective dimensions at the two frequencies, or development of suitable reflector illumination techniques.

7.4 SATELLITE TRANSMITTERS

Several trunk transmitter configurations are shown in Figure 7-6. There are two potential configurations for the FDMA trunk. Individual amplifiers can be provided for each channel, as in Figure 7-6a, or all (or several) of the channels can be combined in a single amplifier, reducing the

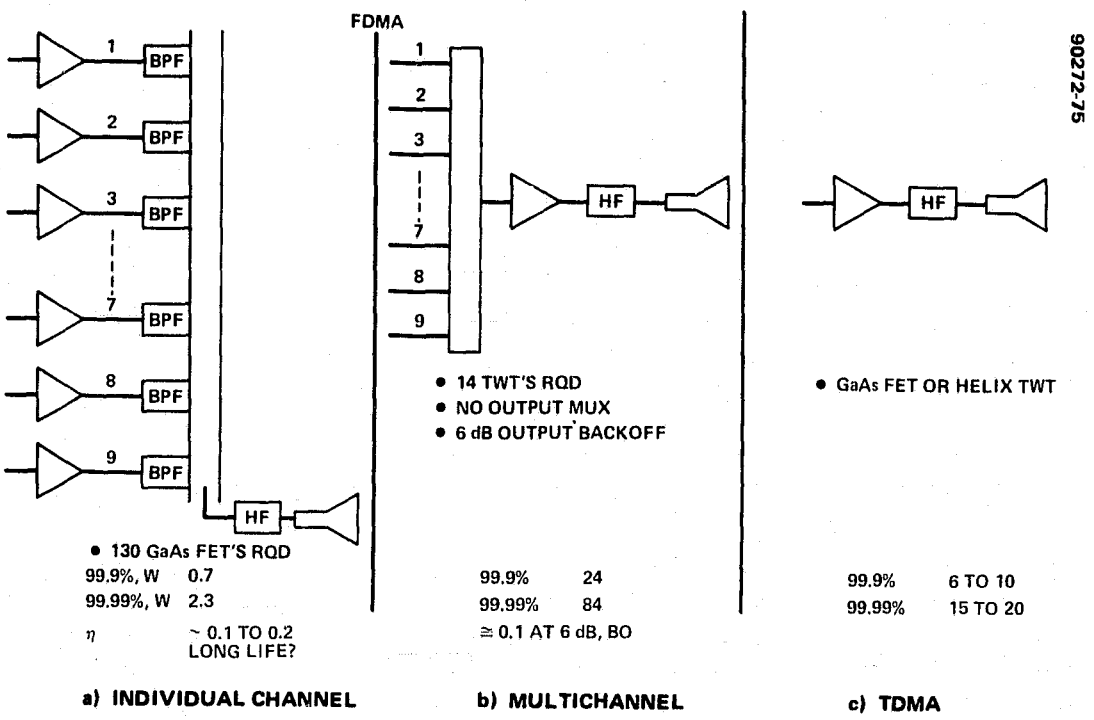

FIGURE 7-6. TRUNK TRANSMITTER CONFIGURATIONS

number of amplifiers but increasing the power capability required of the amplifiers and increasing the primary power requirement by backed off operation. The individual amplifier approach allows use of solid state amplifiers with potentially higher reliability and lower weight; however, long life reliability of GaAs or IMPATT amplifiers at this frequency and power level have yet to be demonstrated. In fact, 20 GHz GaAs amplifiers are not yet commercially available at the power levels required by these systems. Demonstration of long life operation of 20 GHz GaAs FET amplifiers at the level of 1 to 6 watts would be a valuable development. Also, techniques for combining GaAs FET chips to obtain multiwatt capability with long life would be valuable. The efficiency achievable with 20 GHz high power GaAs FET amplifiers also needs considerable improvement. Although some applicable development is being funded by the Department of Defense, it is desirable that this effort be broadened to include a greater number of potential suppliers.

The multichannel approach of Figure 7-6b requires use of a TWT. Multistage collectors can help maintain satisfactory efficiency with backed off operation. The backoff required as a function of the way the spectrum is utilized by digital data requires study. Systematic analysis of the bit error rate degradation produced by various combinations of digital channels at different backoff levels is required to effectively use this approach.

For an FDMA system, the use of the configuration in Figure 7-6b eliminates the serious output multiplexer problem discussed in subsection 7.5.

The TDMA trunk as defined for this study uses a single amplifier per beam. It will probably be difficult to achieve adequate power for this channel with solid state amplifiers, but adequate TWTs have been developed.

7.5 FDMA MULTIPLEXERS

When the single channel per amplifier configuration of Figure 7-6a is used, a serious output multiplexer problem arises. As the number of channels increases beyond about five, it becomes very difficult to simultaneously maintain low output loss and reasonable channel capacity. As the filter skirts are sharpened to allow more spectrum for each channel, the filter losses increase rapidly. Also, fabrication and tuning of the multiplexers becomes extremely difficult and expensive. Techniques for solving these problems are required to allow an FDMA trunk satellite to efficiently use the spectrum.

7.6 MICROWAVE SWITCH MATRIX

A number of technological problems remain to be solved before microwave switch matrix (MSM) modules can be effectively produced. First, there is a need to develop improved techniques for interfacing control signals to switch elements. This interface is important because it is one of the factors which can limit switching speeds of the matrix (other factors are the circuit and devices used). Transmission lines used for carrying the control signals must be of RF quality to minimize any distortions, and still must have flexibility for multiple interconnects to the digital control unit.

The use of multilayer printed microwave circuits is one possible solution. This approach would enable the control signals to be carried on thin substrates located under the main MSM circuitry. Connections between circuits can be via circuit board holes or at the edges. Use of multilayer microwave circuits may also be the solution to the intermodular connection problem. Potential misalignment problems between modules increases with the matrix order because of tolerance buildups associated with higher order matrices. Multilayer technology holds the potential of achieving the required complex intermodular connections and still maintain the capability of repair and replacement of individual modules.

Another problem associated with the MSM is the relatively high cost of fabrication. A development which has the potential of reducing the recurring cost by 50 percent is microwave large scale integration (MLSI). The MLSI process can provide large quantities of active devices on a single chip. Such a process will increase the reliability and cost-effectiveness of the component, for it eliminates many of the manual chip and wire bonding tasks associated with conventional MIC hybrid techniques.

MLSI is important because the N^2 cost factor mentioned earlier would not apply. If MLSI processes are used, active devices are not individually assembled to the main circuit. Thus, the increases in cost associated with the production of higher order matrices will primarily result from the additional hardware and testing required. Integrated circuits on GaAs for microwave applications has considerable interest industry-wide for many applications, so development of portions of this technology will progress in parallel with MSM requirements.

7.7 LOW NOISE AMPLIFIERS

GaAs FET devices hold the potential for adequate noise figures for the satellite receiver front end. Noise figures of 4 dB for the receiver are well within the realm of possibility. The potentially lower noise figures obtainable with parametric amplifiers or through the use of cooling is not justified because of the 290°K sky temperature.

APPENDIX A.

18/30 GHz MULTIPLE SPOT BEAM ANTENNA STUDY

By

David Nakatani, Donald Chang, Hiram Ohta, and
Russel R. Persinger

18/30 GHz MULTIPLE SPOT BEAM ANTENNA STUDY

TABLE OF CONTENTS

1.0	INTRODUCTION	A-3
1.1	Determination of Antenna Aperture Size	A-4
1.2	Comparison of Antenna Systems	A-6
2.0	PRIME FED REFLECTOR SYSTEMS	A-14
2.1	Offset Parabolic Torus	A-14
2.2	Offset Paraboloidal Reflector	A-34
2.3	Spherical Reflector	A-38
3.0	FOLDED OPTICS SYSTEMS	A-45
3.1	Offset Cassegrain Antenna	A-46
3.2	Offset Double Reflector Parabolic Torus	A-50
4.0	LENS ANTENNA SYSTEMS	A-54
4.1	Waveguide Lens	A-54
4.2	Dielectric Lens	A-62
5.0	14-FOOT OFFSET CASSEGRAIN ANTENNA-BASELINE	A-69
6.0	ANTENNA TECHNOLOGY INVESTIGATION	A-76
7.0	DIRECT TO USER ANTENNA	A-80
8.0	CONCLUSION	A-95
	REFERENCES	A-97

1.0 INTRODUCTION

Future generations of satellite communication systems will be required to operate in higher frequency bands of 18 and 30 GHz as the presently utilized 4/6 GHz and 12/14 GHz bands become saturated. The purpose of this study is to analyze, evaluate and trade-off various types of multiple beam antenna systems operating at 18 and 30 GHz suitable for synchronous orbit communication satellites. The final results of the study is to arrive at a recommended antenna configuration and identify key technologies for further research.

This section discusses and presents the results of estimated performance of antenna gain, off-axis gain losses and carrier to interference (C/I) performance for a ten city scenario shown in Figure 1-1 as seen from a satellite positioned at 100 degrees west longitude. The ten cities include New York, Chicago, Atlanta, Houston and Los Angeles, Washington, D.C. St. Paul, Dallas, Denver and San Francisco.

Basic antenna configurations of prime fed reflectors, reflectors employing folded optics and lens antennas were studied for their ability to form spot beams positioned up to 4 degrees from the boresight axis. Among the class of prime fed reflectors, the offset parabolic torus, the offset paraboloids, and spherical reflectors were evaluated because of their relative simple geometry. Offset Cassegrain and offset double reflector parabolic torus were two folded optic designs studied for reducing the package volume of the antennas. Waveguide and dielectric lenses were investigated due to their excellent off-axis beam performance. Antenna arrays were not included because of their difficulty in forming multiple independent beams.

1.1 Determination of Antenna Aperture Size

The spot beam illumination of the ten cities operates in the Frequency Domain Multiple Access (FDMA) mode making beam isolation an important factor for frequency reuse. Ideally, it is desirable to have an uplink and downlink over each city which provide infinite isolation between beams over the other cities. However, an antenna of a practical aperture size produces spot beams each having a finite beamwidth with many sidelobes. These sidelobes are potential sources of interference to the other spot beams and the design and performance of the space segment portion of the 18/30 GHz communication system is dependent upon the amount of interference affecting crosstalk in a multiple beam frequency reuse system.

Spatial beam isolation and polarization isolation are two techniques that can be used to achieve frequency reuse and have been demonstrated for satellite communication by Intelsat IVA[1] and Comstar[2] I respectively. For CONUS city coverage, spatial beam isolation requires a sufficiently large antenna aperture that will produce a beam narrow enough with sidelobes low enough for acceptable isolation. Typically city to city angular separation of several beamwidths are required to keep sidelobe interference to a low level (greater than 25 dB).

Polarization isolation utilizes orthogonally polarized beams to achieve frequency reuse between beams. For the 18/30 GHz system, a combination

of both spatial beam isolation and polarization isolation can be effectively used to achieve nearly equal C/I performance with smaller antenna apertures than if spatial beam isolation only were used.

In order to estimate the required aperture diameter of a frequency reuse antenna using spatial isolation only, a plot of aperture diameter versus angular separation between beams for a circular aperture was prepared and the results are shown in Figure 1-2a for two different values of carrier over interference ratio (C/I). The C/I ratio is a measure of isolation where the gain of the beam of interest is compared with the composite sidelobe gain of other beams as shown in Figure 1-2b. The plots of Figure 1-2a are based on a simple two beam analysis of the radiation patterns shown in Figure 1-3b and with no loss. The assumed amplitude distribution over the aperture was a Bessel function on a 10 dB pedestal shown in Figure 1-3a. Although the sum of the nine sidelobe levels with random phases forms an interfering signal for the ten city scenario, the two beam analysis was used since the sidelobe level of the closest beam is the most significant one and is sufficient to estimate the required aperture size.

For the ten city distribution of Figure 1-1, the closest beam separation is 0.3 degrees between New York and Washington. To achieve a 30 dB C/I ratio, an aperture diameter of about 25 to 30 feet is required if spatial isolation only is implemented. Such a large antenna aperture creates problems of stowage and erection on the spacecraft, more difficulty in fabrication to achieve good reflector tolerance and higher cost of fabrication in tooling materials, and labor. The aperture diameter can be reduced and still maintain nearly the same C/I performance by using orthogonal polarization isolation for half of the beams.

This technique allows the cities to be divided into two groups (one group is vertically polarized and the other group is horizontally polarized) so that the closest beam separation of the cities using spatial isolation increased to approximately 1.2 degrees between Chicago and Atlanta. City divisions are shown in Figure 1-1 where the first group consists of New York, Atlanta, Chicago, Houston and Los Angeles, and the second group consists of Washington, St. Paul, Dallas, Denver and San Francisco. Memphis and Wichita were arbitrarily selected to be the boresight positions of the respective city group for this study.

The two beam analysis of Figure 1-2 indicates that a minimum 6 foot diameter aperture might meet a C/I ratio of 30 dB. If interference effects of other beams are added and the effects of aperture phase error of off-axis beams are included the aperture diameter will be greater than 6 feet to maintain the high C/I ratio. The maximum diameter of solid reflectors is limited to about 14 feet for shuttle launch compatibility. Aperture size greater than 14 feet in diameter will require some type of unfurlable surface. In the analysis to follow, a set of 6 to 14 foot diameter antennas of the different geometries were investigated using both spatial and polarization isolation techniques to achieve independent beam coverage over each city.

1.2 Comparison of Antenna Systems

A comparison of antenna characteristics of various multiple spot beam antennas for 18 and 30 GHz applications is summarized in Figure 1-4. The prime fed reflectors are examples of single reflector geometries with the feeds clustered near the prime focal region. Offset reflectors reduce

blockage and improve aperture efficiency. Double reflector geometries can also be configured to eliminate subreflector blockage. In general, greater offset is required for the double reflectors than single reflectors. The spherical reflector cannot be offset because of its geometry, consequently, its blockage is large. Lens antennas have no blockage and the feed can be positioned near the axis of symmetry.

The off-axis gain loss is one of the primary concerns for the selection of the 18/30 GHz baseline antenna since the outer beams will be positioned more than ten beamwidths from the reflector axis. Off-axis gain loss is minimized by eliminating comatic aberration. This aberration can be eliminated when the Abbe sine condition is satisfied[3]. The basic geometric requirement to satisfy this condition is that the refracting or reflecting surface closest to the focal point be a spherical surface. This condition is readily met for a lens since the surface closest to the focus can be spherically shaped. Thus a lens antenna can be designed to have small off-axis gain loss.

A spherical reflector also meets the Abbe sine condition, however its feed blockage for a multiple beam antenna is significant. The antennas which have the next best off-axis gain performance are the folded optic geometries which have low to moderate off-axis gain loss. Such geometries have an equivalent image reflector of the folded optic geometry consisting of a main reflector and subreflector. When the effective focal length of the image reflector increases to a large value, the image reflector shape begins to approach that of a spherical surface providing good off-axis gain performance.

Bandwidth consideration is another determining factor in the baseline antenna selection. Except for the waveguide lens, bandwidths of the reflector antennas are primarily dependent on feed characteristics over frequency. The waveguide lens is more bandwidth limited because of dispersion and phasing elements of the lens which have a narrower bandwidth than the feed. Thus, use of a waveguide lens antenna requires a separate lens for 18 and 30 GHz. A total of 4 lenses will be required for two orthogonal polarization senses. The fabrication technique and tolerance control at 18/30 GHz become very difficult for waveguide lenses in the 6 to 14 foot diameter class.

For dielectric lens application, several materials were investigated for space communication. Bulk dielectric materials such as teflon, ceramics, and foam are not always suitable because they cannot withstand the thermal range or outgassing requirements of the space environment. Phase delay artificial dielectrics may be used for lens application and can be made from sheets of space approved dielectric material such as metallized Kapton on which an array of metallic discs are etched. The tolerance control of the metallic disc is very critical to obtain a uniform dielectric constant.

The recommended baseline antenna for the 18/30 GHz multiple spot beam application as a result of this study is the offset fed Cassegrain antenna. Two such reflector antennas are required for the proposed antenna system using beam spatial and polarization isolation for a ten city scenario. The diameter of the antenna depends on the C/I performance specification. For a minimum C/I requirement of 30 dB, it is recommended that a 14 foot

diameter aperture be used. The half power beamwidth of this size aperture is approximately 0.2^{o} at 30 GHz and 0.3^{o} at 20 GHz. For reduced C/I requirements, a smaller diameter antenna can be used. Depending upon the selected aperture size adequate performance (C/I) can be obtained with a prime fed offset paraboloid.

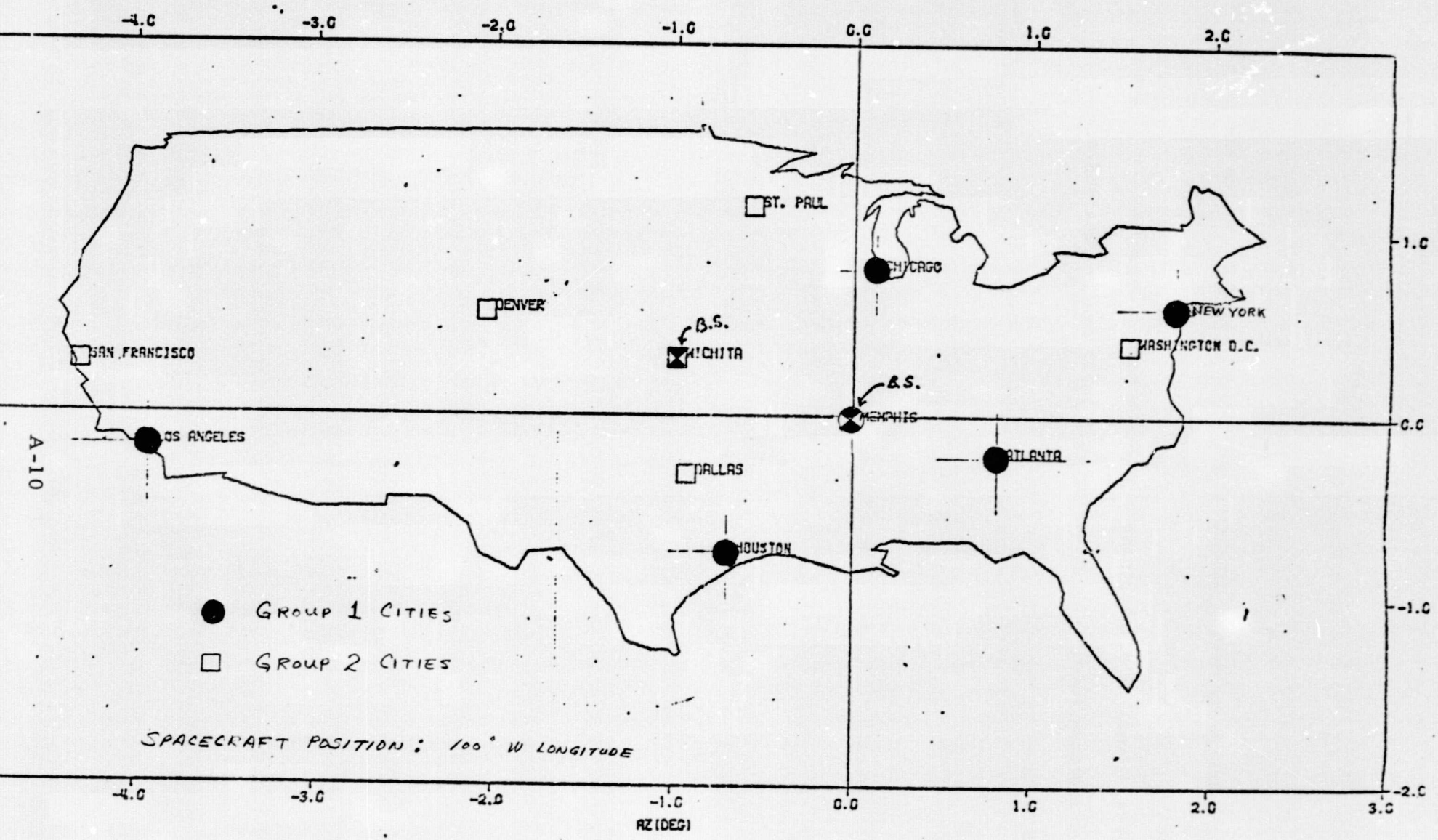

FIGURE 1-1 TEN-CITY ILLUMINATION

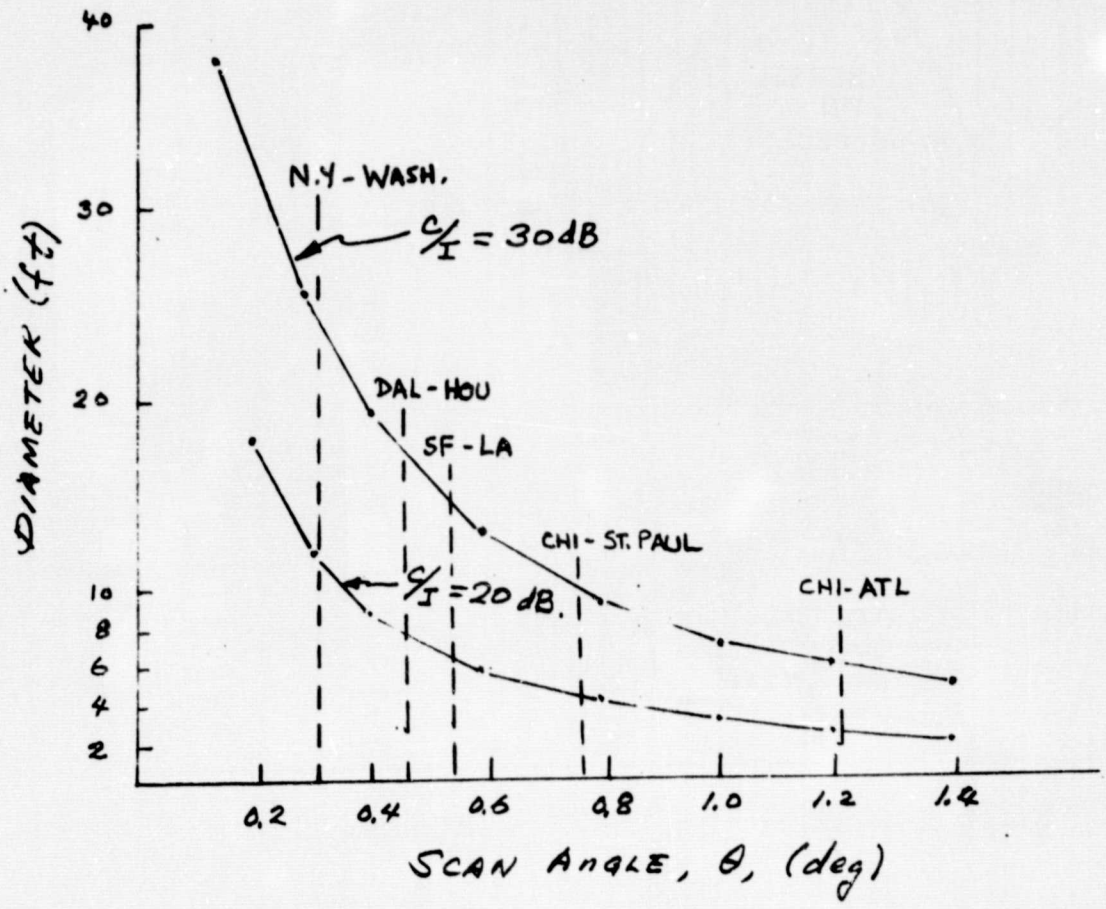

(a) DIAMETER VERSUS SCAN ANGLE

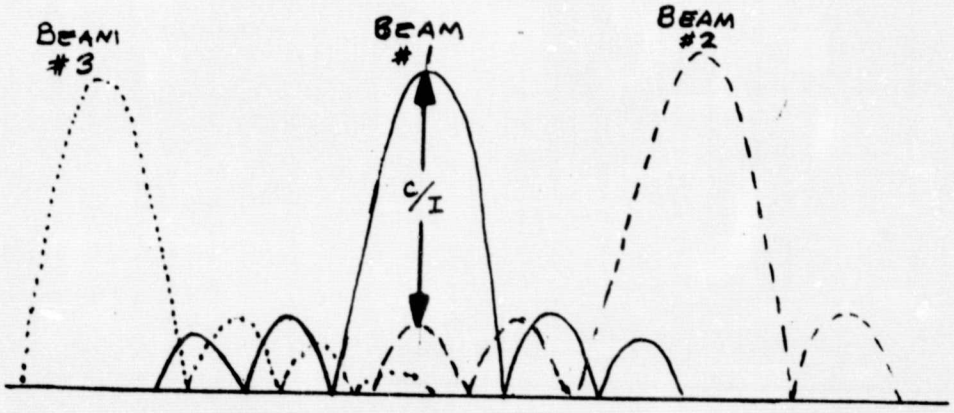

(b) C/I DEFINITION

FIGURE 1-2 C/I PERFORMANCE AND APERTURE DIAMETER

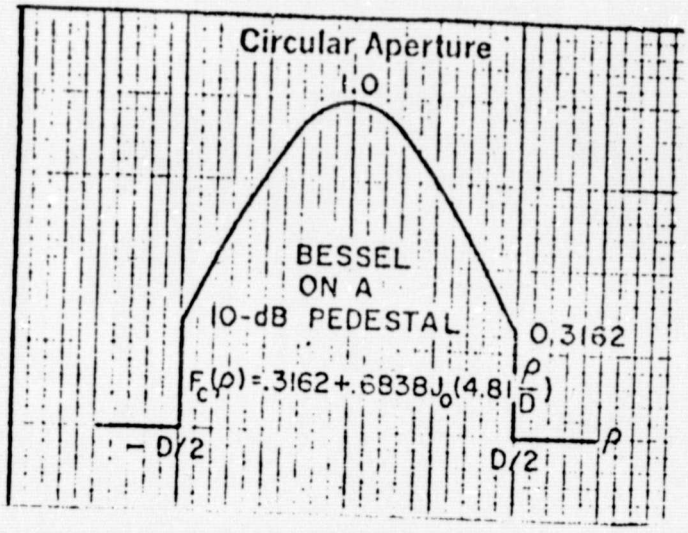

a) Amplitude distribution

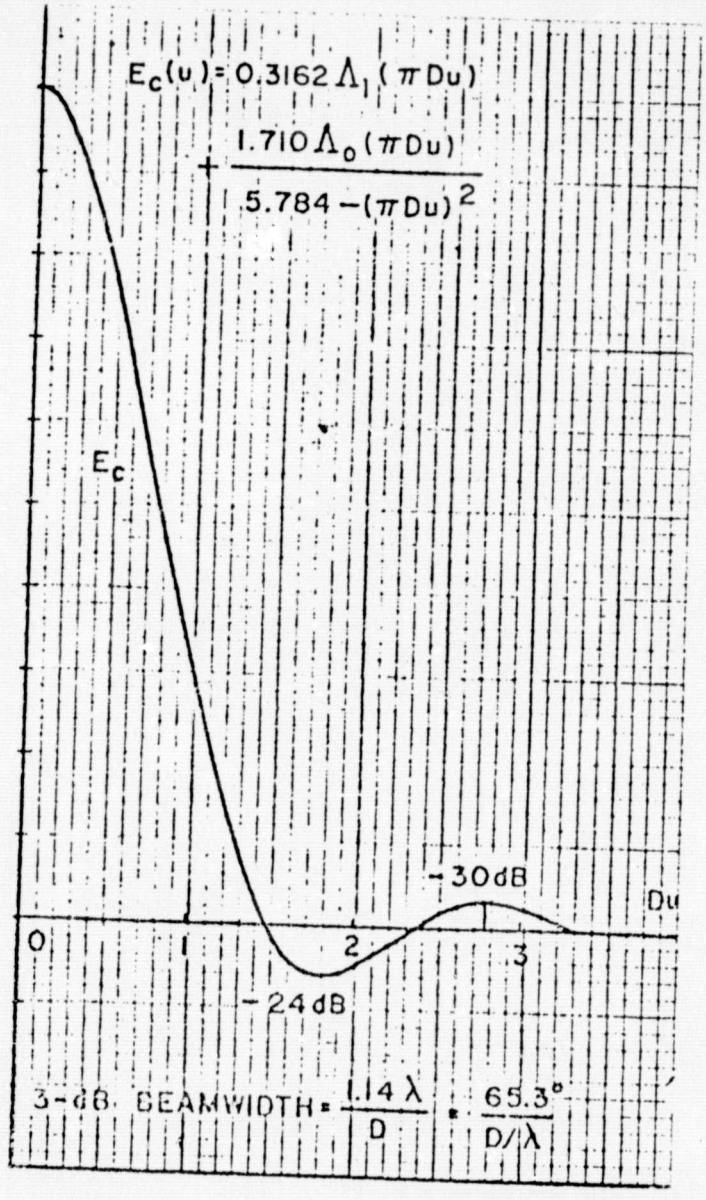

$u = \frac{\sin\theta}{\lambda}$

θ = beam angle

λ = wavelength

D = Diameter

$\Lambda_1(x) = \frac{2J_1(x)}{x}$

$\Lambda_0(x) = J_0(x)$

J_0, J_1 = Bessel functions

(b) Resultant Radiation Pattern

FIGURE 1-3 RADIATION PATTERN OF BESSEL FUNCTION DISTRIBUTION.

Type / Characteristics	PRIME-FED REFLECTOR			DOUBLE REFLECTOR		LENS ANTENNA	
	OFFSET PARABOLIC TORUS	OFFSET PARABOLOID	SPHERICAL REFLECTOR	OFFSET CASSEGRAIN	OFFSET DOUBLE REFL PARABOLIC TORUS	WAVE GUIDE LENS	DIELECTRIC LENS
SIDE VIEW	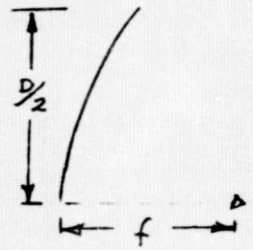	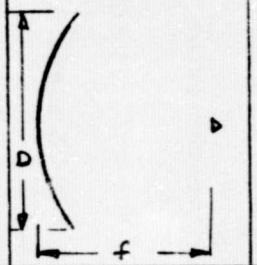	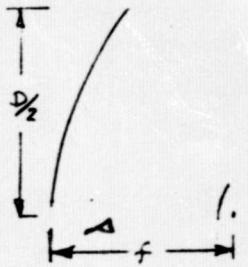	$f_{eff} = f\frac{\epsilon+1}{\epsilon-1}$ $\epsilon > 1$ Eccentricity		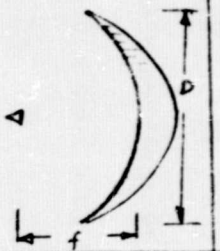	
APERTURE BLOCKAGE	Low	Low	Significant	Low	Low	None	None
OFF-AXIS GAIN LOSS	Low in Azimuth High in Elevation	High	Low	Moderate	Low in Azimuth Moderate in Elevation	Low	Low
BANDWIDTH	*	*	*	*	*	Determined by Lens Waveguide Elements	*
WEIGHT	Light	Light	Moderate	Moderate	Moderate	Heavy	Heavy
REMARKS	Has preferred Orientation on Spacecraft	$\frac{f}{D}$ is Limited by spacecraft geometry	Feed line loss is higher	Capable of reducing Off-axis gain loss by increasing $\frac{f_{eff}}{D}$ within constraint of spacecraft geometry	Has preferred Orientation on Spacecraft	High cost of fabrication Require Separate lenses for 18/30 GHz and dual Polarization need polarizing Screen.	Stability of dielectric materials in space environmental conditions questionable Insertion loss high
Baseline				Baseline Antenna			

* Determined by Feed Characteristics

FIGURE 1-4 COMPARISON OF MULTIPLE SPOT BEAM ANTENNA SYSTEMS FOR 18/30 GHz

2.0 PRIME FED REFLECTOR SYSTEMS

INTRODUCTION

In this chapter, single reflector antennas (the offset parabolic torus, the offset paraboloid and the spherical reflector) are discussed. The major objective is to evaluate the off-axis gain loss and carrier to interference ratio (C/I) for various geometries. The off-axis beams of the system under consideration are positioned within a region $\pm 2^{\circ}$ in elevation and $\pm 4^{\circ}$ in azimuth to cover the major cities of the continental United States (CONUS).

2.1 Offset Parabolic Torus

A toroidal reflector surface (torus) is generated by taking a section of a parabolic curve and rotating it about a fixed axis. The geometry of an offset parabolic torus with f/D=1 is illustrated in Figure 2-1. For this study, the rotation axis is parallel to the latus rectum, the chord drawn through the focus and perpendicular to the axis of the parabola. R_T, the radius of curvature at the vertex in the YZ plane at X=0, is chosen to be $\sim$ 2.083 times the focal length f to minimize the spherical aberration (Li, 1959)[4]. The aperture is a circle with diameter D/2.

Because of the circular crossection in the Y-Z plane, the scanning performance in that plane shall be better than that in the X-Z plane. Thus it is desirable to orient the antenna so that the Y-Z plane and the X-Z plane are in the azimuthal and the elevation direction respectively. Because the reflector geometry inherits spherical aberrations due to the circular geometry a toroidal antenna has a lower gain and higher sidelobes

than a paraboloid. The former shall have a better scan performance than the later at least in one plane (circular plane).

An offset parabolic torus with a 6 foot circular aperture has been studied for two cases (f/D=0.5 and f/D=1 at 20 GHz). Limited studies have been carried out on a 14 foot offset parabolic torus with f/D=1. The results show that for the same aperture size larger f/D goemetries give lower scan loss and lower sidelobes. For the same f/D, a larger aperture size forms a smaller beamwidth and lower interference levels to other cities and hence gives a better performance.

2.1.2 A 6-Foot Diameter Torus with f/D=0.5

An example far field pattern of a 6 foot toroidal reflector of f/D=0.5 is shown in Figure 2-2. The edge taper illumination is about 10 dB in both azimuth (Y-Z plane) and elevation (X-Z plane). It is noticed that the maximum gain is not at the boresight but at -0.2° off the boresight in elevation. The contours are symmetrical in the azimuth direction but not in the elevation direction. The major sidelobe appears to peak in the $\pm 45^{\circ}$ directions in the lower quadrants. The general characteristic of these contours are their triangular beam contours. The orientation of the triangular contours invert at lower gain values of the beam. In this particular example, the 1"x1.3" horn located at the focus is tilted in elevation by 27° to produce a 10 dB taper on the reflector.

The off-axis gain losses in the elevation (X-Z) and the azimuth (Y-Z) direction are shown in Figures 2-3 and 2-4 respectively. The off-axis horn positioned in azimuth has been rotated such that the longitudinal axis of the horn is in the direction of the radius of curvature of the focal arc

(see Figure 2-1) at the corresponding horn location. This direction will be referred to as the radial direction. Scan losses in azimuth for 3 different orientations of the feed horns; toward the center of the reflector, in the direction perpendicular to the Y-axis and in the radial direction are shown in Figure 2-5. Horns oriented in the radial directions provide a better scanning performance because the spillover loss is not the dominant loss factor for a "deep" torus. A horn oriented in the radial direction illuminates most of its radiated energy to the portion of the reflector where the phase distortion on an aperture plane is the smallest. Thus the configuration with horns oriented radially has the best scanning performance at least for the f/D=0.5 geometry studied.

Gain and C/I figures at the five cities are shown in Figure 2-6. The C/I is determined by exciting the horn to find the peak gain (C) and 3 dB beamwidth at the city location. Then the horn of the city in question is turned off and the remaining four horns are all excited with unity power and zero phase to find the gain of the interference signal (I) within the 3 dB beamwidth of the main signal (C) beam. This assumption of horn excitation does not account for power boost of individual beams and, in reality, for random phases among the beams. The maximum, minimum and average C/I are found by subtracting the peak gain of the main signal from the minimum, maximum and average interference signal within the 3 dB main signal beamwidth. The off-axis gain loss for the Los Angeles beam which has the largest gain loss is about 1.1 dB with respect to the on-axis gain. The worst C/I of 14 dB occurs at Atlanta, where the first sidelobe signals of New York and Chicago beams add to increase the interference at Atlanta.

2.1.3 A 6-Foot Torus with f/D=1

An example of a far field pattern for a 6 foot torus with f/D=1 is shown in Figure 2-7. The 2"x3.5" feed horn located at the focus is tilted by 14.25° in elevation.

Gains for the spot beams at the five cities and the corresponding C/I are illustrated in Figure 2-8. Both the gains and C/I figures have been improved over those for the 6 foot torus with f/D=0.5. It is important to point out that the horns in the Y-Z plane (azimuth direction) have been directed to the center of the reflector. This is because the spillover loss becomes more significant than the aberration effect for a shallow torus with f/D=1 when the beam is positioned in azimuth just a few beamwidths away from the axis. To minimize the spillover loss and hence to improve the far field gain, the horns are rotated toward the center in the Y-Z plane.

2.1.4 A 14-Foot Torus with f/D=1

Limited studies have been performed for a 14 foot torus with f/D=1. They include the cases of an on-axis beam, the Atlanta beam which has the worst C/I value and the Los Angeles beam which has the lowest gain. The pattern of the on-axis beam is illustrated in Figure 2-9. The peak gain is 55.5 dBi. Sidelobes are below 20 dBi. A 2"x3.5" horn provides 12 and 16 dB tapers in elevation and a 33 dB taper in azimuth. The far field pattern of the Los Angeles beam is shown in Figure 2-10. The peak gain is 53.7 dBi (1.8 dB scan loss) and sidelobes are below 20 dBi. The C/I figure for Atlanta is better than 35 dB.

2.1.5 Summary of Torus Antenna

The results of the 6 foot tori with f/D=0.5 and f/D=1 are summarized in Table 2-1 and Table 2-2, respectively. The boresight of an antenna on a synchronous satellite at 100° west longitude is chosen to be at Memphis. The 6 foot torus with f/D=1 has better gains and C/I figures than the 6 foot torus with f/D=0.5. For the same f/D tori the larger 14 foot torus has better performance than the 6 foot torus.

The 14 foot torus has a 3 dB beamwidth of 0.35° in azimuth and 0.16° in elevation, much smaller than that of a 6 foot torus (0.66° in azimuth and 0.53° in elevation). However the aperture efficiency of a 14 foot dish is lower than that of the 6 foot torus. The former has 44% efficiency while the later has 56%. That is because, for a given f/D value, the spherical aberration effects becomes pronounced as the torus size increases. Unlike a focal-fed paraboloid in which the path length for each ray from the feed to an aperture plane are identical, the path difference between the ray passing through the center of an aperture and that through the edges becomes larger as the size of the torus increases even with the fixed f/D. Consequently the spherical aberration becomes more pronounced and reduces the aperture efficiency for the larger reflector.

A toroidal reflector generated by rotating a parabolic curve about an axis not parallel to the latus rectum but with a small tilt angle with respect to the latus rectum has been reported to have a better performance (Hyde, et.al, 1974)[5]. Further investigations are needed to determine how large the tilt angle shall be to optimize the far field gain and C/I figures.

It appears that only the 14 foot torus has an acceptable C/I figure for the CONUS city coverage over $\pm 1^{\circ}$ and $\pm 3^{\circ}$ in the elevation and azimuthal directions respectively. Thus the azimuthal scan loss performance is more stringent. A major restriction of this configuration is to place the least off-axis gain loss direction of the antenna (Y-Z plane) parallel to the azimuthal direction in a spacecraft.

For the proposed space segment system, two 14 foot diameter apertures each with a 28 foot focal length must be positioned on the despun shelf of a spin stabilized spacecraft with the orientation shown in Figures 2-11 to allow the Y-Z plane of each antenna to be parallel to the azimuthal direction (East-West over CONUS).

Since the reflector symmetry about the north-south plane must be maintained it is necessary that each reflector and its feed must be deployed. Reflector deployment requires proper design of the necessary mechanisms, booms, and structure and has been demonstrated on NASA programs such as ATS. Feed deployment at 18/30 GHz is a more difficult matter. Moving RF transmission lines such as flexible waveguide or rotary joints are required. The structure and mechanisms required to accurately position the feeds and hold their position in the space thermal environment must be studied completely before implementation.

For a three-axis spacecraft one possible configuration is shown in Figure 2-12. Again, orientation of the reflector must position the North-South symmetry line parallel to the solar panel drive axis to allow the Y-Z

of each antenna to be parallel to the azimuthal direction. This requires the solar panel to be extended further to prevent shadowing and the problems of deployment mentioned above remains. Positioning the antenna on the East-West sides of the spacecraft allows the solar panel to be closer to the body but the deployment of the feeds and reflector are even more complicated (Figure 2-13). Thus, the focal fed parabolic torus has very good electrical performance but its restrictive orientation on any spacecraft limits is usefulness. If the communication system performance can tolerate a smaller aperture with shorter focal length, this type of antenna can be used for a 14 foot diameter spin stabilized spacecraft.

In order to eliminate feed extension, designs employing folded optics such as a Cassegrainian geometry and offset double reflector torus were investigated and are discussed in the next section. These reflector systems have an advantage that their effective focal length can be increased without increasing their physical volume on the spacecraft.

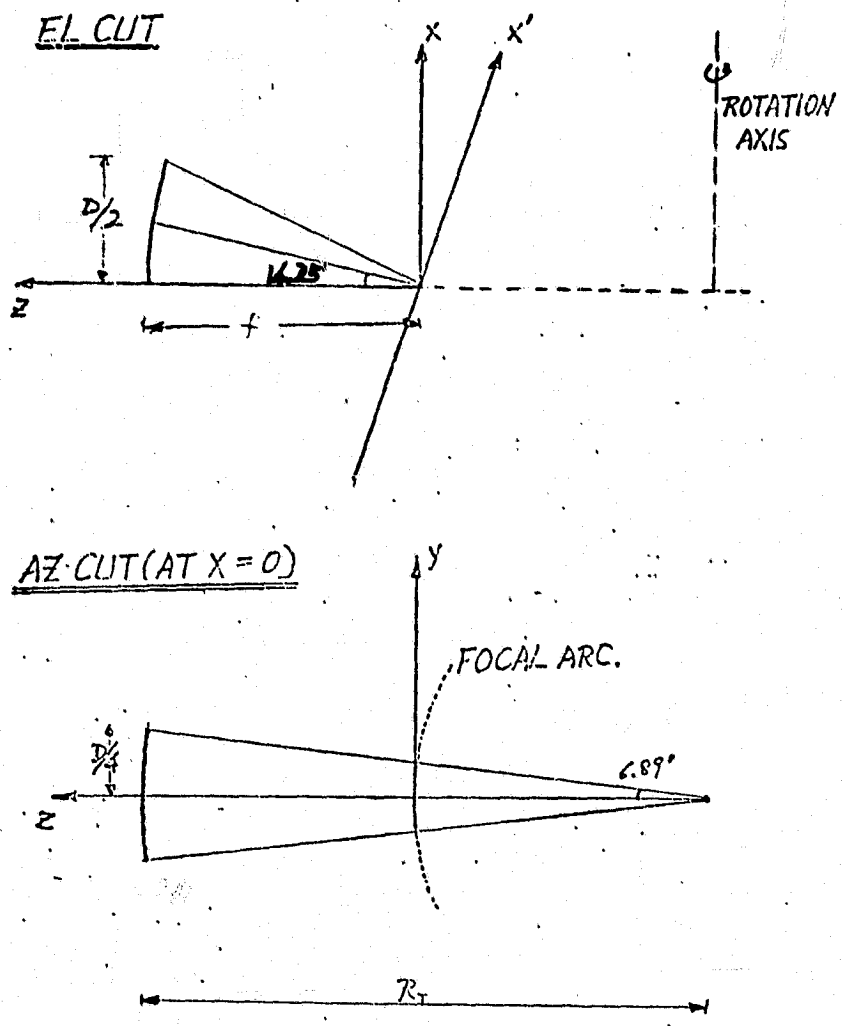

FIGURE 2-1 THE GEOMETRY OF A TORUS ANTENNA (f/D=1)

The focal surface is an elliptical cylinder which is oriented in parallel to X'-axis in such a way that the crossection in a Y-Z plane is a circle.

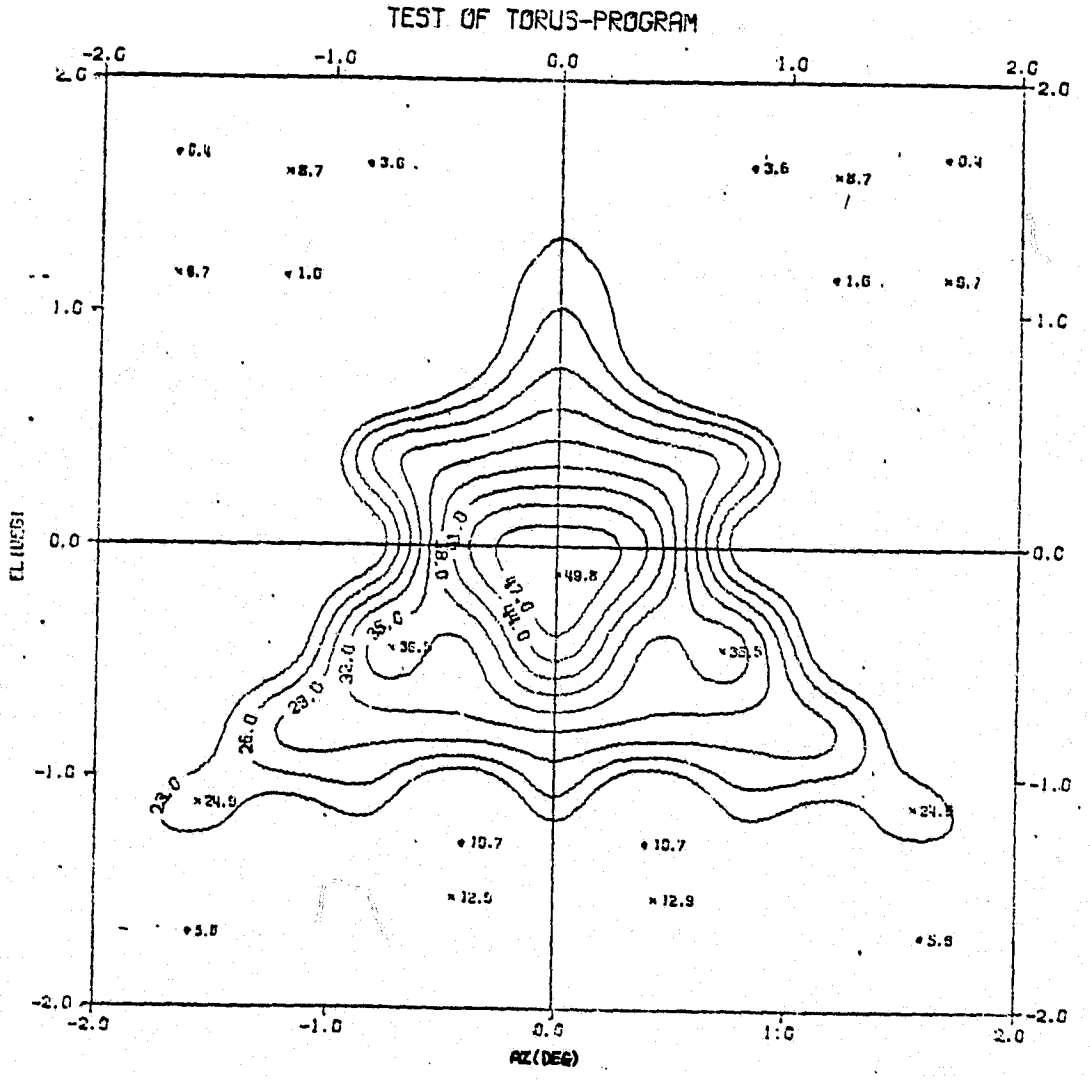

FIGURE 2-2 THE FAR FIELD PATTERN OF A 6 FOOT TORUS WITH f/D=0.5

The 1."x1.3" horn is located at the focus and is tilted in elevation by 27°. The signals are vertically polarized and at 20 GHz.

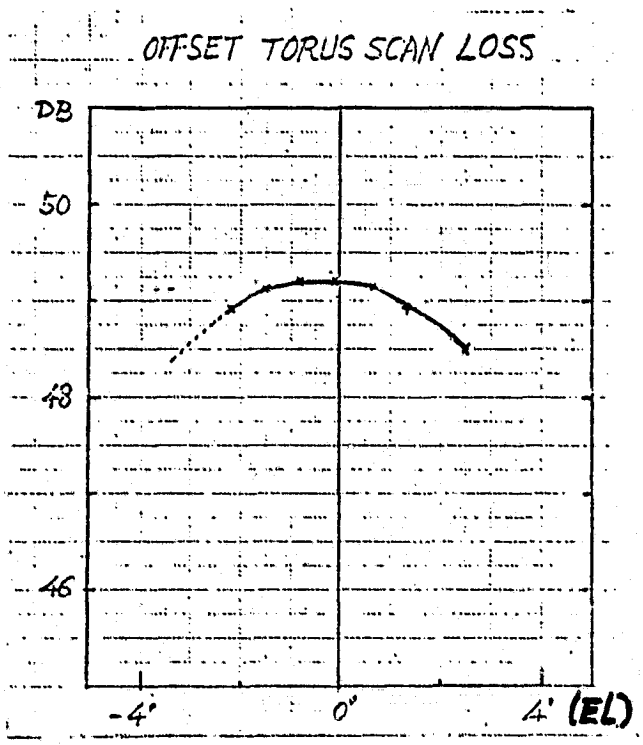

FIGURE 3- THE SCAN LOSS OF A 6 FOOT TORUS WITH f/D=0.5 IN THE ELEVATION DIRECTION

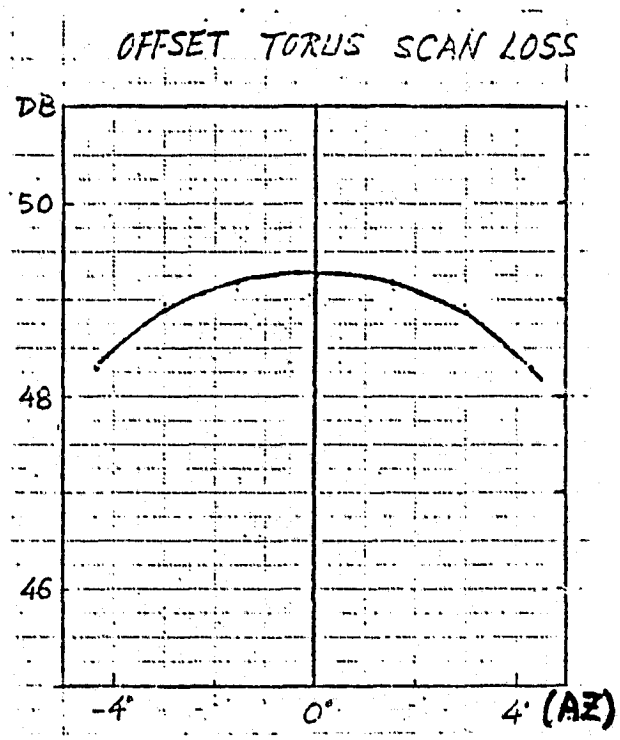

FIGURE 3-4 THE SCAN LOSS OF A 6 FOOT TORUS WITH f/D=0.5 IN THE AZIMUTHAL DIRECTION

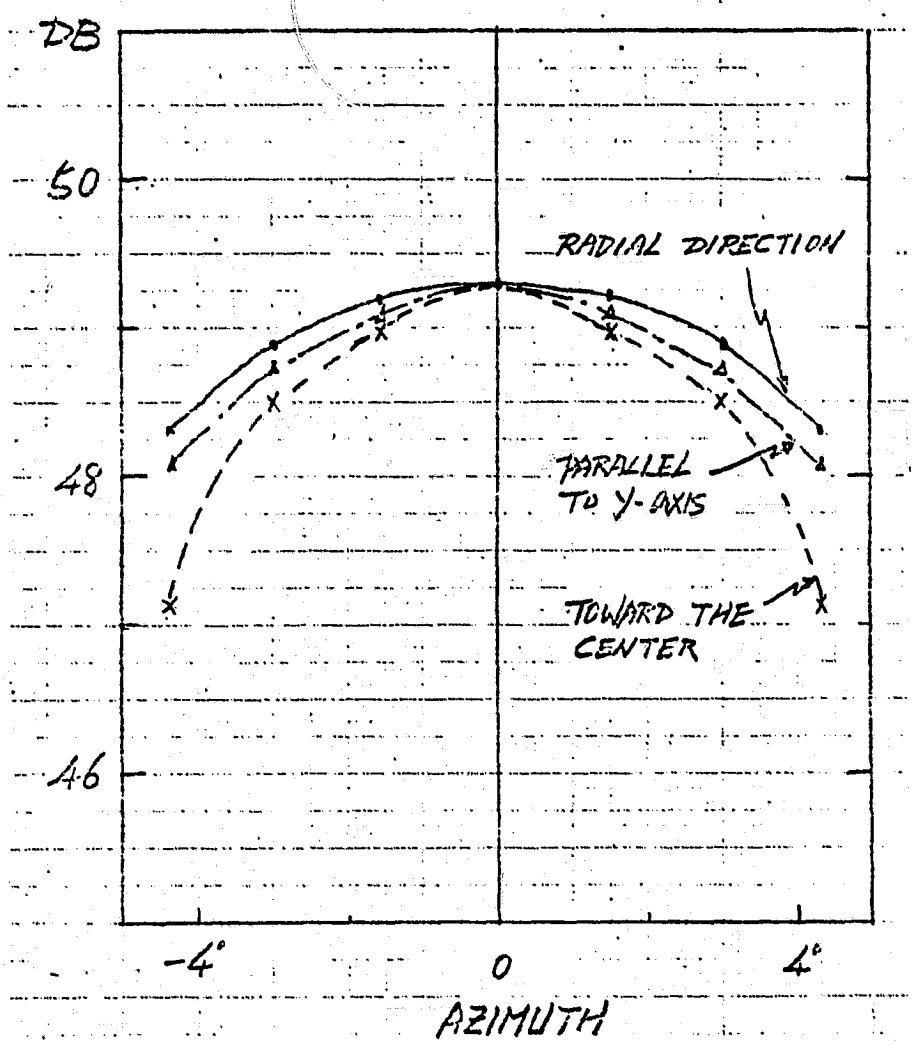

FIGURE 2-5 THE SCAN LOSS IN AZIMUTH FOR A 6-FOOT TORUS WITH f/D=0.5 WHEN THE FEED HORNS ARE ORIENTED IN VARIOUS DIRECTIONS

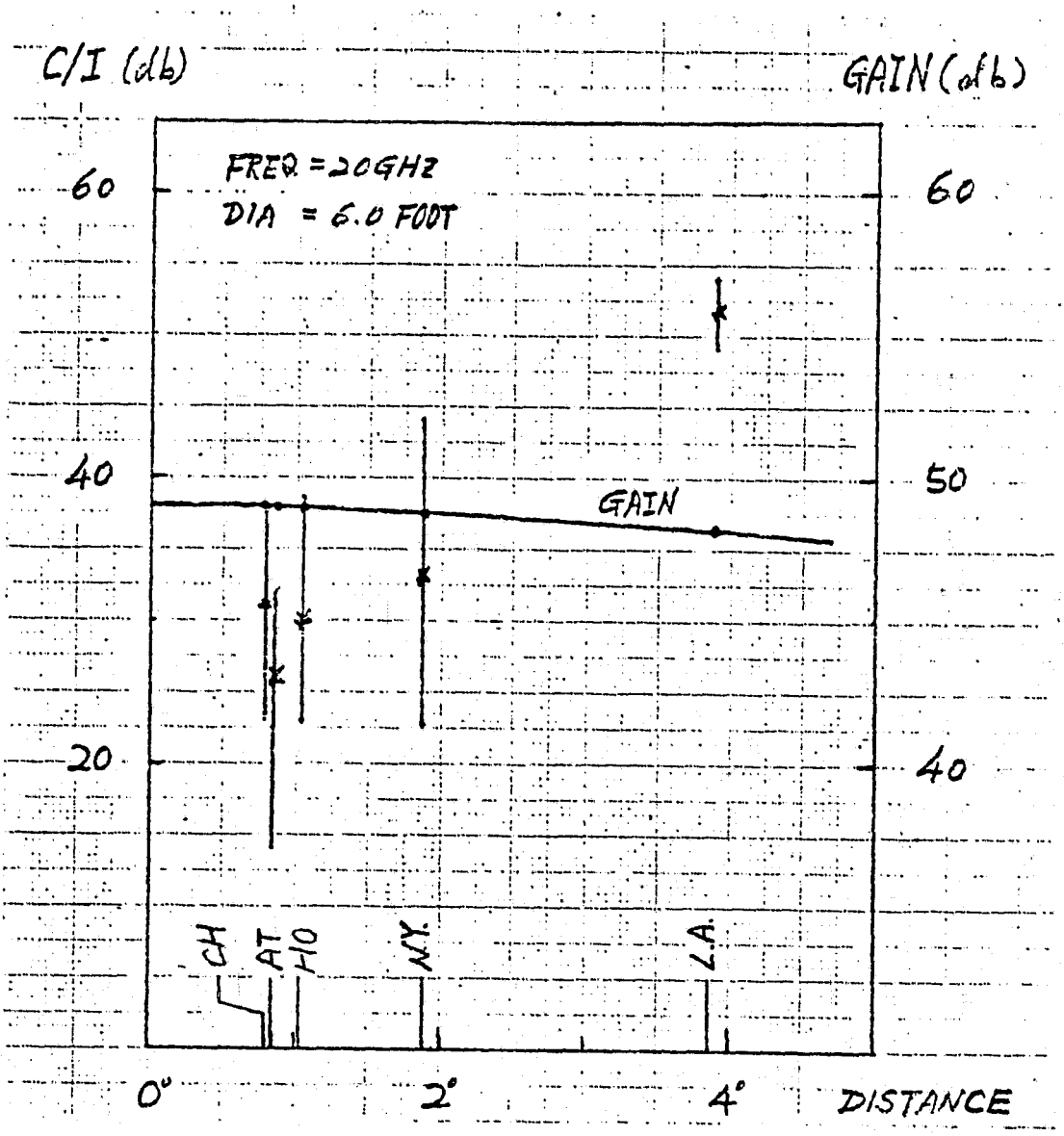

FIGURE 2-2 C/I AND GAIN OF A 6 FOOT TORUS WITH f/D=0.5

The "distance" indicates the far field distance from the boresight (Memphis) in degree.

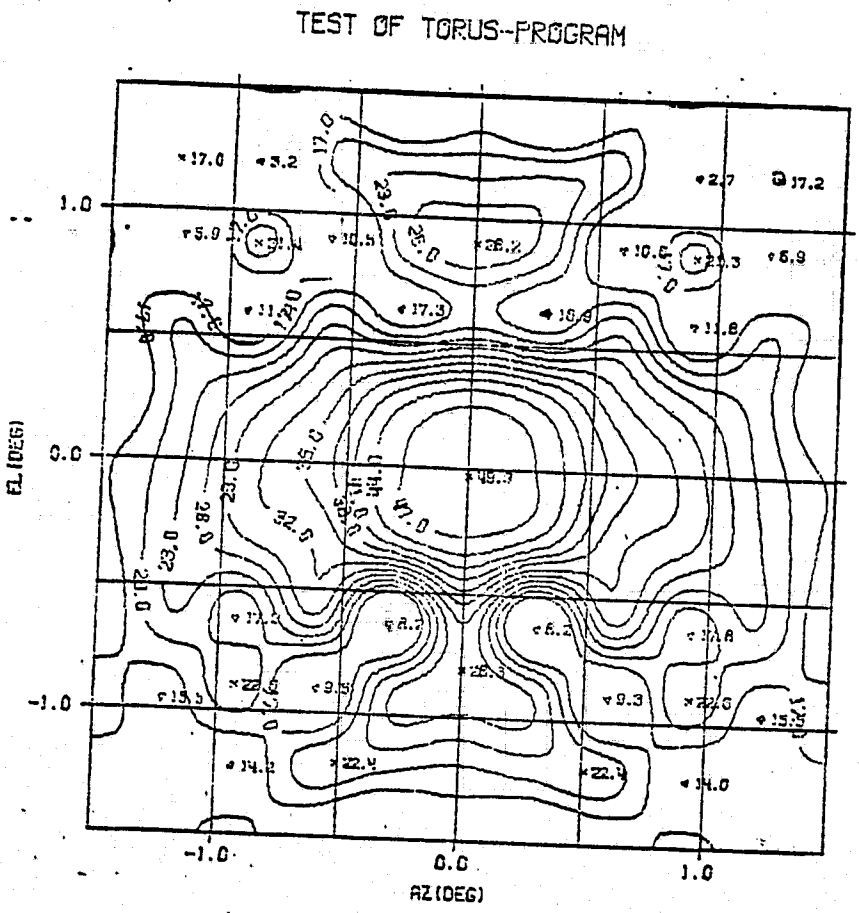

FIGURE 2-7 THE FAR FIELD PATTERN FOR A 6 FOOT TORUS WITH f/D=1

The 1.6"x2.350" horn, located at the focus, is tilted by 14.25°. The 20 GHz signals are vertically polarized.

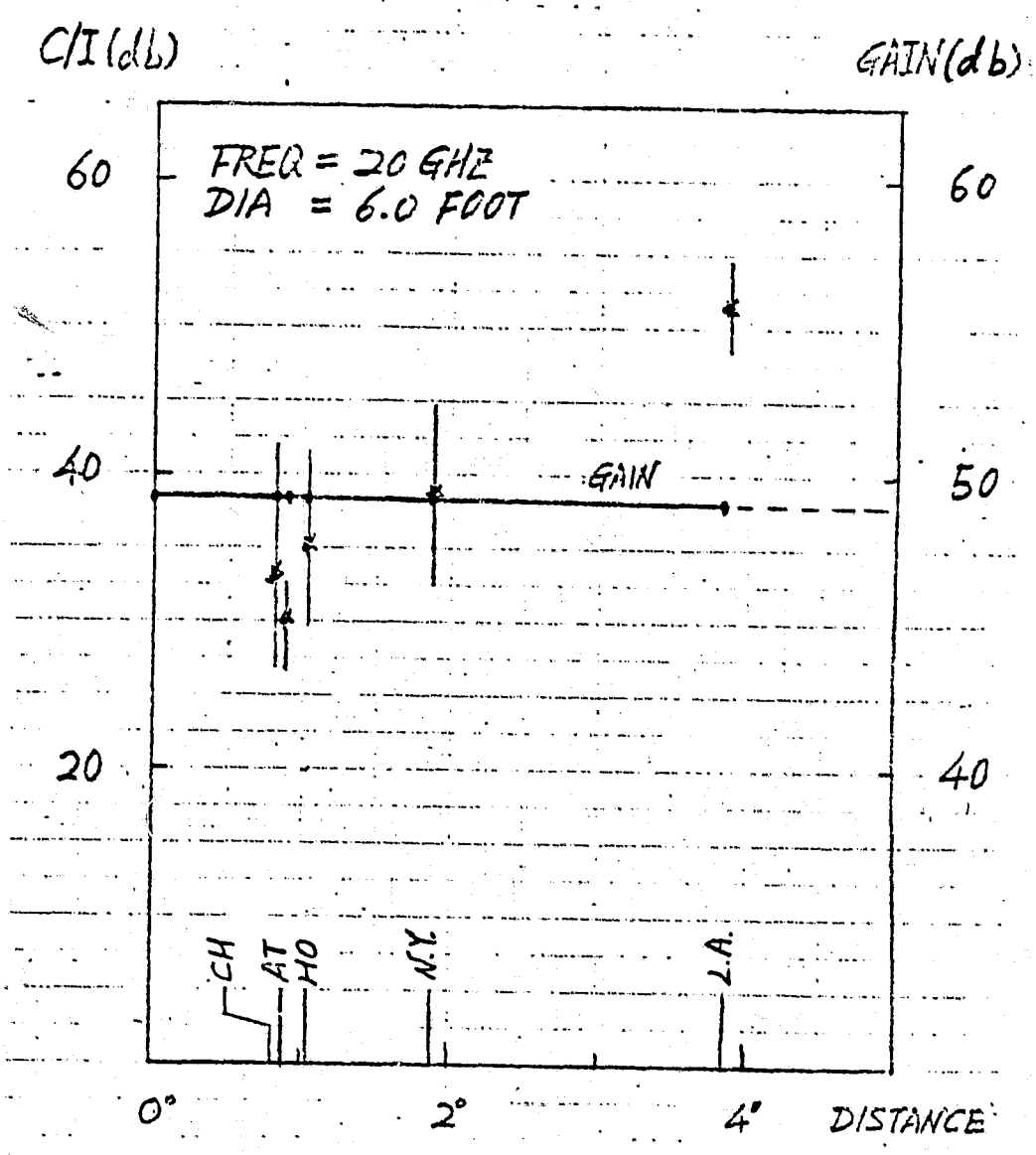

FIGURE 2-8 C/I AND GAIN OF A 6 FOOT TORUS WITH f/D=1

The "distance" indicates the far field distance from the boresight (Memphis) in degrees. Gain values do not include losses.

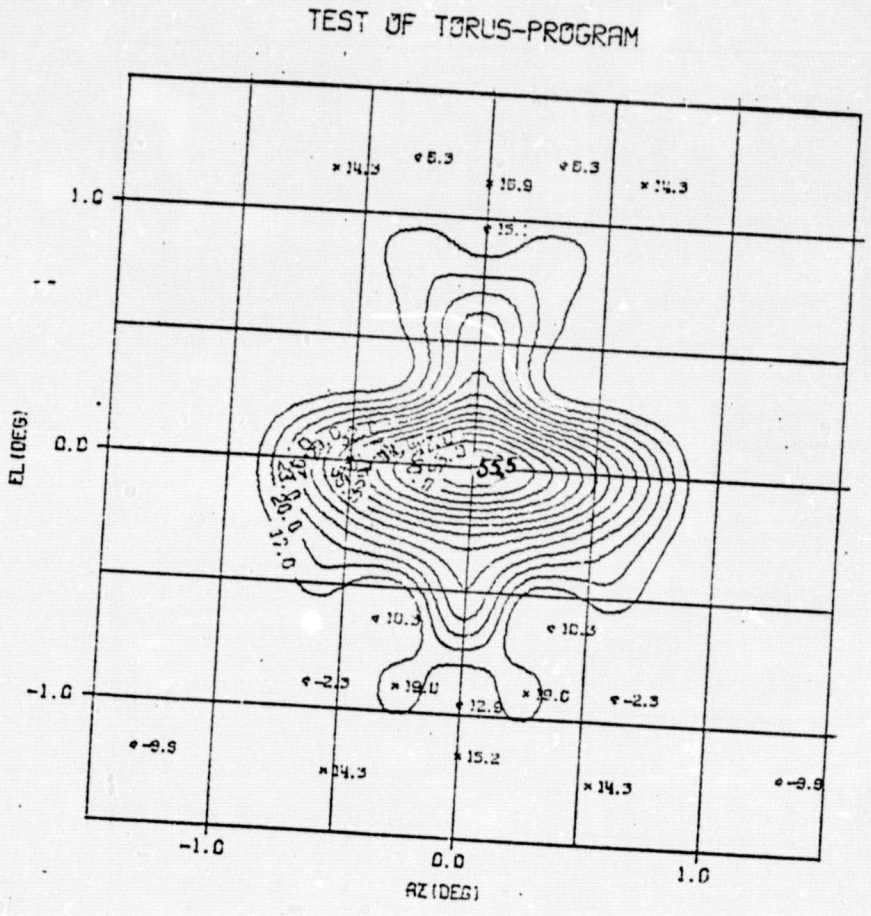

FIGURE 2-9 THE FAR FIELD PATTERN OF A 14 FOOT TORUS WITH f/D=1

The 2"x3.5" feed horn, located at the focus, is tilted by 14.25° in elevation. The peak gain is 56 dB.

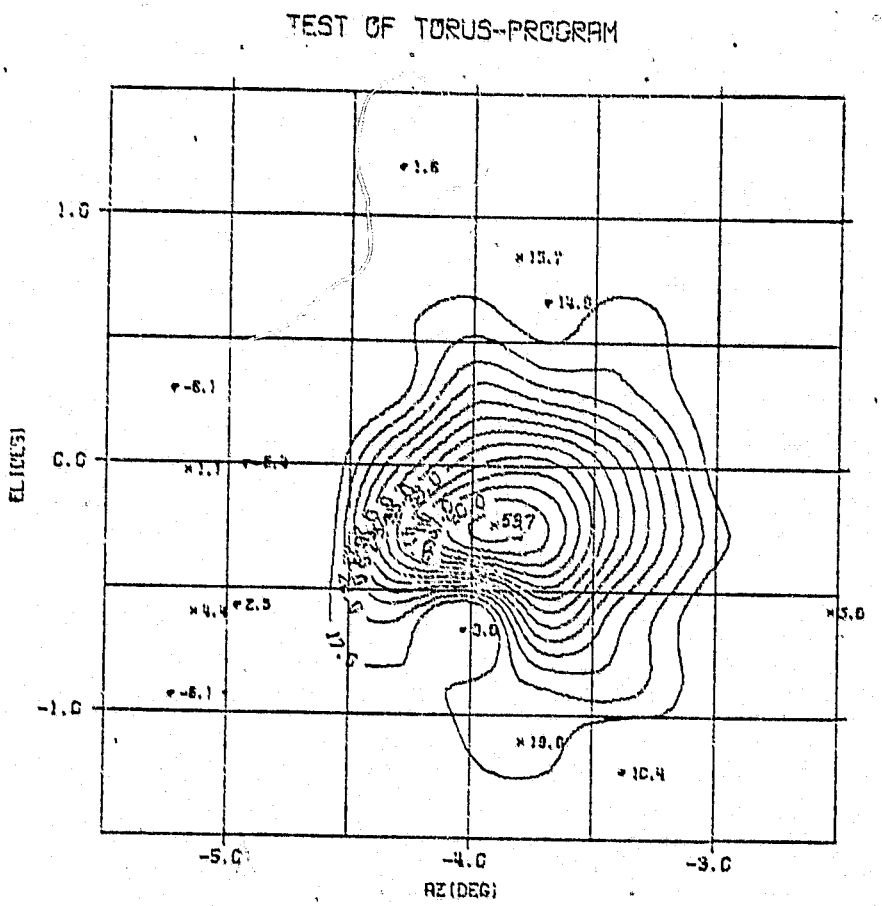

FIGURE 2-10 THE FAR FIELD PATTERN OF THE LOS ANGELES BEAM GENERATED BY A 14 FOOT TORUS WITH f/D=1

The feed is a 2"x3.5" horn. The 20 GHz signals are vertically polarized.

CITY	LOCATION	GAIN (db)	3db BEAMWIDTH	FIRST SIDELOBE	C/I(db)
New York	EL=.595° AZ=1.795°	48.6	EL=0.55° AZ=0.76°	33 db	≥3
CHICAGO	EL=.795° AZ=.120°	48.7	EL=0.51° AZ=0.76°	32db	23
ATLANTA	EL=-.225° AZ=.805°	48.9	EL=0.55° AZ=0.76°	31db	14
HOUSTON	EL=-.735° AZ=-.700°	48.9	EL=0.56° AZ=0.75°	31.2 db	23
L.A.	EL=-.18° AZ=-3.87°	48.1	EL=0.55° AZ=0.78°	34 db	49

TABLE 2-1 GAIN, BEAMWIDTH, SIDELOBE, AND C/I FOR A FIVE CITY SPOT BEAM TORUS ANTENNA WITH A 6 FOOT CIRCULAR APERTURE AND f/D=0.5. THE 20 GHz SIGNALS ARE VERTICALLY POLARIZED AND HORN SIZE IS 1"x2". GAIN VALUES DO NOT INCLUDE LOSSES.

CITY	LOCATION	GAIN (db)	3db BEAMWIDTH	FIRST SIDELOBE	C/I (db)
New York	EL=.595° AZ=1.795°	49.2	EL=0.53° AZ=0.65°	24.1db	32.7
CHICAGO	EL=.795° AZ=.120°	49.3	EL=0.54° AZ=0.63°	25.6db	26.8
ATLANTA	EL=-.225° AZ=.805°	49.2	EL=0.54° AZ=0.65°	24.6db	26.7
HOUSTON	EL=-.735° AZ=-.700°	49.2	EL=0.54° AZ=0.65°	25.1db	29.7
L.A.	EL=-.18° AZ=-3.87°	49.1	EL=0.54° AZ=0.65°	25.7db	48.6

TABLE 2-2 GAIN, BEAMWIDTH, SIDELOBE, AND C/I FOR A FIVE CITY SPOT BEAM TORUS ANTENNA WITH A 6 FOOT CIRCULAR APERTURE AND f/D=1. THE 20 GHz SIGNAL ARE VERTICALLY POLARIZED AND THE HORN SIZE IS 2"x3.5" GAIN VALUES DO NOT INCLUDE LOSSES.

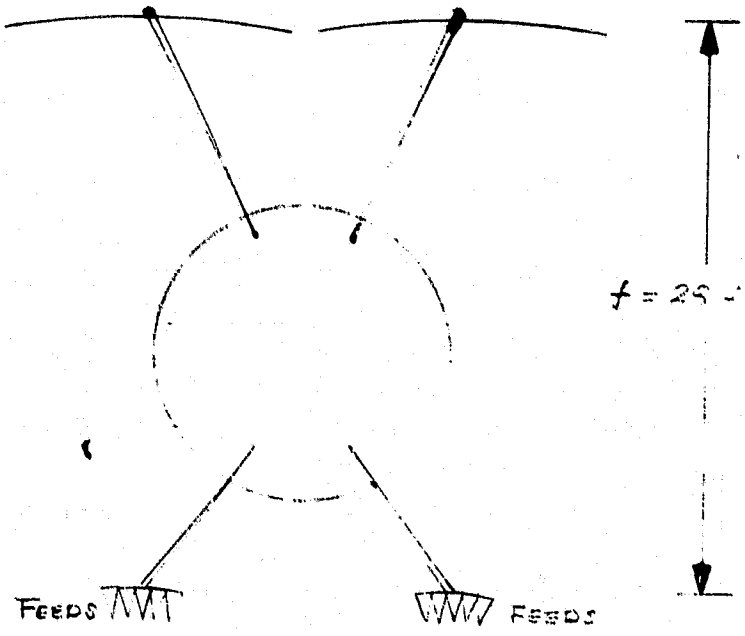

(a) SIDE VIEW

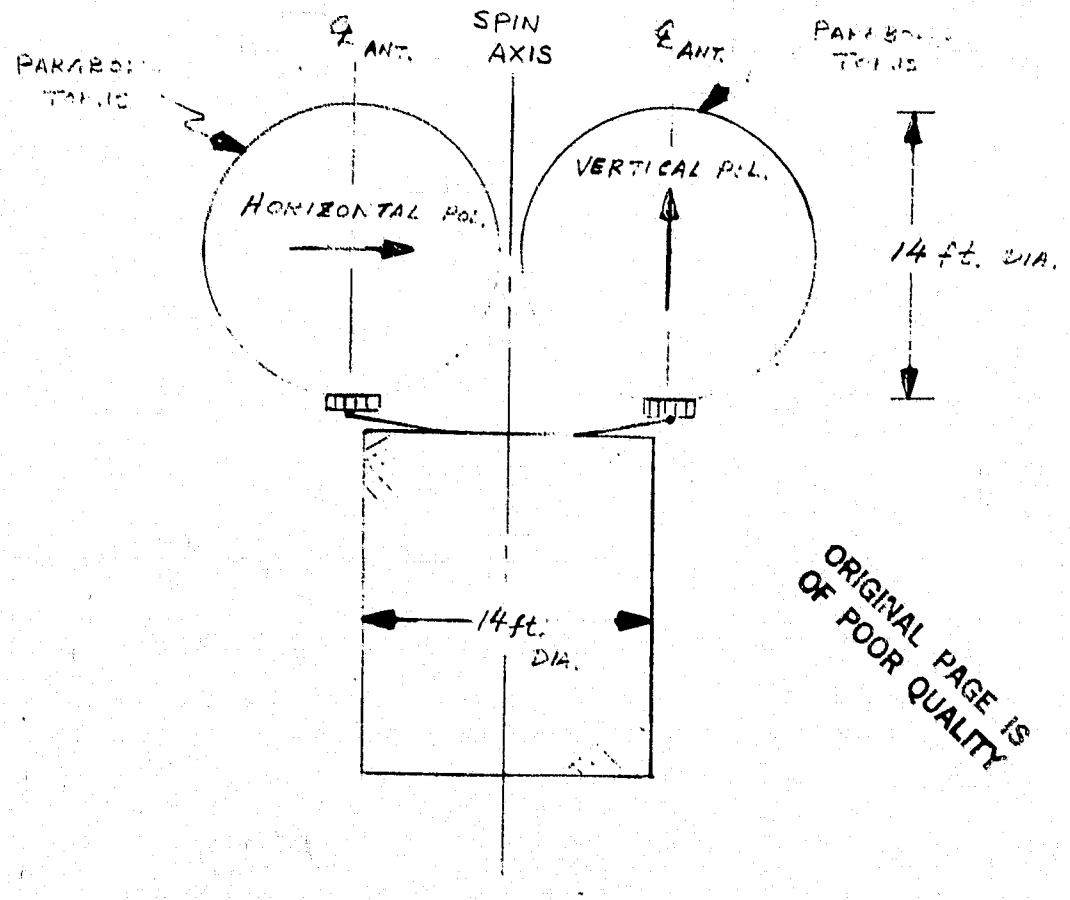

(b) FRONT VIEW

FIGURE 2-11 SPIN STABILIZED SPACE CRAFT ANTENNA GEOMETRY

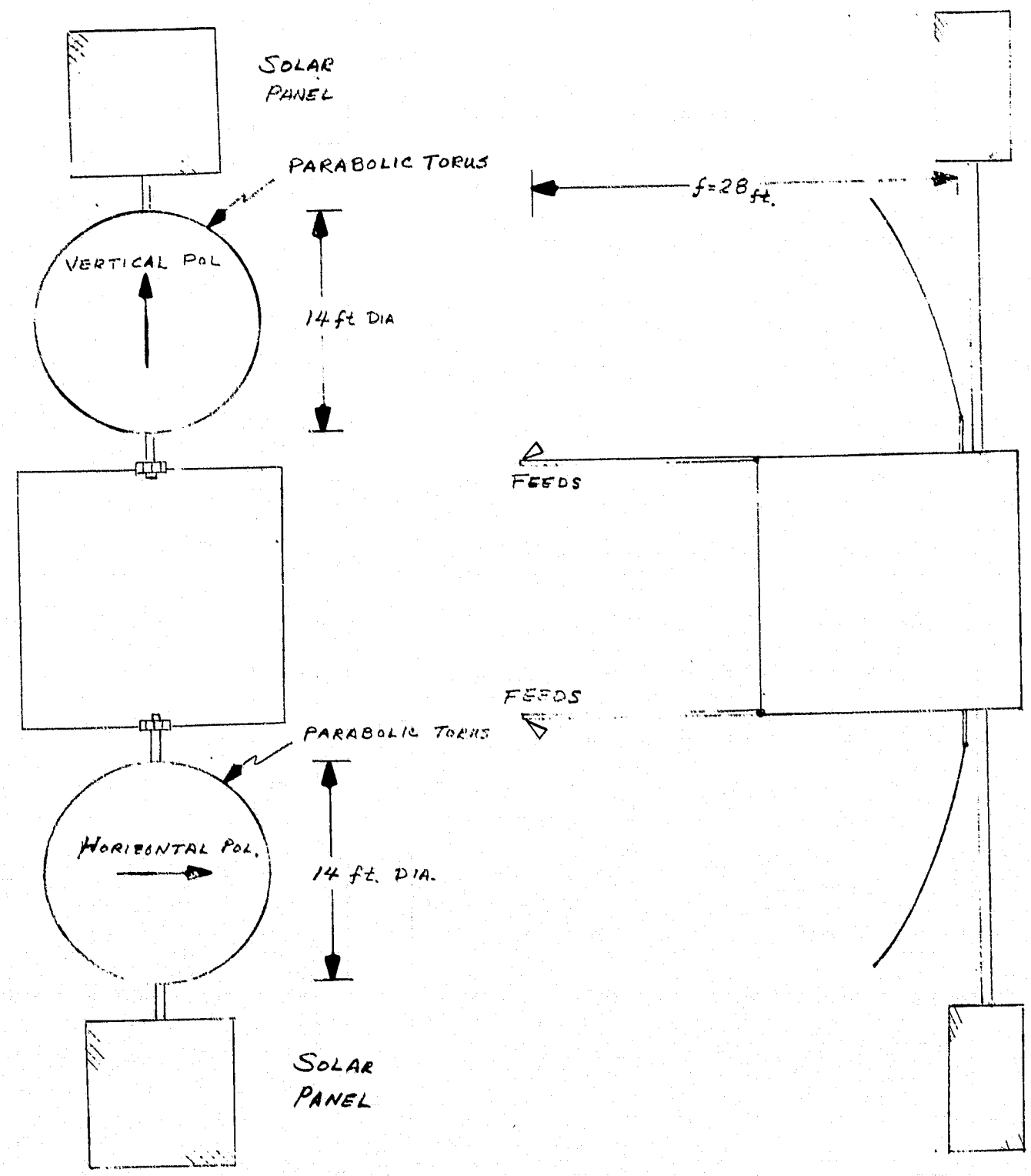

(a) FRONT VIEW

(b) SIDE VIEW

FIGURE 2-12 THREE-AXIS SPACECRAFT ANTENNA GEOMETRY

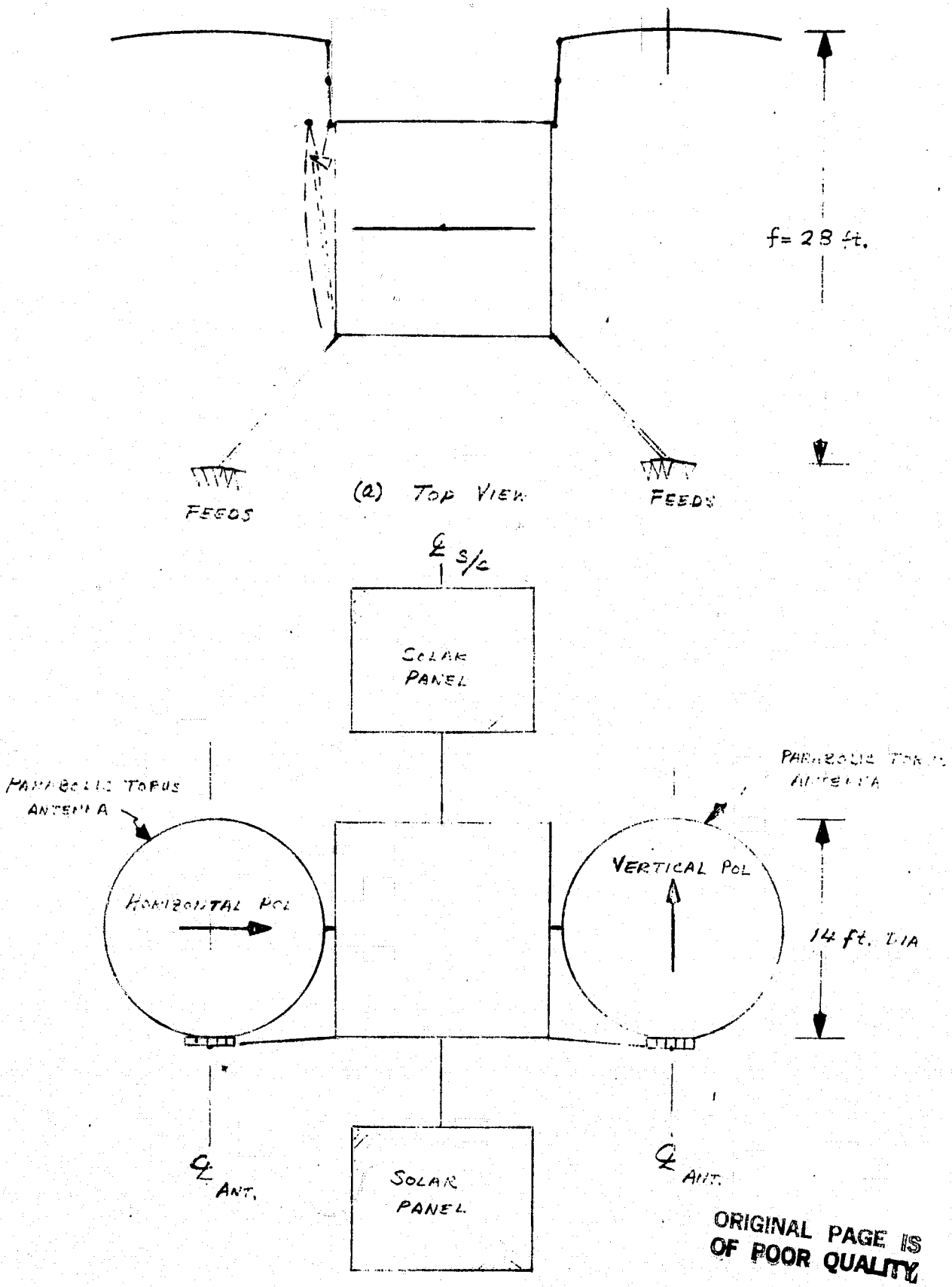

(b) FRONT VIEW

FIGURE 2-13 THREE-AXIS SPACECRAFT ANTENNA GEOMETRY 2

2.2 Offset Paraboloidal Reflector

A paraboloidal reflector is a part of a surface of revolution generated by a parabolic curve rotated about its focal axis. Conventional paraboloidal antennas are symmetric about this axis with usually a single feed at the focal point. For multibeam application, the feed package depending upon the number of beams begins to significantly block the aperture area causing sidelobe levels to increase and peak gain to reduce. By defining the aperture area of the paraboloid to be that portion of the generating surface offset from the focal axis, feed and strut blockage can essentially be eliminated as shown in Figure 2-14 where the reflector bottom edge corresponds to the paraboloid vertex. In practice, the reflector bottom edge will be truncated above the vertex to eliminate the entire feed array blockage. The projected aperture of each reflector studied was circular, and the f/D ratio was calculated by dividing the focal length by twice the reflector diameter.

2.2.1 Analysis

The single solid reflector antenna depicted in Figure 2-14 was one type of antenna system investigated where feed horns are shared by 20 GHz and 30 GHz signals. In this configuration optimization of the feed design is limited to one frequency. The second type of antenna system studied was a shared aperture dual grid reflector depicted in Figure 2-15 where the orthogonally gridded reflectors are placed one in front of the other. Each reflector is polarization sensitive and has a separate focal point allowing independent optimization of feeds. Such a reflector system is under current development for the Anik C and SBS[6] satellite antennas. The analysis of gain and C/I performance of the offset parabolic reflectors was performed using a physical optics vector reflector computer model.

The first analysis conducted was to determine off axis gain loss of a 6 foot diameter dual grid reflector system for two values of f/D (0.5 and 1.0). Feed horns for both the 20 GHz and 30 GHz signals were independently optimized to illuminate the edge of the reflector with a field strength of approximately 10 dB below the peak of the primary beam.

The second analysis performed was to determine the off axis gain loss of a single parabolic reflector of a fixed focal length of 12 feet for two different reflector diameters of 12 feet and 10 feet. The feed horn dimensio were optimized for the downlink signal at 20 GHz but also used to receive the 30 GHz signal where the reflector was under illuminated.

Using the 6 foot diameter dual grid reflector antenna with 12 foot focal length, C/I performance for the first group of five cities was analyzed. The peak gain of the city of interest was determined by exciting its corresponding feed horn with unity power. The interfering signal level was obtained at the city location by the composite sidelobe levels of the other four city beams by exciting the horns with unity power and constant phase as was done for the offset parabolic torus analysis. The difference between the main beam level and the interfering signal level in dB is the resultant C/I ratio.

2.2.2 Discussion of performance

The resultant off axis gain loss characteristics of the 6 foot diameter dual grid reflector with the focal length of 6 foot is shown in Figure 2-16. As noted in the figure the on axis peak gains for both 20 and

30 GHz signals were determined to be 49.8 dB and 53.3 dB corresponding to relatively high efficiency of 65% due to optimization of feeds for both signals (feed and reflector losses are not included). The gain loss for 20 GHz beam is within 2 dB in the range of off axis angle of up to 4^{o}. Gain loss of about twice that of 20 GHz was obtained for the 30 GHz beam.

The effect of increasing the focal length for the 6 foot reflector is shown in Figure 2-17. Off axis gain loss is reduced by approximately one half as f/D ratio increased from 0.5 to 1.0. The wide off-axis capability for the larger f/D ratio is due to the reflector surface approaching Abbe sine condition of spherical surface as discussed in Section 1.2.

The results of the off-axis gain loss of 10 foot and 12 foot diameter reflectors with a 12 foot focal length are plotted in Figures 2-18 and 2-19. The feed horns were optimized at 20 GHz and were shared by the 30 GHz signal. It is interesting to note that the gain loss difference of the two signals is within a few tenths of a dB up to off axis beam of 4^{o}. Again the gain loss is reduced by about a half for the larger f/D value.

The C/I performance was evaluated for the shared aperture configuration of the 6 foot diameter reflector with 12 foot focal lengths. The results of the C/I performance of first group of five cities are as follows:

	Downlink (20 GHz)	Uplink (30 GHz)
New York	34 dB	40 dB
Chicago	34	30
Atlanta	23	29
Houston	25	37
Los Angeles	41	47

The low C/I performance at Atlanta is due to the contribution of sidelobes of Chicago and New York beams where the angular separations to Chicago and New York from Atlanta are about 1.3^{o} so that two sidelobes add to form high interference.

2.2.3 Summary

When the feed horns were optimized at 20 GHz and 30 GHz for the dual grid reflector system, the off axis gain loss for the 30 GHz beams dropped faster than the 20 GHz beams as seen in Figure 2-16. However, when the shared horn was optimized at 20 GHz, the gain loss for both frequency beams became nearly the same, however, the on-axis gain efficien of 30 GHz dropped to 44% (64% at 20 GHz). The reduced efficiency is due t the 20 GHz designed feed being an oversized horn at 30 GHz.

In order to keep the off axis gain loss less than 2 dB, the f/D ratio should be about one as in the previous parabolic torus. To achieve C/I value greater than 30 dB, a 14 foot diameter reflector is required. Therefore, the corresponding focal length for a 14 foot diameter reflector is 28 feet and the same problem of long waveguide runs and deployed feed and reflector is encountered. Therefore, the offset parabolic reflector was not selected as a recommended baseline antenna unless the C/I values less than 30 dB are sufficient.

2.3 Spherical Reflector

A spherical reflector is a truncated portion of a sphere. The feed location is positioned at one half the radius of the sphere as shown in Figure 2-20. Spherical reflectors in general have better scanning performance but lower gain and higher sidelobe levels than paraboloid and parabolic torus reflectors. A typical radiation pattern which is nearly symmetrical in the E and H planes out to the 5 dB beamwidth angle is shown in Figure 2-21. The aperture size of a spherical reflector is somewhat restricted due to spherical aberration. This aberration becomes more serious as the aperture size increases. The following equation estimates the aperture size of the reflector for a given tolerable phase error.[5]

$$\left(\frac{a}{R}\right)^{4}_{max} = 14.7 \frac{\left(\frac{\Delta}{\lambda}\right)_{total}}{\left(\frac{R}{\lambda}\right)}$$

where

a is the radius of the aperture

R is the radius of the spherical surface

λ is the wavelength

Δ is the tolerable phase error in terms of wavelength

A 10 foot aperture operating at 30 GHz requires the radius of the spherical surface to be at least 28 foot in order to maintain a phase error less than $\lambda/16$ over the aperture. The feed is positioned at 14 feet from the reflector surface.

The major drawback of using a spherical reflector for multiple beam application is the feed blockage. Although an offset spherical reflector eliminates feed blockage, such an antenna increases coma as well as spherical aberration and is not recommended for the 18/30 GHz spot beam antenna system.

FIGURE 2-14 OFFSET PARABOLIC REFLECTOR SYSTEM

FIGURE 2-15 SHARE APERTURE GRID REFLECTOR SYSTEM

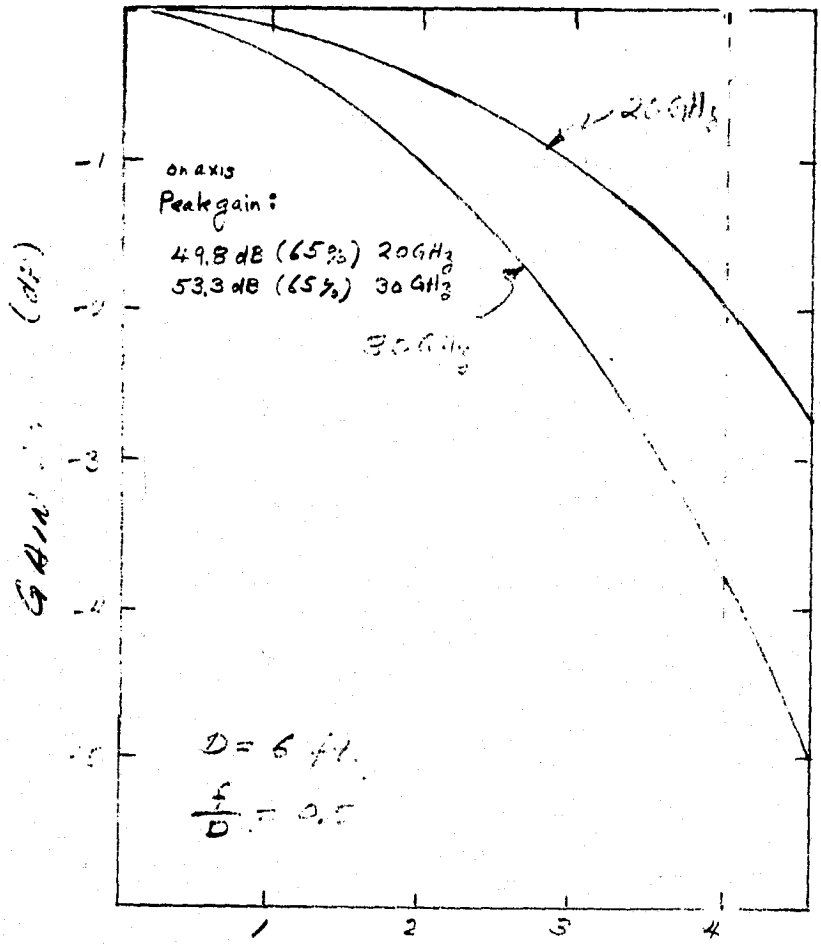

FIGURE 2-16 AS OFF AXIS GAIN LOSS AS A FUNCTION OF FREQUENCY

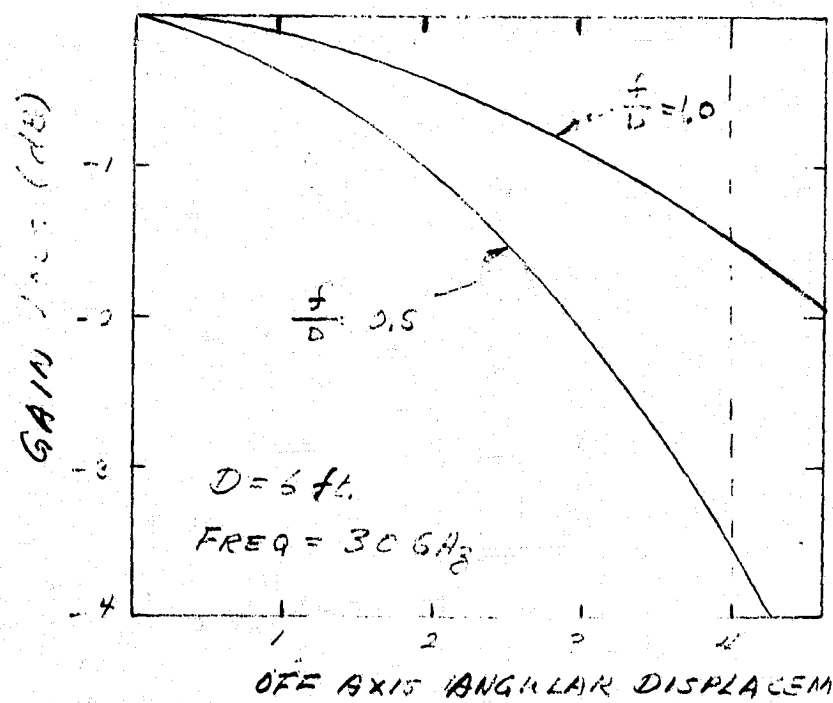

FIGURE 2-17 OFF AXIS GAIN LOSS AS A FUNCTION OF $\frac{f}{D}$

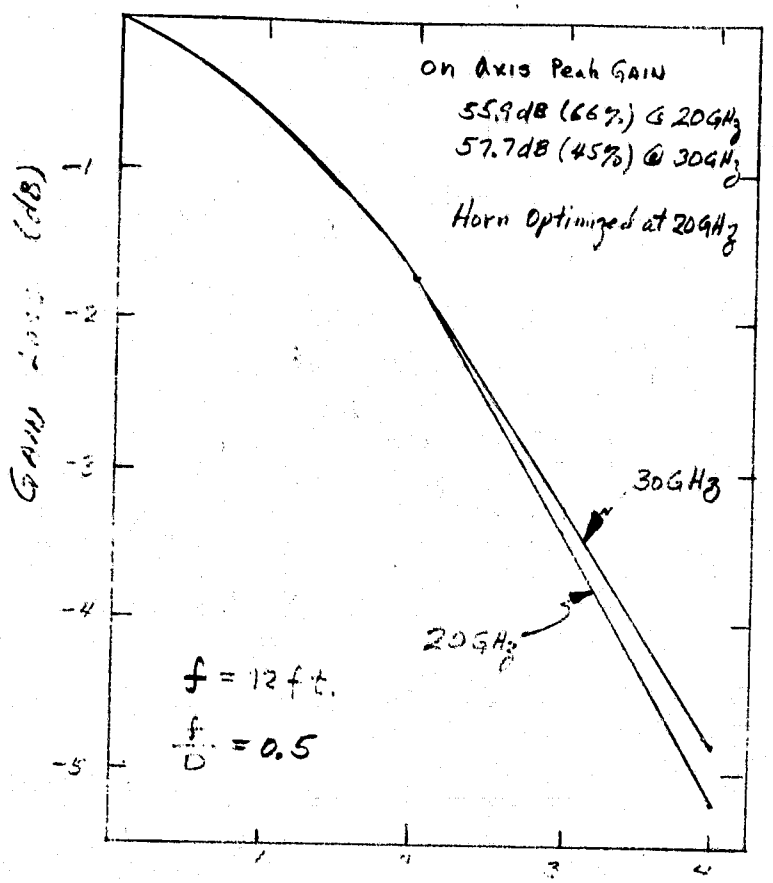

FIGURE 2-18 OFF AXIS GAIN LOSS AS A FUNCTION OF [illegible]

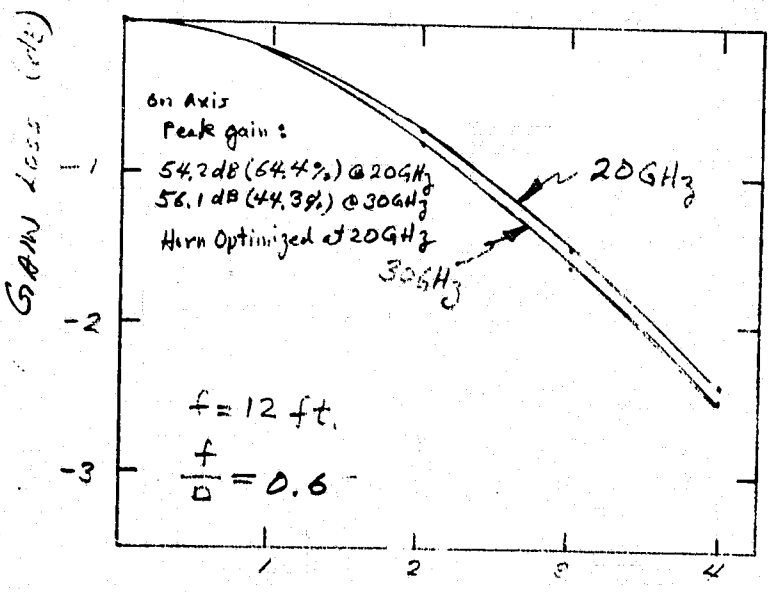

FIGURE 2-19 OFF AXIS GAIN LOSS IS A FUNCTION OF FREQUENCY, f/D

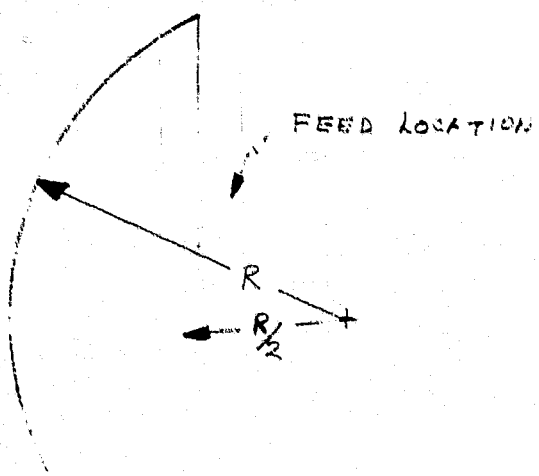

FIGURE 2-20 SPHERICAL REFLECTOR GEOMETRY

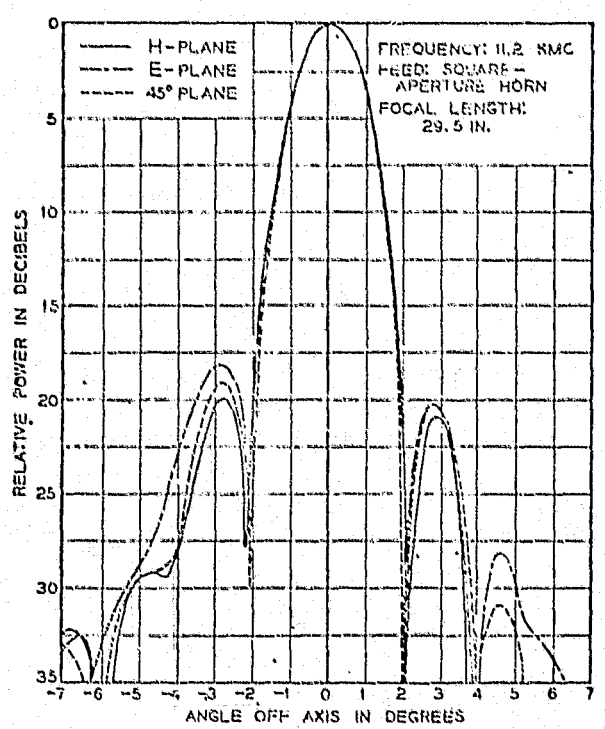

FIGURE 2-21 Radiation patterns of 10-foot spherical reflector.

(Ref: 11)

3.0 FOLDED OPTICS SYSTEMS

3.1 Offset Cassegrain Antenna

3.1.1 Introduction

In multiple spot beam antenna applications the focal length to diameter (f/D) ratio of reflectors and lenses are important. Small values of f/D for paraboloids produce large spherical aberration for beams positioned to tens of beamwidths. A decrease in peak gain and increase in side-lobe levels reduce C/I values. Values of C/I greater than 30 dB require large focal lengths (large f/D value) for a given size reflector. As discussed in section 2.1 and 2.2 focal lengths of 28 feet are required for 14 foot diameter apertures. This makes implementation on the satellite difficult. A way of reducing the physical dimensions of the antenna and still achieve large effective f/D values is to fold the antenna geometry by folded optics technique.

3.1.2 Effective Focal Length

The focal length of single reflector systems is practically limited because of the finite spacecraft dimensions. Placing the focal point beyond the spacecraft geometry creates a difficult feed or reflector design deployment.

In the design of dual reflector Cassegrainian geometry, the effective focal length is set by the subreflector shape. A classical Cassegrainian antenna that consists of a paraboloid and hyperboloid is shown in Figure 3-1. An equivalent paraboloid which is the image of the main reflector is also shown. The effective focal length of the equivalent reflector is determined by the eccentricity ϵ of the hyperboloid.

$$f_{eff} = f \frac{\epsilon + 1}{\epsilon - 1}$$

The focal length f in the above expression is a physical dimension which is the focal length of the main reflector. The value of ϵ changes only the shape of the subreflector without affecting focal length f. Theoretically, any value of f_{eff} greater than f is obtainable by changing the subreflector shape for a fixed value of f. Thus, the volume occupied by the antenna remains constant.

3.1.3 Scalar Double Reflector Model

The Cassegrainian geometry was analyzed using a scalar computer model. The equivalent parabola antenna concept of analysis has been determined to be inadequate for a large off axis angle.[7] The scalar model is based on the geometric optics theory of ray tracing. The rays emmited from a source are traced to the main reflector by the law of reflection. The amplitude of the field distribution on the main reflector is determined by the power density reaching the reflector from a source and the phase distribution is calculated by the ray path length. The radiation pattern is calculated by integrating the amplitude and phase distribution over the main reflector surface.

This analytic model has been compared with experimental data taken on a 50 x 50 inch square aperture offset Cassegrain fabricated several years ago and tested at 20 GHz. The agreement between the measured and calculated off-axis gain loss is within 0.2 dB up to about 8 beamwidths from the on-axis beam as shown in Figure 3-2. At the off-axis beam position of 9 degrees ($\sim$ 10 beamwidths), the measured gain is about 1 dB below the calculated gain loss.

Evaluation of the experimental geometry indicated excessive forward spillover loss of about 0.5 dB for the subreflector at this beam position. This loss can be reduced by proper sizing of the subreflector. For this reason, the measured gain value at 9 degrees was increased by 0.5 dB. Therefore, the model can predict performance of a 50 inch aperture to within 0.5 dB at a scan angle of 9 degrees or 10.8 beamwidths. This accuracy can then also be achieved for a 14 foot aperture at a scan angle of 2.7 degrees which also corresponds to 10.8 beamwidths. It is difficult to apply experimental data taken on the 50 x 50 inch antenna to greater scan angles on the 14 foot antenna because the larger number of beamwidths is equivalent to very large scan angles on the smaller aperture. For example, the 50 x 50 inch aperture antenna was not designed to scan 20 beamwidths (3 degrees at 30 GHz on a 14 foot antenna) which requires the feed to be positioned nearly 60 degrees from the on-axis beam position. For the 14 foot design discussed in this section, the feeds corresponding to beams positioned 3 to 4 degrees off-axis are approximately 20 degrees from the on-axis feed which is much closer to the focal region. Thus, the range of angles traced by rays emanating from the feed to subreflector surface normals are small with the 14 foot antenna and errors caused by the lack of a more precise vector formulation is small. Furthermore, the angular range of feed positions for the 14 foot aperture from the on-axis feed position is less than that for experimental antenna and, thus, the estimated accuracy of the model is judged to be comparable.

3.1.4 Antenna Geometry

A large offset of the main reflector is necessary to avoid subreflector blockage. The focus of the main reflector coincides with one of the hyperboloid foci, and the other focus becomes the focal point of the system.

The analyzed antenna was a 14 foot diameter main reflector with a 4 foot offset and f of 14 feet. The separation of the hyperboloid foci was chosen to be 7 feet, so that the focus of the antenna system will be centered about the spacecraft platform where there is ample space for placement of widely separated feeds. Estimated feed displacement of about ± 3 feet in the horizontal direction and ± 1 foot in the vertical direction is anticipated. Another benefit of centrally located feeds is that the waveguide runs from an electronic shelf to the feeds are short so that waveguide loss will be minimized.

3.1.5 Analysis

The analysis of Cassegrain antennas was performed primarily to assess its off-axis gain. The analysis included two subreflector shapes of eccentricity values of 3 and 2 corresponding to f_{eff} of 2f and 3f respectively. For these two subreflector cases, the diameter and focal length of the main reflector were fixed at 14 feet.

The first analysis performed was to determine off-axis gain as a function of off-axis angular displacement for the subreflector eccentricity of 3 (f_{eff}=28 feet). The feed horn was initially optimized only for the on-axis beam at 20 GHz and was a rectangular aperture of 1.75 by 2.5 in. in E and H dimension respectively. The same horn was used for the 30 GHz signal. The resultant off axis gain performance is shown in Figure 3-3 and 3-4. The off-axis gain loss at 20 GHz was observed to be higher than a single parabolic reflector. Repositioning the off-axis horns along its longitudinal axis as well as re-sizing the off-axis horn apertures improved the off-axis gain performance. The off-axis horns tended to be smaller than the on-axis horn.

The resultant gain characteristic for a larger f_{eff} of 42 feet (ϵ =2) shown in Figure 3-4 indicates better off-axis performance. It was observed in the single parabolic reflector (Figures 2-18 and 2-19) that when the feed is optimized at 20 GHz the gain loss difference of 20 GHz and 30 GHz was comparable. The same phenomenon is observed for the Cassegrain reflector where the difference is within 0.6 dB in the angular range of 4^{o}. The off-axis gain loss at 20 GHz for a 3^{o} off-axis beam is 0.7 dB and for a 4^{o} beam position is 2.4 dB. The gain loss at 30 GHz for a 3^{o} off-axis beam is 1.7 dB and 3.1 dB for a 4^{o} off-axis beam. As discussed in section 3.1.3, the accuracy of the computer model is judged to be comparable to the results compared with an experimental offset Cassegrain. As a conservative upper bound, the predicted gain loss curve is judged to be optimistic by about 1 dB for beams positioned 3 to 4 degrees from the on-axis beam.

The elevation of C/I performance for the offset Cassegrain antenna was not completed due to lack of time. It is assumed that the C/I performance will be comparable to or better than the offset parabolic reflector since the effective focal length is larger and aberrations are smaller. This must be confirmed with further analysis and supported with measured results.

3.1.6 Summary

Analysis show that a 14 foot diameter Cassegrain antenna will provide adequate performance for the 18/30 GHz multiple spot beam application. The geometry of the antenna will fit on a 14 foot diameter spacecraft platform and the feeds can be rigidly placed near the center of the platform. Unlike the single reflector system no long waveguide run or deployment structure is required for the feed. For these reasons, the Cassegrain antenna system was chosen for the recommended 18/30 GHz multiple spot beam application.

3.2 Offset Double Reflector Parabolic Torus

The RF scanning performance of a parabolic torus, as discussed in Section 2-1 is superior than a paraboloid, especially for large f/D systems. However, because of limited space in the spacecraft, systems with double reflectors are incorporated in the design to achieve a longer effective focal length. A parabolic torus can also be folded into a double reflector system.

A Gregorian-corrected toroidal scanning antennas has been studied by Young.[8] In his design, the subreflector is generated by ray-tracing using the principal of equal path length. Therefore minimum scan loss and phase error are achieved simultaneously in the plane in which the main reflector has a circular crossection. The scan loss in this direction mainly comes from the spill over loss. An oversized reflector can overcome this difficulty.

In the 20/30 GHz system considered here, minimum off-axis gain loss is more desirable in the azimuthal direction than in the elevation direction. This design shall have superior off-axis gain performance at least in one direction. To align this favorable performance direction to the desired direction in either a spinner or a three-axis spacecraft is the major problem for large double reflector torus geometries. However for small reflector geometries ($D \leq 10$ ft) a toroidal double reflector system can be fitted into a spin stabilized spacecraft. Therefore it is a potential candidate for the 20/30 GHz spot-beam antenna system.

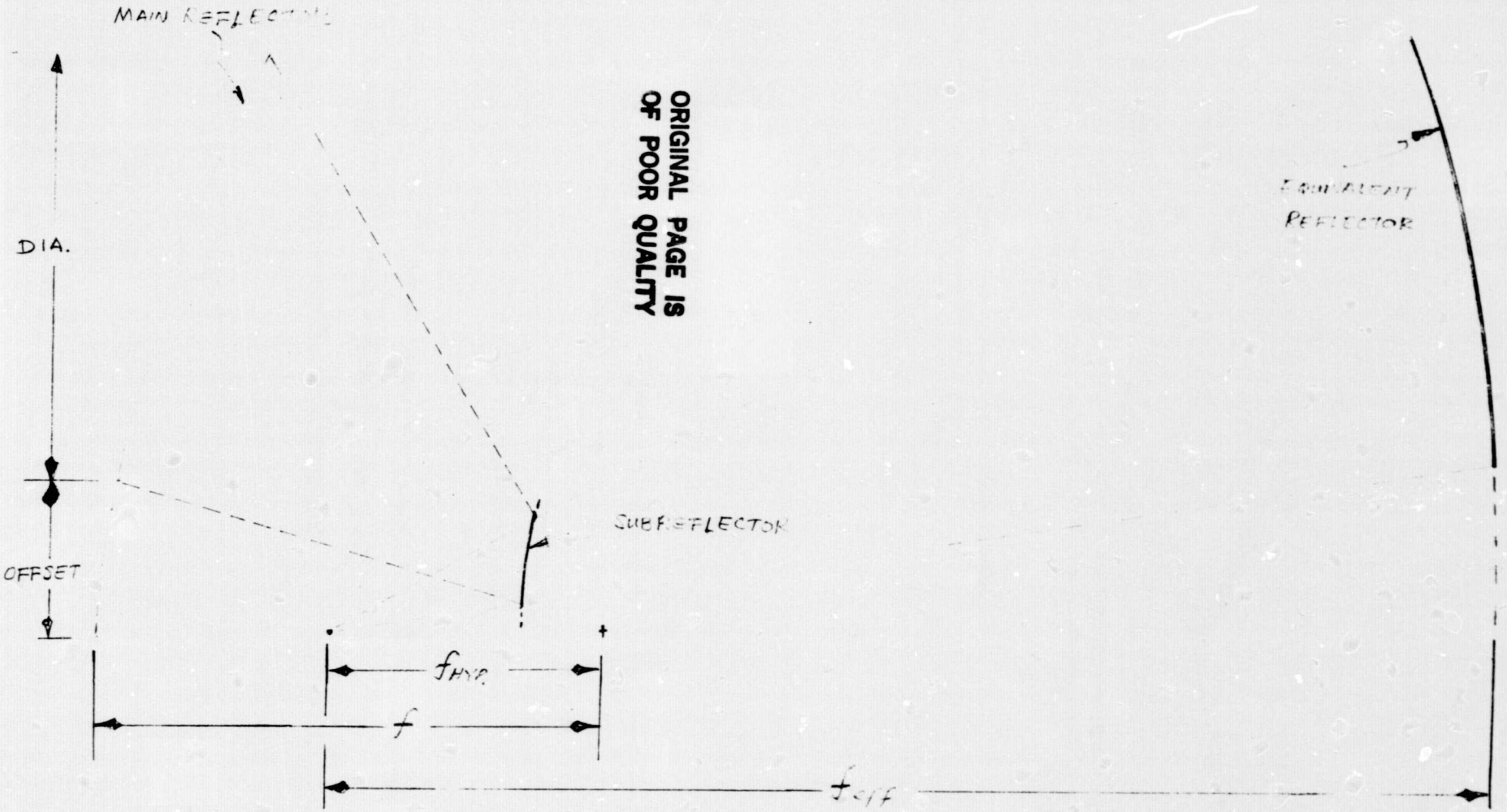

FIGURE 3-1 CASSEGRAIN ANTENNA

$$f_{eff} = f\,\frac{e+1}{e-1}$$

e = ECCENTRICITY OF SUBREFLECTOR.

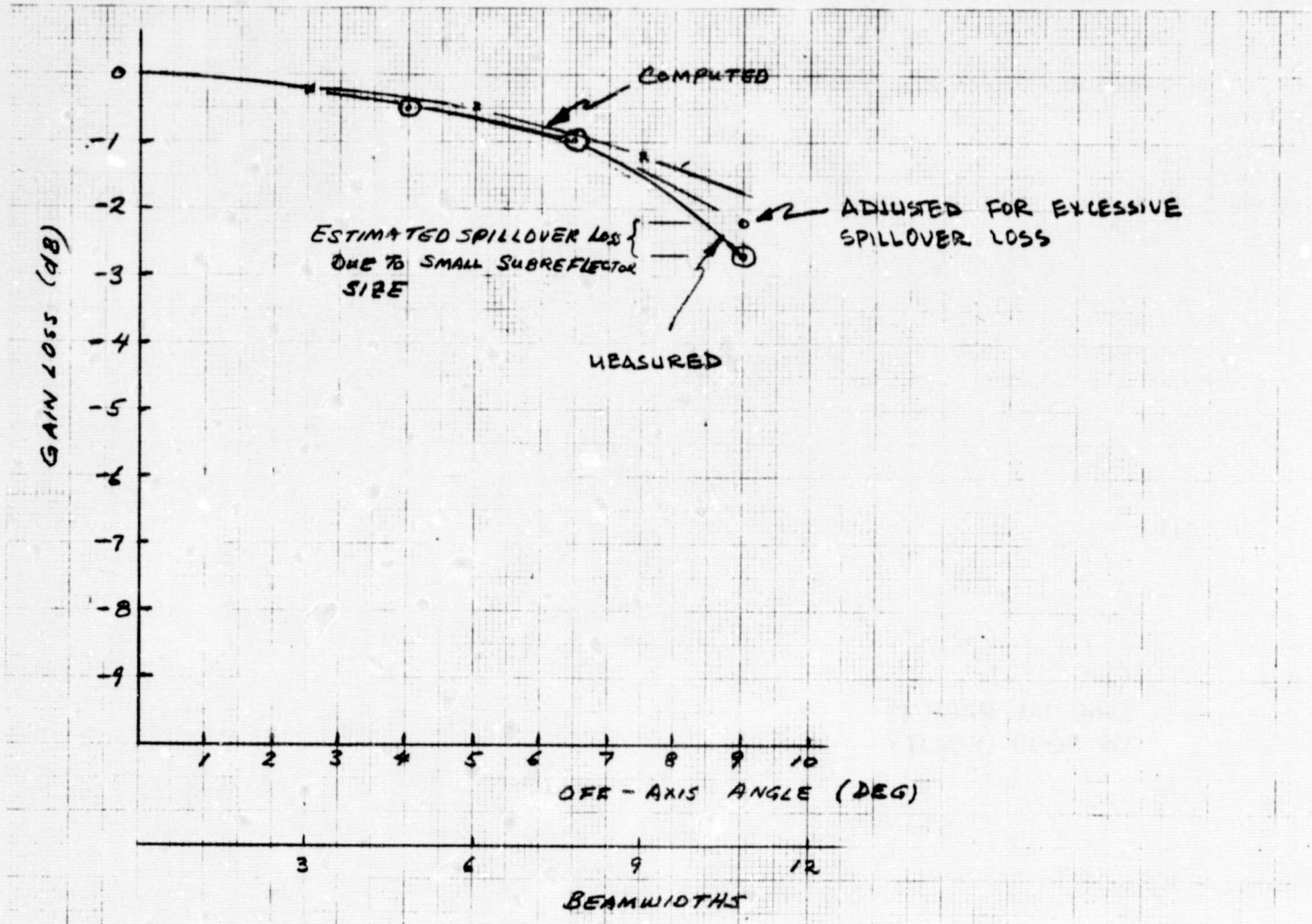

FIGURE 3-2. COMPUTED AND CORRECTED EXPERIMENTAL GAIN LOSS CURVES FOR 50 x 50 IN OFF-SET CASSEGRAIN ANTENNA.

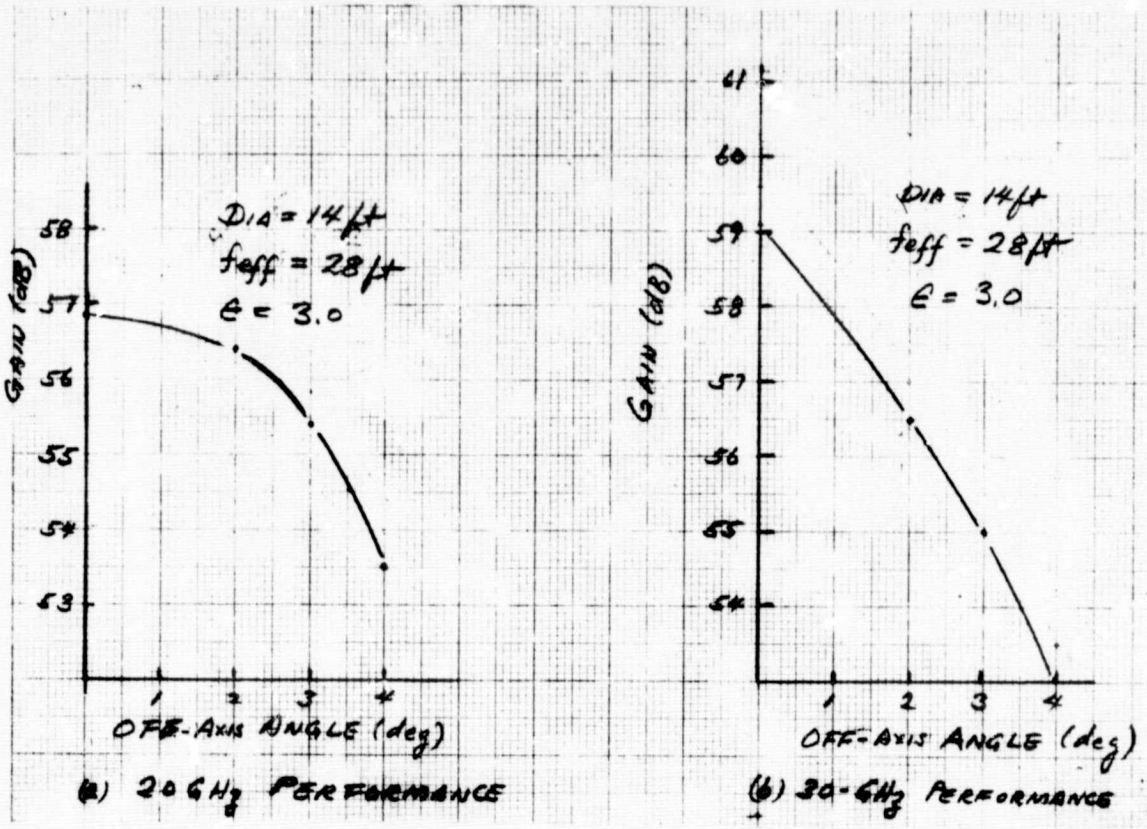

FIGURE 3-3 ANTENNA GAIN OF 14 FOOT DIA CASSEGRAIN ANTENNA WITH A FIXED FEED HORN

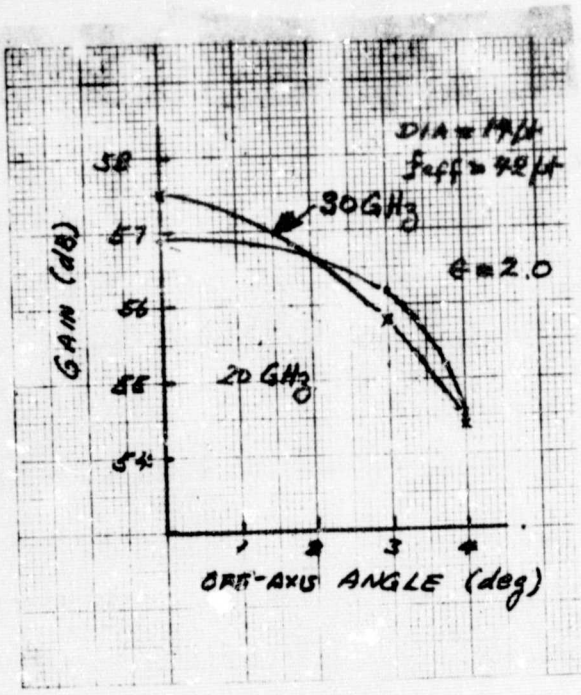

NOTE: FEED [illegible] OPTIMIZED [illegible] GHz for [illegible] STEADY [illegible]

FIGURE 3-4 ANTENNA GAIN OF 14 FOOT DIA. CASSEGRAIN ANTENNA.

4.0 LENS ANTENNA SYSTEM

Lens antennas can be configured to meet the Abbe sine condition discussed in Section 1-2 and thus have excellent off-axis gain performance. Since aperture blockage is zero, the multiple beams will be nearly identical with low sidelobe maintained for the off-axis beams.

Among the class of waveguide lenses, there are three basic types of lenses which were evaluated. The first type includes unzoned waveguide and zoned waveguide lenses which are constructed using only waveguides of varying lengths. A half-wave plate lens is classified as a second type where half-wave plate phase shifters are used to correct for quadratic phase error. Examples of the third type are those employing group delay compensation such as the Coulbourn lens[9] and the equal group delay waveguide lens.[10]

The investigation of dielectric lenses was limited to evaluation of space applicable dielectric material and their limitations.

4.1 Waveguide Lens

Waveguide lenses are frequency limited because the waveguides are dispersive. Various designs have been developed to broaden the lens bandwidth and are summarized in the following paragraphs.

Four of the five waveguide lenses depicted in Figure 4-1 use some technique to broaden their bandwidth. The five lenses were designed to operate at a

e-3

center frequency of 8.138 GHz and the cut-off frequency of the waveguide element was 6.91 GHz corresponding to one inch diameter cylindrical waveguide. The corresponding phase errors shown in Figure 4-2 were calculated at 2 percent below the design frequency of a 4 foot diameter aperture with 6 foot focal length.

4.1.1 Waveguide Lens Analysis

A. Unzoned Waveguide Lens

The unzoned waveguide lens depends solely on the differential phase velocity of the waveguide and free space to form a constant phase plane by adjusting the waveguide lengths at the design frequency. As shown in Figure 4-1 the outer surface of the lens forms a hyperboloid, and for a large aperture antenna the outer most waveguide lengths may reach several wavelengths. These long waveguide elements make this lens the heaviest and bulkiest among the waveguide lenses. Because of the length of the element the unzoned waveguide lens has a large phase error variation at 2 percent off the design frequency. This lens is extremely band limited.

B. Zoned Waveguide Lens

In order to minimize the size of the unzoned lens and to reduce the total phase error, a conventional zoning technique can be used. Positions of the unzoned waveguide lens is removed in discrete steps so that the phase differential is a multiple of 2π radians at the design frequency. The steps in the resultant lens occur concentrically and the step size ΔL is determined by the formula given in Figure 4-1. Although the lens volume is reduced, the step discontinuities at the zone boundaries creates a diffracting surface

resulting in a squinted active element pattern of those waveguides adjacent to a zone. The gain is reduced and the sidelobe levels are increased as a result of this non-uniform aperture distribution.

The lightest weight lens is achieved when the center of the lens is made nearly zero thickness. Such a zoned waveguide lens not only has reduced volume but also has reduced phase error from the unzoned waveguide lens. However, the phase error continues to increase toward the edge of the lens.

C. Half-Wave Plate Lens

The constant thickness lens of Figure 4-1d does not depend on the differential phase of the waveguide and free space to form a plane wave at the aperture. Instead it houses a half-wave plate element in each waveguide. The function of the plate is to correct the quadratic phase error of a spherical wave to form a constant phase plane. However, in order for the plate to function as a phase shifter the incident wave must be circularly polarized and the electrical phase shift is twice the angular rotation of the plate relative to a reference plane. This lens is comparatively light, however, it is band limited since the lens is phase corrected at one frequency. The phase variation of this lens is caused mainly by the differential path length and is a quadratic function of the radius reaching a maximum value of 21 degrees over the 4 percent operating band for the 4 foot diameter lens with 6 foot focal length.

D. Phase-Compensated Half-Wave Plate Lens

The phase-compensated half-wave plate lens has a half-wave plate compensation section as shown in Figure 4-2e. The phase compensation section is configured by using the similar technique used for zoning of the zone lens. At the design frequency the zone step constitutes a phase step of multiple

of 2 π radians, so a constant aperture phase is formed. However, at other frequencies the added waveguide section offsets the phase error as shown in Figure 4-2e to minimize the maximum phase error. As shown in the figure the phase error has been reduced by a third of the uncompensated half-wave plate lens and the maximum phase error is the smallest among the five waveguide lens studied.

Because of the wide band capability, application of the phase compensated half-wave plate lens has been proposed for a future space communication system for a global coverage at X-band frequency. At Hughes, a single step phase-compensated half-wave plate lens of a 4 foot diameter aperture having a 6 foot focal length was built and tested at X-band frequencies. This lens was built with 1732 waveguides of 1.06 inch diameter tubings and 2.08 inch thick half-wave lens section and an additional 3.5 inches of phase compensated waveguide length. The lens itself weighed 15.1 pounds. The experimental gain data of single beams shows that antenna scan loss is less than 0.2 dB for 5 beamwidths scan for a four percent bandwidth.

E. Coulbourn Lens[9]

It has been suggested by Coulbourn that instead of zero thickness at the center, if some thickness is added at the lens axis and proceed the zoning as above, zero mean phase error results as shown in Figure 4-2c. The thickness of lens at the successive step is then gradually reduced. This lens is heavier than the previous zoned lens. The Coulbourn lens also has unavoidable zoning loss as the zoned waveguide lens.

The zero mean phase error reduces the maximum phase errors so that the phase error is evenly distributed between positive and negative values. The overall maximum phase error is reduced significantly to 7 degrees for a 4 percent operating band centered at X-band frequencies.

F. Equal Group Delay Lens[9]

Recently, Messers Ajioka and Ramsey of Hughes GSG proposed a lens using a combination of a waveguide delay section and half-way plate. This new lens has been analyzed for a 4 percent bandwidth at 8.138 GHz design frequency for a 4 foot diameter aperture having a 6 foot focal length. The phase error was calculated to be less than 2° making this lens applicable for a wider bandwidth operation than the phase compensated half-wave plate lens. This wide band characteristic has potential application to the 18/30 GHz requirement.

The lens geometry depicted in Figure 4-3 shows the spherical half-wave plate lens section to which waveguides are added to form an ellipsoidal surface at the front of the lens. For analysis purposes, a 6 foot diameter lens having a 6 foot focal length was selected. A system with adequate performance can be designed using this aperature, and weight and cost become excessive for larger aperatures. The maximum thickness of this lens is approximately 1 foot. The phase error shown in Figure 4-3c is based on a 2.5 GHz bandwidth at design frequency of 20 GHz. The maximum phase error of the 6 foot lens was calculated to be 50° at the band edges. This large phase error occurred because of the higher operating frequency range, wider bandwidth and larger lens diameter in terms of wavelength than the 4 foot lens. Such a large phase error results in undesirable reduction in peak gain and high sidelobe levels which will lower the C/I performance to values lower than 30 dB.

4.1.2 Summary

Although waveguide lenses have low off axis gain loss, they are extremely band limited due to the dispersive characteristic of the waveguide. Among the different designs to broaden the bandwidth, the equal group delay lens appeared to be suitable for the 18/30 GHz application. However, the phase error on the aperture of a 6 foot diameter lens for 12.5 percent bandwidth is too large to provide good C/I performance. Therefore with the present technology, the use of the waveguide lenses for the multiple spot beam application is not recommended.

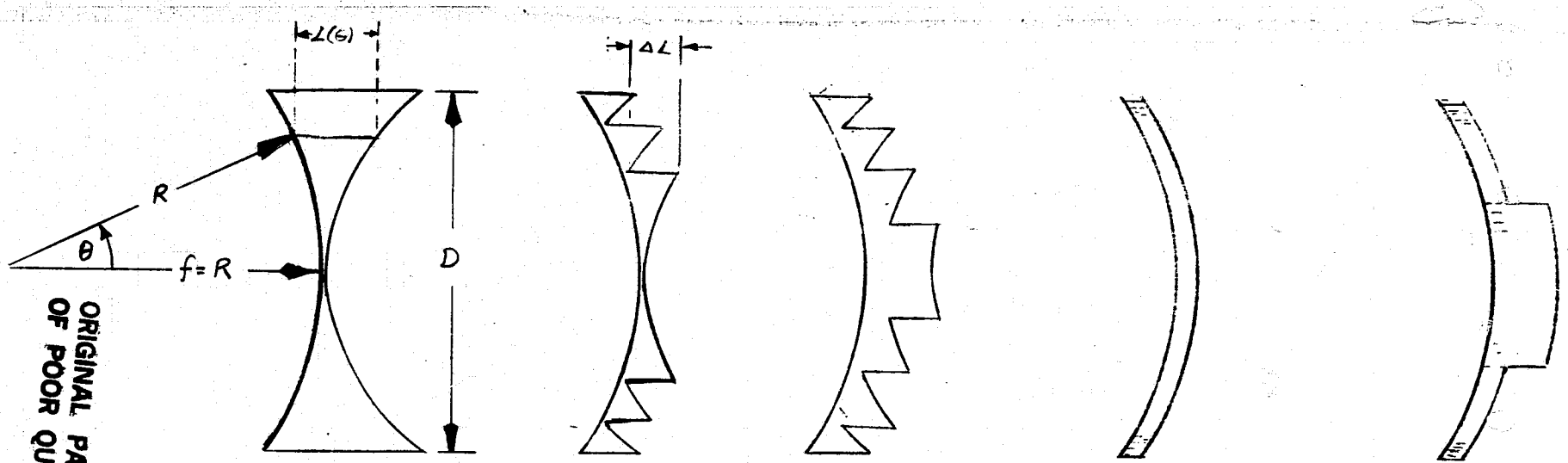

$$L(\theta) = \frac{\lambda_o f}{\lambda_o - \lambda_g}(1 - \cos\theta) \qquad \Delta L = \frac{\lambda_o \lambda_g}{\lambda_o - \lambda_g}$$

λ_o = free space wavelength

λ_g = guide wavelength

(a) Unzoned Lens (b) Zoned Lens (c) Coulbourn Lens (d) Half-wave Plate Lens (e) Phase-Compensated Half-Wave Lens

Figure 4-1 Different Waveguide Lenses

$R = 6$ ft, $D = 4$ ft $\quad freq = (freq)_D (0.98) \quad (freq)_D = 8.14\,GHz$

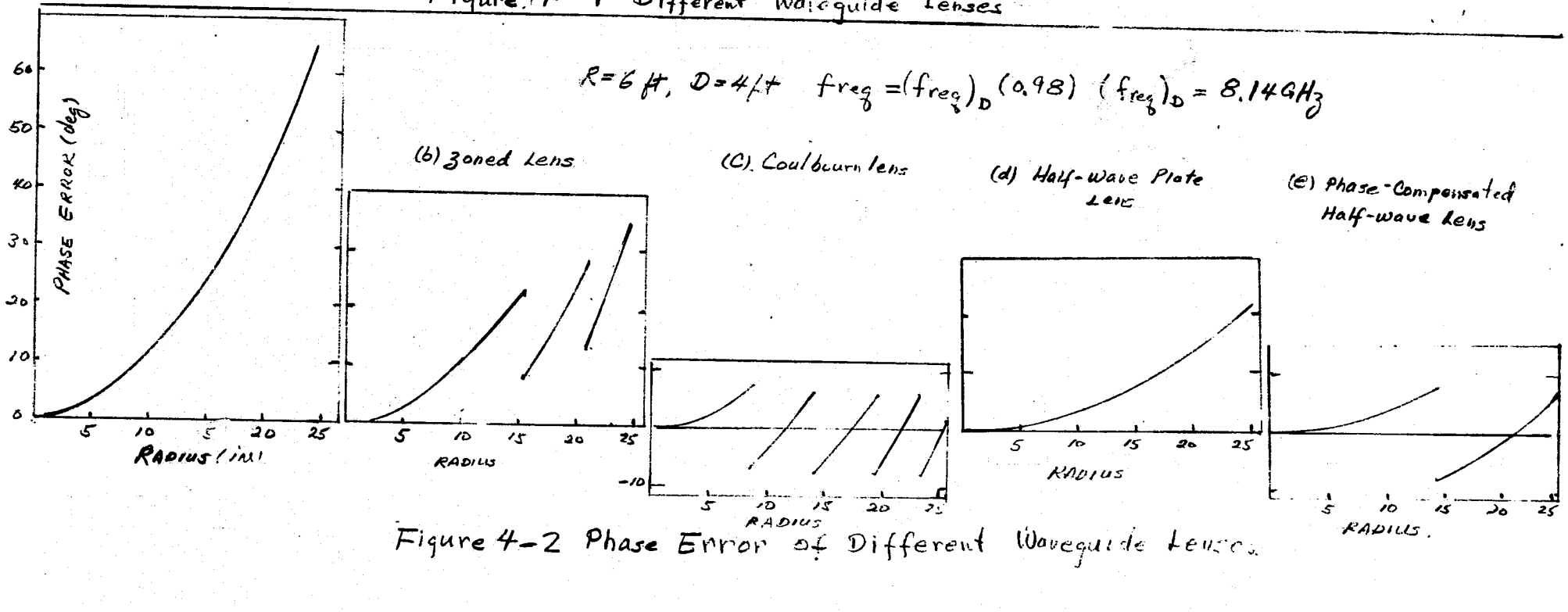

Figure 4-2 Phase Error of Different Waveguide Lenses

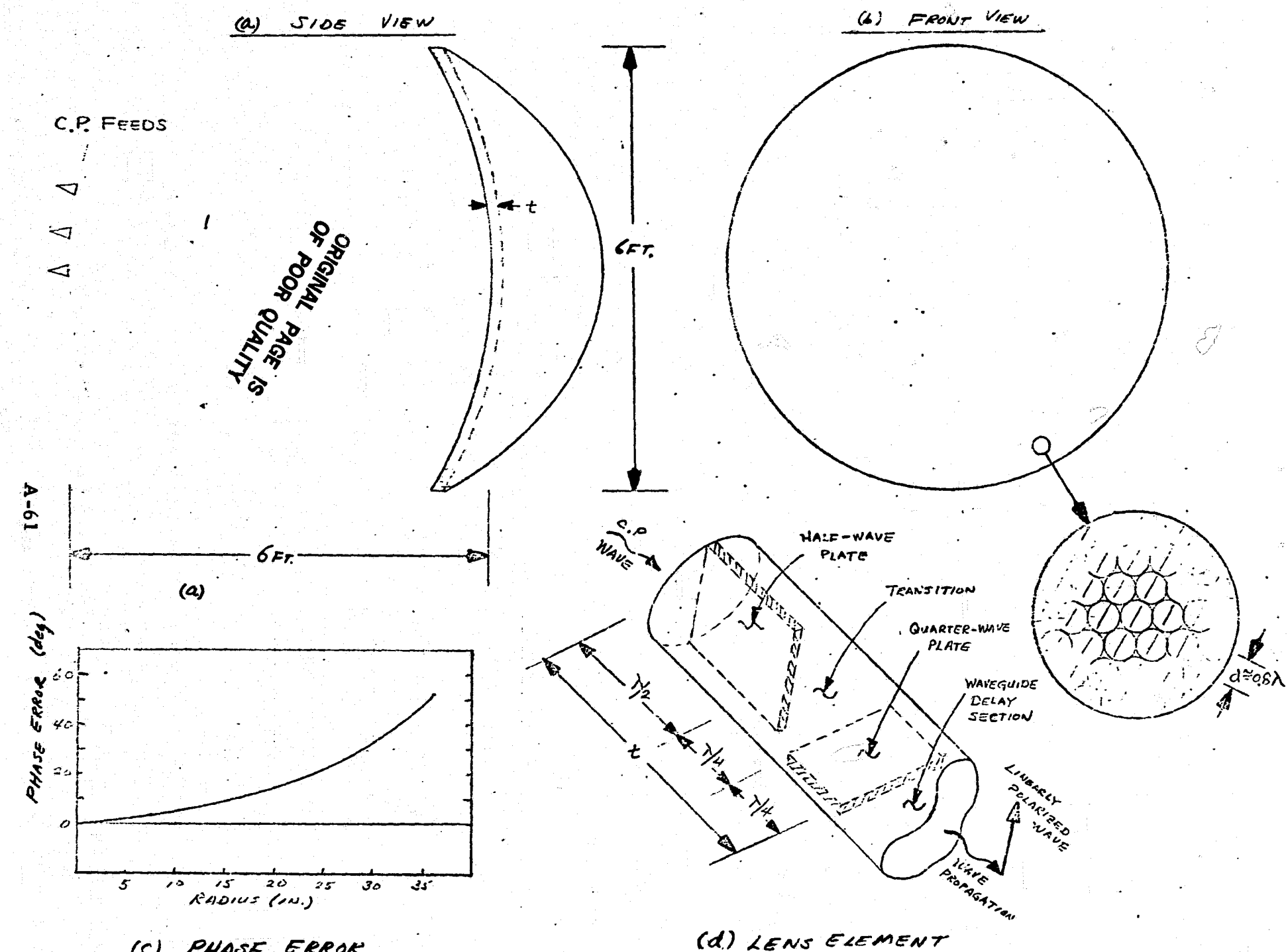

FIGURE 4-3 EQUAL GROUP DELAY LENS

4.2 Dielectric Lens

The geometry of a dielectric lens depends primarily on its index of refraction and focal length f. The surface nearest the focus is spherically shaped to satisfy the Abbe sine condition. The aperture surface is an ellipsoidal contour as shown in Figure 4-4. For this geometry, the lens thickness and volume as a function of the relative dielectric constant ϵ_r have been tabulated for a 6 foot diameter lens with a focal length of 6 feet. Values of ϵ_r less than 2 causes the lens volume to increase rapidly. If the specific gravity of the material is less than 0.2, the weight of the lens will be about 400 pounds for ϵ_r greater 2.

Aside from the dielectric constant and weight concerns, behavior of material properties in the space environment is also a concern. Questions such as material outgassing and thermal distortion due to temperature swings of $\pm 250^{\circ}F$ must be answered. Plastic exposure to ultraviolet rays is known to change material properties which could degrade electrical performance. However, there are ways to shielding the dielectric materials from the sun and ultraviolet rays by thermal coverings and paints. For the size of antenna considered, the stiffness of the material may become a determining factor since cold flow creep due to weight on the earth may become significant. Quality control of bulk material uniformity and batch-to-batch repeatibility must not be overlooked.

The following section discusses particular material properties of some dielectric lens materials and a brief summary of the material properties is listed in Figure 4-5.

4.2.1 Lens Material Choices

Dielectric Plastic Foams

In general, plastic foam materials are light and machinable. Plastic foam materials having a relative dielectric constant of 2.0 at X-band and a specific density of about 0.05 are commercially available. It is recommended that the material be protected from weather exposure. For space application, shielding from the sun is necessary since the maximum allowable temperature is about 170°F. Many plastic foams contain closed air cells and these cells may expand or burst in space. Analysis of such an effect on the electrical performance has not been performed at 18/30 GHz.

There are other material characteristics that affect electrical performance. Thermal distortion, non-uniformity of material, and loss tangent are some other properties affecting the design of plastic foam lens for space application.

Phase Delay Artificial Dielectric

A phase-delay artificial dielectric is made of layers of dielectric sheets on which an array of metallic conductors of 0.1 wavelength diameter is etched. An artificial dielectric is formed when the discs polarize with an electric field. Size and spacing of the discs determine the value of the dielectric constant. At 18/30 GHz, typical required dimensions are 0.040 inch diameter disc, 0.050 inch disc spacing and 0.020 inch spacing of the dielectric sheets to obtain ϵ_r equal to 2.0. If the tolerance control

of these dimensions over a 6 foot diameter can be met, a 24 inch thick lens made of one mil thick Kapton sheet is estimated to weigh about 450 pounds. This weight excludes lens frame, support and any spacers used to keep the layers of sheets from touching.

Teflon and Rexolite

Teflon and rexolite materials have been used extensively for microwave applications. Their dielectric constant is within the desired range for lens application, however, the specific density of rexolite is about 1.1, and a 6 foot diameter foot lens is estimated to weigh about one ton. A teflon lens will weigh two tons. Therefore, teflon and rexolite are not suited for the 18/30 GHz antenna application.

Powdered Glass

Powdered glass known comercially as Cab-O-Sil is a fine powder-like glass material whose particle size measures 7 to 14 millimicrons. This material is cited here since its specific gravity is only 0.03 and may be used for a lightweight lens. Electrically, it has a problem that its dielectric constant is low. However, as in the development of phase-delay artificial dielectric, polarizing elements may be mixed to form a higher value dielectric constant. Mechanically, the material needs to be encapsulated not only to keep the material in place, but also to hermetically shield the material since Cab-O-Sil is hydroscopic. Water particles entrapped in the material is a potential source of rf loss.

4.3 Performance

Neither waveguide lens nor dielectric lens appears practical for the 18/30 GHz.

application. However, analysis was performed using a lens computer model of a half-wave plate lens discussed in 4.1.1. The antenna geometry consisted of a 6 foot diameter lens with a 6 foot focal length. Performance of 14 foot diameter lens was estimated from the 6 foot data for the same f/D value.

The resultant gain and C/I performance for the five city groups are shown in Figure 4-6. The off axis gain loss is less than 0.5 dB within the angular range of 4°. The C/I performance was calculated in the same manner as the reflector in Paragraph 2.2. The gain of a single city beam is calculated over its 3 dB beamwidth by exciting its respective feed with unity power and zero phase. Then, that feed is turned off and the remaining four city horns are excited with unity power and zero phase. The ratio between the gain of a city beam and the combined interference signals from the other four horns is defined as the C/I value. The range of C/I figure is represented by a straight line,and the average value indicated by an asterisk. The wide range observed at New York is due to a null in the interfering signal sidelobe within the half power contour. The minimum C/I performance of 20.5 dB at Atlanta is a result of sidelobes from New York and Chicago beams which are separated by about 1.2°.

The antenna performance of the 14 foot diameter lens shows the same small off axis gain loss. The C/I performance over Atlanta again shows the minimum value of 34.5 dB.

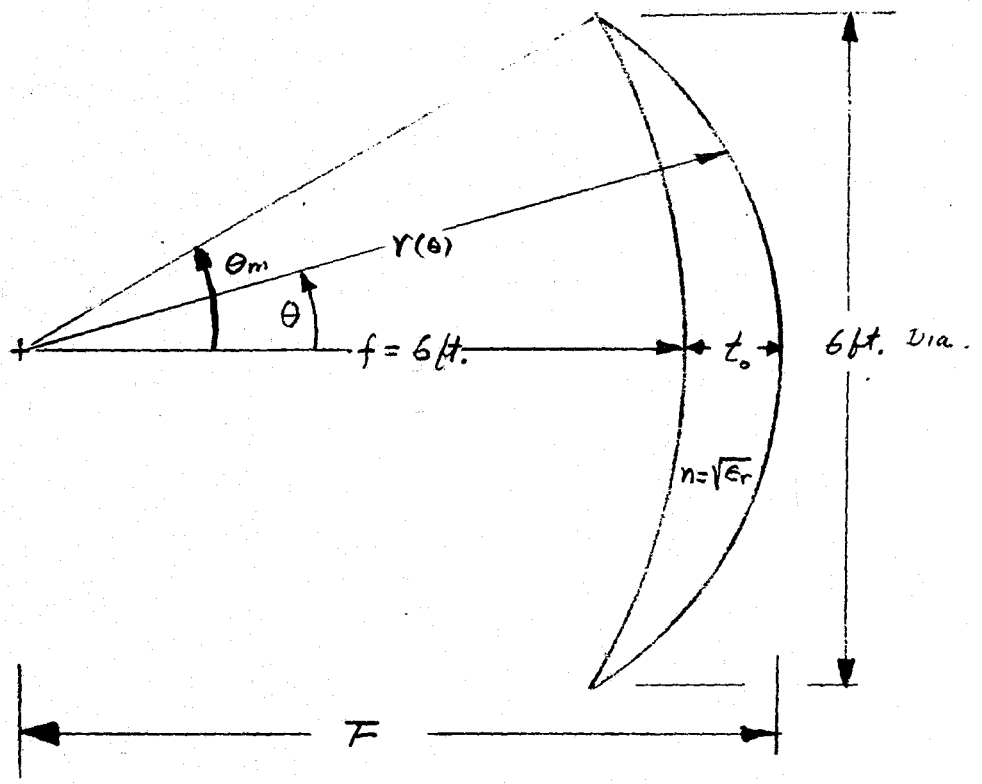

$$r(\theta) = \frac{F(n-1)}{n - \cos\theta}$$

$$F = \frac{f(n - \cos\theta_m)}{n-1}$$

ϵ_r	Δt (ft)	Volume (ft^3)
1.2	8.42	107.3
1.4	4.39	82.7
1.6	3.03	53.7
1.8	2.35	40.3
2.0	1.94	32.6
2.2	1.66	27.5
2.4	1.46	24.0
2.6	1.31	21.4

FIGURE 4-4 DIELECTRIC LENS - GEOMETRIC PARAMETERS

LENS MATERIALS

MATERIAL	DESCRIPTION	ϵ_r	WEIGHT* (lb)	LOSS (dB)	REMARKS
~~REFRIGER~~ DIELECTRIC PLASTIC FOAM	LIGHT-WEIGHT POLYSTYRENE-BASED PLASTIC FOAM MAT'L	2.0	100	2.7	ADVANTAGE: (a) Light material and can get ϵ_r as high as 2.0 (b) machinable. DISADVANTAGE: (a) Low max. operating temperature (167°F) (b) Usual problems of plastic material under space environmental conditions (c) High loss due to material
ARTIFICIAL DIELECTRIC . PHASE-DELAY TYPE	LAYERS OF DIELECTRIC SHEETS WITH ARRAY OF SMALL METALLIC DISKS (0.1 λ DIA.) SPACED AT ABOUT 0.12 λ.	2.0	430	0.4**	ADVANTAGE: (a) Space qualified materials can be used (b) Low loss DISADVANTAGE: (a) moderately heavy lens (b) Tolerance Problem in etching of copper cladded Kapton - disk dia. = 0.050 in. gap = 0.010 in at K-band.
Cab-O-Sil	POWDERED GLASS MATERIAL-COMPRESSIBLE TO FORM DENSE MATERIAL	1.01 1 1.13	***	unknown	ADVANTAGE: (a) Basic material is glass: therefore, no problem under space environment (b) Light and compressible (specific gravity can vary from 0.03 to 0.3) DISADVANTAGE: (a) Has not been used for microwave applications
TEFLON	SOLID	2.0	4500	1.6	DISADVANTAGE: (a) Heavy. (b) Space environment Problem

* Only Lens material and does not include frame or support.
** Based on loss tangent of Kapton. *** Er too small - can't assess weight

FIGURE 4-5 DIELECTRIC LENS MATERIALS

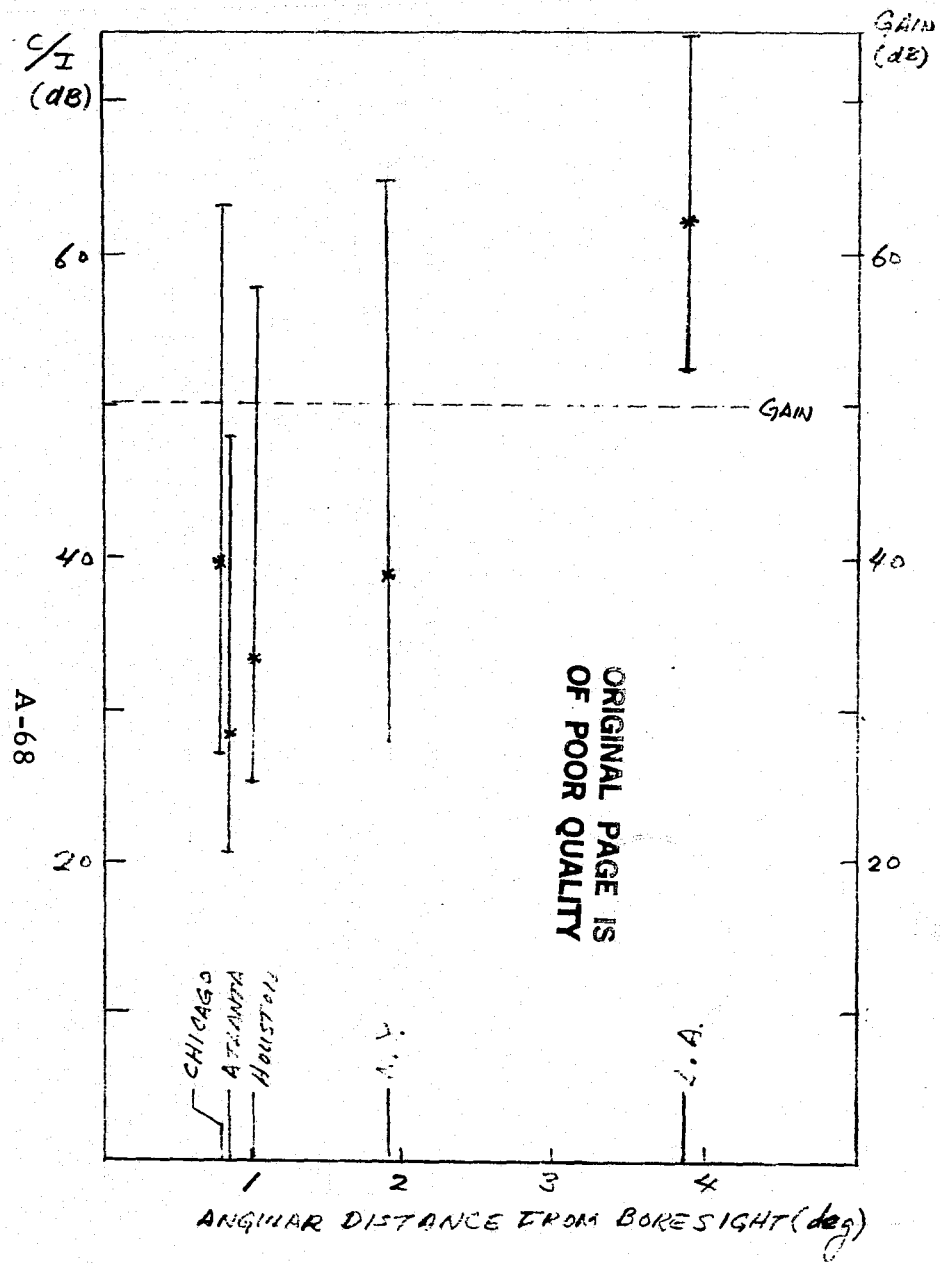

(a) 6 foot DIAMETER LENS
(CALCULATED PERFORMANCE)

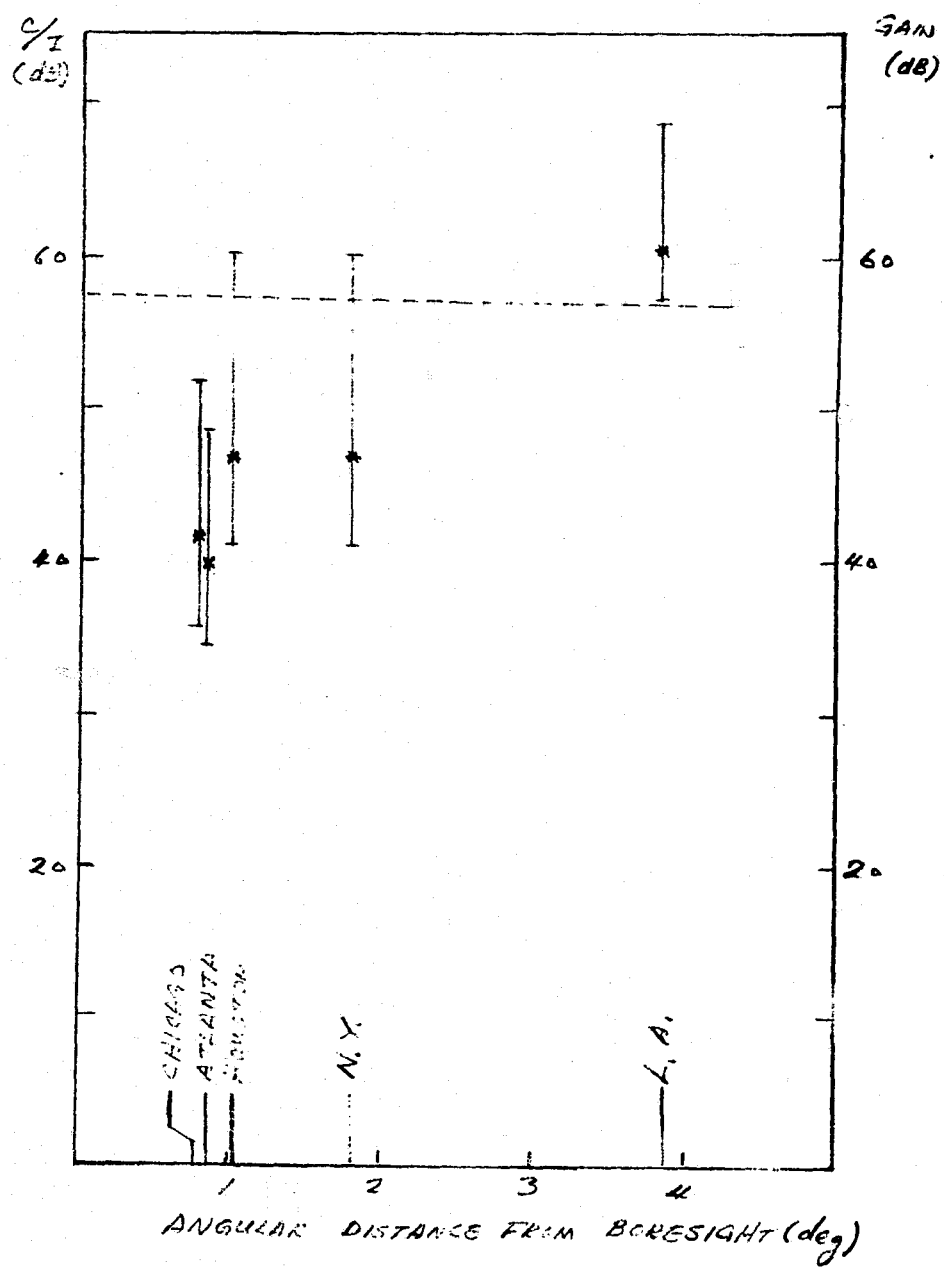

(b) [illegible] DIAMETER LENS
(ESTIMATED PERFORMANCE)

FIGURE 4-6 LENS PERFORMANCE

5.0 14-FOOT OFFEST CASSEGRAIN ANTENNA - TRUNKING BASELINE

5.1 Selection Rationale

The final selection of a baseline satellite antenna configuration depends on many system design factors such as the required EIRP, G/T values, and C/I values. Rain attenuation and depolarization effects must be accounted for in determining the communication link performance between the ground terminals and the satellite. Judgement about these factors will not be made here. Rather, the baseline selection will be made solely on the basis of an assumed C/I performance of greater than 30 dB and to choose an antenna aperture that is the largest practical size consistent with the STS payload envelope. The reflector will be assumed to be solid and not an unfurling mesh design. C/I performance requirements less than 30 dB will allow use of smaller reflector apertures.

As discussed in Section 1.1, reflector apertures 25 feet in diameter are required if spatial beam isolation only is implemented to achieve frequency reuse between beams spaced 0.3 degrees apart (10 city scenario). Reduction to 14 foot aperture is possible by implementing orthogonal polarization isolation between closely spaced beams. The proposed approach provides five of the 10 cities with one sense of linear polarization for both transmit and receive bands with one antenna. The other five cities have spot beams that are orthogonally polarized with beams formed with a second antenna.

Offset single aperture reflectors 14 feet in diameter require focal lengths near 28 feet (f/D=1) to achieve good spatial beam isolation

(C/I 30 dB) for the 10 city scenario. Such long focal lengths make integration to shuttle sized spacecraft difficult because of the deployment required for the reflectors and spacecraft. Torus designs are even more complicated because of their preferred orientation on the spacecraft. Comparable performance is achieved with a smaller antenna volume by folding the offset geometries via a subreflector. This study indicates that an offset Cassegrain can achieve the assumed C/I value of 30 dB with a 14 foot aperture and be implemented on both a spin stablelized or 3-axis stabilized spacecraft. A spin stablelized spacecraft is chosen as an example for this study.

5.2 Antenna Geometry

A stowed and deployed sketch of two identical offset Cassegrainian antennas are shown in Figure 5-1. The feed horns are rigidly mounted to the spacecraft and only the subreflectors and reflectors are deployed. A front view is shown in Figure 5-2. The plane of antenna symmetry is inclined 45 degrees with respect to the axis of the spacecraft. The polarization orthogonality of the two antennas are accomplished by rotating the feed horns of one antenna 90 degrees.

There are several methods in configuring the reflector feeds for independent optimization of the downlink and uplink beams. One is to use a dual grid reflector concept discussed in Section 2.2. For Cassegrain application, a grid subreflector is also required. This approach requires the front grid reflector surface to be RF transparent. The use of graphite is preferred

because of its superior strength and low thermal coefficient of expansion. However it is not RF transparent and cannot be used as the front reflector in a dual grid reflector geometry. Kevlar fabric is RF transparent and has a much lower coefficient of expansion than fiberglass but not as good as graphite. The dual grid reflector for SBS is fabricated from Kevlar and is adequate at 12 and 14 GHz but may be not adequate at 18 and 30 GHz. Further investigation is needed to evaluate the ability of the multiple beams to maintain relative pointing between all the beams under all conditions of thermal distortion.

Another technique for independent optimization of the feeds is to use a dichroic surface to create an image focus.[11] For Cassegrain application, the feed located near the secondary focus would have a flat dichroic surface in front of the horn which would allow the 18 GHz signals to pass through it and reflect the 30 GHz signal to the image point of the 18 GHz feed horn. This allows independent optimization of the feed horns to each band. However for multiple beam application, the use of a common surface for all the feeds or the use of an individual surface for each horn needs to be studied further because of the packaging complexity.

For this study, simple pyramidal horns are assumed where both co-polarized uplink and downlink beams for each city are formed via a single horn. The horn dimensions are chosen for best performance at 18 GHz. The length of the horn to keep the aperture phase error to $\lambda/8$ is about 36 inches. A diplexer attached to the end of each horn is needed to separate the co-polarized uplink and downlink signals. Diplexers are used on the COMSTAR I

antenna system to separate the co-polarized 4 and 6 GHz downlink and uplink signals respectively.[2] The ten city feed horn distribution mounted on the spacecraft is shown in Figure 5-3 where points A and B are focal points of the antenna. It has been found in the course of this study that the subtended angle of a feed by the subreflector increases appreciably as the feed is displaced further from the focal point. For a four degree scanned beam, a reduction of 20 percent in the E-dimension and 25 percent in the H-dimension produces the same reflector edge taper as the on-axis case.

5.3 Performance

The Cassegrain antenna of the chosen geometry has a peak aperture gain of 56.9 dB (efficiency equal to 61 percent) 20 GHz and 57.5 dB at 30 GHz (efficiency equal to 31 percent) for on-axis beam. The off-axis loss at 20 GHz is 0.7 dB and at 30 GHz the loss is 1.4 dB for beams positioned up to 3 degrees. The C/I performance is estimated to be greater than 30 dB based on the results of the 14 foot diameter torus reflector with f/D=1.

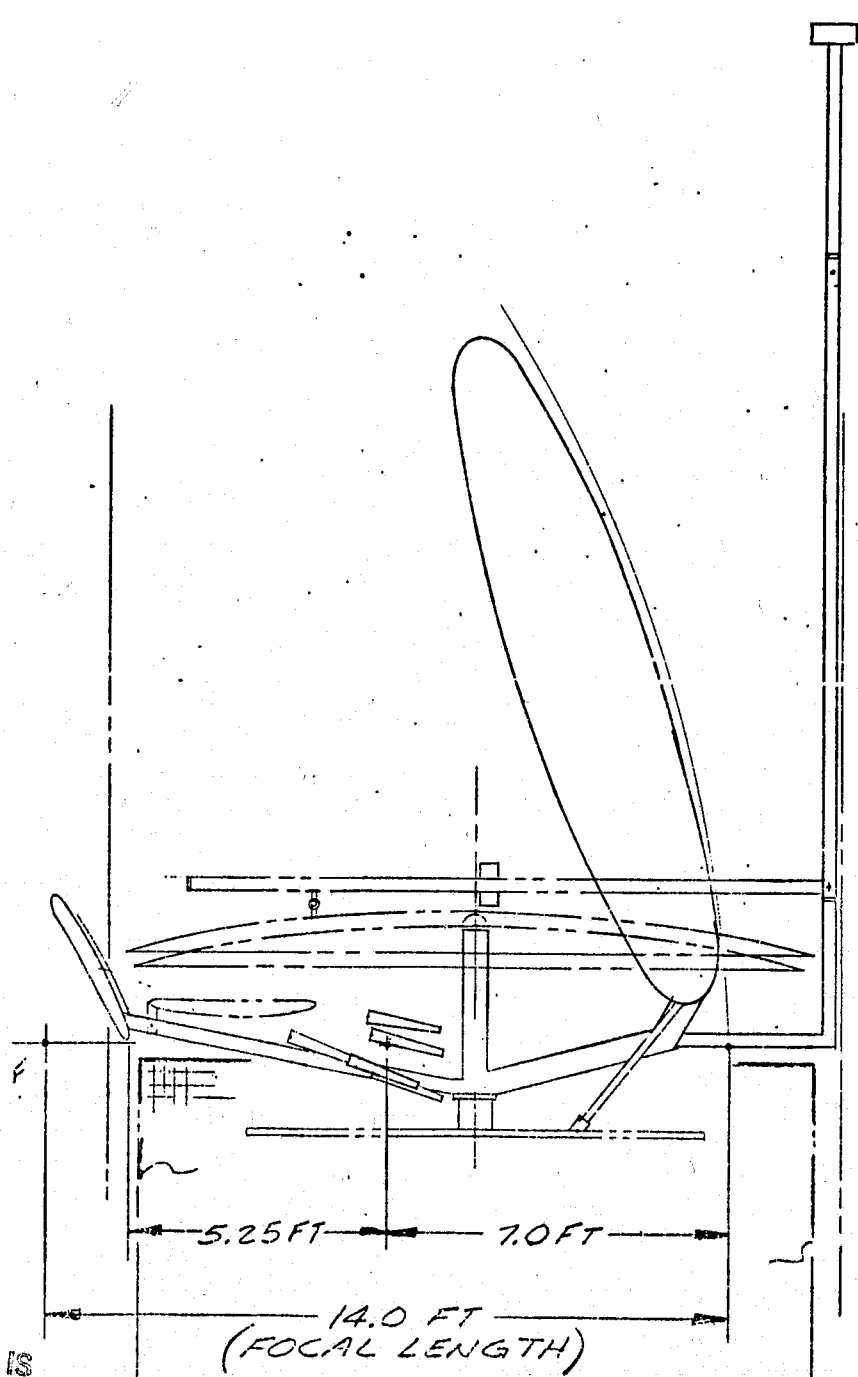

FIGURE 5-1 STOWED AND DEPLOYED ANTENNA POSTION
SIDE VIEW

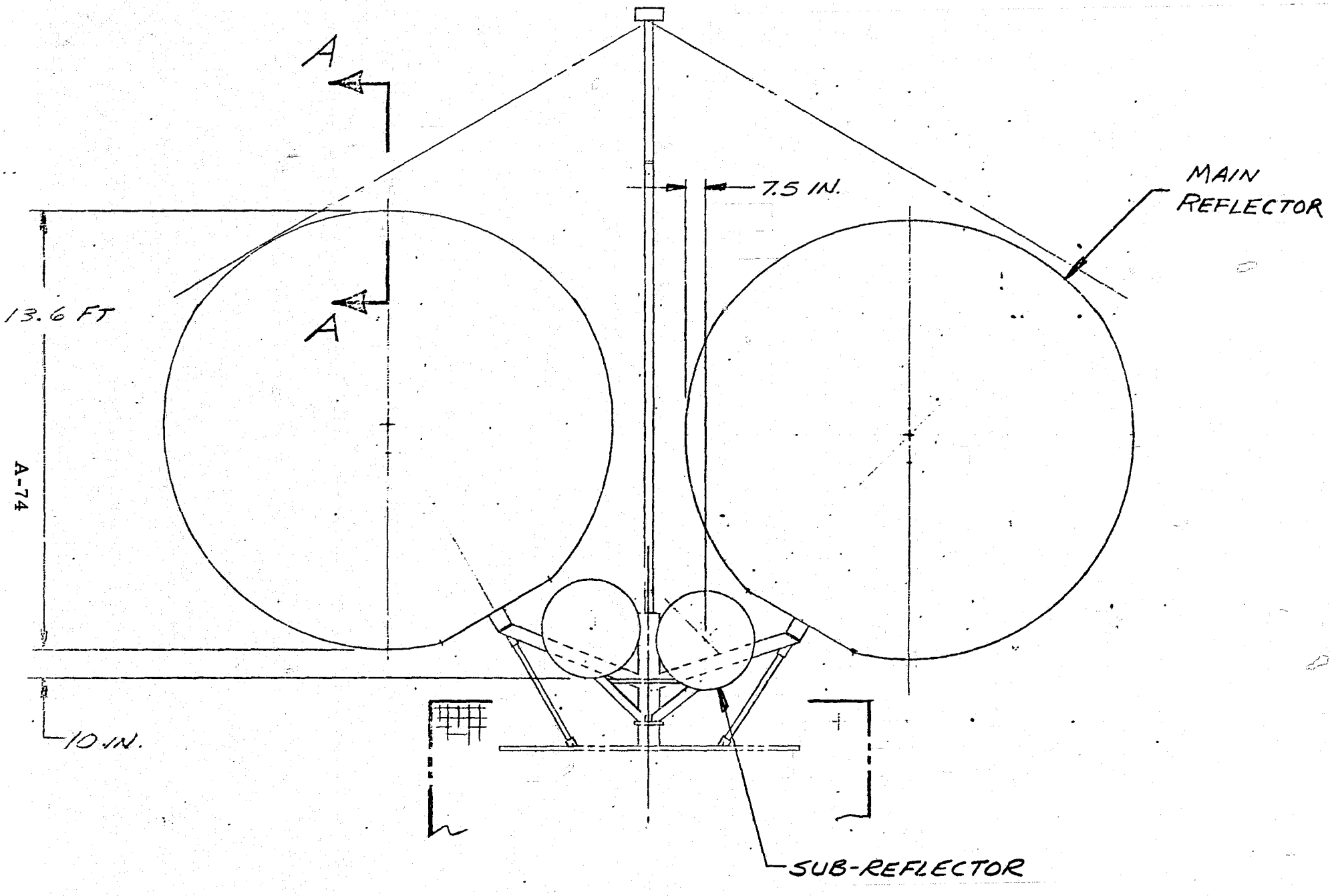

FIGURE 5-2 SPACECRAFT ANTENNA GEOMETRY FRONT VIEW

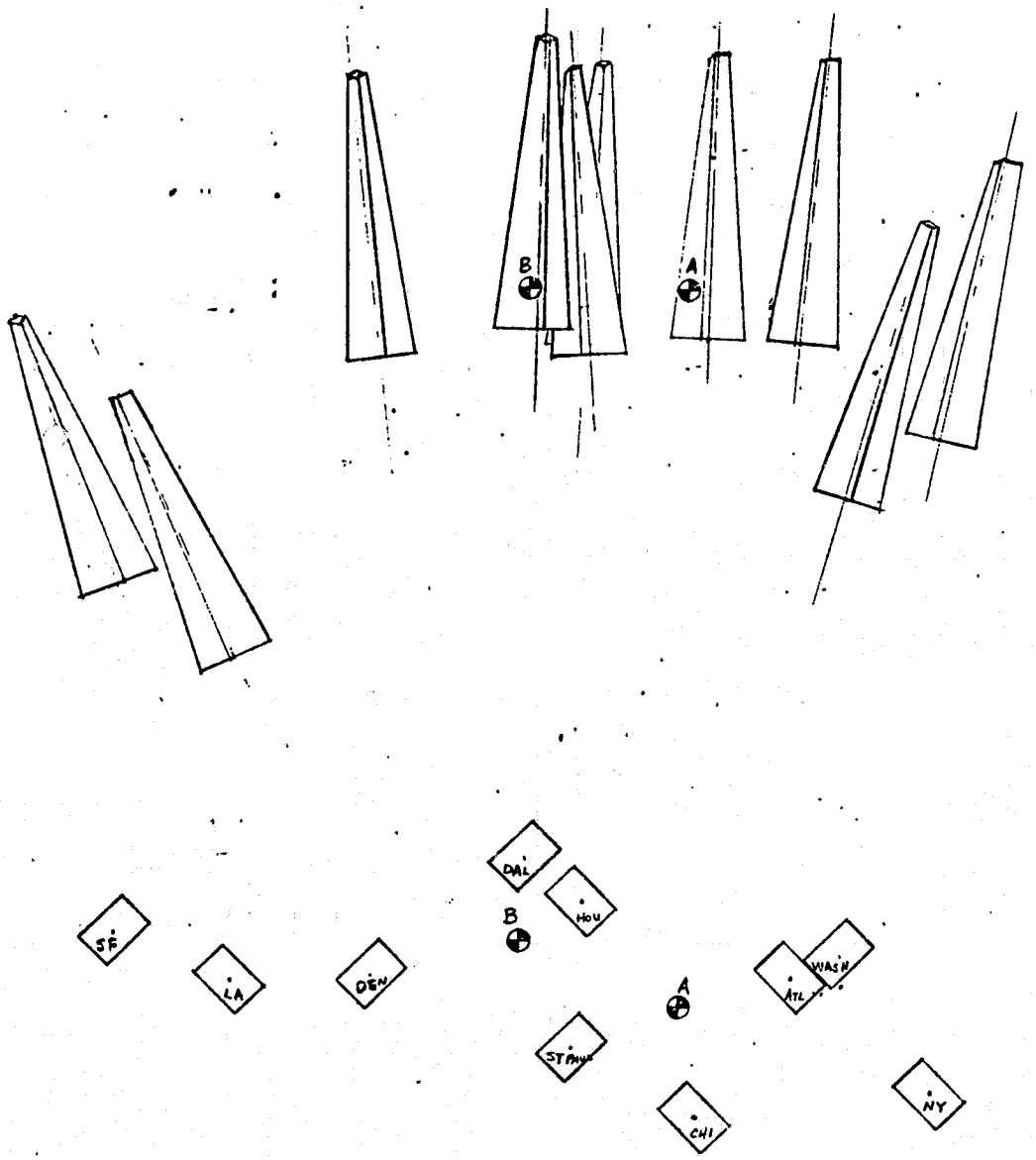

Looking from Subreflector

FIGURE 5-3 FEED GEOMETRY
20/30 CASSEGRAIN ANTENNA.

6.0 ANTENNA TECHNOLOGY INVESTIGATION

In this section, the areas that require further investigation and the technologies that need to be developed for the 18/30GHz multiple spot beam satellite antenna systems are presented.

Scan beam reflector antenna systems have an inherent defocusing characteristic which causes peak gain reduction and sidelobe level increase. Reduction of off axis gain loss and improvement of C/I performance are the two areas needed for further investigation. There are at least two ways to improve the scanning performance. One is by shaping the reflectors, such as the bifocal reflector system currently being developed at HAC. Another is by compensation of phase error in a multiple horn feed geometry for each beam. This approach needs the development of the technologies to design compact feed horns such as partially loaded dielectric horns and low-loss feed networks.

Producing low sidelobe beams to achieve a better spatial isolation is essential in order to improve the C/I performance. Shaping reflectors may improve the sidelobe performances of certain but not all the beams. Therefore, an alternate method of using a multiple horn feed design for each beam appears to be a better approach. This approach also needs the development of compact horns and low loss feed networks to create proper amplitude and phase distributions of the horn array. Another technique of achieving good spatial isolation is to use endfire feeds of highly directive elements such as helical antennas.

A better polarization isolation will improve channel isolation for a frequency reuse system, since the orthogonally polarized beams will have low interference.

The polarization purity is expected to be improved by using grid sub-reflectors and/or grid main reflector. It is pertinent to establish the degree of cross polarization of the grid reflectors to aid in the system design.

When feed horns shared by both the transmit (downlink) and receive (uplink) signals are optimized at the transmit frequency band the uplink beam generally suffers reduction in antenna gain efficiency. In order to improve the efficiency the shared aperture grid reflector system shown in Figure 2-15 has been developed for 12/14 GHz applications. The front reflector may be made to be transparent to vertically polarized waves while it is opaque to horizontally polarized wave, or vice versa. The wave that passes through the front reflector is reflected from the back reflector and re-radiated passing through the front reflector once more. The wave will suffer some loss for passing through the front reflector twice. The focal points of the two reflectors do not coincide; therefore, separate feeds can be used and optimized for each frequency application.

Another way of separating the transmitting and receiving feeds is by using a dichroic plate which can be made to be almost transparent at one frequency and opaque at the other frequency band.

For direct user application where the beams are closely spaced, feed dimensions become a critical packing factor. A highly directive radiating element with physically small aperture is needed for the feed array. A high directivity also helps reduce mutual coupling among the feeds.

Evaluation of thermal distortion of antenna system of the proposed dimensions is essential to ascertain proper beam positioning. Research in this area involves evaluation of thermal characteristics of graphite constructed support structure, reflectors and subreflectors. The honeycomb Kevlar resin structure presently has a coefficient of thermal expansion of 3×10^{-6} in/in/^{o}F. It is desirable that this coefficient be orders of magnitude lower to further reduce any thermal distortion. Such a technology may be developed by using advanced composite materials with low resin.

The above discussions are summarized in Table 6-1.

TABLE 6-1 MULTIPLE BEAM ANTENNA TECHNOLOGY

TOPIC	APPROACHES
SCAN LOSS REDUCTION	o SUBREFLECTOR AND REFLECTOR SHAPING (BIFOCAL TECHNIQUE)
	o PHASE ERROR COMPENSATION VIA MULTIPLE HORN FEED FOR EACH BEAM (POTENTIAL FEED PACKAGE PROBLEMS)
HIGHER SPATIAL BEAM ISOLATION	o HIGH DIRECTIVITY FEEDS (ENDFIRE AIDED DESIGNS)
HIGHER POLARIZATION ISOLATION	o GRID SUBREFLECTOR
	o GRID REFLECTOR (POTENTIAL THERMAL DISTORTION PROBLEMS)
HIGHER UPLINK EFFICIENCY	o SHARED APERTURE GRID REFLECTOR (SEPARATE TRANSMIT AND RECEIVE FEEDS)
	o CONSTANT BEAMWIDTH FEED OVER BOTH BANDS
	o DICHROIC PLATES TO SEPARATE TRANSMIT AND RECEIVE FEEDS (POTENTIAL FEED PACKAGE PROBLEMS)
FEED PACKAGING	o PHYSICALLY SMALL HIGH DIRECTIVITY FEEDS (ENDFIRE DESIGNS)
THERMAL DISTORTION	o GRAPHITE CONSTRUCTION OF SUPPORT STRUCTURE, REFLECTOR, AND SUBREFLECTOR
	o DEVELOPE RESIN SYSTEM FOR KEVLAR WITH LOW THERMAL COEFFICIENT OF EXPANSION $\lesssim 0$, CURRENT TECHNOLOGY = 2 (REQUIRED FOR GRID REFLECTORS)

7.0 DIRECT USER ANTENNAS

7.1 INTRODUCTION

Direct to user antennas in a 18/30 GHz satellite system will be used to generate contiguous pencil beams which can cover the entire U.S. continent. A scenerio with forty pencil beams covering the U.S. is shown in Figure 7-1. The crossover levels of adjacent beams shall be 3 dB or less for both downlink (20 GHz) and uplink (30 GHz) frequency bands.

One purpose of studying direct to user antenna systems is to assess the minimum number of required frequency channels to achieve a reasonable isolation between individual beams (using polarization diversity in a frequency channel is considered as utilizing two frequency channels in this study). Another purpose of this study is to assess the minimum number of antennas needed to pack the feed horns. Investigations have been done for various scenerios, including 9 beam, 18 beam, 31 beam and 40 beam systems.

The beamwidth of each beam is determined graphically for each scenerio. Then the size of the antenna reflectors which generate such a beamwidth is calculated. In order to create the same beamwidth for both 20 GHz and 30 GHz bands, frequency selective surfaces (FSS) are incorporated in the design of the reflector surfaces. Details of this design will be discussed later in this chapter.

The size of feed horns is determined by the desired edge taper on the aperture distribution. In this study, the aperture field is modeled by a simple distribution of $(1-r^2)$ on a 10 dB pedestal. One of the reasons of choosing this distribution is that the corresponding far field pattern of this distribution can be expressed in a closed form. Therefore a minimum computation effort is needed to obtain the far-field pattern.

The number of antennas required to pack the feed horns can then be determined from the size of feed horns. The number of frequency channels is assessed using the sidelobe information and the C/I criteria.

7.2 ANTENNA CONFIGURATION

Frequency selective surfaces (FSS)[12, 13, 14] also known as dichoric surfaces are surfaces that are almost transparent at a frequency band and opaque at another.

The two proposed antenna systems are illustrated in Figures 7-2 and 7-3. Basically they are front-fed offset paraboloids. In the first system shown in Figure 7-2 there is only one set of horns which will be used for both receiving and transmitting. The outer annular ring of the reflector indicated by the cross-hatch area is a FSS which is transparent at 30 GHz and opaque at 20 GHz. The aperture sizes in terms of the wavelengths at these two frequency bands are the same. Therefore the far-field beam-widths will be almost identical. The horns will be optimized at the 20 GHz band. The performance of the system at the 30 GHz bands are in general, not optimal. It is generally true that a larger F/D value gives a better off-axis performance. The F/D of this system is chosen to be ~ 1 at 20 GHz and ~ 1.5 at 30 GHz.

In the second system shown in Figure 7-3, there are two frequency selective surfaces. The cross-hatched crescent area in the main reflector, similar to the dichroic region shown in Figure 7-2, is also transparent at the 30 GHz band and opaque at the 20 GHz band. The aperture size in terms of wavelengths are the same at both frequency bands. Hence the beamwidths at these two frequency bands are identical. The subreflector, a frequency selective plate which is transparent at 20 GHz and opaque at 30 GHz, separates the signals at the 20 GHz band from those at the 30 GHz band spatially. The subreflector guides the signals at the two frequency bands into two separate sets of feed horns which can be optimized independently. The system is a Cassegrain system at 30 GHz and a front fed system at 20 GHz.

The configurations of far field beams for systems with various frequency channels are shown in Figure 7-4. Different beam hash marks indicate various frequency channels. Two different hash marks could also represent the channels of the same frequency but with different polarizations.

7.3 RESULTS AND DISCUSSIONS

The following assumptions are made in this study.

1. The circular aperture field distribution is assumed to be symmetrical in the angular direction and the distribution in the radial direction is modeled by

$$f(r)=0.316 + 0.684\ (1-r^2) \qquad (1)$$

where

$$r = \rho/a$$

a is the radius of the aperture

The far field distribution can be expressed in a closed form as

$$g(U) \propto 0.316 \frac{J_1(U)}{U} + 0.648 \frac{J_2(U)}{U^2} \qquad (2)$$

where

$U = k a \sin \theta$

θ is the angular displacement from the boresight

$g(U)$ is plotted in Figure 7-5. The first sidelobe is about -20.7 dB. This is an approximate model believed to be adequate for this study.

2. The absolute gains are obtained by assuming a 55% aperture efficiency. This assumption is reasonable for offset fed paraboloids.

3. It is assumed that the off-axis gain loss is negligible. When the beam is positioned from boresight by a few beamwidths, the off-axis gain loss of a paraboloid with $f/D \geq 1$ is small. Even in the 40 beam scenario, the outermost beam is positioned only about four beamwidths from the boresight. The maximum gain loss is about 1.2 dB, within the uncertainity of the field distribution model. Therefore the off-axis gain loss has not been taken into account in this study.

4. The beam deviation factor is assumed to be unity. For paraboloid with $F/D \sim 1$, this is a very good approximation.[14]

The flow chart in which the procedures of assessing the systems are summarized is shown in Figure 7-6. The results are summarized in Table 7-1.

It is noted that the C/I value decreases as the number of pencil beams increase for a given number of frequency channels. The C/I value improves as more of the frequency channels are utilized. The 20.7 dB C/I value appears to be a performance limit for 18 beam, 31 beam and 40 beam systems. This is because the first sidelobe of each beam is -20.7 dB. Only when the beams sharing the same frequency channel are separated spatially by at least 3 beamwidths will the C/I value exceed 20.7 dB limit. For a 9 beam system the spacing between beams sharing the same frequency channel becomes more than 3 beamwidths when more than 4 frequency channels are incorporated. Therefore the C/I value becomes better.

The limiting C/I value can be improved by using heavier taper on the aperture distribution. Using a 30 dB taper, the limiting C/I value will become about 24 dB, more than 3 dB better than that of a system with a 10 dB tapered aperture distribution. However the aperture efficiency will become lower. The detailed tradeoffs between using 10 dB tapered and 30 dB tapered aperture distributions remain to be answered.

The sizes of feed horns for the 20 and 30 GHz bands turn out to be almost identical. Because of the difference in the effective areas of the main reflector for the 20 GHz and 30 GHz bands, the subtended angle from the feed position to the edges of the reflecting area for the 20 GHz is about 1.5 times of that for the 30 GHz band. This effect counter balances the

difference of the size of a feed horn in terms of wavelengths in the two frequency bands. Thus the same taper is achieved on the respective edges of the reflector at both 20 GHz and 30 GHz with only one size of feed horn so that the optimal size of feed horns in one frequency band, say 20 GHz, is also the optimal performance at 30 GHz. Thus the configuration is Figure 7-2 appears to be an attractive option for the direct to user antenna system.

The size of a feed horn for both 20 and 30 GHz to create a 10 dB taper on the reflector is about 1.75"x2.50". Assuming the beam deviation factor (BDF) on both azimuth and elevation directions to be unity, the lateral displacements on the feed positions to steer the beams to the prescribed directions can be calculated. The separation between adjacent horns must be greater than the dimension of the horns. Otherwise, the horns physically interfere. A minimum number of 5 antennas is needed to pack the feed horns for all the systems. The antenna size for a 9-beam system is small (about 22" in diameter for 20 GHz and 15" for 30 GHz) in comparison with the size of antennas for a 40-beam system. There is less available space to pack the horns in the 9 beam system than that in the 40 beam system. That is why even the number of beams is small in the 9 beam system, 5 antennas are still needed to pack the feed horns.

When partially dielectrically loaded horns are used, less antennas are needed to pack the horns. The partially loaded horns with smaller dimension can produce almost the same illumination taper on the

reflector. The detailed performance of these horns can be determined in the future when a more accurate assessment is needed.

Another scheme to improve the C/I performance for the transmission band (20 GHz) can be done by sacrificing the simplicity and the radiation power. This basically is a sidelobe cancellation scheme. Each horn serves as the main radiator of a far-field beam and also as an auxiliary radiator for nearby beams. In other words, each horn radiates not only the energy designated to a corresponding far field region but also the energy which would have spilled over to the far field region by other nearby horns. Thus as far as each far field beam is concerned, it is produced by a cluster of horns with a proper combination of phases and amplitudes and has very low sidelobes. The C/I can be improved tremendously. However, the configuration shown in Figure 7-3 has to be utilized to separate the transmitting and receiving feed networks from one another.

The major problem of this scheme is the design in the feed network. Proper phase shift and amplitude adjustment can be done with hybrids in the RF portion of the transmitter. Since only one output arm of each hybrid will be used in each combination of two signals the energy flow through the other arm is lost completely. Thus a tremendous loss (at least 3 dB in the main signal) is inherent in this design. However there is no reason not to combine the signal in the IF portion of the circuitry. More studies are needed to assess this scheme.

7.4 CONCLUSIONS

The following conclusions are drawn from this portion of the study:

1. Using 4 frequency channels in the design of a direct user antenna system can achieve a greater than 20 dB C/I value in the scenerios considered here. In order to further improve the C/I performance, the heavier tapered (greater than 30 dB) aperture distributions are desired. This implies that larger horns and hence more antennas are needed. Forthermore, a scheme of using clusters of horns to cancel sidelobes has been proposed. That scheme might be able to improve the C/I value in both the transmission and the receiving bands. More detailed studies of this scheme are needed to assess this possibility.

2. Five antennas are adequate to pack the feed horns in the scenerios of of interest. In order to use less antennas, the partially dielectrically loaded horns will be used in the design. Detailed performance of these horns will be assessed in the future, when a more accurate assessment becomes necessary.

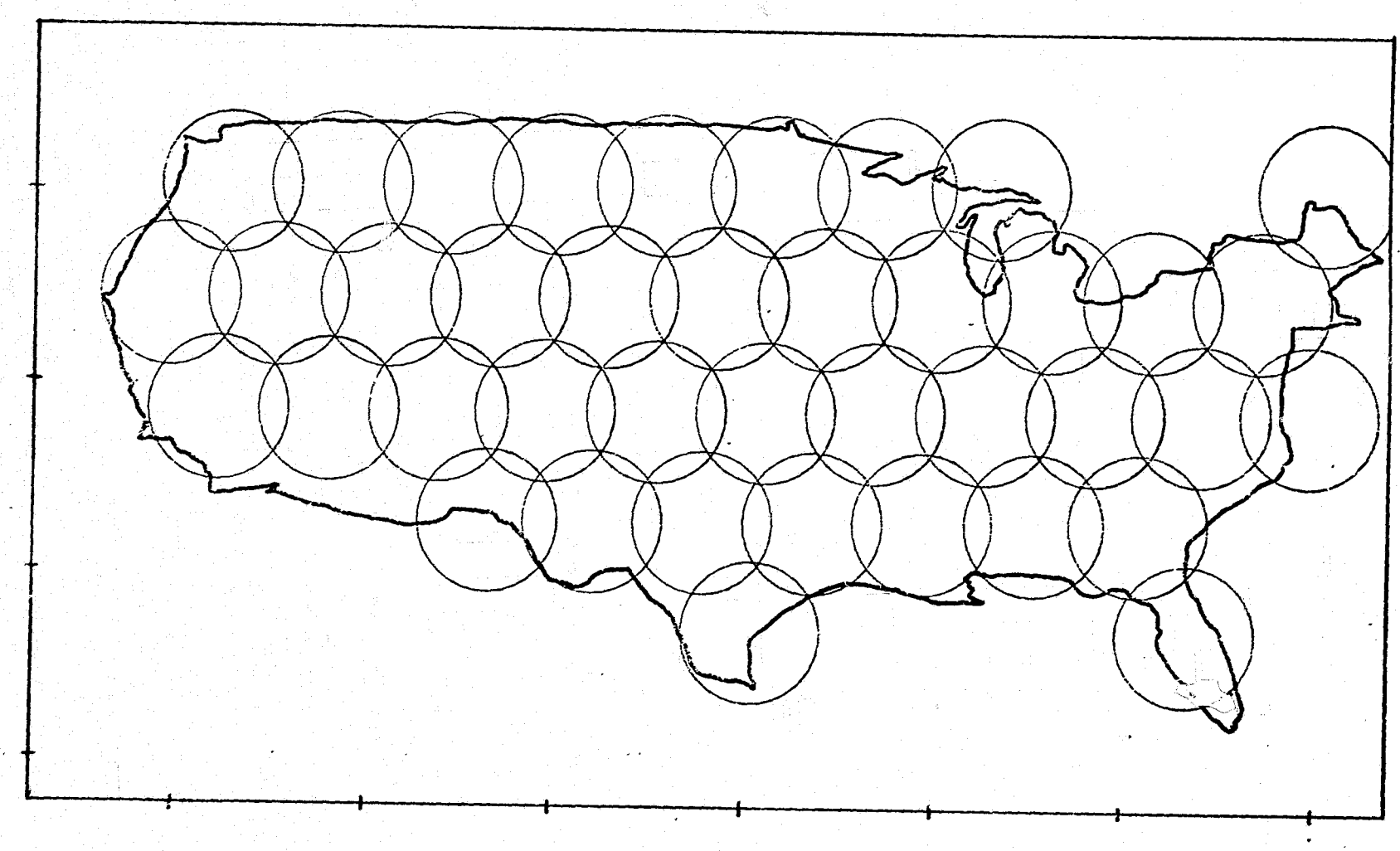

FIGURE 7-1 Forty pencil beams covering the continental United States. The synchronous-orbiting satellite is located at 100°W longitude. The circles represent the 3 dB contours for various beams. The crossover levels for adjacent beams are 3 dB or less.

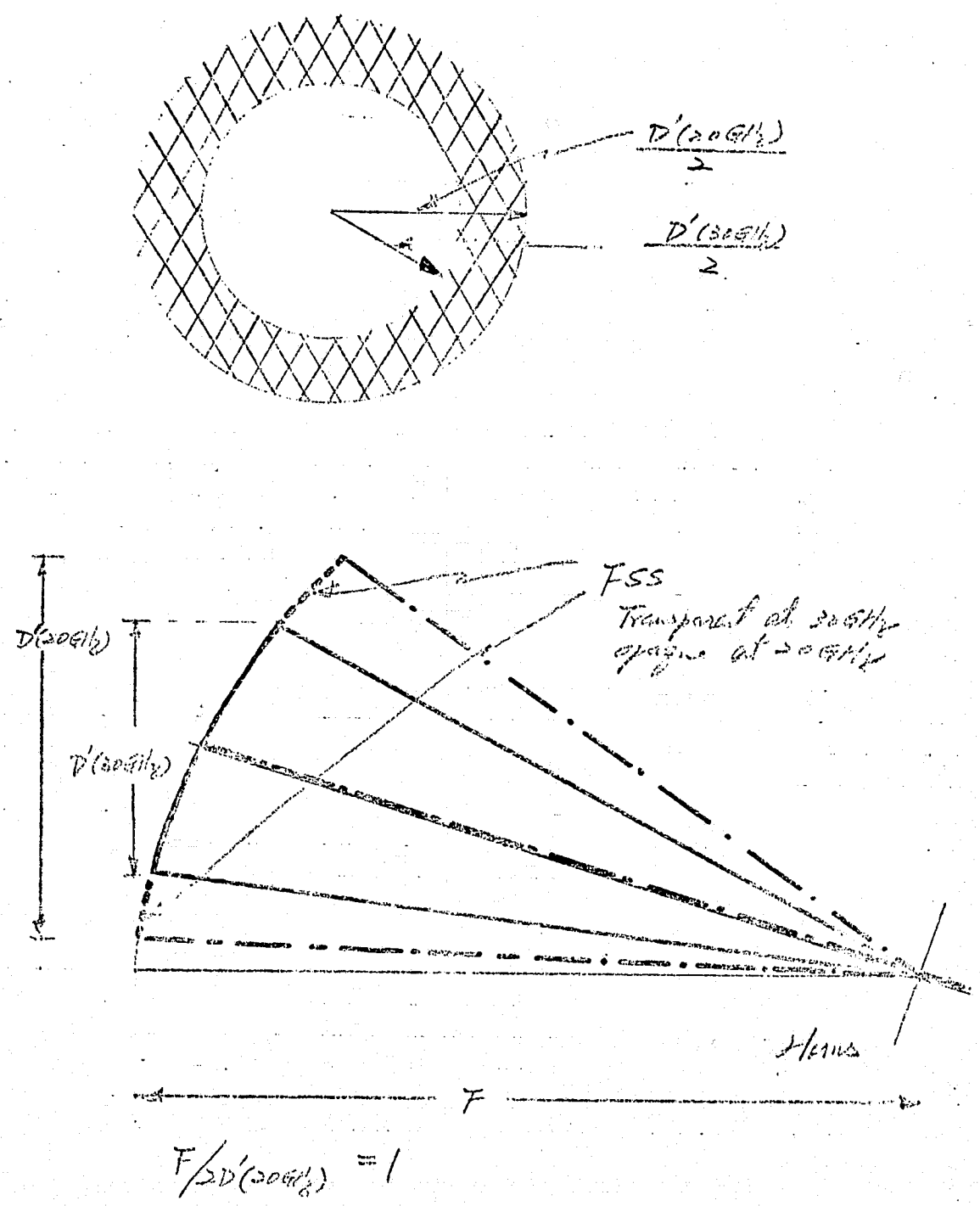

FIGURE 7-2 Antenna system configuration with one set of feed horns. The frequency selective surfaces (FSS's) are indicated by the thatched areas.

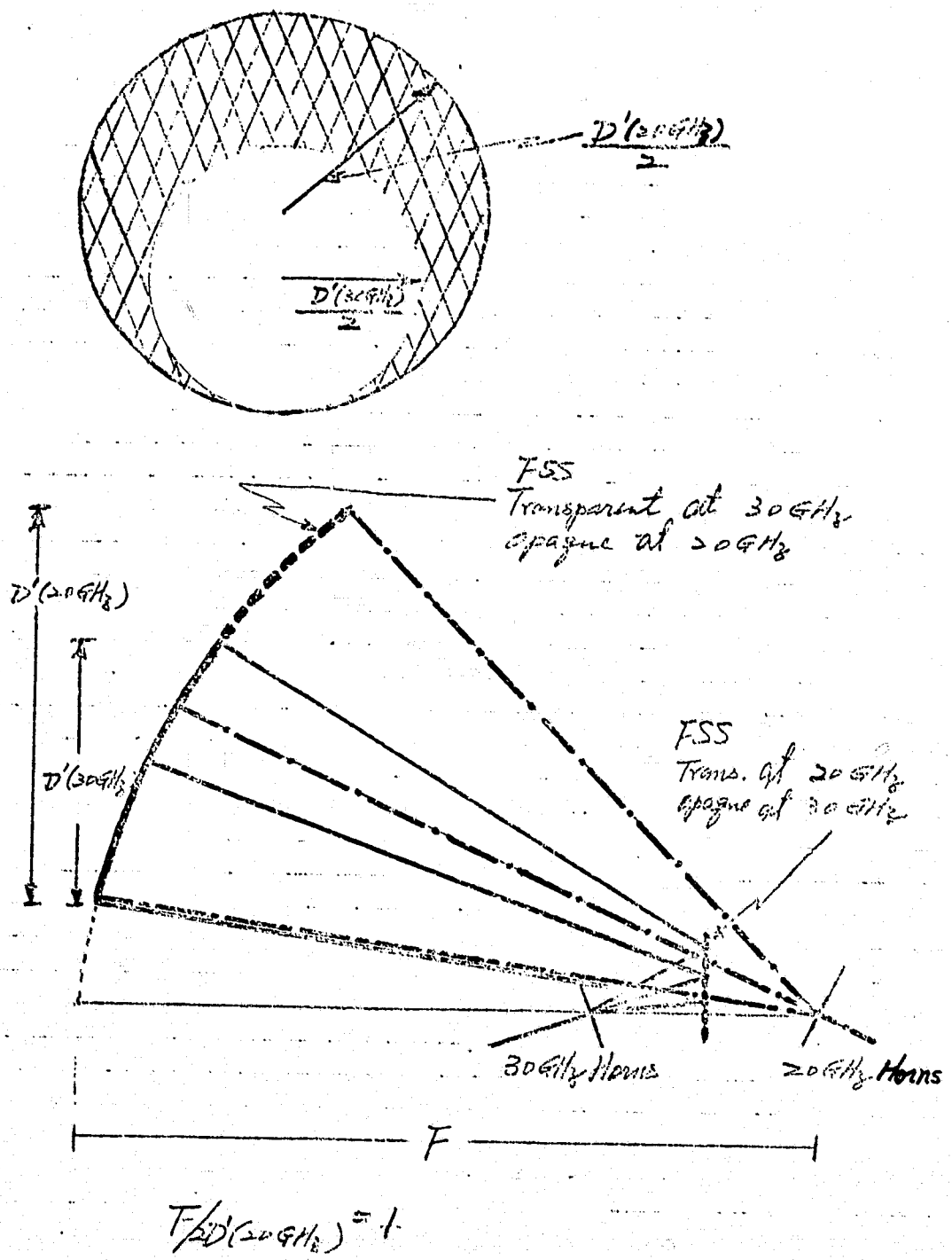

FIGURE 7-3 Antenna system configuration with separated transmitting and receiving feed horns. Two different FSS's are incorporated in this design.

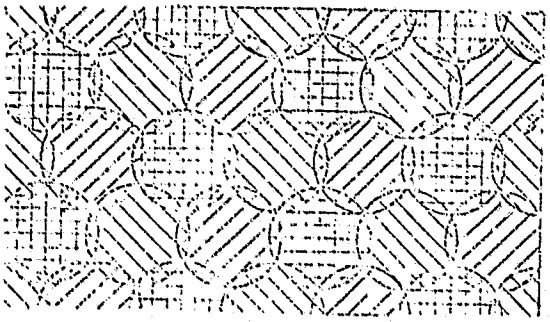

(a)

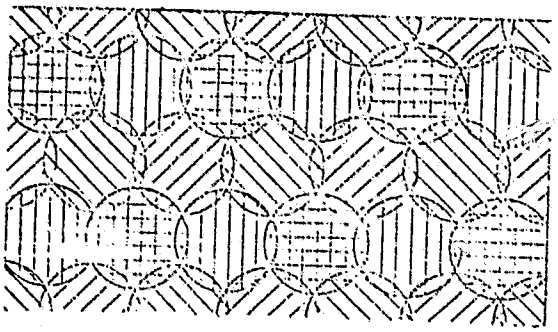

(b)

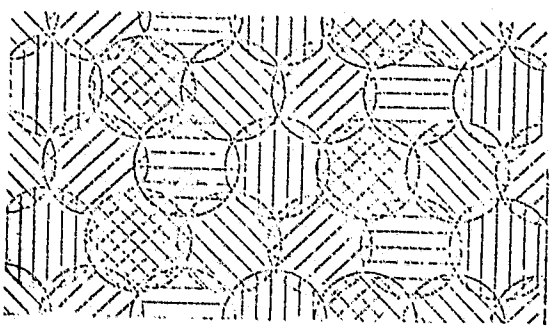

(c)

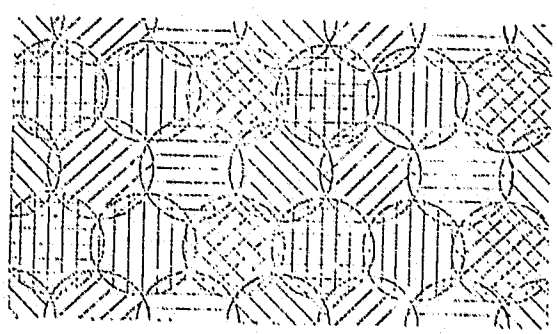

(d)

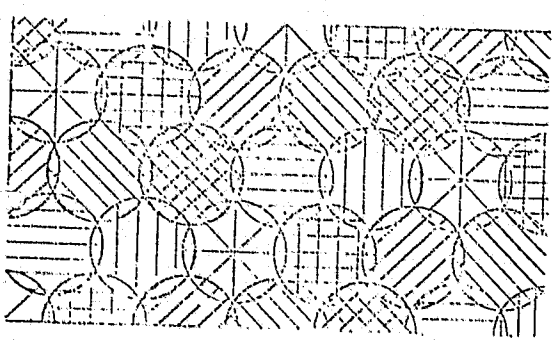

(e)

FIGURE 7-4 Configurations for various numbers of frequency reused beams a) 3-frequency b) 4-frequency, c) 5-frequency d) 6-frequency and e) 7-frequency reused system

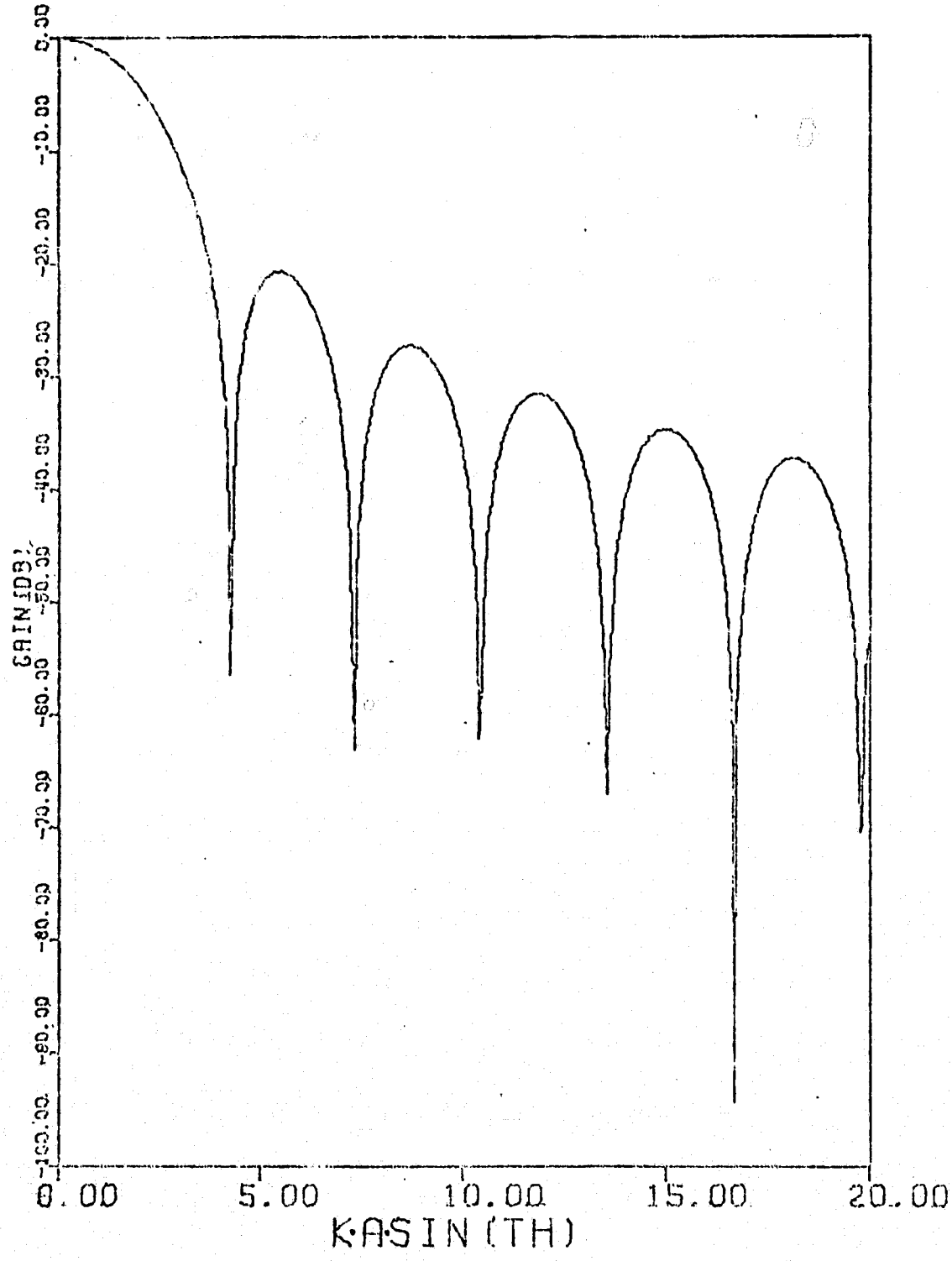

FIGURE 7-5 Far field pattern for the aperture distribution of $f(r)=0.316+0.684(1-r^2)$. K is the wave number A is the radius of the aperture, and θ is the angle away from the boresight.

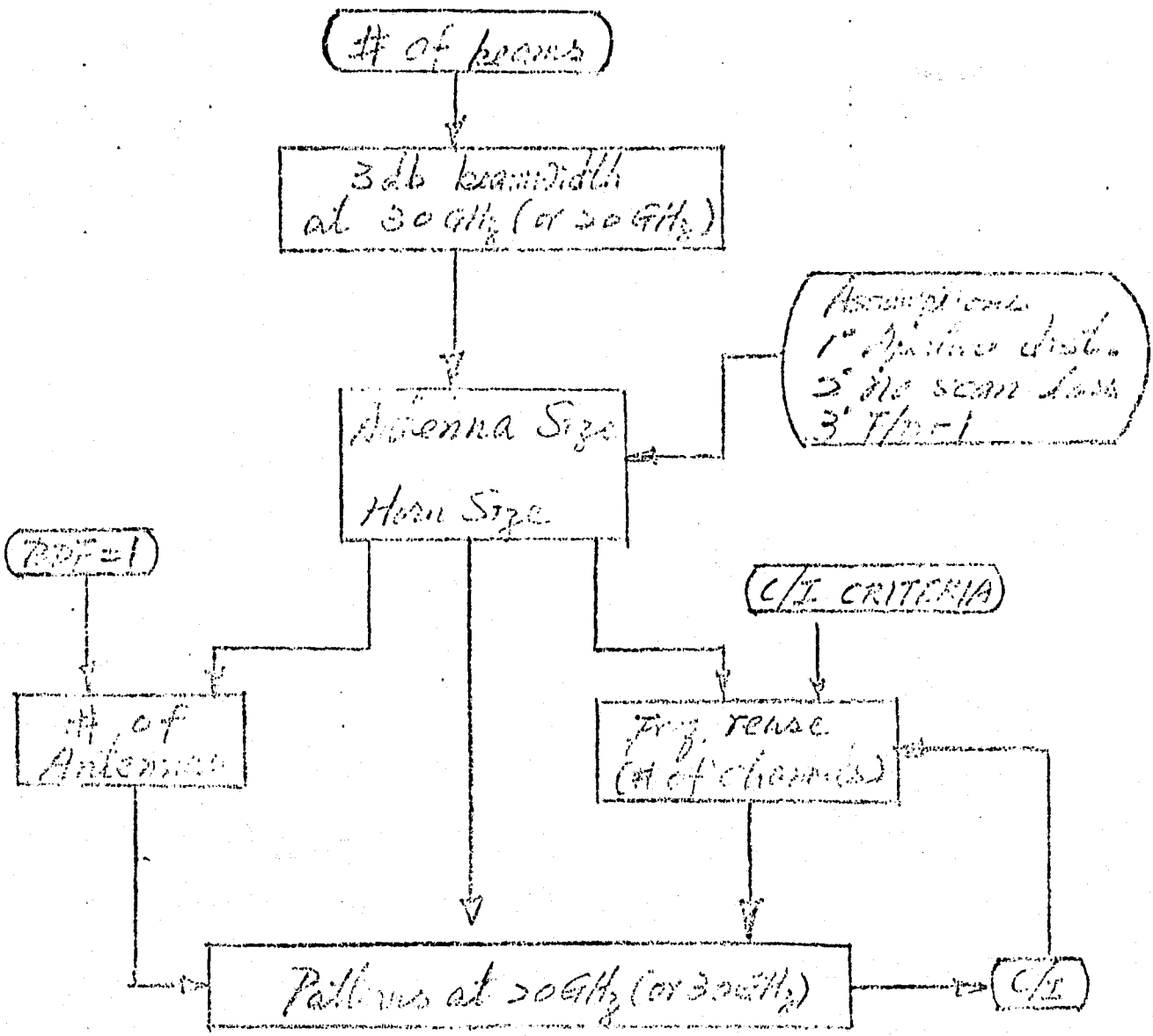

FIGURE 7-6 Flow chart of this investigation

	9-beam	18-beam	31-beam	40-beam
D' (20 GHz)	22.2"	31.4"	42"	50"
D' (30 GHz)	14.8"	20.9"	28"	34"
η	55%	55%	55%	55%
$\frac{\pi D'}{\lambda} = Ka$	118	167	222.82	267.4
Gain (db)	38.8	41.9	44.4	46
Beamwidth ($2\Delta\theta_{3db}$)	1.7°	1.21°	0.9°	0.75°
C/I (worst) 3-freq	+14.7 db	+14.2 db	+12.4 db	+10.5 db
C/I (worst) 4-freq	+20.7 db	+20.7 db	+20.4 db	+20.4 db
C/I (worst) 5-freq	+22 db	+20.7 db	+20.7 db	+20.4 db
C/I (worst) 6-freq	+27.3 db	+20.7 db	+20.7 db	+20.4 db
C/I (worst) 7-freq	—	—	—	+20.7 db
Horn size	1.75"x2.5"	1.75"x2.5"	1.75"x2.5"	1.75"x2.5"
F/D (20 GHz)	1	1	1	1
F/D (30 GHz)	1.5	1.5	1.5	1.5
# of Antennas	5	5	5	5

TABLE 7-1 Results of this investigation. The absolute gains are calculated by using the assumption of 55% aperture efficiency.

8.0 CONCLUSION:

For the 18/30 GHz multiple spot beam antenna, it is necessary to use a system utilizing both the beam spatial isolation and polarization isolation techniques in order to keep the antenna to a practical size of 6 to 14 foot diameters. The analysis included three prime-fed reflectors, two folded optics reflector and two lens antennas. In general, a large diameter antenna improved the carrier to interference (C/I) ratio and a large focal length to diameter ratio (f/D) reduced scan loss.

Of the antennas studied, the lens antennas have superior scan performance; however, the dielectric lens was not chosen because it has potential material deterioration in space environments and has not been tested thoroughly for space applications. The waveguide lens was rejected as a baseline antenna because it is a relatively narrowband device and it would be heavier and more costly than a reflector system.

The baseline antenna chosen was a 14 foot diameter Cassegrain antenna of the folded optics reflector type. This antenna has better performance characteristics than the prime-fed reflectors since a larger effective f/D ratio can be obtained. The scan loss up to 3 degrees for 18 and 30 GHz is 0.7 dB and 1.7 dB respectively. At 4 degree scan, the loss increases significantly to 2.4 dB at 18 GHz and 3.1 dB at 30 GHz. Analysis of the C/I performance of this baseline antenna is left for the next study along with depolarization characteristics.

Preliminary investigation of the offset double reflector parabolic torus indicates that it may have comparable performance characteristics as the Cassegrain antenna. Due to lack of analytical software, comparative data could not be obtained to make its selection for the baseline antenna.

REFERENCES:

1. F.A. Taormina, D.K. McCarty, T.A. Crail and D.T. Nakatani "Intelsat IV Communications Antenna Frequency Reuse Through Spatial Isolation," ICC Conference Record, Vol. 1, Philadelphia, June 1976 pages 4 thru 10 to 4 thru 14.

2. D.T. Nakatani and G.G. Kuhn "COMSTAR I Antenna System," Int. Symposium Digest A&P Society, Stanford University, Jan 1977, pages 337 thru 340.

3. F.A. Jenkins and H.E. White, "Fundamentals of Optics," 3rd Edition, New York: McGraw-Hill, 1957 pages 154 thru 157.

4. Li, T.A., "A Study of Spherical Reflectors as Wide-Angle Scanning Antennas," IEEE Trans. on Antennas and Propagation, July, 1959.

5. Hyde, G., R.W. Krental, and L.V. Smith "The Unattended Earth Terminal Multiple-Beam Torus Antenna," Comsat Tech. Rev., Vol 4, 2, Fall, 1974.

6. P.S. Bains and F.A. Taormina, "SBS Antenna System," Int. Symposium, June 1979.

7. W.C. Wong, "On the Equivalent Parabola Technique to Predice the Performance Characteristics of a Cassegrainian System with an Offset Feed," IEEE Trans. on Antennas and Propagation, Mg 1973,

8. Young, F. "Gregorian-Corrected Toroidal Scanning Antenna" Ph.D. Thesis, University of Southern California, Los Angeles, Ca July, 1978.

9. C.B. Coulbourn, Jr. "Increased Bandwidth Waveguide Lens Antenna," Aerospace Corp. Report TOR-0076 (6403-01)-3, Dec 8, 1975.

10. J.S. Ajioka and V.S. Ramsey, "An Equal Group Delay Waveguide Lens," IEEE, Trans. Antennas Propagation, Vol AP-26, No. 4, pages 519-527, July 1978.

11. Dragone, C. and M.J. Gans, "Imageing Reflector Arrangements To Form a Scaning Beam Using a Small Array," Vol 58, No. 2, February 1979.

12. Arnaud, J.A. and F.A. Pelow, "Resonant-Grid Quasi-Optical Diplexers," The Bell System Technical Journal Vol. 54, No.2, February 1975.

13. Anderson, I., "On the Theory of Self-Resonant Grid," The Bell System Technical Journal Vol. 54, No. 10, December 1975.

14. Cha, A.G., C.C. Chen, and D.T. Nakatani "An Offset Cassegrainian Reflector Antenna System with a Frequency Selective Subreflector," paper presented at AP-S International Symposium, Univ. of Illinois, Urbana Illinois, June 1975 .

15. Ruze, J., "Lateral-Feed Displacement in a Paraboloid," IEEE Trans. Antennas and Propagation, Vol. AP-13, September 1965.

APPENDIX B.

RAIN ATTENUATION AND DEPOLARIZATION AT 20/30 GHz

By: R. R. Persinger

RAIN ATTENUATION AND DEPOLARIZATION AT 20/30 GHz

INTRODUCTION

Because of the extensive amount of literature available on the many facets of rain attenuation and rain depolarization, this section is included simply to give a perspective on the guideline information used in this study. All rain fade and depolarization margins that are used elsewhere in this document are not specifically derived in this section, but can easily be determined by consulting the various references in question. Although the topic of rain attenuation and depolarization is extensively discussed in the literature, no universal point of view has been established. Thus, the work presented here is an overview and represents no one point of view.

BACKGROUND

The atomsphere affects the propagation of millimeter waves on earth-space paths. Although many different effects may be encountered such as rapid amplitude and angle-of-arrival fluctuations, changes in propagation delay, changes in receiver noise and limitations on the bandwidth of the propagation path, the dominant problem caused by the atmosphere is attenuation and depolarization by rain or ice crystals. Other phenomena may cause attenuation such as absorbtion by oxygen and water vapor and attenuation by fog or clouds but the magnitude of the attenuation caused by these phenomena is considerably smaller than that caused by rain.

The purpose of this section is to present rain fade and depolarization estimates that characterize the system impairment induced by rain at 20 and 30 GHz. In the design of a multiple beam system (one scenario considered) rain fade margin estimates and depolarization degradation levels are required for each city of interest associated with the desired system reliability. As a result of a limited measured data base at 20/30 GHz (both in quantity and location), the system design engineer must rely on predictive techniques in the estimation of rain degradation on system performance. In this section measured data at a few locations will be compared to theoretical predictions, the predictive process will be reviewed, and it will be shown that rain attenuation is the dominant problem at 20/30 GHz rather than rain depolarization for the system design engineer to overcome.

MEASURED ATTENUATION DATA - SINGLE EVENT

The first question to be addressed is the frequency dependence of rain fading and the rather high levels associated with the 20/30 GHz frequency bands. Figures 1a, b, c, d present measured data for a single event occurring on August 9, 1977 measured at Blacksburg, Virginia. Figure 1a is a plot of rain rate in mm/hr plotted as a function of time indicating the severity of a typical summer thunder storm. Note the peak rain rate of 125 mm/hr. Figures 1b, c, d illustrate the signal behavior of the Communications Technology Satellite (12 GHz), COMSTAR D2 satellite (19 GHz), and COMSTAR D2 satellite (28 GHz) during the rain event, respectively.

The 12 GHz beacon has a 15 dB fade coincident with the 125 mm/hr peak rain rate. The associated fade at 6 GHz would be on the order of 3 dB. Looking at the signal level of the 19 GHz beacon, a measured fade in

MEASURED DATA
BLACKSBURG, VA

HUGHES

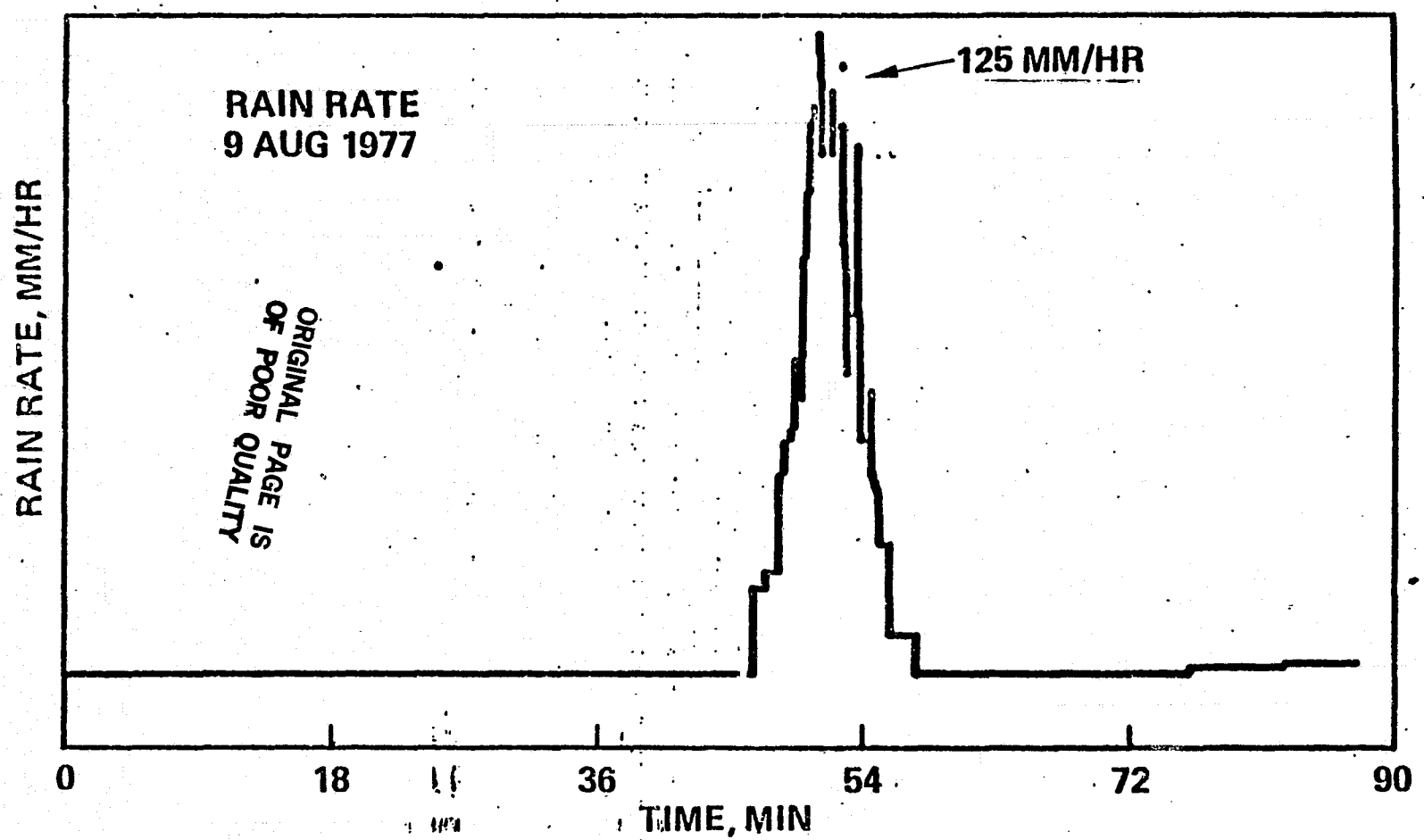

Figure 1a

86776-4

MEASURED DATA
BLACKSBURG, VA

HUGHES

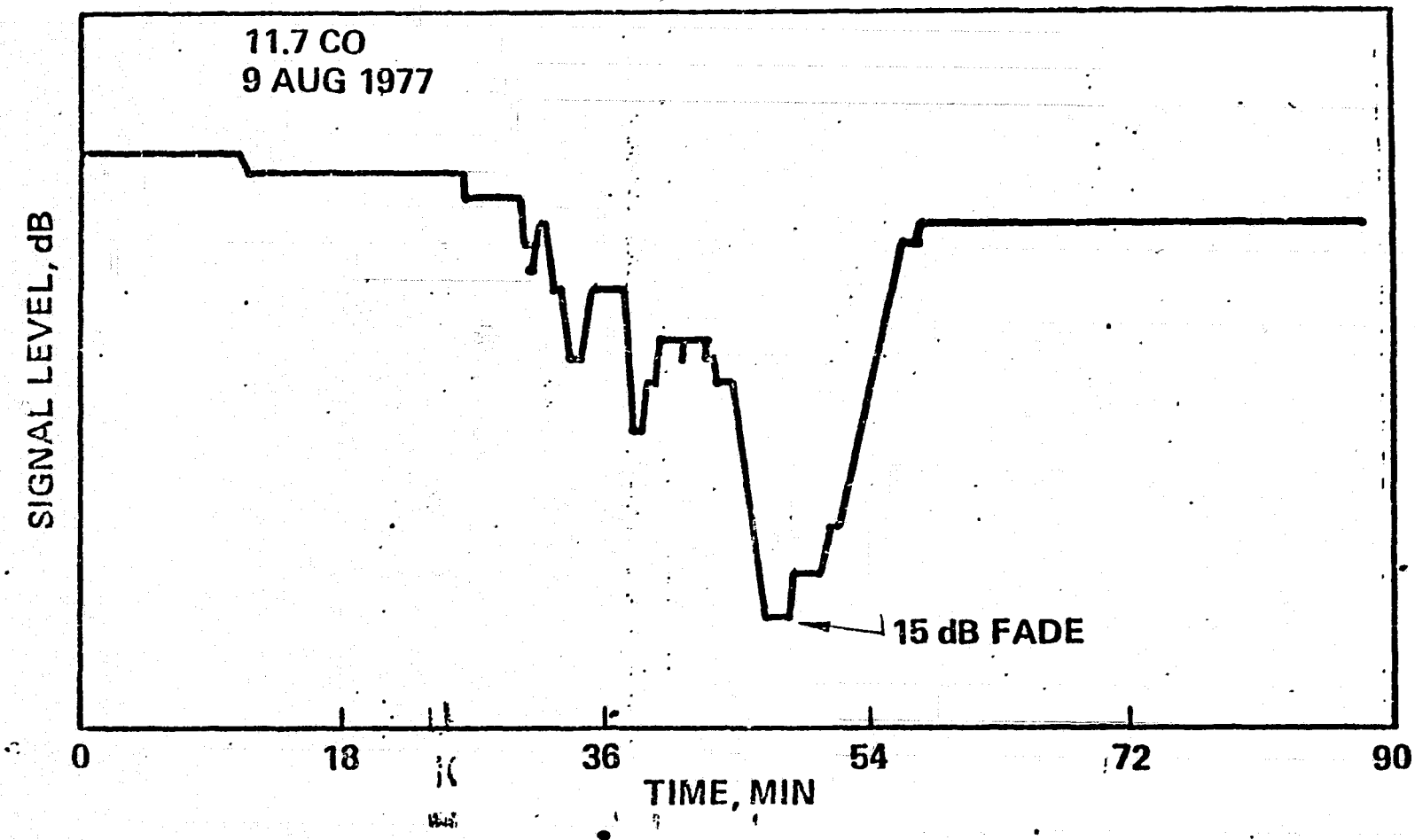

Figure 1b

86776-4X

MEASURED DATA
BLACKSBURG, VA

HUGHES

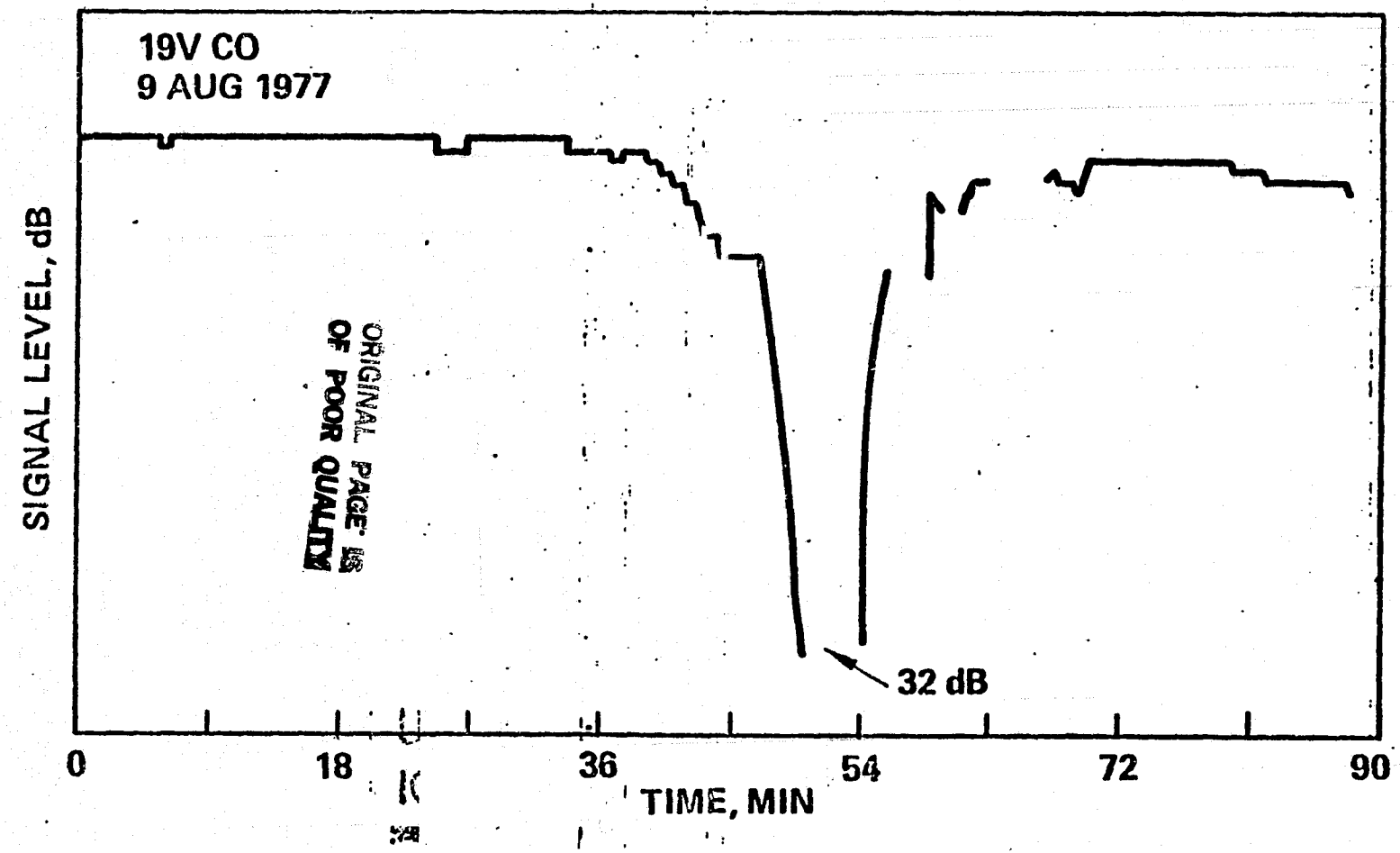

Figure 1c

86776-5

MEASURED DATA
BLACKSBURG, VA

HUGHES

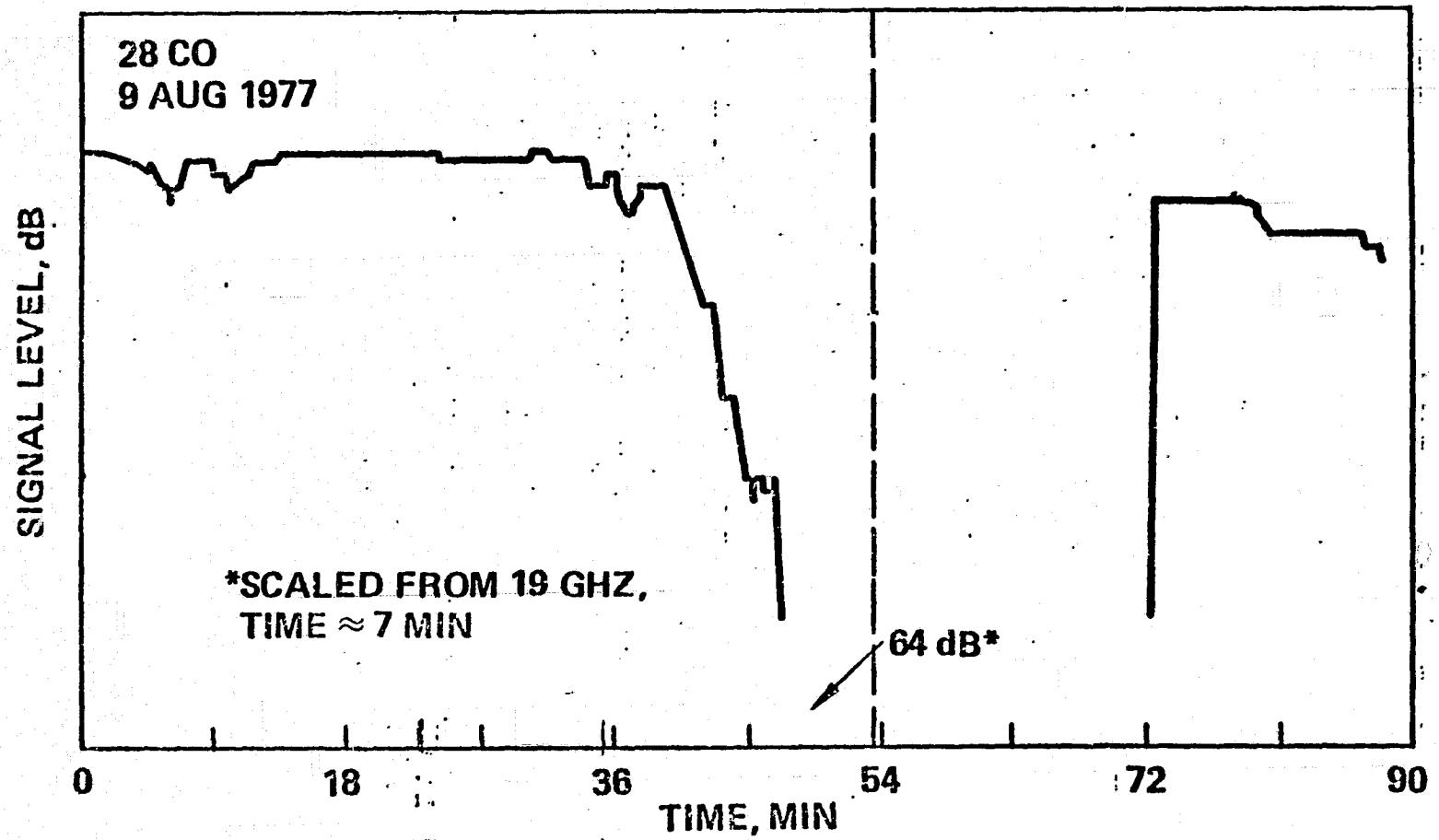

Figure 1d

excess of 32 dB is seen where the phase lock receiver has lost phase lock. Loss of signal is again seen at 28 GHz. Using scaling algorithms (1, 2, 3) and the data at the lower frequencies, a fade in excess of 64 dB is seen for approximately seven (7) minutes indicating the severity of single station fading at 28 GHz.

ATTENUATION STATISTICS - THE PREDICTIVE PROCESS

In order to estimate the required rain fade margin for a communications system with a given reliability, attenuation statistics are needed as illustrated in Figure 2. These single station attenuation statistics were measured by the Blacksburg earth station during the year 1978 for three frequencies, 12, 19 and 28 GHz. As indicated for .01% of the year, an attenuation of 22 dB ror the 28 GHz level and 10 dB ror the 20 GHz level is seen. Also shown in this Figure are theoretical predictions of the Virginia Tech model (1, 2, 3) indicating the ability of predictive models to predict attenuation statistics and rain fade margins. Now that the significance of rain fading at 20 and 30 GHz has been established, predictive modeling on a more global basis can be investigated.

The first step in the predictive process is to estimate the rain statistics for each city of interest. This can be achieved with the use of the Rice-Holmberg rain rate model(4). The Rice-Holmberg model was chosen over the CCIR model (5) in that for each city of interest the rain rate statistics can be expressed directly in terms of annual rain accumulation data which

MEASURED ATTENUATION STATISTICS*
(BLACKSBURG, VA)

HUGHES

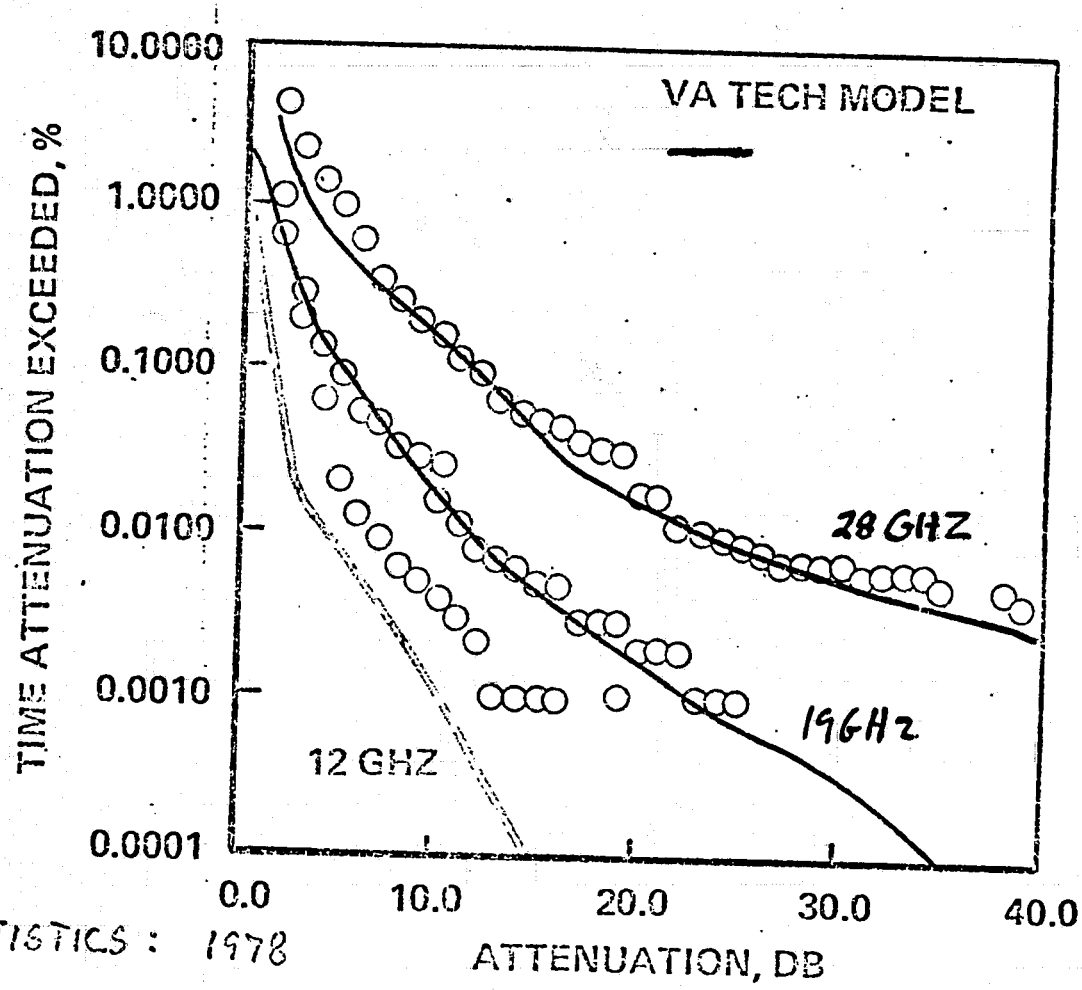

* ANNUAL STATISTICS : 1978

Figure 2

are readily available for each city. The Rice-Holmberg rain rate model is an empirical relation based on 50 years of measured rain statistics. The relation is an exponential expression relating total rain accumulation in MM to the percent of time that a given value of rain rate is equalled or exceeded (see Figure 3). The rain accumulation is represented by the symbol R_o and β is the thunder storm factor. The thunder storm factor is a ratio of thunder storm rain to normal rain and separates rain types that might occur in the Miami region to those found in Seattle, Washington. For Atlanta, Georgia using the National Weather Bureau to obtain annual rain accummulation data and published β values, annual rain statistics for Atlanta can be estimated using the Rice-Holmberg rain rate model.

To give an idea of the accuracy of the Rice-Holmberg model, in Figure 4 theoretical predictions are compared to measured rain statistics for the year 1978 taken at Blacksburg, Virginia. As can be seen rather good agreement is obtained. Although this is only one comparison, many experimenters have checked the validity of the Rice-Holmberg model and found similar results.

The next step in the predictive process is to transform the rain statistics into attenuation statistics with an attenuation vs. rain rate model. These models are usually based on empirical results and relate ground rain rate to attenuation along a slant path. Of course, this model has to be a function of the system parameters such as frequency, elevation angle, polarization angle and location.

RICE-HOLMBERG RAIN RATE MODEL

$$\% T = R_o \left\{ 0.03\,\beta e^{-0.03R} + 0.2(1-\beta)\left\{ e^{-0.25R} + 1.86e^{-1.63R} \right\} \right\}$$

WHERE R_o = RAIN ACCUMULATION FACTOR

β_i = THUNDERSTORM FACTOR

EXAMPLE:

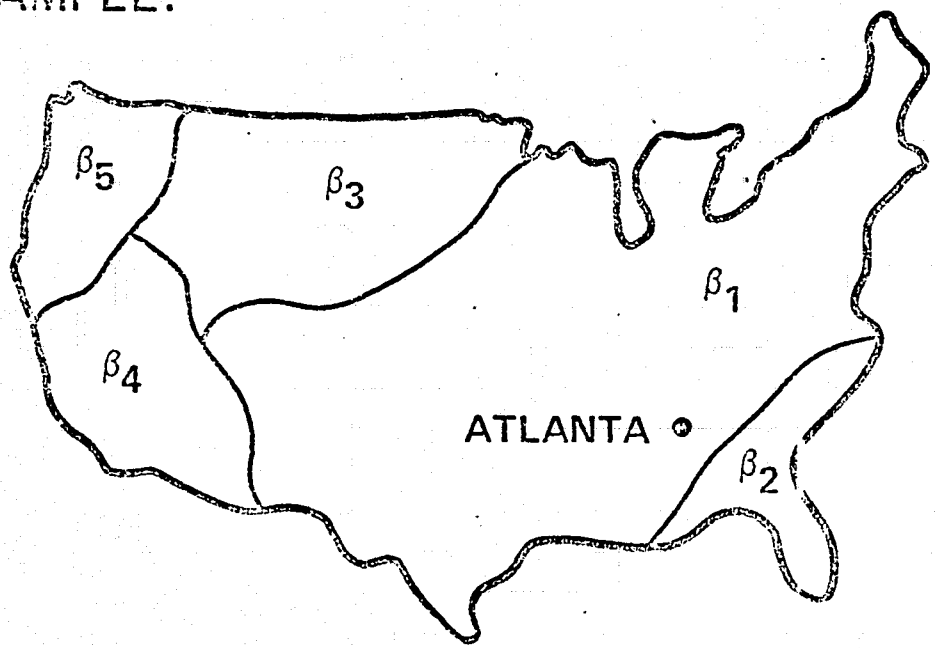

HUGHES

GLOBAL
RAIN STATISTICS

Figure 3

MEASURED RAIN STATISTICS* (BLACKSBURG, VA)

HUGHES

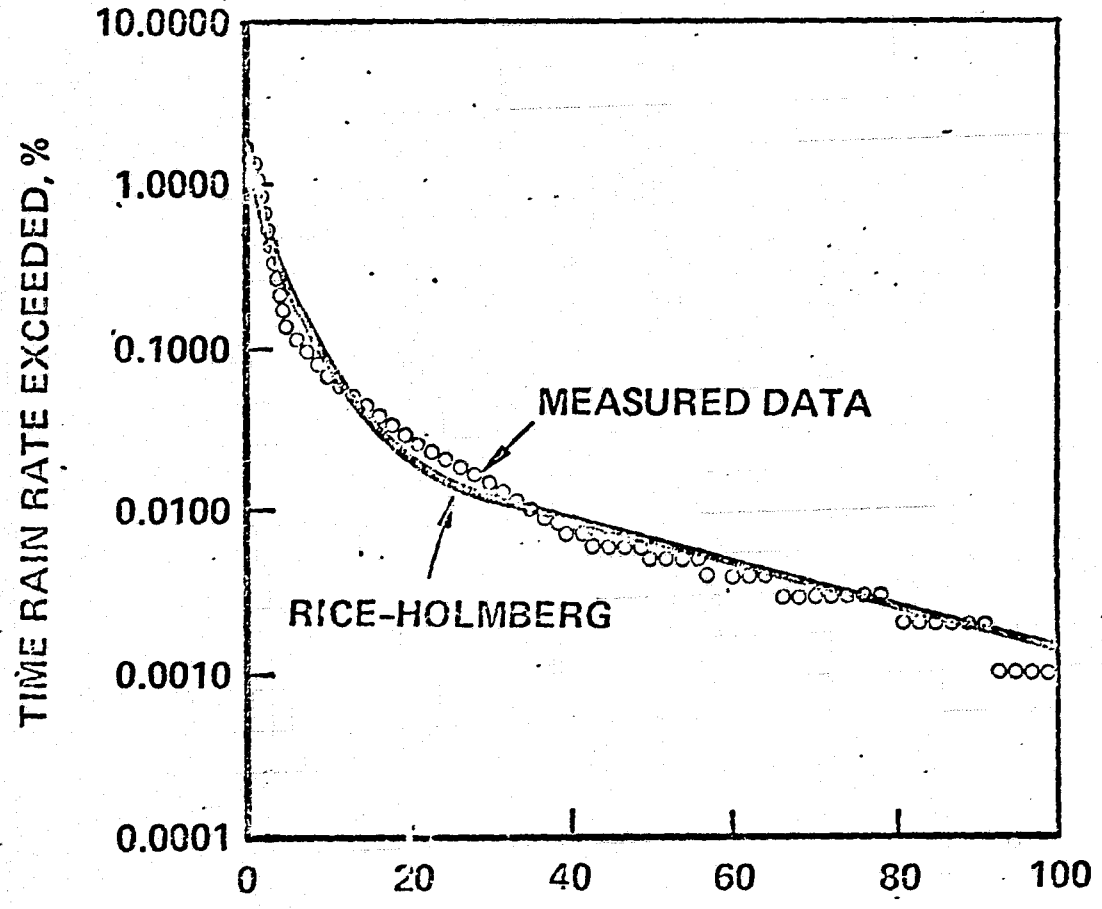

*ANNUAL STATISTICS: 1978

96257-11

Figure 4

Two such models were considered in the HAC study, the CCIR model (5), and the Virginia Tech model (1, 2, 3). Figures 5a, b present the predictions of the two models and the comparison to measured attenuation vs. rain rate data taken at Blacksburg, Virginia using the Comstar D2/D3 spacecrafts during the year 1978. The elevation angle is 44° and the frequencies are 19 GHz and 28 GHz respectively. As can be seen for low rain rates both models agree with the measured data. However, as rain rate increases, the CCIR model begins to deviate in excess of 16 dB for a rain rate of 50 mm/hr.

Comparing the predictions to measured data at another location similar results are seen. Figures 6a, b are plots of measured data taken by Comsat Labs at an elevation angle of 23° and frequencies of 19 GHz and 28 GHz respectively. Note that for the same rain rate, a much higher attenuation is seen as a result of the elevation angle difference when compared to the Blacksburg data. For both locations the 28 GHz attenuation is approximately twice that of the 19 GHz attenuation for the same rain rate [4]. The same trend of the CCIR model predicting excessive fades as compared to the Virginia Tech model was evident in all of the multiple beam predictions. Thus, the system design engineer is faced with a rather significant modeling difference. Very briefly the theoretical reasons for these differences can be examined.

Rain cells of higher rain rates decrease in size as rain rate increases. Thus for higher rain rates, rain on a satellite communications link is very non-uniform. Therefore, this non-uniformity must be accounted for in the attenuation vs. rain rate model. Basically, this is where the two models differ. The proposed CCIR model accounts for this non-

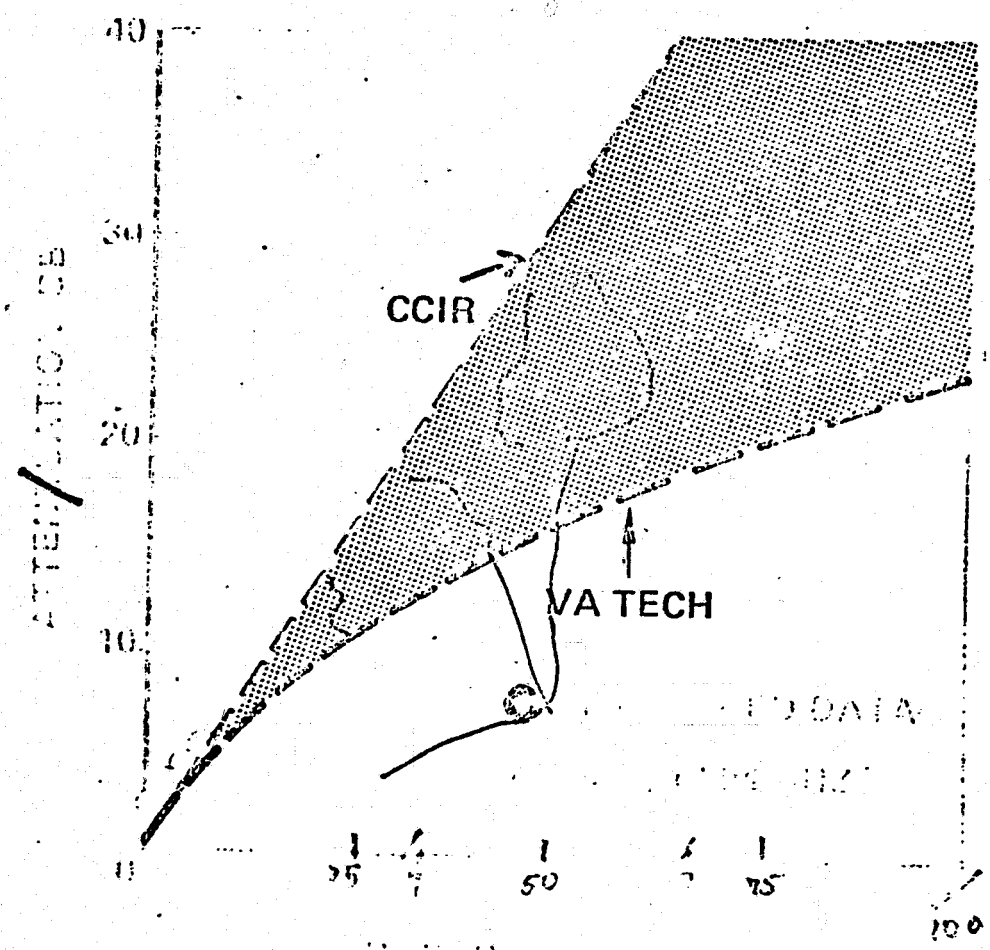

*COMSTAR D 2/
D-3 DATA 1978

FIGURE 5a

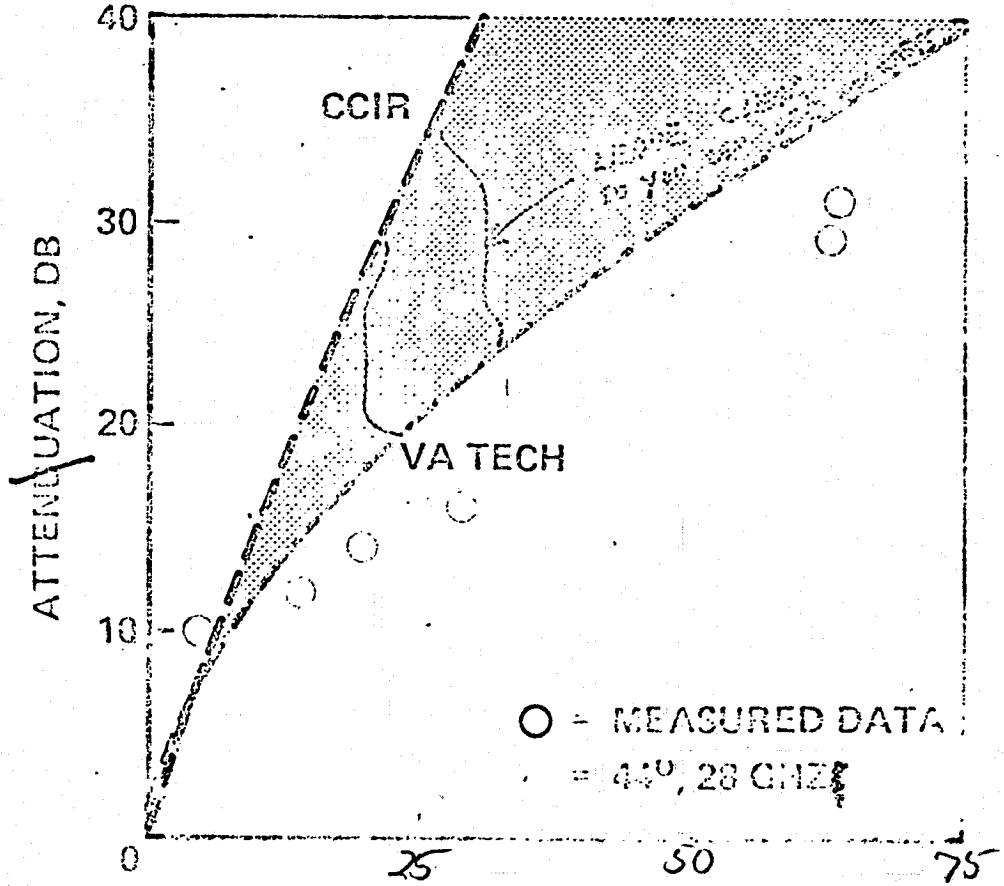

*COMSTAR D-2 DATA: APR, MAY, AND JUN 1978

FIGURE 5b

MEASURED ATTENUATION VS RAIN RATE DATA*
(CLASSIFIED)

HUGHES

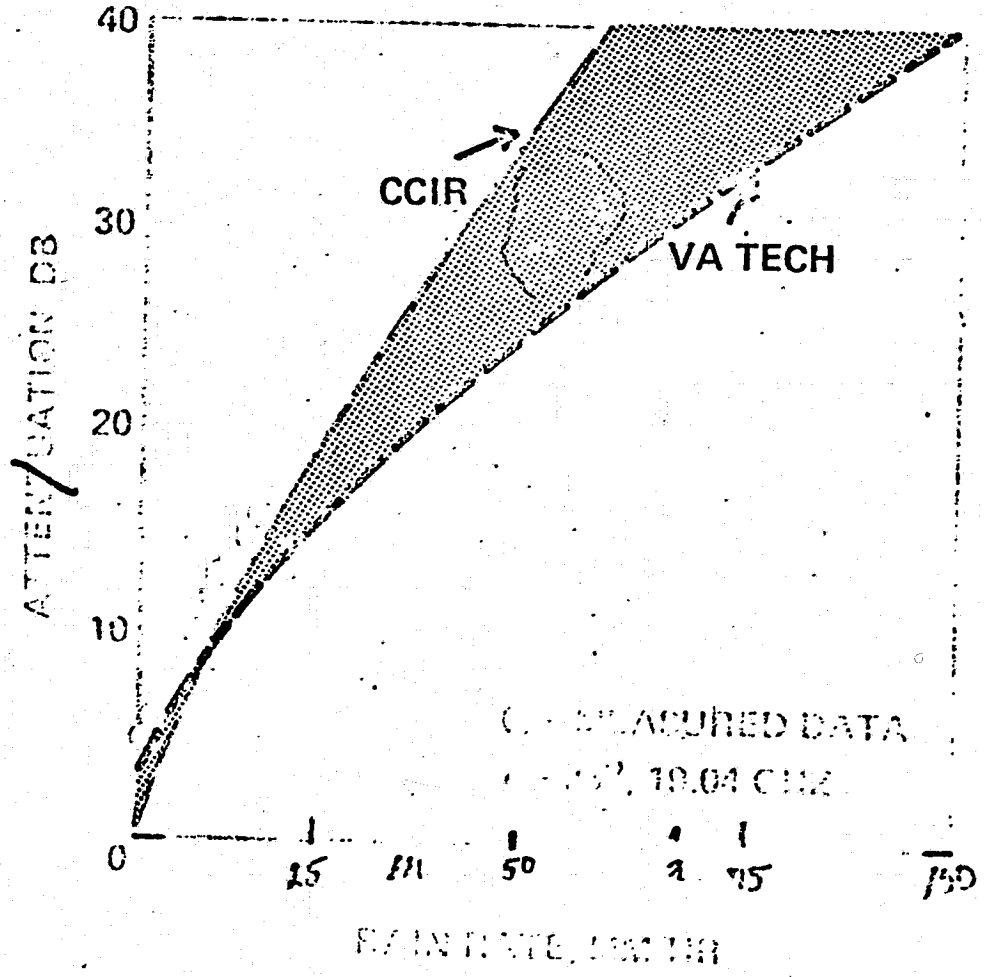

COMSTAR D 1 DATA:
JUL 1976 - JAN 1977

FIGURE 6a

KRD

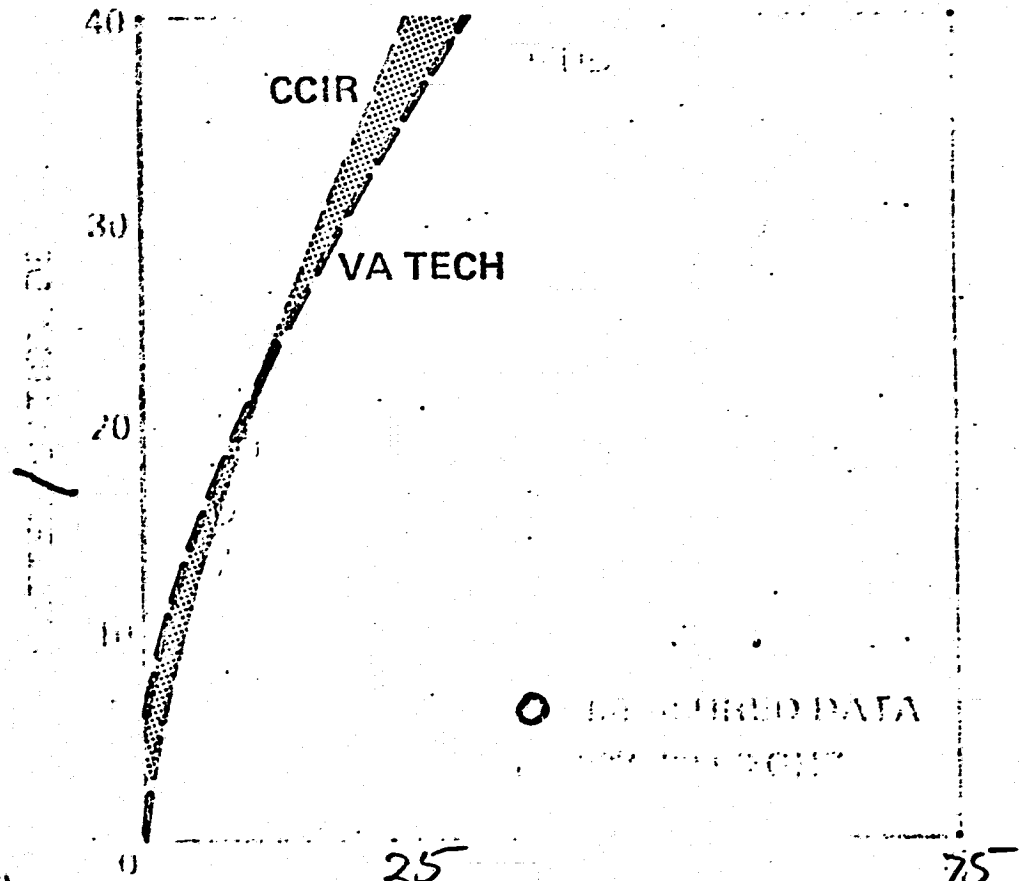

*COMSTAR D TDATA
JUL 1976 JAN 1977

FIGURE 6B

uniformity in the following way (see Figure 7). Given a rain storm on a path of length L, the CCIR model assumes that the path contains a uniform rain. As ground rain rate increases, the length L is shortened to model the non-uniform rain condition. This "effective path length" is based on measured terrestrial rain data referred to as an effective path average factor. Data indicates that this model overestimates the amount of water in the rain path for higher rain rates. The model has a pessimistic overshoot, as illustrated in Figure 8, where the CCIR effective path length is plotted as a function of ground rain rate and compared to measured data.

The Virginia Tech model makes no adjustment on the length, L but accounts for the non-uniform rains directly. In effect, the rain on the path is divided into two different rain levels and the non-uniform nature of the rain is accounted for by a power law relation having an empirical constant which is independent of rain and frequency. This relationship is based on measured earth space attenuation statistics.

Combination of the Rice-Holmberg rain rate model and the Virginia Tech or CCIR attenuation vs. rain rate models yield rain fade estimates as a function of annual reliability for "single station" fading. However, as a result of rather high rain fade margins at 20/30 GHz, the system design engineer must consider the option of the diversity station.

MODEL COMPARISON
(CCIR VS VA TECH)

HUGHES

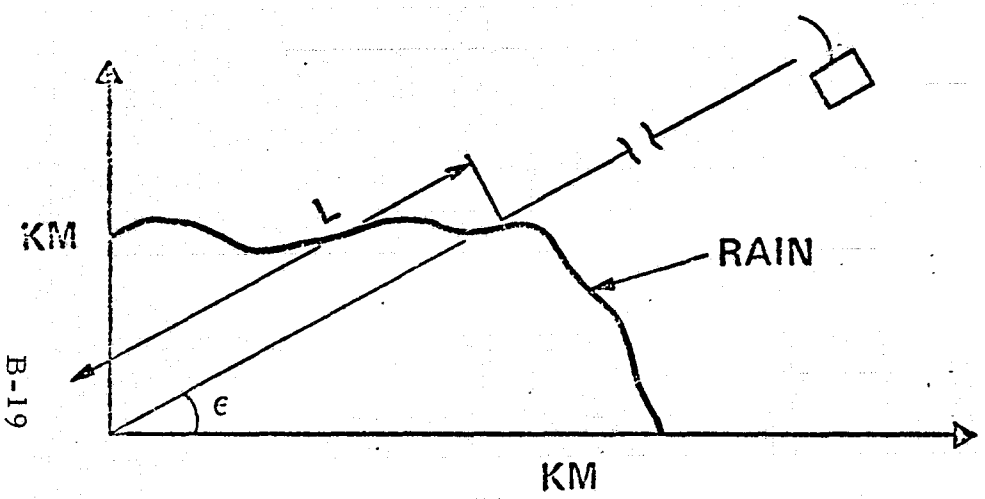

- PROPOSED CCIR MODEL

$$A = \left|H/\sin\epsilon\right| \left|\gamma R^{\delta}\right| \; a_1 R^{b1} \; dB$$

$$= L_{EFF}(R)\, \alpha\,(f, R)\; dB$$

- VA TECH MODEL

$$A = L(\epsilon)\, a_1 \left|0.2\, R^{b1} + 0.8 R_1^{b1}\right| \; dB$$

$$R_1 = R \left\{\frac{R}{10}\right\}^{-0.66} \; MM/HR$$

86776-11A

Figure 7

CCIR EFFECTIVE PATH LENGTH (BLACKSBURG, VA; f = 30 GHZ, ∈ = 45°)

HUGHES

$$L_{EFF} = L\,\gamma R_{POINT}^{-\delta}$$

$$= 10.5 R_{POINT}^{-0.161}$$

$$\Delta L_{EFF} = \approx 3 \text{ KM}$$

$$\Delta A(50 \text{ MM/HR}) = 32.4 \text{ DB}$$

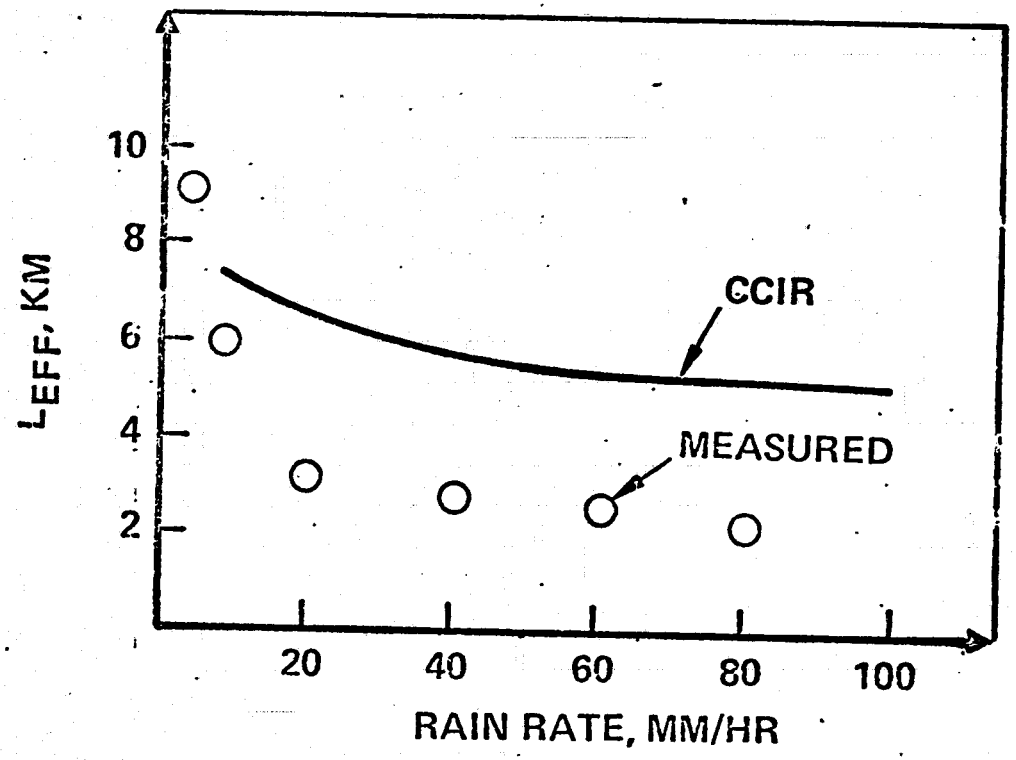

96257-10

FIGURE 8

With the addition of a second earth station the rain fade margin associated with a given system should decrease by taking advantage of the statistical indpendence of localized rain cells. Again measured data is limited and the system engineer must rely on predictive techniques. One such technique uses the concept of diversity gain (6) illustrated in Figure 9. This diversity gain can be added to single station attenuation statistics to obtain an estimate of dual station statistics. However, diversity gain is an empirical relation and existing models are based on single station fading of less than 20 dB. Because fades in excees of 20 dB at the 20 and 30 GHz frequency bands are seen commonly, application of these models to a 20/30 system should only be made with caution. For example, it will be shown that diversity gain is frequency dependent, contrary to previous concept.

Because of limitations on existing diversity gain models, Hughes has investigated a new approach to the diversity prediction problem. Hughes suggests that single station rain statistics can be transformed into dual station rain statistics using a rain diversity ratio curve such as that in Figure 10. On the average, one wishes to relate the rain at the peak station to the rain at the diversity station; thus, describing the statistical independence or dependence of the two stations.

SITE DIVERSITY
(DIVERSITY GAIN)

HUGHES

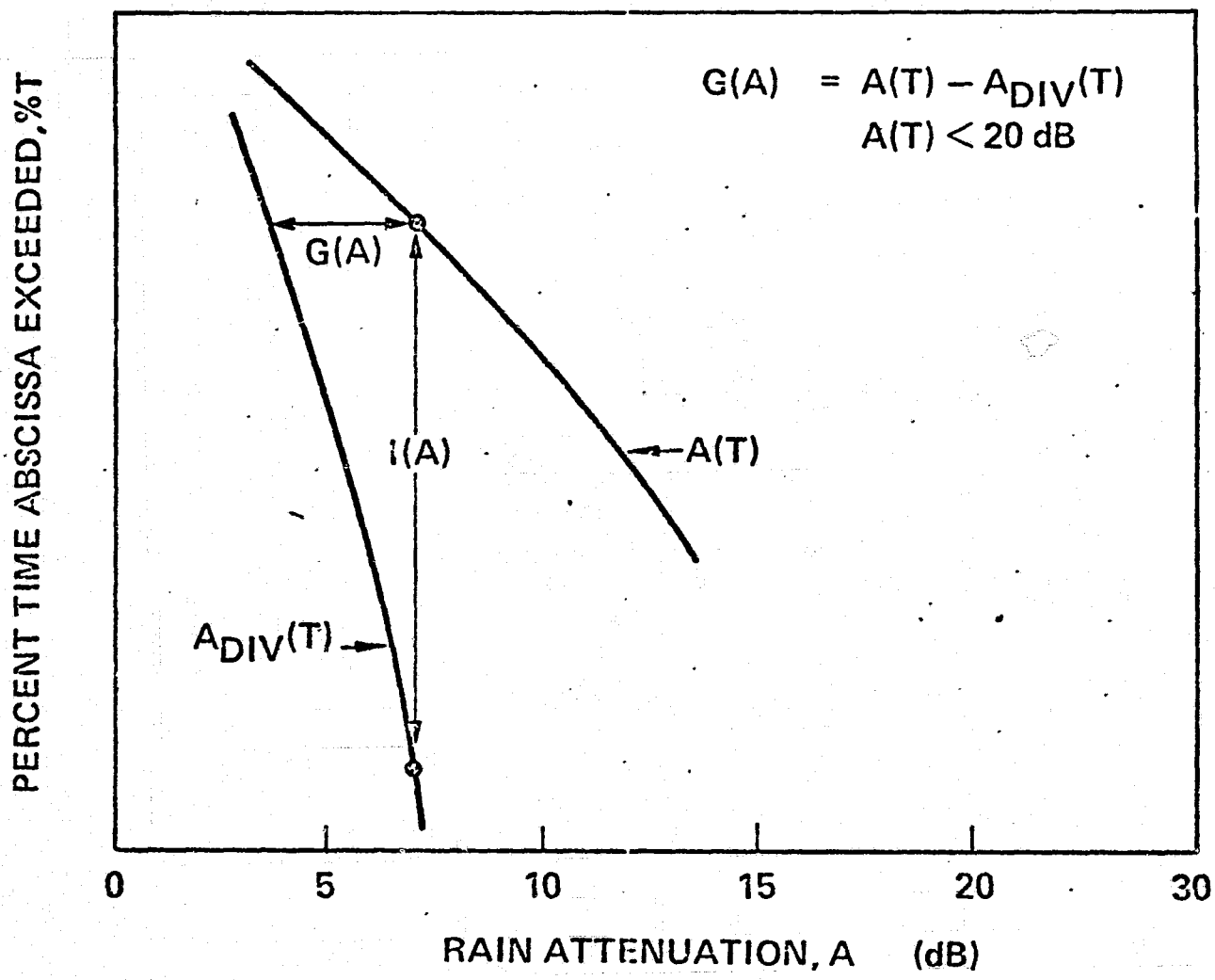

86776-12

Figure 9

RAIN DIVERSITY RATIO

HUGHES

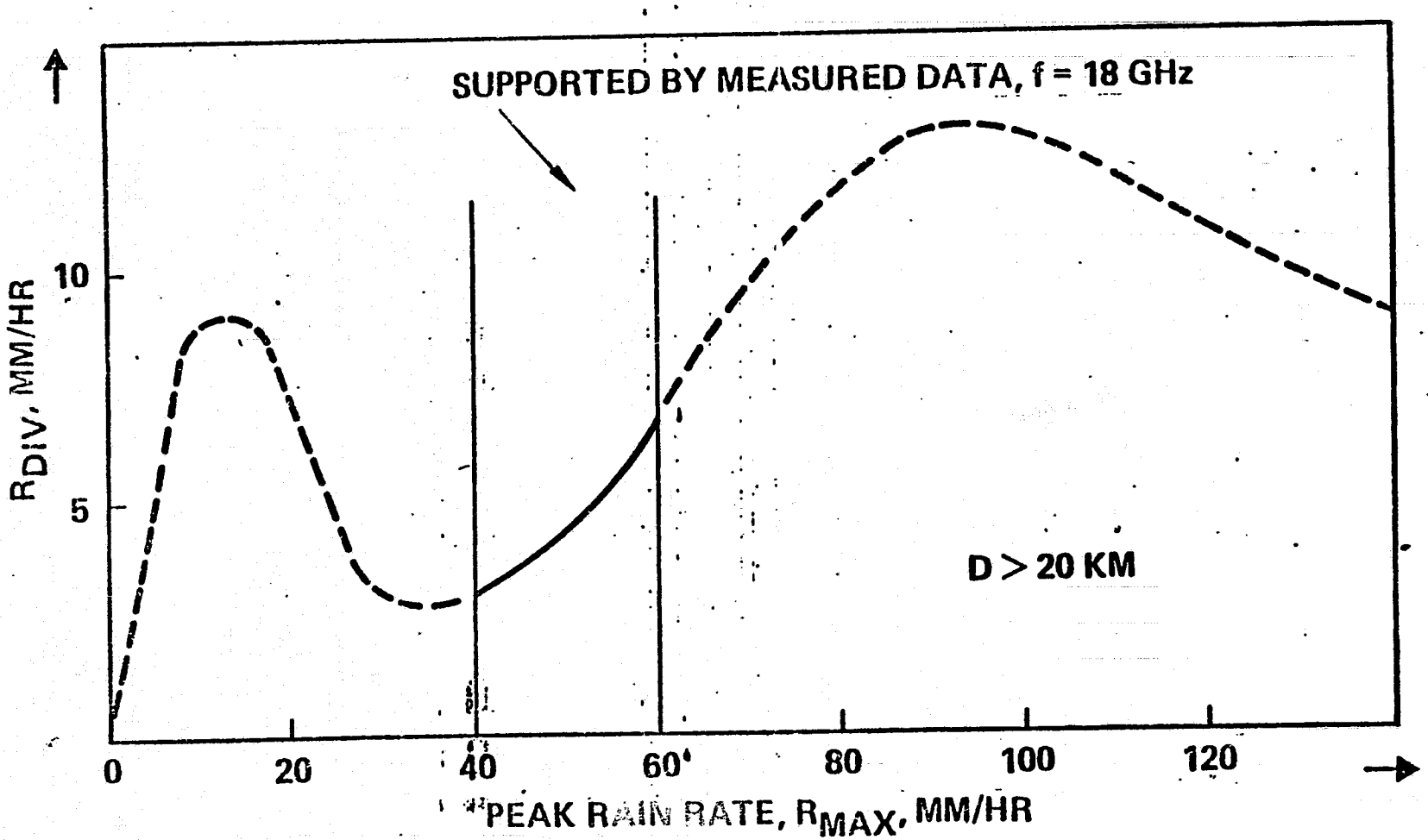

86776-13

Figure 10

First assume that the stations are separated by a distance in excess of 20 KM and there are no local terrain effects such as mountains or lakes, or streams. The first point on the curve is of course (0, 0) which represents a no rain condition. Low rain rate cells are often numerous and wide spread; therefore, for low rain rates the chance of having equal rain rate at both stations is quite high. Thus, a one to one correspondence is seen up to perhaps 10 mm/hr. Then a decrease in the diversity rain rate is seen as the rain rate becomes more intense and the rain cell becomes more localized over the peak rain rate station. However as the peak rain rate increases beyond some level, say 40 mm/hr, an increase in the total amount precipitation in the general area is signified, and one sees a secondary increase in the diversity rain rate. This increase continues, until a second maximum is achieved beyond which very intense, very localized rain conditions exist and an asymtotic decrease in the diversity rain rate is seen. The curve in Figure 9 has been based on huerestic arguments and its quantitative aspects are speculative; however, the model can be quantified and evaluated using data from a single rain gauge network rather than the more expensive attenuation measurements required to evaluate the diversity gain model discussed previously.

Now the rain diversity curve can be used to predict the reduction of attenuations by site diversity. Figure 11 presents rain statistics predictions for Atlanta, Georgia. The single station statistics are those of the Rice-Holmberg rain rate model. They are compared to published statistics by Bell Labs and good agreement is obtained. The diversity curve is derived from Figure 10 and is thus quantitatively speculative; however, if the quantitative arguments of Figure 10 are accepted, it appears that diversity offers a tremendous improvement for highly reliable systems. However, for a reliability of 99.5% there

RAIN STATISTICS PREDICTION
(ATLANTA, $\beta = 0.4$, $R_0 = 14.328$)

HUGHES

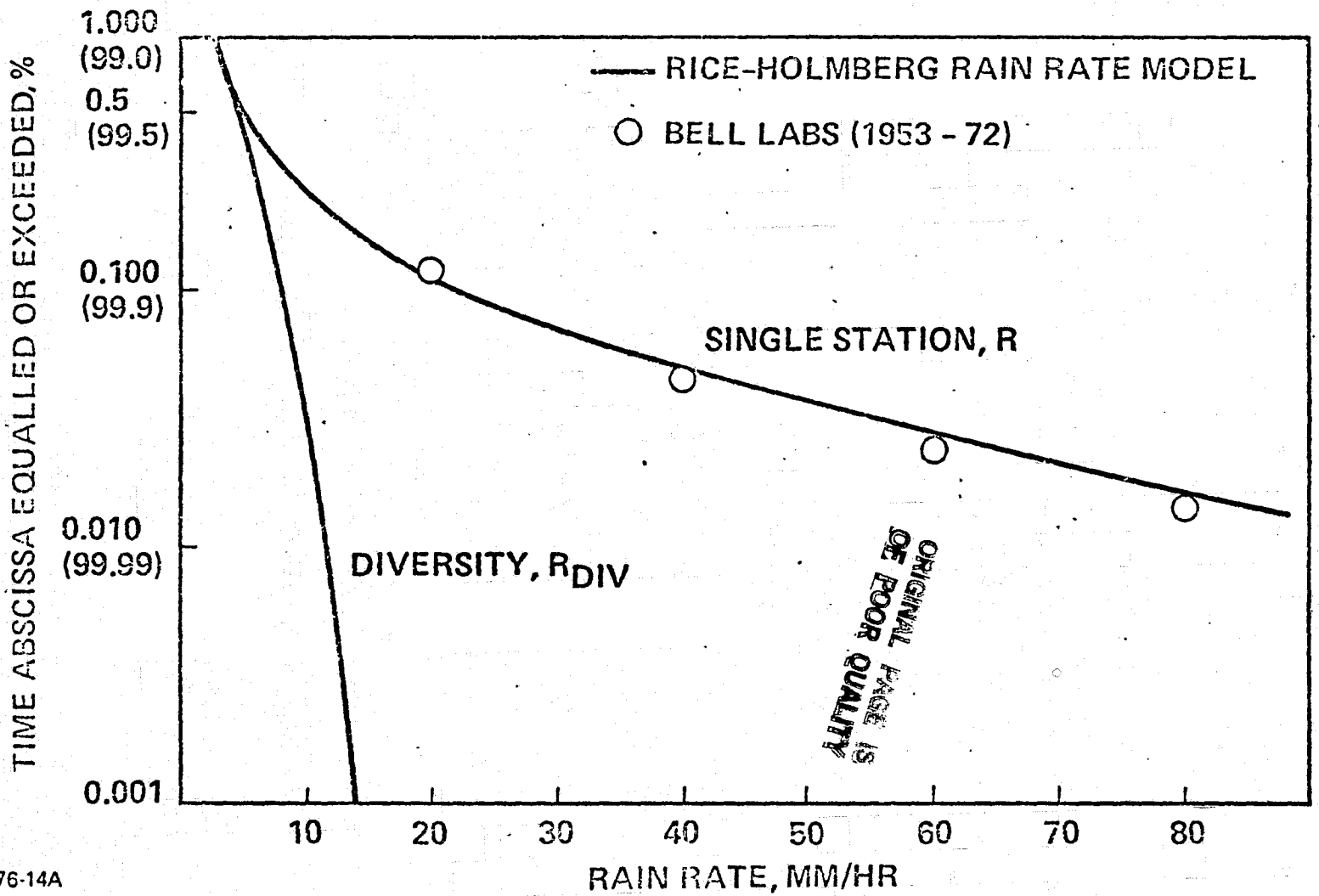

86776-14A

Figure 11

is little help with the addition of the diversity station. Now these rain statistics can be transformed into attenuation statistics and the impact of diversity and modeling differences can be evaluated.

Figure 12 compares predicted attentuation satistics for Atlanta, Georgia at 30 GHz. Again for single station statistics, a difference in excess of 20 dB between the CCIR and Virginia Tech models is seen. However, the associated absolute value of attenuation is greater than 40 dB and the difference of 20 dB may be irrelevant for single station fading. Yet if diversity gain is used to transform these statistics into diversity statistics, an initial 20 dB error results because diversity gain is a function of the single station prediction. Using the rain diversity ratio curve, the improvement with the addition of the diversity station can be estimated. For higher reliability systems, a tremendous improvement is obtained. However, note that for 99.5% reliability little improvement with the addition of the diversity site is achieved. Again this is because of the numerous wide spread low rain rate cells. Because of the lower rain rates, smaller differerences between the Virginia Tech and CCIR models are realized.

The fifth curve on the slide is an extrapolation of diversity gain done by NASA/Lewis. For reliability of 99.5%, an optimistic prediction is seen. This prediction is based on measured attenuation data at 13 GHz where low rain rates have little effect on attenuation statistics. However, low rain rates significantly effect attenuation statistics at 30 GHz. Thus, an apparent frequency dependence is seen in the diversity gain concept. For higher reliability systems a pessimistic overshoot is seen because of the limitations on single station fading. So rain fade margin estimates for a 20/30 GHz system have a significant modeling uncertainty and the impact

ATTENUATION STATISTICS COMPARISON

ATLANTA, f = 30 GHz

HUGHES

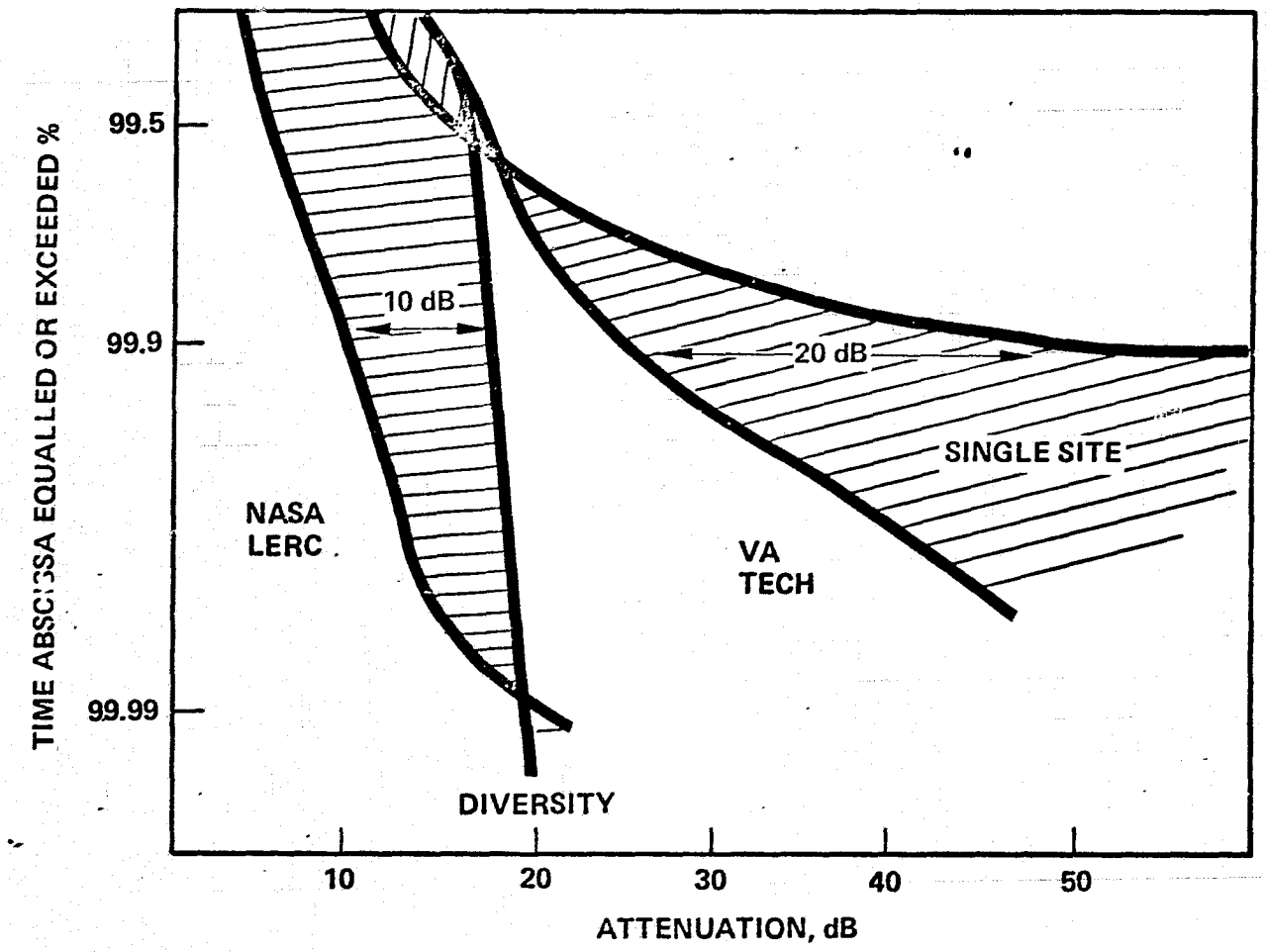

96277-5

of diversity depends on the reliability of interest.

RAIN DEPOLARIZATION

Because of the differential attenuation and differential phase properties of an oblate rain drop, rain can depolarize incident microwave signals (1). Thus, when an orthogonal polarization system is employed to maintain spatial isolation and frequency reuse capabilities, the degradation in Co carrier to Cross interference by rain depolarization must be considered. However, in this section it will become evident that rain depolarization is much less of a problem than rain attenuation at 20/30 GHz.

Because the depolarization phenomena is directly related to the attenuation on a rain-filled path, the isolation between two orthogonal channels is usually plotted as a function of the main channel attenuation as illustrated in Figures 13a, b. The predictions of the Virginia Tech model are compared to measured data using the linearly polarized Comstar D2 spacecraft that was taken by the Blacksburg, Virginia earth station. The theoretical curves a, b, c and d on each figure repreeent various rain drop canting angle and upper ice layer conditions normally found on a rain path. This accounts for the scatter in the data.

Figure 14 illustrates the frequency dependence of orthogonal channel isolation as a function of main channel attenuation. Note that for a given value of attenuation, isolation improves as frequency increases. Thus, if a rain fade margin of 10 and 20 dB is assumed for 20 and 30 GHz respectively, the worst case isolation for either frequency would be

DEPOLARIZATION, 30 GHz
(BLACKSBURG, VA)

HUGHES

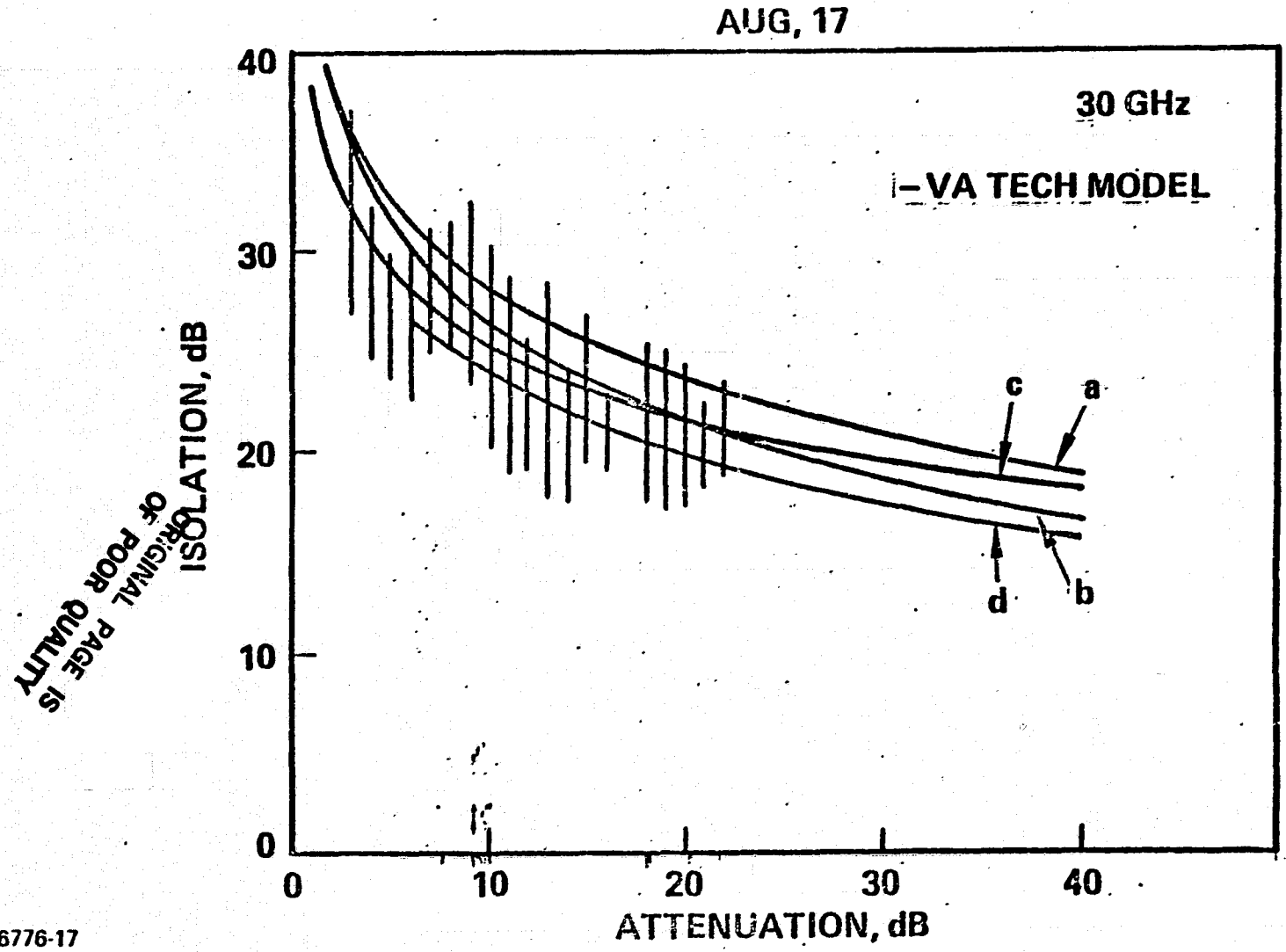

Figure 13a

DEPOLARIZATION, 20 GHz (BLACKSBURG, VA)

HUGHES

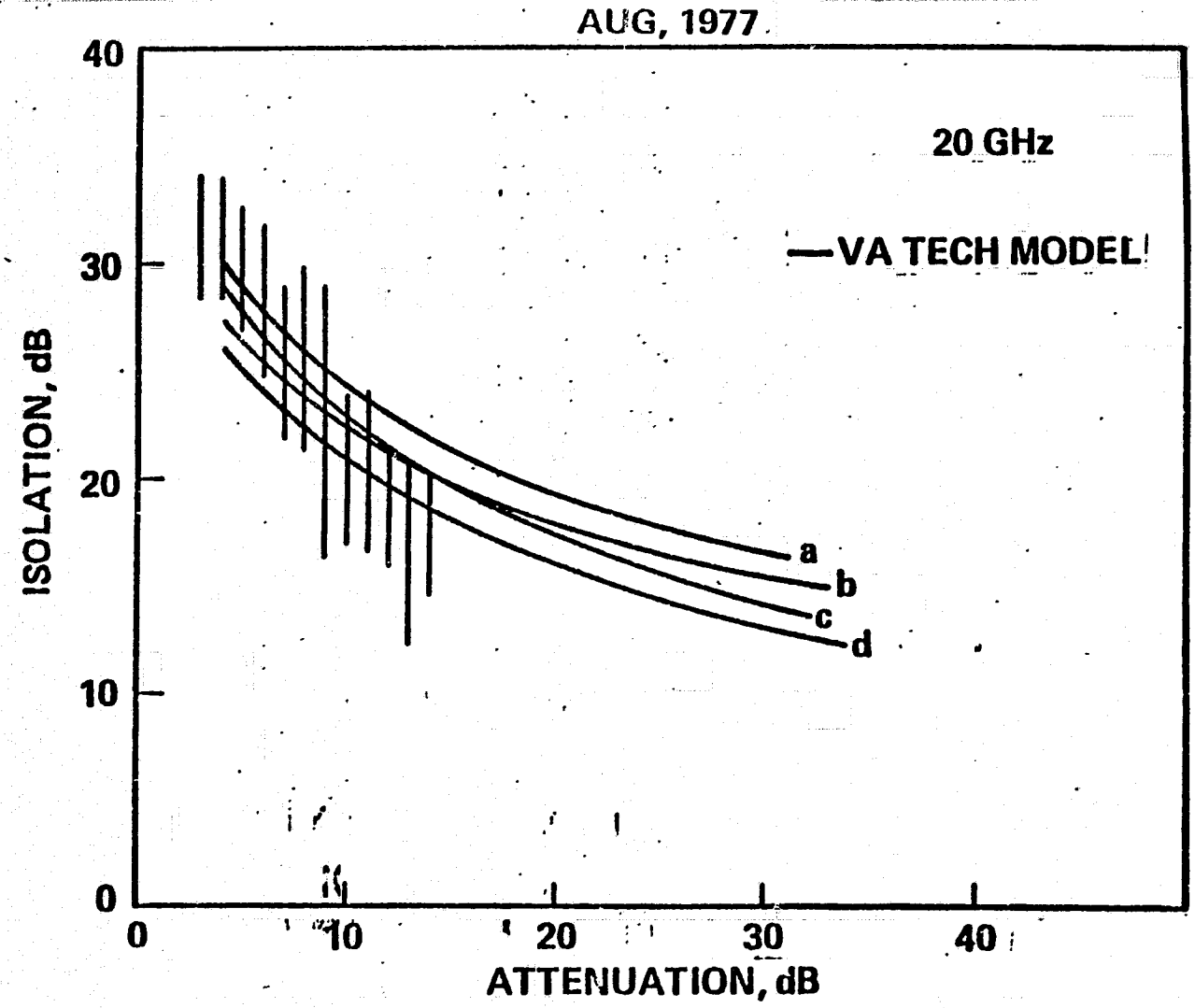

Figure 13b

DEPOLARIZATION COMPARISON
(BLACKSBURG, VA)

HUGHES

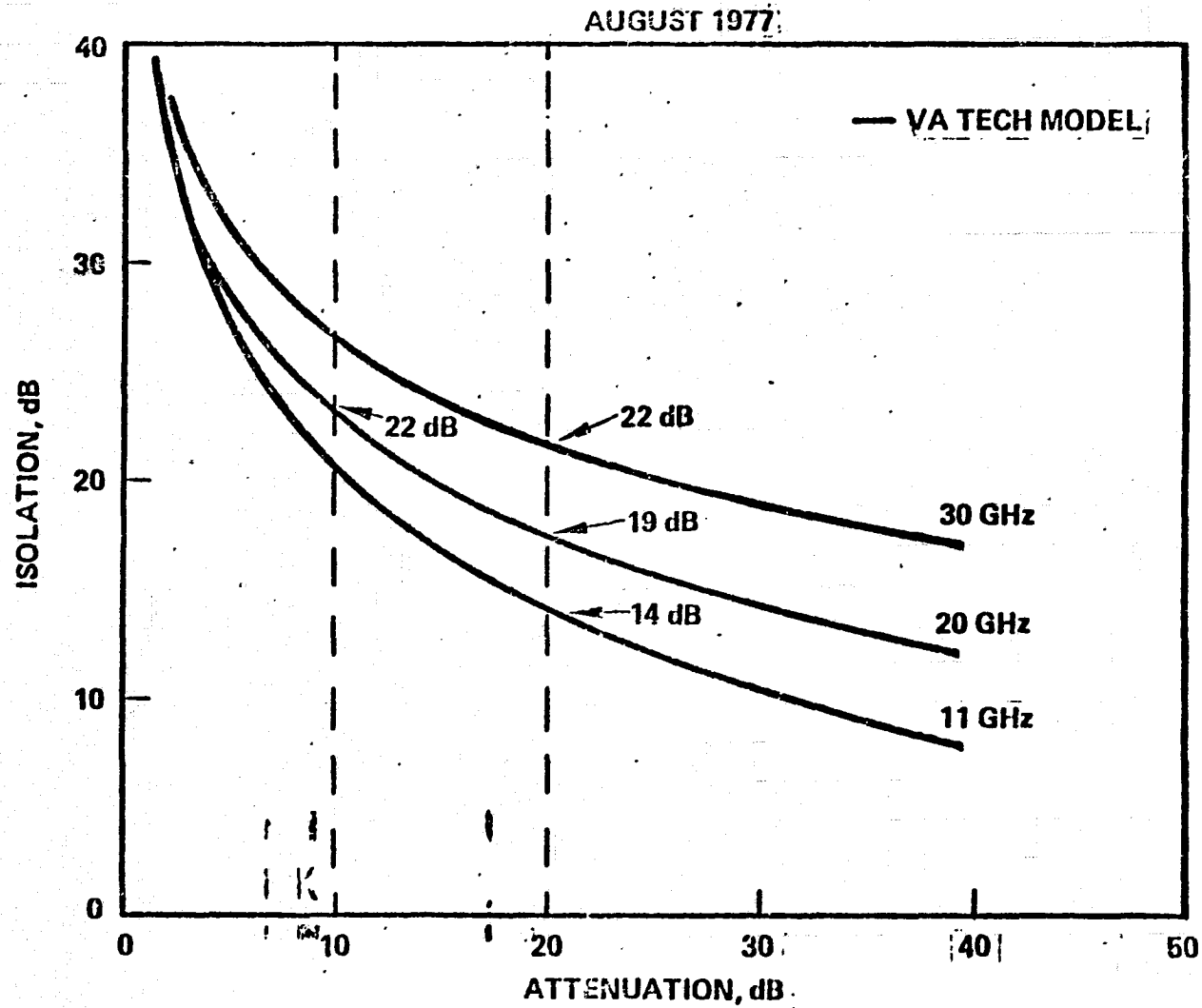

80776-18

Figure 14

approximately 22 dB independent of antenna polarization specifications. (assuming an antenna polarization spec greater than 30 dB). For most digital QPSK systems the 22 dB isolation value is more than adequate for bit error rates of 10^{-6}. Because rain fade margins of 10 and 20 dB are much harder to achieve in the system budget, rain attenuation is more of a dominant problem in a 20/30 system design.

Although rain depolarization is not a serious problem at 20/30 GHz, depolarization by ice crystals alone must be examined also. Ice crystal depolarization is different than rain depolarization in that there is no associated attenuation (1). Thus, ice layers at high altitudes can depolarize microwave signals without effecting the rain fade margin. Fortunately for a digital system, a 10 dB degradation in orthogonal channel isolation can be offset by adding on the order of 2 to 3 dB more power. Thus, symbol error rate levels are maintained. Ice crystal depolarization is being measured around the globe, however the phenomena is somewhat rare and statistically insignificant as compared to rain depolarization.

CONCLUSIONS AND RECOMMENDATIONS

The design of 20/30 GHz multiple beam coverage for service in the continental U.S. requires accurate rain fade estimates. Existing data from 20/30 GHz rain attenuation measurements is insufficient for drawing statistically meaningful conclusions. Also, the number of sites for which data is available is limited. Therefore, the system design engineer must rely on predictive techniques. In the 20 and 30 GHz frequency ranges the rain fades

are much larger than at lower frequencies. Thus, modeling uncertainties can lead to relatively large fade value uncertainties, which have a significant effect on communication system design and cost. Theoretical models should be extensively compared to all available measured data at several frequencies and locations to check the validity of their predictions. Hopefully as the measured data base grows, the various modeling differences will approach zero and one universal model can be adopted.

Site diversity is an important mechanism for increasing system reliability. However, depending on the reliability of interest, station diversity may or may not provide additional margin. The impact of diversity is a major concern at 20/30 GHz and very little work has been done in this area.

The concept of diversity gain is limited and the rain diversity ratio curve is not supported by measured data. More attenuation measurements are needed as related to a diversity system. Also, instantaneous rain gauge measurements are required to determine the statistical independence of the two stations independent of microwave system parameters.

Finally, the system impact of the various rain fade margin uncertainties is significant, but the impact depends on the exact scenario chosen. Thus, the 20/30 system should be designed in such a way as to minimize the impact of rain fade uncertainties.

REFERENCES

1. R.R. Persinger and W.L. Stutzman, "A Depolarization and Attenuation Experiment Using the CTS and COMSTAR Satellites - Millimeter Wave Propagation Modeling of Inhomogeneous Rain Media for Satellite Communication Systems," Interim Report 1978-1, NASA Goddard/DCA Contract NAS5-22577 and U.S. Army Research Office Grant DAAG29-77-G-0083, June, 1978.

2. W.L. Stutzman and C.W. Bostian, "A Millimeter Wave Attenuation and Depolarization Experiment Using the COMSTAR and CTS Satellites," U.S. Army Research Office Grant DAAG29-77-G0083 and NASA Goddard NAS5-22577, April 15, 1979.

3. R.R. Persinger and W.L. Stutzman, "A Synthetic Storm Model for Prediction of Millimeter Wave Rain Attenuation," IEEE Trans. Antennas and Propagation, To Be Published.

4. P.L. Rice and N.R. Holmberg, "Cumulative Time Statistics of Surface-Point Rainfall Rates," IEEE Trans. on Comm., Vol. COM-21, pages 1131-36, Oct. 1973.

5. CCIR Document, DOC P1105-E, Special Preparatory Meeting (WARC-79) Geneva, 1978, 6 June 1978.

6. D.B. Hodge, "Prediction of Path Diversity on Earth-Space Paths," NASA Goddard Contract NAS5-23438, Mod. 68, October, 1978.

APPENDIX C. STATEMENT OF WORK

PREFACE TO EXHIBIT "A"

Analysis of the utilization of satellite communication systems shows trends that would indicate a future need for advanced millimeter-wave satellite systems.

For example, the current communication traffic demand is increasing at the rate of 15-20 percent annually. Specialized services such as data service are growing even faster with a 30-50 percent rate typical of the data service. Extrapolating these trends one obtains two interesting results.

(1) The demand for data services could equal or exceed that for voice by 1990.

(2) The 4/6 GHz satellite bands could be saturated by the mid to late 1980's.

Introduction of 12 GHz systems would provide some relief in this circumstance, perhaps to 1990. However, to insure future demand for satellite services will be met, it may be necessary to develop and implement satellite systems in the millimeter band such as 18/30 GHz and 40/50 GHz.

In order to direct future technology efforts of NASA so that these efforts complement and stimulate the commercial development of these bands, it is necessary to establish probable system configurations of millimeter wave satellite systems and the most critical technology needs. In particular, NASA needs information which resolves:

(1) What type and volume of communication services might be required of 18/30 GHz systems and in what time period.

(2) Whether 18/30 GHz satellite trunking into major terminals would be competitive with present and future communication alternatives (such as buried waveguide, optical fiber, and satellites) and probable methods of implementing this service.

(3) Whether 18/30 GHz satellite systems could technical and economically provide services directly to the users, i.e. via small inexpensive earth terminals, and probable methods of implementing such a service.

(4) What are the advanced technology efforts which need to be carried out to reduce the risks of introducing such a communication system to a normal commercial risk.

(5) Whether the impact of rain attenuation significantly affects the technical and economic viability of 18/30 GHz systems and likely methods of circumventing this problem.

(6) The ultimate cost-effective capacity of the 18/30 GHz bands for domestic fixed service given current and planned technology developments.

To resolve these questions, the Government plans to award separate study contracts in two areas. One effort will specifically address the system and equipment aspects of 18/30 GHz systems while the other will specifically address the service aspects for such systems.

To insure these major areas will be adequately addressed, the Government plans to restrict the system and equipment study effort to communication

service suppliers.

Interaction between the system suppliers and service suppliers throughout these efforts will be encouraged and is specifically called for in the Statement of Work, "Exhibit A". A copy of the Statement of Work of the service study effort is included in this RFP for information only.

This particular study, as defined in "Exhibit A", shall address the system and equipment aspects of 18/30 GHz satellite systems. The depth of the analysis shall be sufficient to provide service costs for selected services and comparison of these costs with those of alternative systems (such as existing terrestrial, satellite, buried waveguide, and optical fiber systems). Also, it is required that sensitivity analyses be performed on these concepts to determine the critical technology areas (e.g. is the service costs sensitive to fade margins required to achieve selected propagation reliabilities). The nature of this study is such that the required assessments and concept formulations will be based as much on previous experience in satellite communication system (including both space and ground segments) concept formulation and design as it will be on in-depth analyses of aspects unique to this study. Consequently, only satellite communication system suppliers, i.e. those with demonstrated experience in concept formulation, design, and actual system integration will be accepted as being qualified.

The scope of the effort involved and the level of detail asked for is expected to require 24-36 man-months of effort to accomplish. The period of performance of this study is nine (9) months.

NASA reserves the right to award more than one technical study contract pertaining to this procurement.

EXHIBIT "A"

STATEMENT OF WORK

18 AND 30 GHZ FIXED SERVICE SATELLITE COMMUNICATIONS SYSTEM STUDY

The contractor shall furnish the necessary personnel, facilities, services and materials and otherwise do all things necessary for or incident to the tasks described below.

TASK 1 - ASSESSMENT OF APPLICABLE STATE-OF-THE-ART AND FORECASTS OF 18/30 GHZ TECHNOLOGY

1.1 Ground Station Technology

The contractor shall assess the state-of-the-art in millimeter ground station technology including that associated with the 18 GHz downlink as well as that associated with the 30 GHz uplink. The contractor shall provide tabular and graphical displays of estimated performance and costs of major subsystems. The contractor shall also provide an assessment of probable developments in these subsystems in the time frame of 1980-1990. As a minimum, the contractor shall specifically address the following subsystems:

1.1.1 Message Processing

(a) Digital Terrestrial Interface - The contractor shall provide an assessment of the capacity, speed, and cost of digital terrestrial interfaces. Terrestrial user input/output digital rates shall span the range 2.4 kbs - 300 mbs. The interface shall include the necessary subsystems for interfacing analog signals as well. The bandwidth of these signals shall span the range 4 KHz - 6 MHz.

(b) Analog Terrestrial Interface - The contractor shall assess the capacity and cost of analog terrestrial interfaces. Terrestrial user input/output bandwidths shall span the range 4 KHz - 6 MHz. Total terminal bandwidth shall range 40 KHz - 1.5 GHz, consistent with user population and bandwidth requirements.

(c) The contractor shall provide schematic diagrams of conceptual interfaces delineating the major elements of these interfaces.

1.1.2 Modulation - Demodulation

(a) Digital Modems - The contractor shall provide an assessment of the capacity, speed, and cost of ground terminal digital modems. The information provided by the contractor shall include 40 kbs - 1.5 gbs. As a minimum, the data on modulation-demodulation methods provided shall include 2, 4, and 8 level PSK.

(b) Analog Modems - The contractor shall assess the capacity and cost of ground terminal analog modems. The data provided shall include modem bandwidths spanning 40 KHz - 1.5 GHz.

1.1.3 Diversity Link

The contractor shall provide an assessment of the capacity, bandwidth and cost of terrestrial microwave systems which provide the interconnect between redundant ground stations at each site. As a minimum, the contractor shall provide data on radio-relay systems, buried waveguide, and buried optical fibers.

1.1.4 Receiver

The contractor shall provide an assessment of the bandwidth, noise performance, and cost of receiver subsystem. This subsystem shall include the downconverter and, as a minimum, the contractor shall provide this data on receivers with:

(a) Cryogenically cooled low-noise amplifier front-ends.

(b) Uncooled low-noise amplifier front-ends.

(c) Mixer front-ends.

1.1.5 Transmitters

The contractor shall provide an assessment of the bandwidth, noise performance, power level, and cost of the transmitter subsystem. This subsystem shall include the upconverter and, as a minimum, the contractor shall provide this data on transmitters of the type:

(a) Completely solid state.

(b) Hybrid with solid state upconverter and TWT power amplifier.

(c) Hybrid with solid state upconverter and Klystron power amplifier.

and the data range shall span:

(a) 0.1 watt - 5 Kw RF power output.

(b) 1 MHz - 1.5 GHz information bandwidth.

1.1.6 Frequency Sources

The contractor shall provide data on the stability, noise performance and cost of frequency sources used for local oscillators in the upconverters and downconverters.

1.1.7 Antennas

The contractor shall provide an assessment of the tolerances, sizes, and costs of ground antenna. As a minimum, the contractor shall include antenna sizes ranging over 0.5 - 30 meters.

1.1.8 Pedestal and Pointing

The contractor shall provide an assessment of the pointing accuracy, antenna size capacity and costs of the pedestal and pointing subsystem.

As a minimum, the contractor shall include antenna sizes ranging over 0.5 - 30 meters and shall include mechanisms of the type:

(a) Fixed

(b) Fixed with manual adjustment

(c) Autotrack

1.2 Satellite Technology

The contractor shall assess the state-of-art in 18/30 GHz satellite technology and provide tabular and graphical displays of estimated performance, weight, and costs of major subsystems. The contractor shall also provide an assessment of probable developments in these subsystems in the time frame of 1980-1990. As a minimum, the contractor shall specifically address the following subsystems:

1.2.1 Receivers

The contractor shall provide an assessment of the bandwidth, noise performance, weight and cost of the receiver subsystem. This subsystem shall include the downconverter and, as a

minimum, the contractor shall provide data on receivers with:

(a) Uncooled low-noise amplifier front-ends.

(b) Mixer front-ends.

1.2.2 Signal Routing and Switching

(a) Time Domain Multiple Access (TDMA) - The contractor shall provide an assessment of the capacity, speed, weight and cost of the signal routing and switching system of a satellite operated in a TDMA mode. As a minimum, the contractor shall provide this data for:

(1) Satellites with no on-board switching.

(2) Satellites with on-board time slot switching.

(3) Satellites with on-board time slot and beam switching.

(b) Frequency Domain Multiple Access (FDMA) - The contractor shall provide an assessment of the capacity, speed, weight and cost of the signal routing and switching system of a satellite operated in a FDMA mode. As a minimum, the contractor shall provide this data for:

(1) Satellites with no on-board switching.

(2) Satellites with on-board frequency channel switching.

(3) Satellites with on-board frequency channel and beam switching.

1.2.3 Transmitters

The contractor shall provide an assessment of the bandwidth, noise performance, power level, weight, and cost of the transmitter subsystem. This subsystem shall include the upconverter and, as a minimum, the contractor shall provide this data on transmitters of the types:

(a) Completely solid state.

(b) Hybrid with solid state upconverter and TWT power amplifier.

The data range shall span:

(a) 0.1 watt - 5 Kw RF power output.

(b) 10 MHz - 1.5 GHz information bandwidth.

1.2.4 Frequency Sources

The contractor shall provide an assessment of the stability, noise performance, weight, and cost of frequency sources used for local oscillators in the upconverters and down-converters.

1.2.5 Antennas

The contractor shall provide an assessment of the gain, sidelobe performance, beam isolation, weight and cost of the antenna subsystem. As a minimum, the contractor shall provide data for:

(a) Multibeam antennas of the reflector type.

(b) Multibeam antennas of the lens type.

The data provided shall span the range of 1 - 50 beams.

1.2.6 Pointing Control

The contractor shall provide an assessment of the pointing accuracy, antenna size capacity, weight and cost of the antenna-pointing subsystem. As a minimum, the contractor shall provide data on:

(a) Fixed pointing - i.e. Spacecraft attitude control subsystem performs pointing function.

(b) Independent pointing - i.e. antenna pointing achieved independent of spacecraft attitude. However, separate beams of a particular antenna may be fixed with respect to the axis of that antenna.

1.2.7 Spacecraft Bus

The contractor shall provide an assessment of the weight and cost of the spacecraft bus which provides the power and otherwise supports the subsystem detailed in Subtasks 1.2.1 - 1.2.6.

TASK 2 - MILLIMETER WAVE SATELLITE/MAJOR TERMINAL TRUNKING CONCEPTS

The contractor shall provide satellite and ground system concepts, subject to NASA project manager approval, for evaluating use of millimeter wave satellites in trunking configuration. Each concept shall include a multibeam satellite and a major ground terminal network. Power margins and/or diversity terminals shall be used as required to achieve the propagation reliabilities specified below. Shuttle/Spin Stabilized Upper Stage (SSUS) and Shuttle/Interim Upper Stage (IUS) shall be the assumed space transportation systems. As a minimum, the contractor shall provide the following:

2.1 FDMA Concepts

2.1.1 Frequency Domain Multiple Access (FDMA), no spacecraft switching

(a) The contractor shall provide a satellite and ground system satellite trunking concept which operates in a FDMA mode without on-board RF switching. This concept shall be arrived at by adjusting the satellite and ground station parameters to arrive at a minimum total system cost on an annual basis. This annual cost shall include all costs associated with the ground segment as well as space segment and prorated over the expected lifetime of the system. The precise method used by the contractor must be approved by the NASA project manager. The following baseline parameters shall be used for this portion of the analysis:

(1) 10 ground stations distributed throughout the U.S.

(2) 200 MHz interconnects between ground stations.

(3) 99.9% propagation reliability.

(4) 10 spot beams on spacecraft, one to each ground station.

(b) The contractor shall provide graphical displays showing system cost sensitivities of the optimum FDMA cost configuration. As a minimum, the contractor shall provide a display of:

(1) Service cost per channel as a function of number of ground terminals. This cost shall be computed for an equivalent 40 MHz channel by using the relationship:

$$\frac{\text{(Total Annual Cost)}}{\text{(Number of Ground Terminals)}} \times \frac{\text{40 MHz}}{\text{(Usable Terminal Bandwidth)}}$$

Full interconnectivity shall be maintained and service bandwidth to each terminal adjusted consistent with spectral allocations. Also the number of spot beams shall coincide with the number of ground stations. The range shall span 5 - 40 terminals.

(2) Service cost per channel as a function of channel bandwidth. The range shall span 40 - 250 MHz.

(3) Service cost per channel as a function of propagation reliability. The range shall span 99.0 - 99.9 per cent.

2.1.2 FDMA, on-board switching

The contractor shall provide an assessment of the impact of adding dynamic on-board switching to the baseline FDMA system specified in Subtask 2.1.1. As a minimum, the contractor shall assess the impacts on service capacity and service cost.

2.2 Resultant FDMA Concept

The contractor shall provide diagrams of the satellite systems and ground systems for the most cost-effective FDMA system arrived at in Subtasks 2.1. Tabular data shall be provided indicating the

major cost elements of the ground system and the major cost and weight elements of the space system.

2.3 TDMA Concepts

2.3.1 Time Division Multiple Access with on-board switching (SS-TDMA)

(a) The contractor shall provide a satellite and ground system satellite trunking concept which operates in a SS-TDMA mode. This concept shall be arrived at by adjusting the satellite and ground station parameters to arrive at a minimum total cost system as specified in Subtask 2.1.1(a). The following baseline parameters shall be used for this portion of the analysis:

(1) 10 ground stations evenly distributed throughout the U.S.

(2) 200 MBS interconnects between ground stations.

(3) QPSK modulation/demodulation with bit error rate of 10^{-6} and no coding.

(4) 99.9% propagation reliability.

(5) 10 spot beams on spacecraft, one to each ground terminal.

(b) The contractor shall provide graphical displays showing system cost sensitivities of the optimum SS-TDMA cost configuration. As a minimum, the contractor shall provide a display of:

(1) Service cost per channel as a function of the number of ground terminals. This cost shall be

computed for an equivalent 40 MBS channel by using the relationship:

$$\frac{\text{Total Annual Cost}}{\text{(Number of Ground Terminals)}} \times \frac{\text{40 MBS}}{\text{Terminal Bit Rate}}$$

Full interconnectivity shall be maintained and service bit rate to each terminal adjusted consistent with spectral allocations. Also, the number of spot beams shall coincide with the number of ground stations. The range shall span 5 - 40 terminals.

(2) Service cost per channel as a function of channel bit rate. The range shall span 40 - 250 MBS per channel.

(3) Service cost per channel as a function of design bit error rate. The range shall be 10^{-3} - 10^{-9}. This evaluation shall be done for 2, 4, and 8 level PSK as a minimum.

(4) Service cost per channel as a function of propagation reliability. The range shall span 99.0 - 99.99 per cent.

2.3.3 TDMA, no on-board switching

The contractor shall provide an assessment of the impact of deleting on-board switching from the baseline TDMA satellite trunking system specified in Subtask 2.3.1. As a minimum, the contractor shall assess the impacts on service cost and service capacity.

2.4 Resultant TDMA Concept

The contractor shall provide diagrams of the satellite systems and ground systems for the most cost-effective TDMA system arrived at in Subtask 2.3. Tabular data shall be provided indicating the major cost elements of the ground system and the major cost and weight of the space system.

TASK 3 - MILLIMETER WAVE SATELLITE DIRECT-TO-USER CONCEPTS

The contractor shall provide satellite and ground system concepts, subject to NASA project manager approval, for evaluating use of millimeter wave satellites in a direct-to-user configuration. Each concept shall include a satellite and network of small terminals. The satellite and ground terminals shall include sufficient margins to accommodate the propagation reliabilities specified in Subtask 3.1. Howaver, only single terminal stations shall be used for this concept. Shuttle/SSUS and Shuttle/IUS shall be the assumed space transportation capability. As a minimum, the contractor shall provide the following:

3.1 FDMA Concepts

3.1.1 FDMA, Conus Coverage, no on-board switching

(a) The contractor shall provide a satellite and ground system direct-to-user concept, operating in a FDMA mode, providing a type of single-carrier-per-channel (SCPC) service, using a CONUS coverage satellite. This concept shall be arrived at by adjusting the satellite and ground station parameters to arrive at a minimum total system cost as defined in Subtask 2.1.1(a). The following parameters shall be used for this analysis:

(1) 10,000 ground stations evenly distributed throughout the U.S.

(2) User channels demand-assigned with ½ capacity devoted to 40 KHz service, ¼ capacity to 1.5 MHz service, and ¼ capacity to 40 MHz service.

(3) 99.5% propagation reliability.

(b) The contractor shall provide graphical displays showing system cost sensitivities of the optimum FDMA SCPC cost configuration. Service costs shall be provided for each of the services specified in Subtask 3.1.1(a) and shall be prorated according to the bandwidth used by each service as done in Subtask 2.1.1(b)(1). As a minimum, the contractor shall provide a display of:

(1) Service cost per equivalent channel and satellite availability as a function of the total number of ground terminals. The range shall span 10^3 - 10^5 terminals. The relative allocation of traffic shall be maintained.

(2) Service cost per equivalent channel as a function of propagation reliability. The range shall span 99.0 - 99.99 per cent.

3.1.2 Multiple beam FDMA, no on-board switching

(a) The contractor shall provide a satellite and ground system direct-to-user concept which operates in an FDMA mode providing a type of single carrier per channel service. This concept shall be arrived at by adjusting the satellite and ground station parameters to arrive at a minimum

total system cost as defined in Subtask 2.1.1(a). The following baseline parameters shall be used for this portion of the analysis:

(1) 10,000 ground stations evenly distributed throughout the U.S.

(2) User channels demand-assigned with ½ capacity devoted to 40 KHz service, ¼ capacity to 1.5 MHz service, and ¼ capacity to 40 MHz service.

(3) 25 spot beams evenly distributed over the U.S. with no direct interconnectivity between beams. Interconnectivity shall be provided by central major terminals and either auxillary trunking channels on the spacecraft or by using services of a separate trunking spacecraft.

(4) 99.5% propagation reliability.

(b) The contractor shall provide graphical displays showing system cost sensitivities of the optimum FDMA-SCPS cost configuration. Service costs shall be provided for each of the services specified in Subtask 3.1.1(a) and shall be prorated according to the bandwidth used by each service as done in Subtask 2.1.1.(b)(1). As a minimum, the contractor shall provide a display of:

(1) Service cost per equivalent channel and satellite availability as a function of the total number of ground terminals. The range shall span 10^3 - 10^5 terminals. The relative allocation of traffic

shall be maintained.

(2) Service cost per equivalent channel as a function of the number of satellite beams. The range shall span 4 - 40 beams.

(3) Service cost per equivalent channel as a function of propagation reliability. The range shall span 90.0 - 99.99 per cent.

3.2 Resultant FDMA Concept

The contractor shall provide diagrams of the satellite systems and ground systems for the most cost-effective FDMA system arrived at in Subtask 3.1. Tabular data shall be provided indicating the major cost elements of the ground system and the major cost and weight elements of the space system.

3.3 TDMA Concepts

3.3.1 TDMA, CONUS Coverage, no on-board switching

(a) The contractor shall provide a satellite and ground system direct-to-user concept, operating in a TDMA mode, using a CONUS coverage satellite. This concept shall be arrived at by adjusting the satellite and ground station parameters to arrive at a minimum total system cost as defined in Subtask 2.1.1(a). The following parameters shall be used for this analysis:

(1) 10,000 ground stations evenly distributed throughout the U.S.

(2) User channels demand-assigned with ½ capacity devoted to 40 KBS service, ¼ capacity to 1.5 MBS service, and ¼ capacity to 40 MBS service.

(3) QPSK modulation/demodulation with bit error rate of 10^{-6} and no coding.

(4) 99.5% propagation reliability.

(b) The contractor shall provide graphical displays showing system cost sensitivities of the optimum TDMA cost configuration. Service costs shall be provided for each of the services specified in Subtask 3.1.1(a) and shall be prorated according to the bandwidth used by each service as done in Subtask 2.3.1(b)(1). As a minimum, the contractor shall provide a display of:

(1) Service cost per equivalent channel and satellite availability as a function of the total number of ground terminals. The range shall span 10^3 - 10^5 terminals. The relative allocation of traffic shall be maintained.

(2) Service cost per equivalent channel as a function of design bit error rate. The range shall span 10^{-3}- 10^{-7}. This evaluation shall be done for 2, 4, and 8 level PSK as a minimum.

(3) Service cost per equivalent channel as a function of propagation reliability. The range shall span 99.0 - 99.99 per cent.

3.3.2 Multibeam TDMA, No On-Board Switching

(a) The contractor shall provide a multibeam satellite and ground system concept which operates in a TDMA mode without on-board switching. This concept shall be arrived

at by adjusting the satellite and ground station parameters to arrive at a minimum service cost to the user as specified in Subtask 2.1.1(a). The following baseline parameters shall be used for this portion of the analysis:

(1) 10,000 ground stations evenly distributed over the U.S.

(2) User channels demand-assigned with ½ capacity devoted to 40 KBS service, ¼ capacity to 1.5 KBS service, and ¼ capacity to 40 MBS service.

(3) QPSK modulation/demodulation with bit error rate of 10^{-6} and no coding.

(4) 99.5% propagation reliability.

(5) 25 spot beams on spacecraft evenly distributed over the U. S. with no direct interconnectivity between beams. Interconnectivity shall be provided as described in Subtask 3.1.2(a)(3).

(b) The contractor shall provide graphical displays showing system cost sensitivities of the optimum TDMA cost configuration in Subtask 3.3.1(a). Service costs shall be provided for each of the services specified in Subtask 3.3.1(a) and shall be prorated according to the bit rate used as done in Subtask 2.3.1(b)(1). As a minimum, the contractor shall provide a display of:

(1) Service cost per channel and satellite availability as a function of the number of ground terminals. The range shall span 10^3 - 10^5 terminals. The relative allocation of traffic shall be maintained.

(2) Service cost per channel as a function of design bit error rate. The range shall be 10^{-3} - 10^{-7}. This evaluation shall be done for 2, 4, 8 level PSK as a minimum.

(3) Service cost per channel as a function of the number of beams. The range shall span 4 - 40 beams.

(4) Service cost per channel as a function of propagation reliability. The range shall span 99.0 - 99.99 per cent.

3.3.3 TDMA, On-Board Switching

The contractor shall provide an assessment of the impact of adding on-board switching to the TDMA systems specified in Subtask 3.3.1 and Subtask 3.3.2. As a minimum, the contractor shall assess the impact on interconnectivity between beams and service cost.

3.4 Resultant TDMA Concept

The contractor shall provide diagrams of the satellite systems and ground systems for the most cost-effective TDMA system arrived at in Subtask 3.3. Tabular data shall be provided indicating the major cost elements of the ground system and the major cost and weight elements of the space system.

TASK 4 - COMPETITIVE ALTERNATIVES TO MILLIMETER WAVE SATELLITE SYSTEMS

The contractor shall provide an assessment of the availability, potential capability, and cost of alternatives to those in Tasks 2 and 3. As a minimum, the contractor shall provide data on the competitiveness of:

(a) Buried waveguide for wideband trunking.

(b) Fiber optic bundles for trunking and direct-to-user wideband service.

(c) Current DOMSAT systems.

TASK 5 - CRITICAL TECHNOLOGIES AND REQUIRED DEVELOPMENTS

The contractor shall provide an assessment of those technologies which are critical to the implementation of the concepts specified in Task 2 and Task 3. This assessment shall include items that have large economic uncertainty as well as items of great technical risk.

The contractor shall provide a tabular display of these technologies as well as a narrative on the nature of the criticality of each item.

The contractor shall recommend a technology program to reduce the technical and economic risks to the level of normal commercial risk. This program may or may not include shuttle flight experiments or an experimental satellite depending on the contractor's judgement as their necessity. Budgetary estimates of cost and schedule shall be provided for the recommended program.

TASK 6 - INTERACTION WITH MARKET STUDY CONTRACTOR

The contractor shall interact with the service study contractor to assure that the system and equipment defined in this study meets the needs of the anticipated service and to provide the service study contractor(s) with information about the system and equipment they need to conduct their study.

(1) Service cost per channel and satellite availability as a function of the number of ground terminals. The range shall span 10^3 - 10^5 terminals. The relative allocation of traffic shall be maintained.

(2) Service cost per channel as a function of design bit error rate. The range shall be 10^{-3} - 10^{-7}. This evaluation shall be done for 2, 4, 8 level PSK as a minimum.

(3) Service cost per channel as a function of the number of beams. The range shall span 4 - 40 beams.

(4) Service cost per channel as a function of propagation reliability. The range shall span 99.0 - 99.99 per cent.

3.3.3 TDMA, On-Board Switching

The contractor shall provide an assessment of the impact of adding on-board switching to the TDMA systems specified in Subtask 3.3.1 and Subtask 3.3.2. As a minimum, the contractor shall assess the impact on interconnectivity between beams and service cost.

3.4 Resultant TDMA Concept

The contractor shall provide diagrams of the satellite systems and ground systems for the most cost-effective TDMA system arrived at in Subtask 3.3. Tabular data shall be provided indicating the major cost elements of the ground system and the major cost and weight elements of the space system.

Task VI - Direct hours and dollars.

Task VII - Direct hours and dollars.

Subtotal

Overhead

Fee

Total Contract

3. A maximum of 10 copies of the Monthly Contractor Performance Analyses Report (NASA 533P). Columns 7-10 inclusive may be omitted. The reporting categories shall be the same as for Form 533M.

   The formal final study report prepared by the contractor shall include as a separate volume an Executive Summary of not more than 20 pages in length.

4. A minimum of three (3) informal presentations at the Lewis Research Center - two of which being reviews of work to date and the third being a final presentation of study results.